

2
2002

**LIBRARY
Michigan State
University**

This is to certify that the

dissertation entitled

ELASTIC DEFORMATIONS IN SHAPE MEMORY ALLOY
FIBER REINFORCED COMPOSITES

presented by

Xinjian FAN

has been accepted towards fulfillment
of the requirements for

Ph. D. degree in Engineering Mechanics

Hungyu Tsai
Major professor



Date 11/05/2001

PLACE IN RETURN BOX to remove this checkout from your record.
TO AVOID FINES return on or before date due.
MAY BE RECALLED with earlier due date if requested.

DATE DUE	DATE DUE	DATE DUE
JUL 22 2005 05		JUL 22 2005

**ELASTIC DEFORMATIONS IN
SHAPE MEMORY ALLOY FIBER REINFORCED COMPOSITES**

By

Xinjian Fan

A DISSERTATION

Submitted to
Michigan State University
in partial fulfilment of the requirements
for the degree of

DOCTOR OF PHILOSOPHY

Department of Mechanical Engineering

2001

ABSTRACT

ELASTIC DEFORMATIONS IN SHAPE MEMORY ALLOY FIBER REINFORCED COMPOSITES

By

Xinjian Fan

The elastic deformations of SMA fibers reinforced composite associated with phase transformations in parts of the SMA fibers are investigated. A simple case involving a single infinite fiber embedded in an infinite elastic matrix is studied. In the study, parts of the fiber are allowed to undergo uniform phase transformation along the axial direction, and there exist sharp boundaries between transformed and untransformed phases. The interaction between the fiber and the matrix is directly described by certain bonding conditions, while the sharp phase boundary in the fiber is directly modeled by piecewise linear constitutive law. The elastostatic problem is simplified as axisymmetrical ones. Two kinds of bonding models (“perfect bonding” and “spring bonding”) and two kinds of stiffness models (“rigid fiber” and “elastic fiber”) are considered. The exact solutions to the distributions of stress, strain, and displacement for each of these models are obtained in integral forms. A single finite segment transformation pattern is discussed in detail to display the local properties at crucial location – the intersection of fiber-matrix interface and phase boundary in the fiber. The asymptotic expansion technique is employed to further analysis the behavior of stresses. In the “perfect bonding” condition, the normal stresses have finite jumps across the phase boundary, whereas the shear stress approaches infinity. The singularities are isolated. The jumps of the normal stresses and the intensity of singularity of the shear stress are determined by the material properties of the matrix and fiber and transformation strain, and are independent of the geometry of the phase transformed region. In the “spring bonding” condition, all stresses are finite and continuous in fiber and matrix. The

shear stress concentrates at the intersection of the fiber-matrix interface and the phase boundary of the fiber. The softer fiber, matrix, and bonding condition will reduce the shear stress concentration. The shear stress concentration increases as the aspect ratio of phase transformed region increases.

ACKNOWLEDGMENTS

I wish to express my sincerest appreciation to my advisor, Dr. Hungyu Tsai, for his valuable guidance and constant support throughout my Ph.D. program and research. Appreciation is extended to Dr. Pence and Dr. Dashing Liu for serving as members of my guidance committee, teaching my courses, and valuable suggestion. Appreciation is also extended to Dr. Zhenfang Zhou for serving as my guidance committee member and assistance.

Special appreciation is due to my wife, Sainan Wei, for her understanding, patience, support, and taking care of our family besides working on her own Ph.D. program. I also owe my appreciation to my daughter, Jingyun Fan, for her understanding and support.

TABLE OF CONTENTS

ACKNOWLEDGMENTS	iv
TABLE OF CONTENTS	v
LIST OF FIGURES	vii
CHAPTER 1	
INTRODUCTION	1
2.1 Literature Review	1
2.2 Objectives	10
CHAPTER 2	
AXISYMMETRICAL DEFORMATIONS	15
2.1 Fundamental Equations	15
2.2 Love's Stress Function	18
2.3 Fourier Transform	20
2.3.1 Fourier Transform in L^1	20
2.3.2 Fourier Transform in S	21
2.3.3 Generalized Fourier Transform in S^*	21
2.4 Basic Equations in the Transformed Domain	24
2.5 General Solutions in the Transformed Domain	25
2.6 General Solutions in the Original Domain	28
2.7 SMA Fiber Reinforced Composite	31
2.8 Single Finite Segment Transformation and Normalization	39
2.9 Asymptotic Expansions for the Modified Bessel Functions	46
CHAPTER 3	
"PERFECT BONDING RIGID FIBER" MODEL	48
3.1 Boundary Conditions	48
3.2 Exact Solutions	49
3.3 Single Finite Segment Transformation	54
3.4 Numerical Evaluation	58
3.5 Analysis of Singularities	65
3.6 Remarks	70
CHAPTER 4	
"PERFECT BONDING ELASTIC FIBER" MODEL	72
4.1 Bonding Conditions	72
4.2 Exact Solutions	73
4.3 Single Finite Segment Transformation	80
4.4 Numerical Evaluation	86
4.5 Reduction to the Perfect Bonding Rigid Fiber Model	94
4.6 Approximations of the Stress Distributions	95
4.7 Analysis of Singularities	111
4.8 Remarks	119
CHAPTER 5	
"SPRING BONDING" MODEL	121
5.1 Bonding Conditions	121
5.2 Exact Solutions	122

5.3 Single Finite Segment Transformation	131
5.4 Numerical Evaluation	137
5.5 Reduction to the Spring Bonding Rigid Fiber Model	144
5.6 Reduction to the Perfect Bonding (Elastic Fiber) Model	151
5.7 Boundedness of the Stress Distributions on the Interface	153
5.8 Maximum shear stress	161
5.9 Remarks	170
 CHAPTER 6	
CONCLUSIONS AND FUTURE WORK	172
 REFERENCES	178

LIST OF FIGURES

CHAPTER 2. AXISYMMETRICAL DEFORMATIONS

- Figure 2.1 The three-dimensional cylindrical region \mathcal{R} and the corresponding two-dimensional domain Ω . (a) A solid cylindrical region, and (b) a hollow cylindrical region. 16
- Figure 2.2 The SMA fiber reinforced composite. (a) A three-dimensional plot of a straight SMA fiber ($\mathcal{R}^{(2)}$) embedded in matrix ($\mathcal{R}^{(1)}$). (b) The corresponding two-dimensional domains $\Omega^{(1)}$ and $\Omega^{(2)}$ 32
- Figure 2.3 The SMA fiber reinforced composite with a fiber of which a single finite segment of length $2L$ undergoes phase transformation. (a) A three-dimensional plot of regions $\mathcal{R}^{(1)}$ and $\mathcal{R}^{(2)}$. (b) The corresponding two-dimensional domains $\Omega^{(1)}$ and $\Omega^{(2)}$ 41
- Figure 2.4 A fiber with a single finite segment of length $2L$ undergoing phase transformation. (a) The phase transformation characteristic function. (b) The displacement phase transformation characteristic function. 42

CHAPTER 3. "PERFECT BONDING RIGID FIBER" MODEL

- Figure 3.1 The 3D plots of stress distributions for $\nu^{(1)} = 0.25$ and $\alpha = 10$. (a) $\frac{\bar{\sigma}_{rr}^{(1)}}{E^{(1)}\gamma T}$, (b) $\frac{\bar{\sigma}_{\theta\theta}^{(1)}}{E^{(1)}\gamma T}$, (c) $\frac{\bar{\sigma}_{zz}^{(1)}}{E^{(1)}\gamma T}$, and (d) $\frac{\bar{\sigma}_{rz}^{(1)}}{E^{(1)}\gamma T}$ 59-60
- Figure 3.2 The 3D plots of strain distributions for $\nu^{(1)} = 0.25$ and $\alpha = 10$. (a) $\frac{\bar{\gamma}_{rz}^{(1)}}{\gamma T}$, (b) $\frac{\bar{\gamma}_{\theta\theta}^{(1)}}{\gamma T}$, (c) $\frac{\bar{\gamma}_{zz}^{(1)}}{\gamma T}$, and (d) $\frac{\bar{\gamma}_{rz}^{(1)}}{\gamma T}$ 61-62
- Figure 3.3 The 3D plots of displacements for $\nu^{(1)} = 0.25$ and $\alpha = 10$. (a) $\frac{\bar{u}_r^{(1)}}{a\gamma T}$, and (b) $\frac{\bar{u}_z^{(1)}}{a\gamma T}$ 63
- Figure 3.4 The distributions of the stresses on the fiber-matrix interface for $\nu^{(1)} = 0.25$ and $\alpha = 10$ 64
- Figure 3.5 The shear stress distributions, $\frac{\bar{\sigma}_{rz}^{(1)}}{E^{(1)}\gamma T}$, on the fiber-matrix interface for $\nu^{(1)} = 0.25$ and $\alpha = 1, 5, 10$, and 20, respectively. 64

CHAPTER 4. "PERFECT BONDING ELASTIC FIBER" MODEL

- Figure 4.1 The 3D plots of stress distributions for $w = 0.000096$, $\nu^{(1)} = 0.35$, $\nu^{(2)} = 0.29$, and $\alpha = 10$. (a) $\frac{\bar{\sigma}_{rr}^{(1)}}{E^{(1)}\gamma T}$, (b) $\frac{\bar{\sigma}_{\theta\theta}^{(1)}}{E^{(1)}\gamma T}$, (c) $\frac{\bar{\sigma}_{zz}^{(1)}}{E^{(1)}\gamma T}$, and (d) $\frac{\bar{\sigma}_{rz}^{(1)}}{E^{(1)}\gamma T}$ 87-88

Figure 4.2 The 3D plots of strain distributions for $w = 0.000096$, $\nu^{(1)} = 0.35$, $\nu^{(2)} = 0.29$, and $\alpha = 10$. (a) $\frac{\tilde{\gamma}_{rr}}{\gamma^T}$, (b) $\frac{\tilde{\gamma}_{\theta\theta}}{\gamma^T}$, (c) $\frac{\tilde{\gamma}_{zz}}{\gamma^T}$, and (d) $\frac{\tilde{\gamma}_{rz}}{\gamma^T}$ 89-90

Figure 4.3 The 3D plots of displacements for $w = 0.000096$, $\nu^{(1)} = 0.35$, $\nu^{(2)} = 0.29$, and $\alpha = 10$. (a) $\frac{\tilde{u}_r}{a\gamma^T}$, and (b) $\frac{\tilde{u}_z}{a\gamma^T}$ 91

Figure 4.4 The stress distributions of the matrix on the fiber-matrix interface for $w = 0.000096$, $\nu^{(1)} = 0.35$, $\nu^{(2)} = 0.29$, and $\alpha = 10$ 92

Figure 4.5 The stress distributions of the fiber on the fiber-matrix interface for $w = 0.000096$, $\nu^{(1)} = 0.35$, $\nu^{(2)} = 0.29$, and $\alpha = 10$ 92

Figure 4.6 The maximum constrained strain of the fiber, $\frac{\tilde{\gamma}_{zz}^{(2)} - \gamma^T}{\gamma^T}$, against the logarithm of w for $\alpha = 1, 10$, and 100 , with $\nu^{(1)} = \nu^{(2)} = 0.3$. Here, w is the ratio of the shear modulus of the fiber $G^{(1)}$ to the shear modulus of the matrix $G^{(2)}$: $w = \frac{G^{(1)}}{G^{(2)}} = \frac{(1+\nu^{(2)})E^{(1)}}{(1+\nu^{(1)})E^{(2)}}$ 93

CHAPTER 5. “SPRING BONDING” MODEL

Figure 5.1 The 3D plots of stress distributions for $E^{(1)} = 1\text{GPa}$, $E^{(2)} = 100\text{GPa}$, $\nu^{(1)} = \nu^{(2)} = 0.3$, $\bar{k} = 10^{-5}$, and $\alpha = 10$. (a) $\frac{\tilde{\sigma}_{rr}}{E^{(1)}\gamma^T}$, (b) $\frac{\tilde{\sigma}_{\theta\theta}}{E^{(1)}\gamma^T}$, (c) $\frac{\tilde{\sigma}_{zz}}{E^{(1)}\gamma^T}$, and (d) $\frac{\tilde{\sigma}_{rz}}{E^{(1)}\gamma^T}$ 138-139

Figure 5.2 The 3D plots of strain distributions for $E^{(1)} = 1\text{GPa}$, $E^{(2)} = 100\text{GPa}$, $\nu^{(1)} = \nu^{(2)} = 0.3$, $\bar{k} = 10^{-5}$, and $\alpha = 10$. (a) $\frac{\tilde{\gamma}_{rr}}{\gamma^T}$, (b) $\frac{\tilde{\gamma}_{\theta\theta}}{\gamma^T}$, (c) $\frac{\tilde{\gamma}_{zz}}{\gamma^T}$, and (d) $\frac{\tilde{\gamma}_{rz}}{\gamma^T}$ 140-141

Figure 5.3 The 3D plots of displacements for $E^{(1)} = 1\text{GPa}$, $E^{(2)} = 100\text{GPa}$, $\nu^{(1)} = \nu^{(2)} = 0.3$, $\bar{k} = 10^{-5}$, and $\alpha = 10$. (a) $\frac{\tilde{u}_r}{a\gamma^T}$, and (b) $\frac{\tilde{u}_z}{a\gamma^T}$ 142

Figure 5.4 The stress distributions of matrix on the fiber-matrix interface for $E^{(1)} = 1\text{GPa}$, $E^{(2)} = 100\text{GPa}$, $\nu^{(1)} = \nu^{(2)} = 0.3$, $\bar{k} = 10^{-5}$, and $\alpha = 10$ 143

Figure 5.5 The stress distributions of fiber on the fiber-matrix interface for $E^{(1)} = 1\text{GPa}$, $E^{(2)} = 100\text{GPa}$, $\nu^{(1)} = \nu^{(2)} = 0.3$, $\bar{k} = 10^{-5}$, and $\alpha = 10$ 143

Figure 5.6 The shear stress distributions $\frac{\tilde{\sigma}_{rz}^{(n)}}{E^{(n)}\gamma^T}$ on the fiber-matrix interface for $\nu^{(1)} = \nu^{(2)} = 0.3$, $\alpha = 10$, $\bar{k} = 10^{-3}$, and various ratios of shear modulus of fiber to that of matrix: $w = 10^{-5}, 10^{-4}, 10^{-3}, 10^{-2}$, and 10^{-1} . (a) For matrix, and (b) for fiber. 150

Figure 5.7 The displacement distributions $\frac{\tilde{u}_z^{(n)}}{a\gamma^T}$ on the fiber-matrix interface for

$E^{(1)} = 1\text{GPa}$, $E^{(2)} = 100\text{GPa}$, $\nu^{(1)} = \nu^{(2)} = 0.3$, and $\alpha = 10$, and various stiffnesses ($\bar{k} = 0, 10^{-5}, 10^{-4}, 10^{-3}, 10^{-2}$, and 10^{-1}). The solid curves are for fiber and dashed ones for matrix. 152

Figure 5.8 The shear stress distributions $\frac{\bar{\sigma}_{rz}}{E^{(1)}\gamma^T}$ on the fiber-matrix interface for $E^{(1)} = 1\text{GPa}$, $E^{(2)} = 100\text{GPa}$, $\nu^{(1)} = \nu^{(2)} = 0.3$, and $\alpha = 10$, and various stiffnesses ($\bar{k} = 0, 10^{-5}, 10^{-4}, 10^{-3}, 10^{-2}$, and 10^{-1}). 152

Figure 5.9 The variation of maximum shear stress $\bar{\sigma}_{rz}^{max}$ with the ratio of shear moduli $w = G^{(1)}/G^{(2)}$ for fixed $E^{(1)}$, $\alpha = 10$, and $\bar{k} = 10^{-5}$ 164

Figure 5.10 The variation of maximum shear stress $\bar{\sigma}_{rz}^{max}$ with \bar{k} for fixed $\alpha = 10$, and $w = 10^{-2}$ 164

Figure 5.11 The variation of maximum shear stress $\bar{\sigma}_{rz}^{max}$ with parameters α for fixed $w = 10^{-2}$ and $\bar{k} = 10^{-5}$ 165

Figure 5.12 The maximum shear stress $\bar{\sigma}_{rz}^{max}$ as a function of parameters w and \bar{k} for fixed $\alpha = 10$. (a) The 3D plot, (b) the contour plot. 166

Figure 5.13 The variation of maximum shear stress $\bar{\sigma}_{rz}^{max}$ with $\bar{k} - w$ for $\alpha = 10$. 167

Figure 5.14 The maximum shear stress $\bar{\sigma}_{rz}^{max}$ as a function of parameters w and α for fixed $\bar{k} = 10^{-5}$. (a) The 3D plot, (b) the contour plot. 168

Figure 5.15 The maximum shear stress $\bar{\sigma}_{rz}^{max}$ as a function of parameters \bar{k} and α for fixed $w = 10^{-2}$. (a) The 3D plot, (b) the contour plot. 169

CHAPTER 1. INTRODUCTION

1.1 Literature Review

Recently, smart materials have attracted increasing attention for their extensive application prospects in a variety of fields, such as aerospace, automotives, and biomechanics. These novel materials have intrinsic sensing, actuating, and controlling capabilities, so that they are capable of responding to the external stimuli according to a prescribed manner and extent in an appropriate time (see, for example, Wei et al. 1998a, 1998b; Birman 1997; Crawley, 1994; Rogers et al. 1989). Since such properties are not found in traditional engineering materials (except probably in some biomaterials), one attempts to create them artificially by integrating several materials with special functions into hybrid composites (Wei et al. 1998a, 1998c; Nozaki and Takahashi 1994).

Shape memory alloy (SMA) hybrid composites is one class of the most promising smart materials due to the unique characteristics of SMAs, such as the shape memory effects (SME), pseudoelasticity, and high damping capacity. A variety of alloys, including Nitinol, Cu-Zn-Al and Cu-Al-Ni, have been found to exhibit SME (Hodgson et al. 1990; Perkins 1986; Wei et al. 1998a). For example, the most popular SMA, Nitinol, has not only prominent shape memory performance, but also excellent mechanical properties, good processibility, good corrosion resistance, and good biocompatibility (Wei et al. 1998a). For Nitinol, a few percent of inelastic strains can be completely recovered. All the unique characteristics of SMAs, in general, originate from the ability of the SMAs to undergo phase transformation (Wayman and Duerig 1990, Shaw and Kyriakides 1995).

Although many of the SMAs can be readily fabricated into a large variety of shapes, such as particles, fibers, ribbons, and thin films, the SMA fiber reinforced composites are more often employed in practical applications and more intensively

studied. This might be partly because most experiments for characterizing the behavior of SMA are one-dimensional in nature. On the other hand, with the dominant dimension in the longitudinal direction of the fibers, one can more efficiently take advantage of SME or control the SME in some specific directions. For the design, analysis, and application of either SMA fiber itself or SMA fiber reinforced composites, a sound mechanical model for SMA fiber is essential in addition to extensive experimental studies.

Generally, a model of SMA associated with phase transformation consists of two coupled parts: a constitutive relation governing the thermomechanical response and an evolution relation describing the state of phase transformation. Some models emphasize on the local property, while the others aim at the global behavior. To describe local property of SMA associated with phase transformation, a non-convex thermodynamical potential energy is often employed. To obtain global behavior, different approximation schemes from the local property are used such as mixture rule (volume average), statistical mechanics, and self-consistent method. To describe the state of phase transformation, internal variables, such as the position of phase boundary, the phase fraction, or fractions of variants, are introduced depending on what scale and property of phase transformation are considered in the model. The evolution of the internal variables is determined according to physical law or macroscopic experimental phenomenology.

The following are some typical models of SMA. Based on purely mechanical continuum nonlinear elasticity, Ericksen (1975) developed a one-dimensional theory on elastic bar, which is capable of undergoing stress-induced phase transformation. The material constitution of the bar is given by a non-convex strain energy that leads to a non-monotonic relation between the longitudinal strain and the stress. The stress-strain curve consists of three branches. The slopes of the strain-stress curve of the first, second, and third branches go from positive to negative and back

to positive values. Each branch of the stress-strain curve is associated with a phase of the material. It was shown that the branch with negative slope corresponds to an unstable phase. Particles of the material can stay only on either branch with positive slope, one corresponding to low strain phase and the other high strain phase. The sudden change of the state of a material particle in the strain-stress curve from the low strain phase to the high strain phase, or vice versa, is described as phase transformation. The inelastic strain associated with the phase transformation is called the transformation strain. From the potential energy point of view, the phase transformation corresponds to the jump of material state from one potential well to another. Fosdick and James (1981) investigated an analogous situation in the bending of a homogeneous inextensible elastica with a non-convex moment-curvature relation.

The theory given by Ericksen (1975) characterizes the phase transformation from the point of view of stability of material state. Because the stress is no longer a monotonic function of the strain in that model, a given boundary condition generally does not lead to a unique equilibrium solution. For example, a given tensile force applied at the end of the bar (hard device problem) or a given displacement at the end of the bar (soft device problem), may result in infinitely many equilibrium states involving a mixture of phases. To obtain the unique solution, one viewed the position of the phase boundary as an internal variable and presented a supplementary constitutive relation to govern the evolution of the phase boundary (Abeyaratne and Knowles 1988). This kinetic relation connects the driving traction acting on a moving phase boundary with the velocity of the quasi-static motion of the phase boundary. It was found that the kinetic relation, together with a nucleation criterion that signals the initiation of phase boundary, is sufficient to single out a unique solution. To take the thermal effect into account, a more general model of a one-dimensional thermoelastic bar that is capable of undergoing phase

tr
p
cr
m
at
h
g
w
t
i
o
a
i
s
i

transformation was developed (Abeyaratne and Knowles 1993). An explicit example of the Helmholtz free energy density, the kinetic relation, and the nucleation criterion were constructed. In that model, the stress-strain curve at each temperature is trilinear. The mechanical cycling at constant temperature, thermal cycling at constant stress, and the SME involving a combination of mechanical and thermal loading were studied and compared qualitatively with experimental results.

Instead of considering quasi-static processes, Pence (1986) investigated the fully dynamical motion of phase boundary. A semi-infinite compressible elastic bar, whose normal stress versus normal strain relation is non-monotonic, is subjected to a monotonically increasing load at the end. The problem is formulated as an initial-boundary value problem in one-dimension. The emergence and propagation of phase boundary are discussed in detail. With the same mathematical structure, an analogous problem with full dynamics effects was studied in a specific class of incompressible homogeneous isotropic hyperelastic materials in which the stress-strain relation in simple shear is not monotonic (Pence 1991a, 1991b). A single internal pre-existing shear stress-induced stationary phase boundary can be set in motion by external applied dynamical shear. Two-dimensional motion of twin boundaries are studied by Rosakis and Tsai (1995) and Tsai and Rosakis (2001) in the setting of anti-plane shear.

To describe the phenomena associated with phase transformation of SMA, Falk (1980, 1983) developed a one-dimensional model of SMAs in a special shear direction of phase transformation. The state equation is given in terms of the Helmholtz free energy density as a function of the shear strain and temperature. According to the crystallography of a single crystal undergoing phase transformation, the simplest form of the Helmholtz free energy density is proposed to be a polynomial of shear strain. In that model, the stress-induced phase transformation, the temperature-induced phase transformation, and the shape memory effect of SMAs

a

te

f

st

i

n

at

fr

ti

un

be

l

un

a

su

iv

tr

ste

on

co

B

n

pl

va

th

are qualitatively reflected.

Tanaka (1986b) presented a one-dimensional thermomechanical model of material subject to phase transformation. To characterize the extent of phase transformation, the martensitic volume fraction is introduced as an independent internal state variable. The strain, temperature, and martensitic volume fraction together form a complete set of state variables to describe the thermomechanical behavior of materials involving phase transformation. The forms of the constitutive equations are derived with the restriction of the Clausius-Duhem inequality on Helmholtz free energy. The evolution of the martensitic volume fraction is determined by the dissipation potential. An explicit form of the evolution of the martensitic volume fraction is suggested to be an exponential function of temperature and stress based on the phase transformation phenomena (Tanaka, 1986a). Liang and Rogers (1990) improved Tanaka's model by describing the evolution of the martensitic volume fraction with a cosine function of temperature and stress. Then, Zhang et al. (1992) extended the model to include the two-way shape memory effect. Brinson (1993) further distinguished the twinned martensite phase and detwinned one by introducing separate fractions so more behavior of SMA can be captured. The transformation kinetics is expressed by algebraic equations with a few material constants. The transformation region is described with the aid of phase diagram. Based on this model, a lot of behaviors of SMA have been discussed by Brinson and his colleagues (Brinson et al. 1996, Brinson and Huang 1996, Bekker and Brinson 1997, Bekker and Brinson 1998, Bekker et al. 1998).

Ivshin and Pence (1994a, 1994b) developed a one-dimensional constitutive model for describing the thermomechanical behavior of mixture of two phases. Each phase allows one variant. The fraction of austenite phase is used as an internal variable. Based on a series arrangement of individual pure phase at microscale level, the overall thermomechanical behavior is calculated by mixture law from individual

behavior of each pure phase. A restriction condition on the phase fraction is derived from Maxwell relation. An algorithm to determine the evolution of the phase fraction is developed for given temperature history (Ivshin and Pence 1994a) or for given both temperature and stress histories (Ivshin and Pence 1994b). Further, Wu and Pence (1998) studied a model of SMA involving austenite and two variants of martensite.

Following the statistic mechanics approach, Muller (1979) presented a snap-spring model to simulate the thermomechanical behavior of SMAs. The basic element of the model is a loaded snap-spring, which has one or two stable equilibrium configurations according to the magnitude of the applying load. The model is built up by the loaded snap-spring. Assume the snap-spring can exchange energy with its surroundings and with other snap-springs. As a result the snap-spring can move around irregularly in the neighborhood of the equilibrium position. Based on the statistical mechanics, the global behavior of the SMA body is described according to the energy of local snap-spring and the temperature.

Also based on the statistical mechanics, Achenbach and Muller (1985) developed a stacked lattice particle model. Differing from the snap-spring model, the basic element is modeled as lattice particle, which represents a small part of the metallic lattice to reflect the microscopic properties. The lattice particle is capable of assuming three equilibrium configurations to describe austenite phase and martensite twins according to minima of the potential energy. The SMA body is then built up by stacking up the layers and in each layer the lattice particles have the same equilibrium configuration. The phase transformation depends on the load and temperature and is governed by a rate law of the lattice particle fraction based on transition possibility. The temperature follows a rate law according to the balance of energy in the heat transfer with the environment and the heat for the phase transformation.

US
et al. 1
local be
of the
fraction
of plas
is emp
stress a
is also

A
each p
The ex
fraction
marter
of SM.

O
round-
fibers.
tions a
additi
on the
the SM
structu
ites.

To
approac
standards

Using micromechanical approach, Patoor et al. (Buisson et al. 1991, Berveiller et al. 1991, Patoor et al. 1996) developed a thermomechanical model of SMA. The local behavior of an elementary representative volume is described by the kinematics of the martensitic phase transformation and thermodynamical potential. Volume fractions of the different variants of martensite are used to describe the evolution of phase transformation. Based on defect theory, the self-consistent approximation is employed to obtain the global behavior. By taking into account in the internal stress associated with the oriented defect produced in training sequences, the model is also used to study two way memory effect (Patoor et al. 1991).

Another way to model the SMA associated with phase transformation is to take each phase of SMA as an component of a composite (Boyd and Lagoudas 1994). The extent of phase transformation in SMA is described by martensite volume fraction, which is determined by a function of temperature and stress. Assuming the martensite phase is distributed randomly in the SMA body, the effective properties of SMA can be obtained from theories of composites.

On the setting of SMA fiber reinforced composites, the SMA fibers are surrounded by the matrix. To accommodate the transformation strains in the SMA fibers, the matrix is forced to deform in order to maintain certain bonding conditions at the fiber-matrix interface. In turn, the deformation in the matrix induces additional deformation in the SMA fibers with the possibility to impose constraints on the phase transformation in the SMA fibers. Therefore, the interaction between the SMA fibers and the matrix determines the overall mechanical properties of the structure and hence plays a crucial role in the design and analysis of such composites.

To deal with the interactions between the SMA fibers and the matrix, one approach is to employ averaging schemes or some kind of mixture rule used in standard composite theory without phase transformation. This approach states

that the composite properties are the sum of the corresponding properties of each constituent weighted by some kinds of concentration factors, usually the volume fraction. This approach can be used to study the overall effective properties of the SMA fiber reinforced composites.

For example, Yamada, Taya, and Watanabe (1993) studied Nitinol particle with metal matrix composite. Based on the Eshelby's equivalent inclusion method (Eshelby 1957, 1959) or self-consistent method (Hill 1965), the residual stress caused by the shape memory effect is solved. The Young's modulus, yield stress, and work-hardening rate of the composite are predicted.

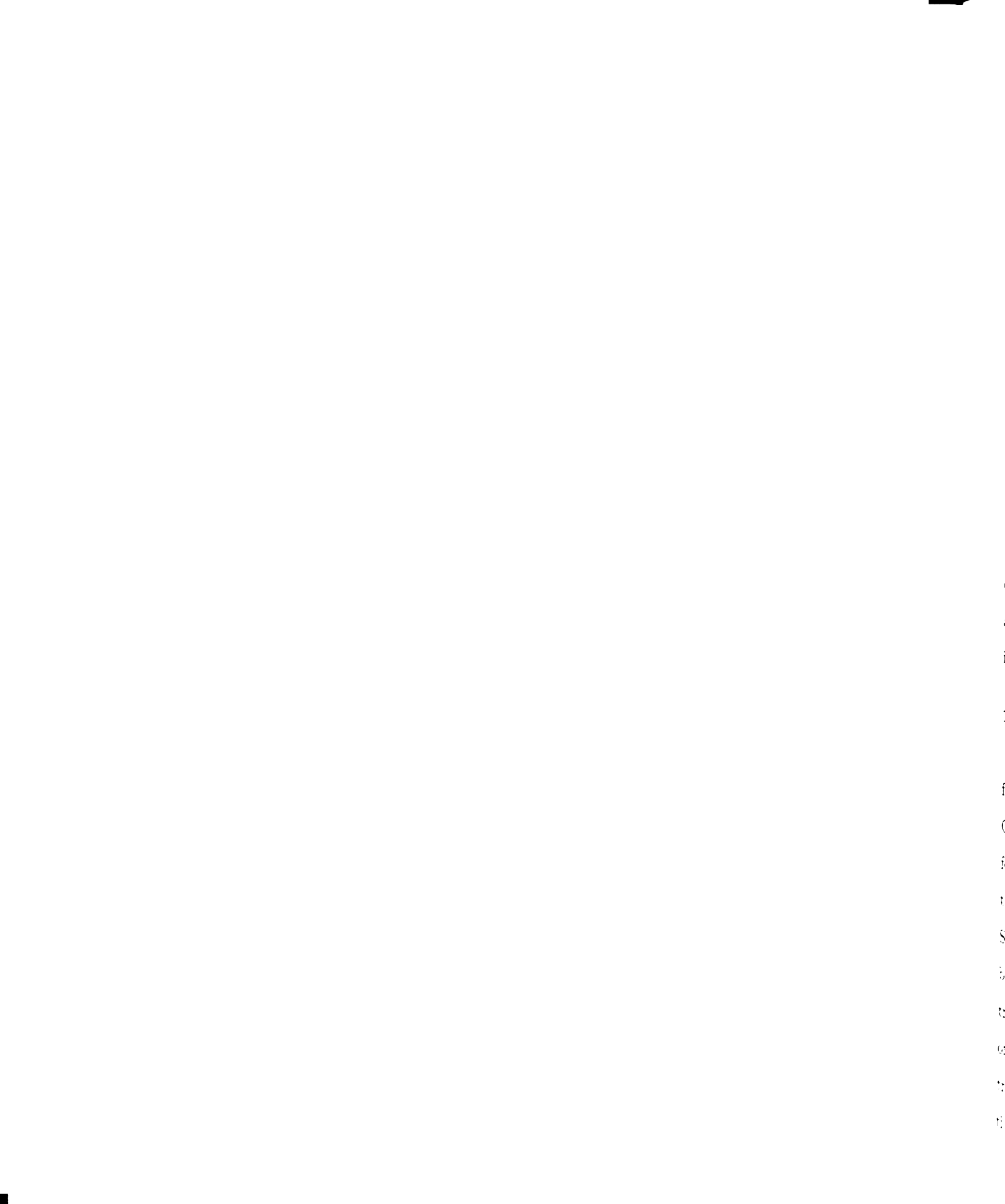
For the SMA fibers reinforced composites, Lagoudas, Boyd, and Bo (1994) and Boyd and Lagoudas (1994) present a micromechanical model to predict the effective thermomechanical properties. The SMA fiber is treated as an elastic composite consisting of martensite and austenite. The phase transformation in fibers is described by an exponential decay of martensite volume fraction with temperature and a von-Mises type effective stress. The transformation strain rate is proportional to the rate of martensite volume fraction. The effective thermomechanical properties of the SMA fibers are obtained by using Mori-Tanaka micromechanical averaging schemes. Then, the Mori-Tanaka micromechanical averaging method is used again to get the overall effective thermomechanical properties of the composites in terms of the thermomechanical properties of the matrix and the effective thermomechanical properties of the fibers. In order to model path dependent thermomechanical loading, the incremental thermomechanical constitutive relations are used and within each stress and temperature increment the martensite volume fraction is assumed remaining constant in the fibers.

In order to analyze the stress of SMA fiber composite in detail, Berman and White (1996) and Birman and Hopkins (1996) developed a three-phase concentric cylinder model. This model consists of a SMA fiber, a cylinder matrix, and

an infinite composite cylinder. The extent of phase transformation in the SMA fiber is described by martensite volume fraction and then the fiber is homogenized as isotropic elastic material using mixture rule. The introduction of the infinite composite cylinder is to consider the interactions of fiber and matrix with the surrounding fiber and matrix (Birman and Hopkins, 1996), or to describe an internal control system protected from the environment (Berman and White, 1996). The surrounding composite is modeled as homogeneous transversely isotropic and elastic material and the corresponding equivalent properties of the composite are obtained by using micromechanical approach. By requiring continuities of the radial stress and radial displacement, the properties are determined by a boundary value problem of axisymmetric plane strain deformation. The problem then can be solved numerically.

Another way to deal with the interactions between the SMA fibers and the matrix is to directly consider the interaction by explicitly describing the bonding conditions. Compared with the previous approach, this way gives more details about the behaviors of the composites, such as the distributions of stress, strain, and displacement. Eshelby's model (Eshelby 1957, 1959) is a typical one of this kind. In this model, Eshelby considered a general solid problem in which an isolated inclusion in an infinite homogeneous isotropic elastic medium undergoes a change of shape and size. Provided the inclusion has an ellipsoidal shape and the entire inclusion undergoes uniform deformation, a closed form solution to the elastic fields was found by using a set of imaginary cutting, straining, and welding operations. The Eshelby's method can be used to derive many other models (Mura 1982) and is found of great usefulness in the studies of regular composites and SMA hybrid composites.

In the case of SMA fiber reinforced composite during phase transition, however, only part of the SMA fiber undergoes phase transformation. In this situation,



across the phase boundary between the transformed and the untransformed parts of the SMA fiber, the strains suffer finite jumps, while the displacements remain continuous. These jumps of the strains across the phase boundary make the problem more interesting and more complicated. A good understanding of the behavior of material near the phase boundary, such as the stress distributions, is critical for the design and application of SMA fiber reinforced composites. The homogenization technique used by most researchers introduces martensite volume fraction and mixture rule to describe phase transformation in SMA fibers (Boyd and Lagoudas 1994, Birman and Hopkins 1996, Berman and White 1996). It only shows constituent average properties. In addition, the assumption of plane strain deformation can not completely characterize the behavior of the deformation, especially in the axial direction. Thus, in those models, the important shear deformation, which plays a crucial role in the analysis such as debonding, is not considered. For this concern, a new model is needed in which both the phase boundary in the SMA fiber and the interaction between the SMA fiber and the matrix should be described explicitly.

1.2 Objectives

In this dissertation, I investigate the elastic deformations of SMA fibers reinforced composite associated with phase transformations in parts of the SMA fibers. Generally, the deformations of the composite depend on the property of phase transformation in the SMA fiber, the material properties of the SMA fibers and the matrix, and the interaction between the SMA fibers and the matrix. As parts of the SMA fibers undergo phase transformation, their shapes are changed inelastically by the corresponding transformation strain (typically a few percent), with the matrix being elastic and isotropic. Under certain bonding condition, the deformation of the fibers forces the matrix to deform elastically in order to accommodate the transformation strain. In turn, additional elastic deformation besides the deformation from the phase transformation is induced in the fibers in order to maintain

the equilibrium at the fiber-matrix interface. Therefore, while the deformation in the matrix is induced only by the interaction between fiber and matrix since the phase transformation in the SMA fibers, the deformation in the fiber consists of two parts: the inelastic deformation from the phase transformation and the elastic deformation imposed by the constraint of the matrix. Generally, the transformation strain is the dominant strain in the SMA fibers.

Since the interaction between the SMA fibers and the matrix plays a key role in determining the mechanical properties of the composite, I will concentrate my attention upon a simple case involving a single infinite fiber embedded in an infinite elastic matrix. Assume parts of the fiber are allowed to undergo uniform phase transformation along the axial direction, and there exist sharp boundaries between the transformed phases and the untransformed phases. The strain in the fiber suffers finite jumps across these sharp phase boundaries. The lengths of the transformed parts of the fiber are changed by the corresponding transformation strain. In this case, the phase transformation of the SMA fiber is described by the magnitude of transformation strain and the transformation regions in the fiber, so it can be described by a so-called phase transformation characteristic function. Two kinds of phase transformation patterns are discussed: the general transformation and the single finite segment transformation. The case of single finite segment transformation is important because it gives (1) a detailed description of the local behavior, especially at some crucial locations, and (2) a description of the overall behavior for general transformation pattern by superposition principle.

The interaction between fiber and matrix is modeled through certain bonding conditions. Two kinds of bonding models are studied in this dissertation: the “perfect bonding” model and the “spring bonding” model. For the “perfect bonding” model, the displacement is assumed to be continuous across the fiber-matrix interface. The corresponding bonding conditions are given by geometry constraints

and equilibrium at the fiber-matrix interface. In the “spring bonding” model, on the other hand, the radial displacement maintains continuous while the axial displacement is allowed for discontinuity across the fiber-matrix interface. Such an axial displacement jump results in a shear stress with magnitude proportional to the magnitude of the jump. The corresponding bonding conditions are given by geometry constraints, equilibrium, and other interaction relations between fiber and matrix. The “perfect bonding” is the simplest assumption to the interaction between fiber and matrix. The “spring bonding” model is an attempt to account for more complex interactions.

The relative stiffness between fiber and matrix is an important factor for determining the behavior of the composite. In this dissertation, both the fiber and matrix are considered as elastic and isotropic. Thus, their material properties are determined by the Young’s moduli and Poisson’s ratios. With different assumptions about stiffness of the fiber relative to that of the matrix, we will study the “rigid fiber” model and the “elastic fiber” model. In the “rigid fiber” model, the elasticity of the fiber is ignored so that matrix exert no influence on the fiber. The only deformation considered in the SMA fiber is the phase transformation, which gives the boundary condition for the deformation of the matrix. The results of “rigid fiber” model provide good approximations to the cases in which the fiber is much stronger than the matrix. In the “elastic fiber” model, the elastic deformation of the fiber will be taken into account.

All the assumptions made for the geometry, material properties, phase transformation, and bonding conditions are axisymmetrical, so are the deformations. Mathematically, the problems are two-dimensional. We follow the formulation used by Muki and Sternberg (1969) on a problem with similar settings but without phase transformations. We begin with the description of the problem and the governing equations. Then, the Love’s stress function is introduced to reduce the problem to

a boundary value problem of PDE with only one unknown function. After applying (generalized) Fourier transform, the problem is further reduced to an ODE. The general solution to the Love's stress function in the Fourier transformed space is obtained in terms of the modified Bessel functions of the first and the second kinds. Thus, the general solutions to stresses, strains, and displacements of the problem can also be expressed in terms of the modified Bessel functions of the first and the second kinds. For each model, by solving the linear algebraic equations for the corresponding boundary conditions in the Fourier transformed domain, the exact elasticity solutions (in integral form) are found.

According to the assumptions on the bonding condition, the models are classified into "perfect bonding" and "spring bonding" models. On the other hand, based on the assumptions on the material properties, the models are classified into "rigid fiber" and "elastic fiber" models. In this dissertation, the "perfect bonding rigid fiber" model, the "perfect bonding elastic fiber" model, and the "spring bonding (elastic fiber)" model are studied in details in separate chapters, and the "spring bonding rigid fiber" model is dealt with as the special case of the "spring bonding" model. For each model, the results for both cases of general phase transformation and single finite segment phase transformation are presented. The following outline the dissertation.

In Chapter 2, we review the general approach for solving axisymmetrical elastic problems. The purpose of this chapter is to include materials that are common to our studies on each model so that it will not have to be repeated in the subsequent chapters. Since the phase transformation in SMA fiber is described by a function that is not absolutely integrable, we have to deal with the Fourier transform of generalized functions. The fundamental formula and properties of both standard and generalized Fourier transforms are reviewed. The general solution to the axisymmetrical elastic deformation for a general cylindrical body is derived first. The

De

in

ti

at

fo

ot

as

C

ti

at

ia

ex

in

ri

ot

be

fi

bu

ot

st

be

st

fo

results are then extended to composite with one SMA fiber embedded in elastic matrix.

As the preliminary step of the research, we study the “perfect bonding rigid fiber” model in Chapter 3. The exact solutions to the deformation of the matrix are derived according to the boundary conditions that are given by the phase transformation in the fiber. The numerical evaluation of the exact solutions is carried out. The behavior near the phase boundary of the fiber is further analyzed by using asymptotic expansion technique.

The study on the “perfect bonding elastic fiber” model is carried out in Chapter 4. The exact solutions are developed based on the perfect bonding conditions. The numerical evaluation of the solutions is carried out. The boundedness and continuity of the solution inside the fiber and matrix are shown and the singularities of the stresses on the fiber-matrix interface are isolated by using asymptotic expansion. The influence of matrix on the deformation and phase transformation in the fiber is discussed. The reduction of the results to those of “perfect bonding rigid fiber” model are also shown.

Chapter 5 is devoted to the “spring bonding” model. The exact solutions are obtained by applying spring bonding conditions. Then, the results are illustrated by numerical evaluation. As a special case, the results for the “spring bonding rigid fiber” model are presented. The reduction of the results to those of the “perfect bonding elastic fiber” model is shown. The boundedness of the stress distributions on the fiber-matrix interface, so on the whole domain, is proved for finite spring stiffness. Based on the numerical calculation, the influence of material properties, bonding stiffness, and geometry of phase transformed part of the fiber on the shear stress concentration are discussed.

Chapter 6 provides a summary to the results for all those models. Some topics for future work are suggested.

CHAPTER 2. AXISYMMETRICAL DEFORMATIONS

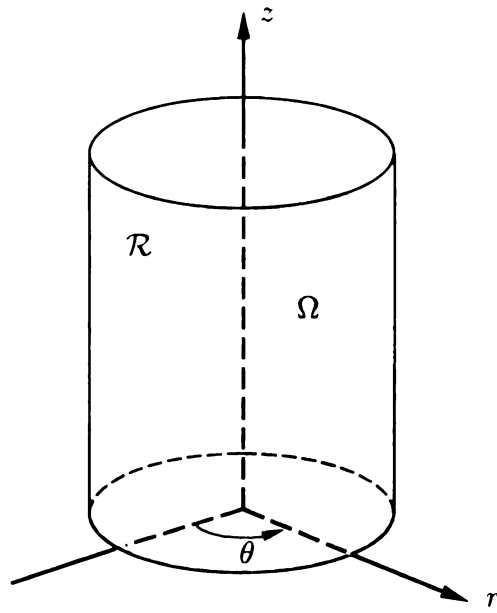
In this Chapter, we review the general approach for solving axisymmetrical elastostatic problems in linear elasticity. First, we consider a general cylindrical body made of homogeneous, isotropic, and linearly elastic materials. Under axisymmetrical deformations, the general solutions to stresses, strains, and displacements are derived. Then, the results are extended to composite with one SMA fiber embedded in elastic matrix. Particularly, the fiber is allowed to undergo phase transformation along the axial direction of the fiber. Since the phase transformation in SMA fiber, which is the main concern of this study, is described by a function that is not absolutely integrable, we have to deal with the Fourier transform of generalized functions. The fundamental formula and properties of both standard and generalized Fourier transforms are also reviewed.

2.1 Fundamental (Governing) Equations

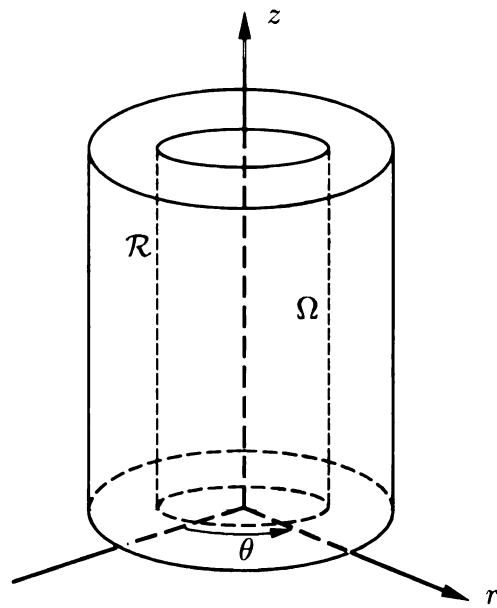
Let \mathcal{R} be a three-dimensional cylindrical region occupied by a body in its undeformed configuration. The cylindrical region \mathcal{R} could be either solid or hollow. Choose cylindrical coordinates (r, θ, z) with z -direction along the axis of symmetry of the body. The region \mathcal{R} can be given by the revolution about z -axis of a two-dimensional domain Ω in the rz -plane, as shown in Figure 2.1. Thus, the three-dimensional region \mathcal{R} can be expressed as the direct sum of the two-dimensional domain Ω and the one-dimensional interval $[0, 2\pi)$:

$$\mathcal{R} = \{(r, \theta, z) \mid (r, z) \in \Omega, \theta \in [0, 2\pi)\}. \quad (2.1)$$

For axisymmetric deformations with respect to the z -axis, all the quantities are independent of θ so that the problem is reduced to a two-dimensional one on domain Ω . The non-trivial displacement components are u_r and u_z , with the non-trivial elastic strain components γ_{rr} , $\gamma_{\theta\theta}$, γ_{zz} , and γ_{rz} . All these components are



(a)



(b)

Figure 2.1. The three-dimensional cylindrical region \mathcal{R} and the corresponding two-dimensional domain Ω . (a) A solid cylindrical region, and (b) a hollow cylindrical region.

fu

ca

ce

of

T

of

fo

functions of r and z only. The strain–displacement relations are given by

$$\gamma_{rr} = \frac{\partial u_r}{\partial r}, \quad \gamma_{\theta\theta} = \frac{u_r}{r}, \quad \gamma_{zz} = \frac{\partial u_z}{\partial z}, \quad \gamma_{rz} = \frac{1}{2} \left(\frac{\partial u_r}{\partial z} + \frac{\partial u_z}{\partial r} \right) \quad \text{on } \mathcal{R}. \quad (2.2)$$

Consider a body which is homogeneous, isotropic, and elastic. The mechanical properties are determined by Young’s modulus E and Poisson’s ratio ν . The constitutive equations are given by

$$\begin{aligned} \sigma_{rr} &= \frac{E}{(1+\nu)(1-2\nu)} [(1-\nu)\gamma_{rr} + \nu(\gamma_{\theta\theta} + \gamma_{zz})], \\ \sigma_{\theta\theta} &= \frac{E}{(1+\nu)(1-2\nu)} [(1-\nu)\gamma_{\theta\theta} + \nu(\gamma_{rr} + \gamma_{zz})], \\ \sigma_{zz} &= \frac{E}{(1+\nu)(1-2\nu)} [(1-\nu)\gamma_{zz} + \nu(\gamma_{rr} + \gamma_{\theta\theta})], \\ \sigma_{rz} &= \frac{E}{1+\nu} \gamma_{rz} \quad \text{on } \mathcal{R}, \end{aligned} \quad (2.3)$$

or alternatively,

$$\begin{aligned} \gamma_{rr} &= \frac{1}{E} [\sigma_{rr} - \nu(\sigma_{\theta\theta} + \sigma_{zz})], \\ \gamma_{\theta\theta} &= \frac{1}{E} [\sigma_{\theta\theta} - \nu(\sigma_{rr} + \sigma_{zz})], \\ \gamma_{zz} &= \frac{1}{E} [\sigma_{zz} - \nu(\sigma_{rr} + \sigma_{\theta\theta})], \\ \gamma_{rz} &= \frac{1+\nu}{E} \sigma_{rz} \quad \text{on } \mathcal{R}. \end{aligned} \quad (2.4)$$

Thus, the non-trivial stress components σ_{rr} , $\sigma_{\theta\theta}$, σ_{zz} , and σ_{rz} are also functions of r and z only. In this setting, the equilibrium equations (in the absence of body forces) reduce to

$$\begin{aligned} \frac{\partial \sigma_{rr}}{\partial r} + \frac{\partial \sigma_{rz}}{\partial z} + \frac{\sigma_{rr} - \sigma_{\theta\theta}}{r} &= 0, \\ \frac{\partial \sigma_{rz}}{\partial r} + \frac{\partial \sigma_{zz}}{\partial z} + \frac{\sigma_{rz}}{r} &= 0 \quad \text{on } \mathcal{R}. \end{aligned} \quad (2.5)$$

In terms of stress, the compatibility equations for axisymmetrical deformations are in the following forms (Timoshenko and Goodier, 1951, p.346)

$$\begin{aligned}\nabla^2 \sigma_{rr} - \frac{2}{r^2}(\sigma_{rr} - \sigma_{\theta\theta}) + \frac{1}{1+\nu} \frac{\partial^2 \Theta}{\partial r^2} &= 0, \\ \nabla^2 \sigma_{\theta\theta} + \frac{2}{r^2}(\sigma_{rr} - \sigma_{\theta\theta}) + \frac{1}{1+\nu} \frac{1}{r} \frac{\partial \Theta}{\partial r} &= 0, \\ \nabla^2 \sigma_{zz} + \frac{1}{1+\nu} \frac{\partial^2 \Theta}{\partial z^2} &= 0, \\ \nabla^2 \sigma_{rz} - \frac{1}{r^2} \sigma_{rz} + \frac{1}{1+\nu} \frac{\partial^2 \Theta}{\partial r \partial z} &= 0 \quad \text{on } \mathcal{R},\end{aligned}\tag{2.6}$$

where ∇^2 is the axisymmetric Laplacian operator given by

$$\nabla^2 = \frac{\partial^2}{\partial r^2} + \frac{1}{r} \frac{\partial}{\partial r} + \frac{\partial^2}{\partial z^2},\tag{2.7}$$

and Θ is the trace of the stress tensor:

$$\Theta = \sigma_{rr} + \sigma_{\theta\theta} + \sigma_{zz}.\tag{2.8}$$

Mathematically, the above governing equations (2.2), (2.3), (2.5), and (2.6) together with certain boundary conditions and some necessary restriction conditions form a two-dimensional boundary value problem.

2.2 Love's Stress Function

A standard way to solve the above elastostatic problem is to introduce the Love's stress function $\Phi = \Phi(r, z)$, (Love, 1927; Timoshenko and Goodier, 1951), such that the stresses are given by

$$\begin{aligned}\sigma_{rr} &= \frac{\partial}{\partial z} \left[\nu \nabla^2 \Phi - \frac{\partial^2 \Phi}{\partial r^2} \right], \\ \sigma_{\theta\theta} &= \frac{\partial}{\partial z} \left[\nu \nabla^2 \Phi - \frac{1}{r} \frac{\partial \Phi}{\partial r} \right],\end{aligned}$$

T

T

t

(

m

d

g

o

$$\begin{aligned}\sigma_{zz} &= \frac{\partial}{\partial z} \left[(2 - \nu) \nabla^2 \Phi - \frac{\partial^2 \Phi}{\partial z^2} \right], \\ \sigma_{rz} &= \frac{\partial}{\partial r} \left[(1 - \nu) \nabla^2 \Phi - \frac{\partial^2 \Phi}{\partial z^2} \right] \quad \text{on } \Omega.\end{aligned}\quad (2.9)$$

The stresses defined by (2.9) automatically satisfy the compatibility equations (2.6). The equilibrium equations (2.5) are satisfied by (2.9) provided that the stress function Φ are biharmonic:

$$\nabla^2 \nabla^2 \Phi = 0 \quad \text{on } \Omega. \quad (2.10)$$

By substituting (2.9) into the constitutive equation (2.4), the strain components can be solved in terms of the stress function Φ as

$$\begin{aligned}\gamma_{rr} &= -\frac{1 + \nu}{E} \frac{\partial^3 \Phi}{\partial r^2 \partial z}, \\ \gamma_{\theta\theta} &= -\frac{1 + \nu}{Er} \frac{\partial^2 \Phi}{\partial r \partial z}, \\ \gamma_{zz} &= \frac{1 + \nu}{E} \frac{\partial}{\partial z} \left[2(1 - \nu) \nabla^2 \Phi - \frac{\partial^2 \Phi}{\partial z^2} \right], \\ \gamma_{rz} &= \frac{1 + \nu}{E} \frac{\partial}{\partial r} \left[(1 - \nu) \nabla^2 \Phi - \frac{\partial^2 \Phi}{\partial z^2} \right] \quad \text{on } \Omega.\end{aligned}\quad (2.11)$$

By substituting (2.11) into the strain-displacement relation (2.2), the displacement components in terms of Φ can be found as

$$\begin{aligned}u_r &= -\frac{1 + \nu}{E} \frac{\partial^2 \Phi}{\partial r \partial z}, \\ u_z &= \frac{1 + \nu}{E} \left[2(1 - \nu) \nabla^2 \Phi - \frac{\partial^2 \Phi}{\partial z^2} \right] \quad \text{on } \Omega.\end{aligned}\quad (2.12)$$

The axisymmetrical elastostatic problem under present consideration thus reduces to the determination of a biharmonic function Φ such that the displacements given by (2.12) and the stresses given by (2.9) satisfy the corresponding boundary conditions and the restriction conditions.

2.3 Fourier Transform

To solve the biharmonic function Φ from (2.10), and to further determine the corresponding stresses, strains, and displacements from (2.9), (2.11), and (2.12), respectively, it is convenient to introduce the Fourier transform. Later, we will consider the phase transformation in SMA fiber, which is described by a function that is not absolutely integrable. Therefore, we have to deal with the Fourier transform of generalized functions. In this section, we review the fundamental formula and properties of both standard and generalized Fourier transforms for later use.

2.3.1 Fourier Transform in L^1

First, we consider the standard Fourier transform in space $L^1(-\infty, \infty)$, which consists of all absolutely integrable functions. For an absolutely integrable function $\phi \in L^1(-\infty, \infty)$, the Fourier transform of ϕ is defined by

$$\tilde{\phi}(\eta) \equiv \mathcal{F}[\phi] = \int_{-\infty}^{\infty} \phi(z) e^{i\eta z} dz, \quad -\infty < \eta < \infty, \quad (2.13)$$

where η is the independent variable in the Fourier transformed space, and i is the imaginary unit ($i^2 = -1$). The inverse Fourier transform of $\tilde{\phi} \in L^1(-\infty, \infty)$ is defined by

$$\mathcal{F}^{-1}[\tilde{\phi}] = \frac{1}{2\pi} \int_{-\infty}^{\infty} \tilde{\phi}(\eta) e^{-i\eta z} d\eta, \quad -\infty < z < \infty. \quad (2.14)$$

If ϕ is also continuous and piecewise smooth, then one has

$$\phi = \mathcal{F}^{-1}[\mathcal{F}[\phi]], \quad -\infty < z < \infty. \quad (2.15)$$

If ϕ is n differentiable, the following formula for the Fourier transform of the derivatives of ϕ is useful

$$\mathcal{F}\left[\frac{d^n \phi}{dz^n}\right] = (-i\eta)^n \mathcal{F}[\phi], \quad -\infty < \eta < \infty. \quad (2.16)$$

2

6

G

"

S

S

w

S

1

4

S

h

e

a

w

h

t

2.3.2 Fourier Transform in S

In order to extend the Fourier transform to cover more general functions, we consider the space S , which consists of all functions of rapid decay (See, for example, Griffel, 1981). A function of rapid decay ϕ is a smooth function such that for all $m, n \geq 0$, one has

$$z^m \frac{d^n \phi(z)}{dz^n} \rightarrow 0 \quad \text{as } |z| \rightarrow \infty. \quad (2.17)$$

Since functions of rapid decay are absolutely integrable, S is a subspace of L^1 , i.e., $S \subset L^1$. Thus, both the Fourier transform and the inverse Fourier transform are well defined in S , and the properties (2.15) and (2.16) hold. Moreover, the space S is closed under the Fourier transform and the inverse Fourier transform (Griffel, 1981). This property is stated as the following.

Property 2.1 If $\phi \in S$, then $\mathcal{F}[\phi] \in S$ and $\mathcal{F}^{-1}[\phi] \in S$.

2.3.3 Generalized Fourier Transform in S^*

Now, we consider the dual space S^* of S . The generalized function space S^* consists of all slow growth functions, that is, function $\phi^* \in S^*$ if it is locally integrable and there exists some n such that $\phi^*(z) = o(z^n)$ as $|z| \rightarrow \infty$.

For generalized function $\phi^* \in S^*$, the generalized Fourier transform and generalized inverse Fourier transform are defined respectively as follows:

$$\langle \mathcal{F}[\phi^*], \phi \rangle = \langle \phi^*, \mathcal{F}[\phi] \rangle \quad \text{for any } \phi \in S, \quad (2.18)$$

and

$$\langle \mathcal{F}^{-1}[\phi^*], \phi \rangle = \langle \phi^*, \mathcal{F}^{-1}[\phi] \rangle \quad \text{for any } \phi \in S, \quad (2.19)$$

where $\langle f, \phi \rangle$ denotes the action of the generalized function $f \in S^*$ on the test function $\phi \in S$. The properties (2.15) and (2.16) also hold for generalized Fourier transform on S^* . Similarly, the space S^* is also closed under the generalized Fourier

t

s

d

2

3

r

I

2

k

s

f

3

6

transform and the generalized inverse Fourier transform (Griffel, 1981), which is stated as the following property.

Property 2.2 If $\phi^* \in S^*$, then $\mathcal{F}[\phi^*] \in S^*$ and $\mathcal{F}^{-1}[\phi^*] \in S^*$.

According to the Property 2.1 and Property 2.2, one has the following Theorem.

Theorem 2.3 If $\phi_n^*, \phi_0^* \in S^*$ and $\phi_n^* \rightarrow \phi_0^*$ as $n \rightarrow \infty$, then $\mathcal{F}[\phi_n^*] \rightarrow \mathcal{F}[\phi_0^*]$ and $\mathcal{F}^{-1}[\phi_n^*] \rightarrow \mathcal{F}^{-1}[\phi_0^*]$ as $n \rightarrow \infty$.

Proof. Assume $\phi_n^* \rightarrow \phi_0^*$ as $n \rightarrow \infty$. By the definition of convergence of generalized function, for any $\phi \in S$ one has $\langle \phi_n^*, \phi \rangle \rightarrow \langle \phi_0^*, \phi \rangle$ as $n \rightarrow \infty$. Since $\tilde{\phi} = \mathcal{F}[\phi]$ also belongs to S by Property 2.1, one has $\langle \phi_n^*, \tilde{\phi} \rangle \rightarrow \langle \phi_0^*, \tilde{\phi} \rangle$ as $n \rightarrow \infty$. So,

$$\langle \mathcal{F}[\phi_n^*], \phi \rangle = \langle \phi_n^*, \tilde{\phi} \rangle \rightarrow \langle \phi_0^*, \tilde{\phi} \rangle = \langle \mathcal{F}[\phi_0^*], \phi \rangle \quad \text{as } n \rightarrow \infty.$$

This shows that $\mathcal{F}[\phi_n^*] \rightarrow \mathcal{F}[\phi_0^*]$ as $n \rightarrow \infty$. Similarly, one can show $\mathcal{F}^{-1}[\phi_n^*] \rightarrow \mathcal{F}^{-1}[\phi_0^*]$ as $n \rightarrow \infty$. This finishes the proof of the theorem.

The theorem 2.3 is useful for studying the mechanical behavior on the boundary. Particularly, we will use this theorem to discuss the distributions of stress, strain, and displacement on the fiber-matrix interface associated with phase transformation, which is the main topic of this dissertation.

For later use, let us look at some examples of generalized Fourier transform on generalized functions.

Example 1 For Dirac-delta function, $\delta(z)$, one has $\mathcal{F}[\delta] = 1$. This is because of that

$$\langle \mathcal{F}[\delta], \phi \rangle = \langle \delta, \tilde{\phi} \rangle = \tilde{\phi}(0) = \int_{-\infty}^{\infty} \phi(z) dz = \langle 1, \phi \rangle \quad \forall \phi \in S.$$

Example 2 $\mathcal{F}[\delta(z - a)] = e^{ia\eta}$. This is because $\forall \phi \in S$, one has

$$\langle \mathcal{F}[\delta(z - a)], \phi \rangle = \langle \delta(z - a), \tilde{\phi} \rangle = \tilde{\phi}(a) = \int_{-\infty}^{\infty} \phi(z) e^{iaz} dz = \langle e^{ia\eta}, \phi \rangle.$$

Example 3 For the square-impulse function defined by

$$\gamma^* = \gamma^*(z) \equiv \begin{cases} \gamma^T & |z| \leq L, \\ 0 & |z| > L, \end{cases} \quad (2.20)$$

one has

$$\tilde{\gamma}^* = \tilde{\gamma}^*(\eta) = \frac{2\gamma^T}{\eta} \sin(L\eta). \quad (2.21)$$

Since function γ^* can be expressed in terms of the step functions H as

$$\gamma^* = \gamma^T [H(z + L) - H(z - L)],$$

one has

$$(\gamma^*)' = \gamma^T [\delta(z + L) - \delta(z - L)].$$

Applying Fourier transform and keep in mind (2.16) and example 2, one arrives at

$$-i\eta\tilde{\gamma}^* = \gamma^T [e^{-iL\eta} - e^{iL\eta}].$$

So, one has

$$\tilde{\gamma}^* = \gamma^T \frac{e^{-iL\eta} - e^{iL\eta}}{-i\eta} = \frac{2\gamma^T}{\eta} \sin(L\eta).$$

Example 4 For the piecewise-linear function defined by

$$u^* = u^*(z) \equiv \begin{cases} \gamma^T L & z > L, \\ \gamma^T z & |z| \leq L, \\ -\gamma^T L & z < -L. \end{cases} \quad (2.22)$$

one has

$$\tilde{u}^* = \tilde{u}^*(\eta) = i \frac{2\gamma^T}{\eta^2} \sin(L\eta). \quad (2.23)$$

This is because of the relation $(u^*)' = \gamma^*$. Using (2.16), one has

$$-i\eta\tilde{u}^* = \tilde{\gamma}^*.$$

Substituting (2.21) into above and dividing both sides of above by $-i\eta$, one arrives at (2.23).

2.4 Basic Equations in the Transformed Domain

Now, applying the Fourier transform with respect to z to (2.9) and using (2.16), one has the Fourier transformed stresses:

$$\begin{aligned}\bar{\sigma}_{rr}(r; \eta) &= -i\eta \left[\nu \tilde{\nabla}^2 \tilde{\Phi} - \frac{d^2 \tilde{\Phi}}{dr^2} \right], \\ \bar{\sigma}_{\theta\theta}(r; \eta) &= -i\eta \left[\nu \tilde{\nabla}^2 \tilde{\Phi} - \frac{1}{r} \frac{d\tilde{\Phi}}{dr} \right], \\ \bar{\sigma}_{zz}(r; \eta) &= -i\eta \left[(2 - \nu) \tilde{\nabla}^2 \tilde{\Phi} + \eta^2 \tilde{\Phi} \right], \\ \bar{\sigma}_{rz}(r; \eta) &= \frac{d}{dr} \left[(1 - \nu) \tilde{\nabla}^2 \tilde{\Phi} + \eta^2 \tilde{\Phi} \right] \quad \text{on } \tilde{\Omega},\end{aligned}\tag{2.24}$$

where $\tilde{\Phi} = \tilde{\Phi}(r; \eta) = \mathcal{F}[\Phi]$ is the Fourier transform of Φ and $\tilde{\Omega} = \{(r; \eta)\}$ is the Fourier transformed domain of Ω . The symbol $\tilde{\nabla}^2$ denotes the corresponding axisymmetric Laplacian operator after the Fourier transform:

$$\tilde{\nabla}^2 = \frac{d^2}{dr^2} + \frac{1}{r} \frac{d}{dr} - \eta^2.\tag{2.25}$$

Similarly, applying Fourier transform with respect to z to (2.11) and (2.12) with the aid of (2.16), one finds the corresponding Fourier transformed strains in terms of $\tilde{\Phi}$:

$$\begin{aligned}\tilde{\gamma}_{rr}(r; \eta) &= i \frac{1 + \nu}{E} \eta \frac{d^2 \tilde{\Phi}}{dr^2}, \\ \tilde{\gamma}_{\theta\theta}(r; \eta) &= i \frac{1 + \nu}{E} \eta \frac{d\tilde{\Phi}}{r dr}, \\ \tilde{\gamma}_{zz}(r; \eta) &= -i \frac{1 + \nu}{E} \eta \left[2(1 - \nu) \tilde{\nabla}^2 \tilde{\Phi} + \eta^2 \tilde{\Phi} \right], \\ \tilde{\gamma}_{rz}(r; \eta) &= \frac{1 + \nu}{E} \frac{d}{dr} \left[(1 - \nu) \tilde{\nabla}^2 \tilde{\Phi} + \eta^2 \tilde{\Phi} \right] \quad \text{on } \tilde{\Omega},\end{aligned}\tag{2.26}$$

and the corresponding Fourier transformed displacements in terms of $\tilde{\Phi}$:

$$\tilde{u}_r(r; \eta) = i \frac{1 + \nu}{E} \eta \frac{d\tilde{\Phi}}{dr},$$

$$\tilde{u}_z(r; \eta) = \frac{1 + \nu}{E} \left[2(1 - \nu) \tilde{\nabla}^2 \tilde{\Phi} + \eta^2 \tilde{\Phi} \right] \quad \text{on } \tilde{\Omega}. \quad (2.27)$$

Applying the Fourier transform with respect to z to (2.10), one arrives at the biharmonic equation in the transformed domain:

$$\tilde{\nabla}^2 \tilde{\nabla}^2 \tilde{\Phi} = 0 \quad \text{on } \tilde{\Omega}. \quad (2.28)$$

It is worthy to notice that by applying Fourier transform with respect to z , the PDE (2.10) transforms to ODE (2.28). By solving for $\tilde{\Phi}$ from the ODE (2.28), one can obtain the Fourier transformed stresses, strains, and displacements from (2.24), (2.26), and (2.27), respectively.

2.5 General Solutions in the Transformed Domain

Solving (2.28), one has the general solution to the Fourier transformed Love's stress function

$$\begin{aligned} \tilde{\Phi}(r; \eta) = & A_1(\eta) K_0(|\eta|r) + B_1(\eta) |\eta|r K_1(|\eta|r) \\ & + A_2(\eta) I_0(|\eta|r) + B_2(\eta) |\eta|r I_1(|\eta|r) \quad \text{on } \tilde{\Omega}, \end{aligned} \quad (2.29)$$

where $A_1(\eta)$, $B_1(\eta)$, $A_2(\eta)$, and $B_2(\eta)$ are unknown functions. And K_0 and K_1 are the modified Bessel's functions of the second kind of zero and one order, while I_0 and I_1 are the modified Bessel's functions of the first kind of zero and one order, respectively.

Among Bessel functions and their derivatives there exist the following recurrence relations (Bell, 1968, pp113-116)

$$\begin{aligned} K_0'(r) = -K_1(r), \quad K_1'(r) = -K_0(r) - \frac{1}{r} K_1(r), \\ I_0'(r) = I_1(r), \quad I_1'(r) = I_0(r) - \frac{1}{r} I_1(r). \end{aligned} \quad (2.30)$$

Utilizing the above recurrence relations (2.30), one finds the following expressions

for the derivatives of $\tilde{\Phi}$:

$$\begin{aligned} \frac{d\tilde{\Phi}}{dr} &= \left\{ -|\eta|K_1(|\eta|r)A_1(\eta) - \eta^2 r K_0(|\eta|r)B_1(\eta) \right. \\ &\quad \left. + |\eta|I_1(|\eta|r)A_2(\eta) + \eta^2 r I_0(|\eta|r)B_2(\eta) \right\}, \\ \frac{d^2\tilde{\Phi}}{dr^2} &= \eta^2 \left\{ \left[K_0(|\eta|r) + \frac{1}{|\eta|r} K_1(|\eta|r) \right] A_1(\eta) + \left[K_0(|\eta|r) + |\eta|r K_1(|\eta|r) \right] B_1(\eta) \right. \\ &\quad \left. + \left[I_0(|\eta|r) - \frac{1}{|\eta|r} I_1(|\eta|r) \right] A_2(\eta) + \left[I_0(|\eta|r) + |\eta|r I_1(|\eta|r) \right] B_2(\eta) \right\}, \\ \tilde{\nabla}^2 \tilde{\Phi} &= 2\eta^2 \left[-K_0(|\eta|r)B_1(\eta) + I_0(|\eta|r)B_2(\eta) \right]. \end{aligned} \quad (2.31)$$

Substituting (2.29) into (2.24) with the aid of (2.31), one finds the Fourier transformed stresses:

$$\begin{aligned} \tilde{\sigma}_{rr}(r; \eta) &= i\eta^3 \left\{ \left[K_0(|\eta|r) + \frac{1}{|\eta|r} K_1(|\eta|r) \right] A_1(\eta) \right. \\ &\quad \left. + \left[-(1 - 2\nu)K_0(|\eta|r) + |\eta|r K_1(|\eta|r) \right] B_1(\eta) \right. \\ &\quad \left. + \left[I_0(|\eta|r) - \frac{1}{|\eta|r} I_1(|\eta|r) \right] A_2(\eta) \right. \\ &\quad \left. + \left[(1 - 2\nu)I_0(|\eta|r) + |\eta|r I_1(|\eta|r) \right] B_2(\eta) \right\}, \\ \tilde{\sigma}_{\theta\theta}(r; \eta) &= i\eta^3 \left\{ -\frac{1}{|\eta|r} K_1(|\eta|r)A_1(\eta) - (1 - 2\nu)K_0(|\eta|r)B_1(\eta) \right. \\ &\quad \left. + \frac{1}{|\eta|r} I_1(|\eta|r)A_2(\eta) + (1 - 2\nu)I_0(|\eta|r)B_2(\eta) \right\}, \\ \tilde{\sigma}_{zz}(r; \eta) &= -i\eta^3 \left\{ K_0(|\eta|r)A_1(\eta) + \left[-2(2 - \nu)K_0(|\eta|r) + |\eta|r K_1(|\eta|r) \right] B_1(\eta) \right. \\ &\quad \left. + I_0(|\eta|r)A_2(\eta) + \left[2(2 - \nu)I_0(|\eta|r) + |\eta|r I_1(|\eta|r) \right] B_2(\eta) \right\}, \end{aligned}$$

$$\begin{aligned}
\bar{\sigma}_{rz}(r; \eta) = \eta^2 |\eta| \left\{ -K_1(|\eta|r) A_1(\eta) + \left[-|\eta|r K_0(|\eta|r) \right. \right. \\
+ 2(1 - \nu) K_1(|\eta|r) \left. \left. \right] B_1(\eta) + I_1(|\eta|r) A_2(\eta) \right. \\
\left. + \left[|\eta|r I_0(|\eta|r) + 2(1 - \nu) I_1(|\eta|r) \right] B_2(\eta) \right\} \quad \text{on } \tilde{\Omega}. \quad (2.32)
\end{aligned}$$

Similarly, substituting (2.29) into (2.26) and (2.27) with the aid of (2.31), one finds the Fourier transformed strains:

$$\begin{aligned}
\tilde{\gamma}_{rr}(r; \eta) = i \frac{1 + \nu}{E} \eta^3 \left\{ \left[K_0(|\eta|r) + \frac{1}{|\eta|r} K_1(|\eta|r) \right] A_1(\eta) \right. \\
+ \left[-K_0(|\eta|r) + |\eta|r K_1(|\eta|r) \right] B_1(\eta) \\
+ \left[I_0(|\eta|r) - \frac{1}{|\eta|r} I_1(|\eta|r) \right] A_2(\eta) \\
\left. + \left[I_0(|\eta|r) + |\eta|r I_1(|\eta|r) \right] B_2(\eta) \right\}, \\
\tilde{\gamma}_{\theta\theta}(r; \eta) = i \frac{1 + \nu}{E} \eta^3 \left\{ -\frac{1}{|\eta|r} K_1(|\eta|r) A_1(\eta) - K_0(|\eta|r) B_1(\eta) \right. \\
\left. + \frac{1}{|\eta|r} I_1(|\eta|r) A_2(\eta) + I_0(|\eta|r) B_2(\eta) \right\}, \\
\tilde{\gamma}_{zz}(r; \eta) = -i \frac{1 + \nu}{E} \eta^3 \left\{ K_0(|\eta|r) A_1(\eta) \right. \\
+ \left[-4(1 - \nu) K_0(|\eta|r) + |\eta|r K_1(|\eta|r) \right] B_1(\eta) + I_0(|\eta|r) A_2(\eta) \\
\left. + \left[4(1 - \nu) I_0(|\eta|r) + |\eta|r I_1(|\eta|r) \right] B_2(\eta) \right\}, \\
\tilde{\gamma}_{rz}(r; \eta) = \frac{1 + \nu}{E} \eta^2 |\eta| \left\{ -K_1(|\eta|r) A_1(\eta) + \left[-|\eta|r K_0(|\eta|r) + 2(1 - \nu) K_1(|\eta|r) \right] B_1(\eta) \right. \\
\left. + I_1(|\eta|r) A_2(\eta) + \left[|\eta|r I_0(|\eta|r) + 2(1 - \nu) I_1(|\eta|r) \right] B_2(\eta) \right\} \quad \text{on } \tilde{\Omega}, \quad (2.33)
\end{aligned}$$

and the Fourier transformed displacements:

$$\begin{aligned}\tilde{u}_r(r; \eta) &= i \frac{1+\nu}{E} \eta |\eta| \left\{ -K_1(|\eta|r) A_1(\eta) - |\eta|r K_0(|\eta|r) B_1(\eta) \right. \\ &\quad \left. + I_1(|\eta|r) A_2(\eta) + |\eta|r I_0(|\eta|r) B_2(\eta) \right\}, \\ \tilde{u}_z(r; \eta) &= \frac{1+\nu}{E} \eta^2 \left\{ K_0(|\eta|r) A_1(\eta) + \left[-4(1-\nu) K_0(|\eta|r) + |\eta|r K_1(|\eta|r) \right] B_1(\eta) \right. \\ &\quad \left. + I_0(|\eta|r) A_2(\eta) + \left[4(1-\nu) I_0(|\eta|r) + |\eta|r I_1(|\eta|r) \right] B_2(\eta) \right\} \quad \text{on } \tilde{\Omega}. \quad (2.34)\end{aligned}$$

The above equations (2.32), (2.33), and (2.34) give the general solutions to stresses, strains, and displacements. To obtain exact solutions to special problems, one can determine the unknown functions $A_1(\eta)$, $B_1(\eta)$, $A_2(\eta)$, and $B_2(\eta)$ from the corresponding boundary conditions and restriction conditions.

2.6 General Solutions in the Original Domain

Now, one can perform the inverse Fourier transform on (2.29) to obtain the Love's stress function in the original coordinates:

$$\begin{aligned}\Phi(r, z) &= \frac{1}{2\pi} \int_{-\infty}^{\infty} \left\{ A_1(\eta) K_0(|\eta|r) + B_1(\eta) |\eta|r K_1(|\eta|r) \right. \\ &\quad \left. + A_2(\eta) I_0(|\eta|r) + B_2(\eta) |\eta|r I_1(|\eta|r) \right\} e^{-i\eta z} d\eta \quad \text{on } \Omega, \quad (2.35)\end{aligned}$$

Similarly, performing the inverse Fourier transform on (2.32), (2.33), and (2.34), one obtains the stress, strain, and displacement fields in the original coordinates.

The stresses in terms of the original coordinates are

$$\sigma_{rr}(r, z) = i \frac{1}{2\pi} \int_{-\infty}^{\infty} \eta^3 \left\{ \left[K_0(|\eta|r) + \frac{1}{|\eta|r} K_1(|\eta|r) \right] A_1(\eta) \right.$$

$$\begin{aligned}
& + \left[- (1 - 2\nu)K_0(|\eta|r) + |\eta|rK_1(|\eta|r) \right] B_1(\eta) \\
& + \left[I_0(|\eta|r) - \frac{1}{|\eta|r}I_1(|\eta|r) \right] A_2(\eta) \\
& + \left[(1 - 2\nu)I_0(|\eta|r) + |\eta|rI_1(|\eta|r) \right] B_2(\eta) \Big\} e^{-i\eta z} d\eta, \\
\sigma_{\theta\theta}(r, z) &= i \frac{1}{2\pi} \int_{-\infty}^{\infty} \eta^3 \left\{ - \frac{1}{|\eta|r} K_1(|\eta|r) A_1(\eta) - (1 - 2\nu) K_0(|\eta|r) B_1(\eta) \right. \\
& \left. + \frac{1}{|\eta|r} I_1(|\eta|r) A_2(\eta) + (1 - 2\nu) I_0(|\eta|r) B_2(\eta) \right\} e^{-i\eta z} d\eta, \\
\sigma_{zz}(r, z) &= -i \frac{1}{2\pi} \int_{-\infty}^{\infty} \eta^3 \left\{ K_0(|\eta|r) A_1(\eta) + \left[- 2(2 - \nu) K_0(|\eta|r) \right. \right. \\
& \left. \left. + |\eta|r K_1(|\eta|r) \right] B_1(\eta) + I_0(|\eta|r) A_2(\eta) \right. \\
& \left. + \left[2(2 - \nu) I_0(|\eta|r) + |\eta|r I_1(|\eta|r) \right] B_2(\eta) \right\} e^{-i\eta z} d\eta, \\
\sigma_{rz}(r, z) &= \frac{1}{2\pi} \int_{-\infty}^{\infty} \eta^2 |\eta| \left\{ - K_1(|\eta|r) A_1(\eta) + \left[- |\eta|r K_0(|\eta|r) \right. \right. \\
& \left. \left. + 2(1 - \nu) K_1(|\eta|r) \right] B_1(\eta) + I_1(|\eta|r) A_2(\eta) \right. \\
& \left. + \left[|\eta|r I_0(|\eta|r) + 2(1 - \nu) I_1(|\eta|r) \right] B_2(\eta) \right\} e^{-i\eta z} d\eta \quad \text{on } \Omega. \quad (2.36)
\end{aligned}$$

The strains in terms of the original coordinates are

$$\begin{aligned}
\gamma_{rr}(r, z) &= i \frac{1 + \nu}{2\pi E} \int_{-\infty}^{\infty} \eta^3 \left\{ \left[K_0(|\eta|r) + \frac{1}{|\eta|r} K_1(|\eta|r) \right] A_1(\eta) \right. \\
& \left. + \left[- K_0(|\eta|r) + |\eta|r K_1(|\eta|r) \right] B_1(\eta) \right. \\
& \left. + \left[I_0(|\eta|r) - \frac{1}{|\eta|r} I_1(|\eta|r) \right] A_2(\eta) \right.
\end{aligned}$$

$$\begin{aligned}
& + \left[I_0(|\eta|r) + |\eta|r I_1(|\eta|r) \right] B_2(\eta) \Big\} e^{-i\eta z} d\eta, \\
\gamma_{\theta\theta}(r, z) &= i \frac{1+\nu}{2\pi E} \int_{-\infty}^{\infty} \eta^3 \left\{ -\frac{1}{|\eta|r} K_1(|\eta|r) A_1(\eta) - K_0(|\eta|r) B_1(\eta) \right. \\
& \quad \left. + \frac{1}{|\eta|r} I_1(|\eta|r) A_2(\eta) + I_0(|\eta|r) B_2(\eta) \right\} e^{-i\eta z} d\eta, \\
\gamma_{zz}(r, z) &= -i \frac{1+\nu}{2\pi E} \int_{-\infty}^{\infty} \eta^3 \left\{ K_0(|\eta|r) A_1(\eta) \right. \\
& \quad \left. + \left[-4(1-\nu)K_0(|\eta|r) + |\eta|r K_1(|\eta|r) \right] B_1(\eta) + I_0(|\eta|r) A_2(\eta) \right. \\
& \quad \left. + \left[4(1-\nu)I_0(|\eta|r) + |\eta|r I_1(|\eta|r) \right] B_2(\eta) \right\} e^{-i\eta z} d\eta, \\
\gamma_{rz}(r, z) &= \frac{1+\nu}{2\pi E} \int_{-\infty}^{\infty} \eta^2 |\eta| \left\{ -K_1(|\eta|r) A_1(\eta) + \left[-|\eta|r K_0(|\eta|r) \right. \right. \\
& \quad \left. \left. + 2(1-\nu)K_1(|\eta|r) \right] B_1(\eta) + I_1(|\eta|r) A_2(\eta) \right. \\
& \quad \left. + \left[|\eta|r I_0(|\eta|r) + 2(1-\nu)I_1(|\eta|r) \right] B_2(\eta) \right\} e^{-i\eta z} d\eta \quad \text{on } \Omega. \tag{2.37}
\end{aligned}$$

The displacements in terms of the original coordinates are

$$\begin{aligned}
u_r(r, z) &= i \frac{1+\nu}{2\pi E} \int_{-\infty}^{\infty} \eta |\eta| \left\{ -K_1(|\eta|r) A_1(\eta) - |\eta|r K_0(|\eta|r) B_1(\eta) \right. \\
& \quad \left. + I_1(|\eta|r) A_2(\eta) + |\eta|r I_0(|\eta|r) B_2(\eta) \right\} e^{-i\eta z} d\eta, \\
u_z(r, z) &= \frac{1+\nu}{2\pi E} \int_{-\infty}^{\infty} \eta^2 \left\{ K_0(|\eta|r) A_1(\eta) + \left[-4(1-\nu)K_0(|\eta|r) \right. \right. \\
& \quad \left. \left. + |\eta|r K_1(|\eta|r) \right] B_1(\eta) + I_0(|\eta|r) A_2(\eta) \right. \\
& \quad \left. + \left[4(1-\nu)I_0(|\eta|r) + |\eta|r I_1(|\eta|r) \right] B_2(\eta) \right\} e^{-i\eta z} d\eta \quad \text{on } \Omega. \tag{2.38}
\end{aligned}$$

2.7 SMA Fiber Reinforced Composite

Let $\mathcal{R}^{(1)}$ and $\mathcal{R}^{(2)}$ be two three-dimensional regions occupied by the matrix and the fiber of a continuous fiber reinforced composite in its undeformed configuration, respectively. Throughout this paper, the superscript “(1)” indicates quantities associated with matrix and superscript “(2)” with fiber, respectively. For convenience, the general superscript is denoted by “(n)”, $n = 1$ or 2 . Assume the fiber is straight with a circular cross-section of radius a . Choose cylindrical coordinates (r, θ, z) with z -direction along the longitudinal axis of the fiber. Then, one has

$$\begin{aligned}\mathcal{R}^{(1)} &= \{(r, \theta, z) | a < r < \infty, 0 \leq \theta < 2\pi, -\infty < z < \infty\}, \\ \mathcal{R}^{(2)} &= \{(r, \theta, z) | 0 \leq r < a, 0 \leq \theta < 2\pi, -\infty < z < \infty\}.\end{aligned}\quad (2.39)$$

The interface between the fiber and the matrix is given by surface

$$\mathcal{P} = \{(r, \theta, z) | r = a, 0 \leq \theta < 2\pi, -\infty < z < \infty\}.\quad (2.40)$$

By axisymmetry, it is convenient to take the regions $\mathcal{R}^{(n)}$ as the revolution about z -axis of the following two-dimensional domains $\Omega^{(n)}$ on the half rz -plane:

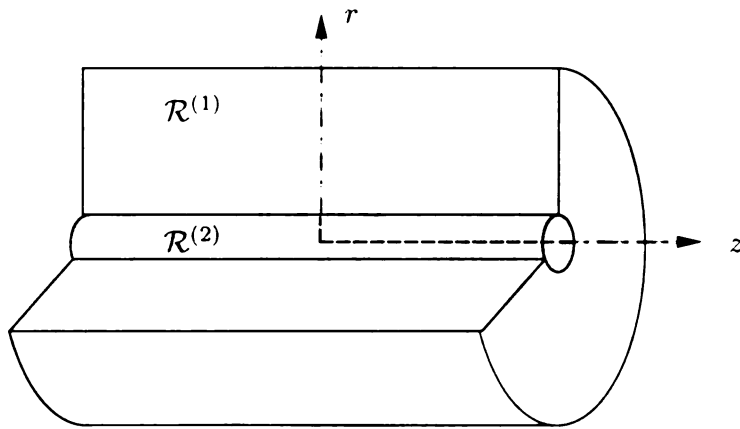
$$\begin{aligned}\Omega^{(1)} &= \{(r, z) | a < r < \infty, -\infty < z < \infty\}, \\ \Omega^{(2)} &= \{(r, z) | 0 \leq r < a, -\infty < z < \infty\},\end{aligned}\quad (2.41)$$

and the interface \mathcal{P} as the revolution about z -axis of the following straight line Π on the half rz -plane:

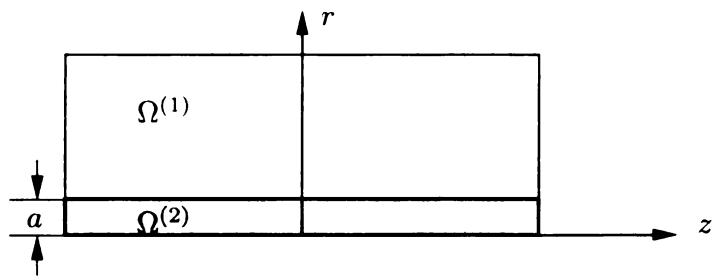
$$\Pi = \{(a, z) | -\infty < z < \infty\}.\quad (2.42)$$

The regions $\mathcal{R}^{(n)}$ and domains $\Omega^{(n)}$ are showed in Figure 2.2.

Now, assume the matrix is made of a homogeneous, isotropic, and linearly elastic material with Young's modulus $E^{(1)}$ and Poisson's ratio $\nu^{(1)}$. The fiber is capable of undergoing a displacive phase transformation along the axial direction.



(a)



(b)

Figure 2.2. The SMA fiber reinforced composite. (a) A three-dimensional plot of a straight SMA fiber ($\mathcal{R}^{(2)}$) embedded in matrix ($\mathcal{R}^{(1)}$). (b) The corresponding two-dimensional domains $\Omega^{(1)}$ and $\Omega^{(2)}$.

The transformation strain is denoted by γ^T . Within each phase, we assume the fiber is linearly elastic and isotropic with Young's modulus $E^{(2)}$ and Poisson's ratio $\nu^{(2)}$. We model the deformations associated with a SMA fiber reinforced composite with a partially transformed fiber as follows.

Assume that part of the fiber undergoes phase transformation with the constant transformation strain γ^T along z -direction. The sharp phase boundaries in the fiber are assumed perpendicular to the longitudinal axis of the fiber. The phase transformed region of the fiber is characterized by the subset Λ of z -axis such that the z coordinate of the points of transformed region belong to it. The transformation strain in the fiber is given by the (strain) phase transformation characteristic function:

$$\gamma^* = \gamma^*(z) \equiv \begin{cases} \gamma^T & z \in \Lambda, \\ 0 & z \notin \Lambda. \end{cases} \quad (2.43)$$

Since the fiber is embedded in the matrix, the fiber and the matrix interact with each other under certain bonding conditions. Elastic deformations in the matrix arise as a result of the phase transformation in the fiber, which at the same time induces additional elastic deformation in the fiber in order to maintain equilibrium at the interface. Therefore, in general, the deformation of the fiber consists of two parts: the deformation from the phase transformation and the elastic deformation imposed by the constraint of the matrix. The elastic axial normal strain in the fiber is $\gamma_{zz}^{(2)} - \gamma^*$, where $\gamma_{zz}^{(2)}$ is the total normal strain in axial direction in the fiber.

For any axisymmetrical bonding conditions between the fiber and the matrix, namely the bonding conditions are independent of the angle θ , the deformations in both the fiber and the matrix are axisymmetrical. Thus, for the composite system considered here, the strain–displacement relations are given by

$$\begin{aligned} \gamma_{rr}^{(n)} &= \frac{\partial u_r^{(n)}}{\partial r}, \quad \gamma_{\theta\theta}^{(n)} = \frac{u_r^{(n)}}{r}, \quad \gamma_{zz}^{(n)} = \frac{\partial u_z^{(n)}}{\partial z}, \\ \gamma_{rz}^{(n)} &= \frac{1}{2} \left(\frac{\partial u_r^{(n)}}{\partial z} + \frac{\partial u_z^{(n)}}{\partial r} \right) \quad \text{on } \mathcal{R}^{(n)}. \end{aligned} \quad (2.44)$$

The equilibrium equations are given by

$$\begin{aligned}\frac{\partial \sigma_{rr}^{(n)}}{\partial r} + \frac{\partial \sigma_{rz}^{(n)}}{\partial z} + \frac{\sigma_{rr}^{(n)} - \sigma_{\theta\theta}^{(n)}}{r} &= 0, \\ \frac{\partial \sigma_{rz}^{(n)}}{\partial r} + \frac{\partial \sigma_{zz}^{(n)}}{\partial z} + \frac{\sigma_{rz}^{(n)}}{r} &= 0 \quad \text{on } \mathcal{R}^{(n)}.\end{aligned}\tag{2.45}$$

And the constitutive equations are, in general, given by

$$\begin{aligned}\gamma_{rr}^{(n)} &= \frac{1}{E^{(n)}} [\sigma_{rr}^{(n)} - \nu^{(n)} (\sigma_{\theta\theta}^{(n)} + \sigma_{zz}^{(n)})], \\ \gamma_{\theta\theta}^{(n)} &= \frac{1}{E^{(n)}} [\sigma_{\theta\theta}^{(n)} - \nu^{(n)} (\sigma_{rr}^{(n)} + \sigma_{zz}^{(n)})], \\ \gamma_{zz}^{(n)} &= \frac{1}{E^{(n)}} [\sigma_{zz}^{(n)} - \nu^{(n)} (\sigma_{rr}^{(n)} + \sigma_{\theta\theta}^{(n)})] + \delta_{n2} \gamma^*, \\ \gamma_{rz}^{(n)} &= \frac{1 + \nu^{(n)}}{E^{(n)}} \sigma_{rz}^{(n)} \quad \text{on } \mathcal{R}^{(n)},\end{aligned}\tag{2.46}$$

where δ_{ij} is the Kronecker delta.

In addition, in the absence of any loads at infinity and for regularity at the center of the fiber, the stresses are required to satisfy the restriction conditions

$$\sigma_{rr}^{(n)} = o(1), \quad \sigma_{\theta\theta}^{(n)} = o(1), \quad \sigma_{zz}^{(n)} = o(1), \quad \sigma_{rz}^{(n)} = o(1) \quad \text{as } r^2 + z^2 \rightarrow \infty, \tag{2.47}$$

and

$$\sigma_{rr}^{(2)} = O(1), \quad \sigma_{\theta\theta}^{(2)} = O(1), \quad \sigma_{zz}^{(2)} = O(1), \quad \sigma_{rz}^{(2)} = O(1) \quad \text{as } r \rightarrow 0. \tag{2.48}$$

Thus, the elastostatic problems for both fiber and matrix are axisymmetric as described in section 2.1, with restriction conditions (2.47) and (2.48). The general solutions to the elastostatic problem at hand can be obtained by using previous results in the Sections 2.2-2.6 and taking account for the restriction conditions (2.47) and (2.48).

By applying Fourier transform with respect to z and noticing Theorem 2.3, the restriction conditions (2.47) in the Fourier transformed domain become

$$\tilde{\sigma}_{rr}^{(n)} = o(1), \quad \tilde{\sigma}_{\theta\theta}^{(n)} = o(1), \quad \tilde{\sigma}_{zz}^{(n)} = o(1), \quad \tilde{\sigma}_{rz}^{(n)} = o(1) \quad \text{as } |r| \rightarrow \infty. \quad (2.49)$$

In addition, we require that the Fourier transformed stresses are bounded at the center of the fiber:

$$\tilde{\sigma}_{rr}^{(2)} = O(1), \quad \tilde{\sigma}_{\theta\theta}^{(2)} = O(1), \quad \tilde{\sigma}_{zz}^{(2)} = O(1), \quad \tilde{\sigma}_{rz}^{(2)} = O(1) \quad \text{as } r \rightarrow 0. \quad (2.50)$$

The general solutions to stresses for both fiber and matrix in the Fourier transformed domain are (2.32). Considering the restriction conditions (2.49) and (2.50) and the behavior of the Bessel functions as $r \rightarrow \infty$ and $r \rightarrow 0$, one has

$$A_2^{(1)}(\eta) = B_2^{(1)}(\eta) = A_1^{(2)}(\eta) = B_1^{(2)}(\eta) \equiv 0, \quad -\infty < \eta < \infty. \quad (2.51)$$

Using (2.29), the general solutions to the Fourier transformed Love's stress functions for fiber and matrix are

$$\tilde{\Phi}^{(n)}(r; \eta) = A^{(n)}(\eta)R_0^{(n)}(|\eta|r) + B^{(n)}(\eta)|\eta|rR_1^{(n)}(|\eta|r) \quad \text{on } \tilde{\Omega}^{(n)}, \quad (2.52)$$

where

$$\begin{aligned} \tilde{\Omega}^{(1)} &= \{(r; \eta) | a < r < \infty, -\infty < \eta < \infty\}, \\ \tilde{\Omega}^{(2)} &= \{(r; \eta) | 0 \leq r < a, -\infty < \eta < \infty\}. \end{aligned} \quad (2.53)$$

The modified Bessel's functions of the second and the first kinds are redenoted as

$$R_0^{(1)} = K_0, \quad R_1^{(1)} = K_1 \quad (2.54)$$

and

$$R_0^{(2)} = I_0, \quad R_1^{(2)} = I_1, \quad (2.55)$$

respectively; while unknown functions are denoted as

$$A^{(1)}(\eta) = A_1^{(1)}(\eta), \quad B^{(1)}(\eta) = B_1^{(1)}(\eta) \quad (2.56)$$

and

$$A^{(2)}(\eta) = A_2^{(2)}(\eta), \quad B^{(2)}(\eta) = B_2^{(2)}(\eta), \quad (2.57)$$

respectively.

By using (2.32), the Fourier transformed stresses for fiber and matrix are

$$\begin{aligned} \tilde{\sigma}_{rr}^{(n)}(r; \eta) &= i\eta^3 \left\{ \left[R_0^{(n)}(|\eta|r) - \frac{(-1)^n}{|\eta|r} R_1^{(n)}(|\eta|r) \right] A^{(n)}(\eta) \right. \\ &\quad \left. + \left[(-1)^n (1 - 2\nu^{(n)}) R_0^{(n)}(|\eta|r) + |\eta|r R_1^{(n)}(|\eta|r) \right] B^{(n)}(\eta) \right\}, \\ \tilde{\sigma}_{\theta\theta}^{(n)}(r; \eta) &= i(-1)^n \eta^3 \left\{ \frac{1}{|\eta|r} R_1^{(n)}(|\eta|r) A^{(n)}(\eta) + (1 - 2\nu^{(n)}) R_0^{(n)}(|\eta|r) B^{(n)}(\eta) \right\}, \\ \tilde{\sigma}_{zz}^{(n)}(r; \eta) &= -i\eta^3 \left\{ R_0^{(n)}(|\eta|r) A^{(n)}(\eta) \right. \\ &\quad \left. + \left[(-1)^n 2(2 - \nu^{(n)}) R_0^{(n)}(|\eta|r) + |\eta|r R_1^{(n)}(|\eta|r) \right] B^{(n)}(\eta) \right\}, \\ \tilde{\sigma}_{rz}^{(n)}(r; \eta) &= \eta^2 |\eta| \left\{ (-1)^n R_1^{(n)}(|\eta|r) A^{(n)}(\eta) + \left[(-1)^n |\eta|r R_0^{(n)}(|\eta|r) \right. \right. \\ &\quad \left. \left. + 2(1 - \nu^{(n)}) R_1^{(n)}(|\eta|r) \right] B^{(n)}(\eta) \right\} \quad \text{on } \tilde{\Omega}^{(n)}. \end{aligned} \quad (2.58)$$

Using (2.33), the Fourier transformed strains for fiber and matrix are

$$\begin{aligned} \tilde{\gamma}_{rr}^{(n)}(r; \eta) &= i \frac{1 + \nu^{(n)}}{E^{(n)}} \eta^3 \left\{ \left[R_0^{(n)}(|\eta|r) - \frac{(-1)^n}{|\eta|r} R_1^{(n)}(|\eta|r) \right] A^{(n)}(\eta) \right. \\ &\quad \left. + \left[(-1)^n R_0^{(n)}(|\eta|r) + |\eta|r R_1^{(n)}(|\eta|r) \right] B^{(n)}(\eta) \right\}, \\ \tilde{\gamma}_{\theta\theta}^{(n)}(r; \eta) &= i(-1)^n \frac{1 + \nu^{(n)}}{E^{(n)}} \eta^3 \left\{ \frac{1}{|\eta|r} R_1^{(n)}(|\eta|r) A^{(n)}(\eta) + R_0^{(n)}(|\eta|r) B^{(n)}(\eta) \right\}, \end{aligned}$$

$$\begin{aligned}
\tilde{\gamma}_{zz}^{(n)}(r; \eta) &= -i \frac{1 + \nu^{(n)}}{E^{(n)}} \eta^3 \left\{ R_0^{(n)}(|\eta|r) A^{(n)}(\eta) + \left[(-1)^n 4(1 - \nu^{(n)}) R_0^{(n)}(|\eta|r) \right. \right. \\
&\quad \left. \left. + |\eta|r R_1^{(n)}(|\eta|r) \right] B^{(n)}(\eta) \right\} + \delta_{i2} \tilde{\gamma}^*(\eta), \\
\tilde{\gamma}_{rz}^{(n)}(r; \eta) &= \frac{1 + \nu^{(n)}}{E^{(n)}} \eta^2 |\eta| \left\{ (-1)^n R_1^{(n)}(|\eta|r) A^{(n)}(\eta) + \left[(-1)^n |\eta|r R_0^{(n)}(|\eta|r) \right. \right. \\
&\quad \left. \left. + 2(1 - \nu^{(n)}) R_1^{(n)}(|\eta|r) \right] B^{(n)}(\eta) \right\} \quad \text{on } \tilde{\Omega}^{(n)}. \tag{2.59}
\end{aligned}$$

Using (2.34), the Fourier transformed displacements for fiber and matrix are

$$\begin{aligned}
\tilde{u}_r^{(n)}(r; \eta) &= i(-1)^n \frac{1 + \nu^{(n)}}{E^{(n)}} \eta |\eta| \left\{ R_1^{(n)}(|\eta|r) A^{(n)}(\eta) + |\eta|r R_0^{(n)}(|\eta|r) B^{(n)}(\eta) \right\}, \\
\tilde{u}_z^{(n)}(r; \eta) &= \frac{1 + \nu^{(n)}}{E^{(n)}} \eta^2 \left\{ R_0^{(n)}(|\eta|r) A^{(n)}(\eta) + \left[(-1)^n 4(1 - \nu^{(n)}) R_0^{(n)}(|\eta|r) \right. \right. \\
&\quad \left. \left. + |\eta|r R_1^{(n)}(|\eta|r) \right] B^{(n)}(\eta) \right\} + i \delta_{i2} \frac{1}{\eta} \tilde{\gamma}^*(\eta) \quad \text{on } \tilde{\Omega}^{(n)}. \tag{2.60}
\end{aligned}$$

Performing the inverse Fourier transform on (2.52), or directly using (2.35) and considering (2.51), one obtains the Love's stress functions for the fiber and matrix in the original coordinates

$$\Phi^{(n)}(r, z) = \frac{1}{2\pi} \int_{-\infty}^{\infty} \left\{ A^{(n)}(\eta) R_0^{(n)}(|\eta|r) + B^{(n)}(\eta) |\eta|r R_1^{(n)}(|\eta|r) \right\} e^{-i\eta z} d\eta \quad \text{on } \Omega^{(n)}. \tag{2.61}$$

Similarly, one has the stress, strain, and displacement fields in the original coordinates for fiber and matrix. The stresses are

$$\begin{aligned}
\sigma_{rr}^{(n)}(r, z) &= i \frac{1}{2\pi} \int_{-\infty}^{\infty} \eta^3 \left\{ \left[R_0^{(n)}(|\eta|r) - \frac{(-1)^n}{|\eta|r} R_1^{(n)}(|\eta|r) \right] A^{(n)}(\eta) \right. \\
&\quad \left. + \left[(-1)^n (1 - 2\nu^{(n)}) R_0^{(n)}(|\eta|r) + |\eta|r R_1^{(n)}(|\eta|r) \right] B^{(n)}(\eta) \right\} e^{-i\eta z} d\eta,
\end{aligned}$$

$$\begin{aligned}
\sigma_{\theta\theta}^{(n)}(r, z) &= i \frac{(-1)^n}{2\pi} \int_{-\infty}^{\infty} \eta^3 \left\{ \frac{1}{|\eta|r} R_1^{(n)}(|\eta|r) A^{(n)}(\eta) \right. \\
&\quad \left. + (1 - 2\nu^{(n)}) R_0^{(n)}(|\eta|r) B^{(n)}(\eta) \right\} e^{-i\eta z} d\eta, \\
\sigma_{zz}^{(n)}(r, z) &= -i \frac{1}{2\pi} \int_{-\infty}^{\infty} \eta^3 \left\{ R_0^{(n)}(|\eta|r) A^{(n)}(\eta) \right. \\
&\quad \left. + [(-1)^n 2(2 - \nu^{(n)}) R_0^{(n)}(|\eta|r) + |\eta|r R_1^{(n)}(|\eta|r)] B^{(n)}(\eta) \right\} e^{-i\eta z} d\eta, \\
\sigma_{rz}^{(n)}(r, z) &= \frac{1}{2\pi} \int_{-\infty}^{\infty} \eta^2 |\eta| \left\{ (-1)^n R_1^{(n)}(|\eta|r) A^{(n)}(\eta) + [(-1)^n |\eta|r R_0^{(n)}(|\eta|r) \right. \\
&\quad \left. + 2(1 - \nu^{(n)}) R_1^{(n)}(|\eta|r)] B^{(n)}(\eta) \right\} e^{-i\eta z} d\eta \quad \text{on } \Omega^{(n)}. \tag{2.62}
\end{aligned}$$

The strains are

$$\begin{aligned}
\gamma_{rr}^{(n)}(r, z) &= i \frac{1 + \nu^{(n)}}{2\pi E^{(n)}} \int_{-\infty}^{\infty} \eta^3 \left\{ \left[R_0^{(n)}(|\eta|r) - \frac{(-1)^n}{|\eta|r} R_1^{(n)}(|\eta|r) \right] A^{(n)}(\eta) \right. \\
&\quad \left. + [(-1)^n R_0^{(n)}(|\eta|r) + |\eta|r R_1^{(n)}(|\eta|r)] B^{(n)}(\eta) \right\} e^{-i\eta z} d\eta, \\
\gamma_{\theta\theta}^{(n)}(r, z) &= i (-1)^n \frac{1 + \nu^{(n)}}{2\pi E^{(n)}} \int_{-\infty}^{\infty} \eta^3 \left\{ \frac{1}{|\eta|r} R_1^{(n)}(|\eta|r) A^{(n)}(\eta) \right. \\
&\quad \left. + R_0^{(n)}(|\eta|r) B^{(n)}(\eta) \right\} e^{-i\eta z} d\eta, \\
\gamma_{zz}^{(n)}(r, z) &= -i \frac{1 + \nu^{(n)}}{2\pi E^{(n)}} \int_{-\infty}^{\infty} \eta^3 \left\{ R_0^{(n)}(|\eta|r) A^{(n)}(\eta) + [(-1)^n 4(1 - \nu^{(n)}) R_0^{(n)}(|\eta|r) \right. \\
&\quad \left. + |\eta|r R_1^{(n)}(|\eta|r)] B^{(n)}(\eta) \right\} e^{-i\eta z} d\eta + \delta_{i2} \gamma^*(z), \\
\gamma_{rz}^{(n)}(r, z) &= \frac{1 + \nu^{(n)}}{2\pi E^{(n)}} \int_{-\infty}^{\infty} \eta^2 |\eta| \left\{ (-1)^n R_1^{(n)}(|\eta|r) A^{(n)}(\eta) + [(-1)^n |\eta|r R_0^{(n)}(|\eta|r) \right.
\end{aligned}$$

$$+2(1 - \nu^{(n)})R_1^{(n)}(|\eta|r)]B^{(n)}(\eta)\}e^{-i\eta z}d\eta \quad \text{on } \Omega^{(n)}, \quad (2.63)$$

where $\gamma^*(z)$ is the phase transformation characteristic function (2.43).

The displacements are

$$\begin{aligned} u_r^{(n)}(r, z) &= i(-1)^n \frac{1 + \nu^{(n)}}{2\pi E^{(n)}} \int_{-\infty}^{\infty} \eta|\eta| \left\{ R_1^{(n)}(|\eta|r)A^{(n)}(\eta) \right. \\ &\quad \left. + |\eta|rR_0^{(n)}(|\eta|r)B^{(n)}(\eta) \right\} e^{-i\eta z} d\eta, \\ u_z^{(n)}(r, z) &= \frac{1 + \nu^{(n)}}{2\pi E^{(n)}} \int_{-\infty}^{\infty} \eta^2 \left\{ R_0^{(n)}(|\eta|r)A^{(n)}(\eta) + \left[(-1)^n 4(1 - \nu^{(n)})R_0^{(n)}(|\eta|r) \right. \right. \\ &\quad \left. \left. + |\eta|rR_1^{(n)}(|\eta|r) \right] B^{(n)}(\eta) \right\} e^{-i\eta z} d\eta + \delta_{i2}u^*(z) \quad \text{on } \Omega^{(n)}, \end{aligned} \quad (2.64)$$

where $u^*(z)$ is the displacement phase transformation characteristic function given by

$$u^*(z) = \int_{z_0}^z \gamma^*(s) ds. \quad (2.65)$$

2.8 Single Finite Segment Transformation and Normalization

For composites, the interaction between their constituents plays a important role in determining the mechanical properties. Therefore, the local behavior near the interface between their constituents is of great interest. As for SMA fiber reinforced composites associated with phase transformation, the local behavior near the intersection between fiber-matrix interface and phase boundary in the fiber is crucial. In order to study this local behavior, a model including only one single finite segment undergoing phase transformation is fundamental, i.e., $\Lambda = [-L, L]$, (see figure 2.3). This model is not only simple but also practical. In the setting of linear elastic deformation, it gives all the information for general transformation

pattern of fiber by superposition principle. For this sake, attention is paid to the case that only one single finite segment of length $2L$ of the fiber undergoes phase transformation along z -direction. After the phase transformation, the length of this segment becomes $2L(1 + \gamma^T)$. The (strain) phase transformation characteristic function in this case is

$$\gamma^* = \gamma^*(z) \equiv \begin{cases} \gamma^T & |z| \leq L, \\ 0 & |z| > L. \end{cases} \quad (2.66)$$

(See Figure 2.4(a)). The displacement phase transformation characteristic function u^* given by piecewise linear function

$$u^* = u^*(z) \equiv \begin{cases} \gamma^T L & z > L, \\ \gamma^T z & |z| \leq L, \\ -\gamma^T L & z < -L, \end{cases} \quad (2.67)$$

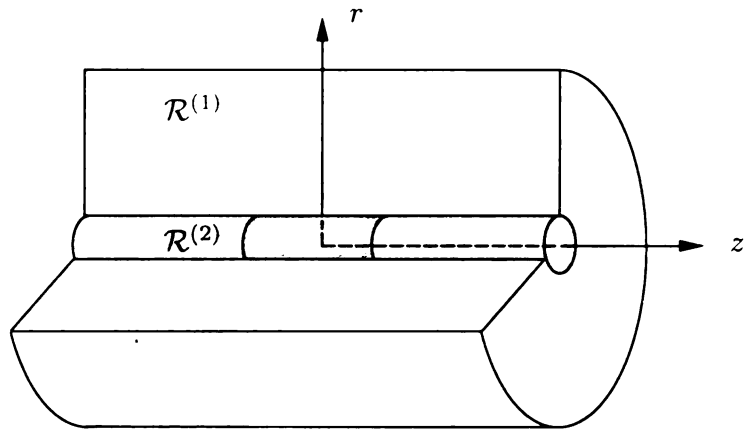
(See Figure 2.4 (b)).

The general solutions are given by (2.61), (2.62), (2.63), and (2.64), with γ^* given by (2.66) and u^* given by (2.67).

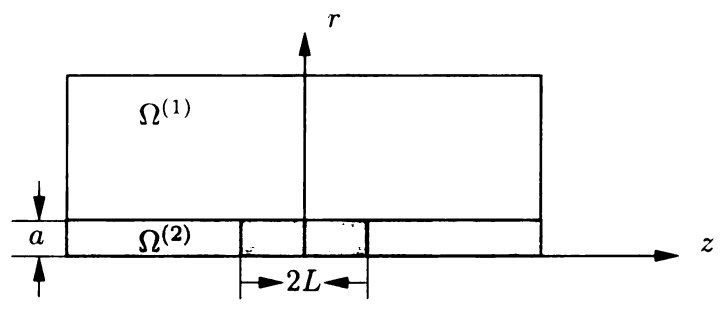
The mechanical responses of the composite to the phase transformation of the MSA fiber depend not only on the material properties and the geometry of the matrix and the fiber, but also on the geometry of the transformed region of the fiber. To investigate the effect of the geometry of the transformed region of the fiber, we introduce the dimensionless normalized coordinates (\bar{r}, \bar{z}) and normalized variable of the Fourier transformed domain $\bar{\eta}$ as follow

$$\bar{r} = \frac{r}{a}, \quad \bar{z} = \frac{z}{L}, \quad \bar{\eta} = a\eta. \quad (2.68)$$

To describe the geometry of the transformed region of the fiber, we introduce the aspect ratio α , which is defined by the ratio of the length ($2L$) of phased transformed portion of the fiber to the fiber diameter ($2a$)

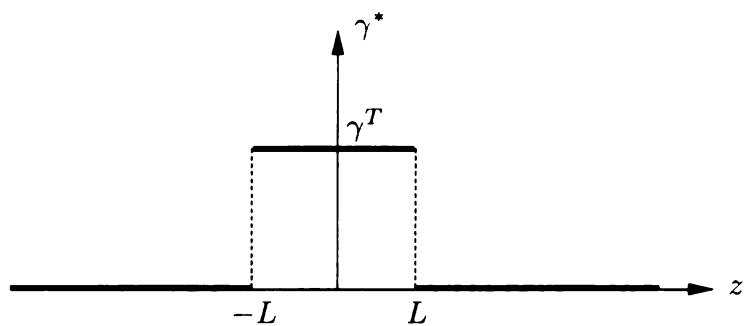


(a)

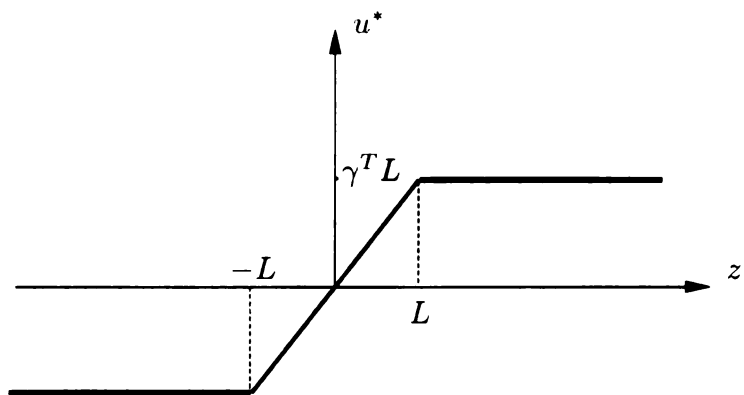


(b)

Figure 2.3. The SMA fiber reinforced composite with a fiber of which a single finite segment of length $2L$ undergoes phase transformation. (a) A three-dimensional plot of regions $\mathcal{R}^{(1)}$ and $\mathcal{R}^{(2)}$. (b) The corresponding two-dimensional domains $\Omega^{(1)}$ and $\Omega^{(2)}$.



(a)



(b)

Figure 2.4. A fiber with a single finite segment of length $2L$ undergoing phase transformation. (a) The phase transformation characteristic function. (b) The displacement phase transformation characteristic function.

$$\alpha = \frac{L}{a}. \quad (2.69)$$

For a function $f(r, z)$, we use the notation \bar{f} to express the change of variables of f from (r, z) to (\bar{r}, \bar{z}) :

$$\bar{f}(\bar{r}, \bar{z}) = f(r, z)|_{r=a\bar{r}, z=L\bar{z}}. \quad (2.70)$$

By using this notation, the Love's stress functions (2.61) can be expressed in the normalized variables as

$$\bar{\Phi}^{(n)}(\bar{r}, \bar{z}) = \frac{1}{2a\pi} \int_{-\infty}^{\infty} \left\{ \bar{A}^{(n)}(\bar{\eta}) R_0^{(n)}(|\bar{\eta}|\bar{r}) + \bar{B}^{(n)}(\bar{\eta}) |\bar{\eta}|\bar{r} R_1^{(n)}(|\bar{\eta}|\bar{r}) \right\} e^{-i\alpha\bar{\eta}\bar{z}} d\bar{\eta} \quad (2.71)$$

on $\bar{\Omega}^{(n)}$, where $\bar{A}^{(n)}$ and $\bar{B}^{(n)}$ are given by

$$\bar{A}^{(n)}(\bar{\eta}) = A^{(n)}\left(\frac{\bar{\eta}}{a}\right), \quad \bar{B}^{(n)}(\bar{\eta}) = B^{(n)}\left(\frac{\bar{\eta}}{a}\right). \quad (2.72)$$

The domains are

$$\bar{\mathcal{R}}^{(1)} = \{(\bar{r}, \bar{\theta}, \bar{z}) | 1 < \bar{r} < \infty, 0 \leq \bar{\theta} < 2\pi, -\infty < \bar{z} < \infty\},$$

$$\bar{\mathcal{R}}^{(2)} = \{(\bar{r}, \bar{\theta}, \bar{z}) | 0 \leq \bar{r} < 1, 0 \leq \bar{\theta} < 2\pi, -\infty < \bar{z} < \infty\}, \quad (2.73)$$

with $\bar{\theta} = \theta$, and

$$\bar{\Omega}^{(1)} = \{(\bar{r}, \bar{z}) | 1 < \bar{r} < \infty, -\infty < \bar{z} < \infty\},$$

$$\bar{\Omega}^{(2)} = \{(\bar{r}, \bar{z}) | 0 \leq \bar{r} < 1, -\infty < \bar{z} < \infty\}. \quad (2.74)$$

Similarly, the stress components can be expressed in the normalized variables as

$$\begin{aligned} \bar{\sigma}_{rr}^{(n)}(\bar{r}, \bar{z}) = & i \frac{1}{2\pi} \int_{-\infty}^{\infty} \frac{\bar{\eta}^3}{a^4} \left\{ \left[R_0^{(n)}(|\bar{\eta}|\bar{r}) - \frac{(-1)^n}{|\bar{\eta}|\bar{r}} R_1^{(n)}(|\bar{\eta}|\bar{r}) \right] \bar{A}^{(n)}(\bar{\eta}) \right. \\ & \left. + \left[(-1)^n (1 - 2\nu^{(n)}) R_0^{(n)}(|\bar{\eta}|\bar{r}) + |\bar{\eta}|\bar{r} R_1^{(n)}(|\bar{\eta}|\bar{r}) \right] \bar{B}^{(n)}(\bar{\eta}) \right\} e^{-i\alpha\bar{\eta}\bar{z}} d\bar{\eta}, \end{aligned}$$

$$\begin{aligned}
\bar{\sigma}_{\theta\theta}^{(n)}(\bar{r}, \bar{z}) &= i \frac{(-1)^n}{2\pi} \int_{-\infty}^{\infty} \frac{\bar{\eta}^3}{a^4} \left\{ \frac{1}{|\bar{\eta}|\bar{r}} R_1^{(n)}(|\bar{\eta}|\bar{r}) \bar{A}^{(n)}(\bar{\eta}) \right. \\
&\quad \left. + (1 - 2\nu^{(n)}) R_0^{(n)}(|\bar{\eta}|\bar{r}) \bar{B}^{(n)}(\bar{\eta}) \right\} e^{-i\alpha\bar{\eta}\bar{z}} d\bar{\eta}, \\
\bar{\sigma}_{zz}^{(n)}(\bar{r}, \bar{z}) &= -i \frac{1}{2\pi} \int_{-\infty}^{\infty} \frac{\bar{\eta}^3}{a^4} \left\{ R_0^{(n)}(|\bar{\eta}|\bar{r}) \bar{A}^{(n)}(\bar{\eta}) \right. \\
&\quad \left. + \left[(-1)^n 2(2 - \nu^{(n)}) R_0^{(n)}(|\bar{\eta}|\bar{r}) + |\bar{\eta}|\bar{r} R_1^{(n)}(|\bar{\eta}|\bar{r}) \right] \bar{B}^{(n)}(\bar{\eta}) \right\} e^{-i\alpha\bar{\eta}\bar{z}} d\bar{\eta}, \\
\bar{\sigma}_{rz}^{(n)}(\bar{r}, \bar{z}) &= \frac{1}{2\pi} \int_{-\infty}^{\infty} \frac{\bar{\eta}^2 |\bar{\eta}|}{a^4} \left\{ (-1)^n R_1^{(n)}(|\bar{\eta}|\bar{r}) \bar{A}^{(n)}(\bar{\eta}) + \left[(-1)^n |\bar{\eta}|\bar{r} R_0^{(n)}(|\bar{\eta}|\bar{r}) \right. \right. \\
&\quad \left. \left. + 2(1 - \nu^{(n)}) R_1^{(n)}(|\bar{\eta}|\bar{r}) \right] \bar{B}^{(n)}(\bar{\eta}) \right\} e^{-i\alpha\bar{\eta}\bar{z}} d\bar{\eta} \quad \text{on } \bar{\Omega}^{(n)}. \quad (2.75)
\end{aligned}$$

The strain components can be written in terms of the normalized variables as

$$\begin{aligned}
\bar{\gamma}_{rr}^{(n)}(\bar{r}, \bar{z}) &= i \frac{1 + \nu^{(n)}}{2\pi E^{(n)}} \int_{-\infty}^{\infty} \frac{\bar{\eta}^3}{a^4} \left\{ \left[R_0^{(n)}(|\bar{\eta}|\bar{r}) - \frac{(-1)^n}{|\bar{\eta}|\bar{r}} R_1^{(n)}(|\bar{\eta}|\bar{r}) \right] \bar{A}^{(n)}(\bar{\eta}) \right. \\
&\quad \left. + \left[(-1)^n R_0^{(n)}(|\bar{\eta}|\bar{r}) + |\bar{\eta}|\bar{r} R_1^{(n)}(|\bar{\eta}|\bar{r}) \right] \bar{B}^{(n)}(\bar{\eta}) \right\} e^{-i\alpha\bar{\eta}\bar{z}} d\bar{\eta}, \\
\bar{\gamma}_{\theta\theta}^{(n)}(\bar{r}, \bar{z}) &= i(-1)^n \frac{1 + \nu^{(n)}}{2\pi E^{(n)}} \int_{-\infty}^{\infty} \frac{\bar{\eta}^3}{a^4} \left\{ \frac{1}{|\bar{\eta}|\bar{r}} R_1^{(n)}(|\bar{\eta}|\bar{r}) \bar{A}^{(n)}(\bar{\eta}) \right. \\
&\quad \left. + R_0^{(n)}(|\bar{\eta}|\bar{r}) \bar{B}^{(n)}(\bar{\eta}) \right\} e^{-i\alpha\bar{\eta}\bar{z}} d\bar{\eta}, \\
\bar{\gamma}_{zz}^{(n)}(\bar{r}, \bar{z}) &= -i \frac{1 + \nu^{(n)}}{2\pi E^{(n)}} \int_{-\infty}^{\infty} \frac{\bar{\eta}^3}{a^4} \left\{ R_0^{(n)}(|\bar{\eta}|\bar{r}) \bar{A}^{(n)}(\bar{\eta}) + \left[(-1)^n 4(1 - \nu^{(n)}) R_0^{(n)}(|\bar{\eta}|\bar{r}) \right. \right. \\
&\quad \left. \left. + |\bar{\eta}|\bar{r} R_1^{(n)}(|\bar{\eta}|\bar{r}) \right] \bar{B}^{(n)}(\bar{\eta}) \right\} e^{-i\alpha\bar{\eta}\bar{z}} d\bar{\eta} + \delta_{i2} \bar{\gamma}^*(\bar{z}), \\
\bar{\gamma}_{rz}^{(n)}(\bar{r}, \bar{z}) &= \frac{1 + \nu^{(n)}}{2\pi E^{(n)}} \int_{-\infty}^{\infty} \frac{\bar{\eta}^2 |\bar{\eta}|}{a^4} \left\{ (-1)^n R_1^{(n)}(|\bar{\eta}|\bar{r}) \bar{A}^{(n)}(\bar{\eta}) + \left[(-1)^n |\bar{\eta}|\bar{r} R_0^{(n)}(|\bar{\eta}|\bar{r}) \right. \right.
\end{aligned}$$

$$+2(1 - \nu^{(n)})R_1^{(n)}(|\bar{\eta}|\bar{r}) \Big] \bar{B}^{(n)}(\bar{\eta}) \Big\} e^{-i\alpha\bar{\eta}\bar{z}} d\bar{\eta} \quad \text{on } \bar{\Omega}^{(n)}, \quad (2.76)$$

where

$$\bar{\gamma}^* = \bar{\gamma}^*(\bar{z}) \equiv \begin{cases} \gamma^T & |\bar{z}| \leq 1, \\ 0 & |\bar{z}| > 1. \end{cases} \quad (2.77)$$

The displacement components, in terms of \bar{r} and \bar{z} , are

$$\begin{aligned} \bar{u}_r^{(n)}(\bar{r}, \bar{z}) &= i(-1)^n \frac{1 + \nu^{(n)}}{2\pi E^{(n)}} \int_{-\infty}^{\infty} \frac{\bar{\eta}|\bar{\eta}|}{a^3} \left\{ R_1^{(n)}(|\bar{\eta}|\bar{r}) \bar{A}^{(n)}(\bar{\eta}) \right. \\ &\quad \left. + |\bar{\eta}|\bar{r} R_0^{(n)}(|\bar{\eta}|\bar{r}) \bar{B}^{(n)}(\bar{\eta}) \right\} e^{-i\alpha\bar{\eta}\bar{z}} d\bar{\eta}, \\ \bar{u}_z^{(n)}(\bar{r}, \bar{z}) &= \frac{1 + \nu^{(n)}}{2\pi E^{(n)}} \int_{-\infty}^{\infty} \frac{\bar{\eta}^2}{a^3} \left\{ R_0^{(n)}(|\bar{\eta}|\bar{r}) \bar{A}^{(n)}(\bar{\eta}) + \left[(-1)^n 4(1 - \nu^{(n)}) R_0^{(n)}(|\bar{\eta}|\bar{r}) \right. \right. \\ &\quad \left. \left. + |\bar{\eta}|\bar{r} R_1^{(n)}(|\bar{\eta}|\bar{r}) \right] \bar{B}^{(n)}(\bar{\eta}) \right\} e^{-i\alpha\bar{\eta}\bar{z}} d\bar{\eta} + \delta_{i2} \bar{u}^*(\bar{z}) \quad \text{on } \bar{\Omega}^{(n)}, \quad (2.78) \end{aligned}$$

where

$$\bar{u}^* = \bar{u}^*(z) \equiv \begin{cases} \gamma^T L & \bar{z} > 1, \\ \gamma^T L \bar{z} & |\bar{z}| \leq 1, \\ -\gamma^T L & \bar{z} < -1. \end{cases} \quad (2.79)$$

In the following chapters, we will further discuss the exact solutions for three different models. In Chapter 3, we discuss the “perfect bonding rigid fiber” model, in which the fiber and the matrix is perfectly bonded and the fiber is much stronger than the matrix so that the elastic deformation in the fiber is ignored. In Chapter 4, the “perfect bonding elastic fiber” model is studied. The fiber and the matrix is still assumed perfectly bonded but the elastic deformation in the fiber is taken into account. In Chapter 5, the “spring bonding” model is investigated, in which the perfect bonding condition is relaxed to allow for displacement discontinuity across the fiber-matrix interface. Such a displacement jump results in a shear stress with magnitude proportional to the magnitude of the displacement jump.

2.9 Asymptotic Expansions for the Modified Bessel Functions

For later use, here we present the asymptotic expansions for the modified Bessel functions of the first kinds and the second kinds.

As $\bar{\eta} \rightarrow \infty$, the modified Bessel functions have the following asymptotic expansions (Olver, 1974):

$$\begin{aligned}
 R_0^{(1)}(\bar{\eta}) &= K_0(\bar{\eta}) \sim \sqrt{\frac{\pi}{2\bar{\eta}}} e^{-\bar{\eta}} \left[1 - \frac{1}{8\bar{\eta}} + \frac{9}{128\bar{\eta}^2} - \frac{75}{1024\bar{\eta}^3} + \cdots \right], \\
 R_1^{(1)}(\bar{\eta}) &= K_1(\bar{\eta}) \sim \sqrt{\frac{\pi}{2\bar{\eta}}} e^{-\bar{\eta}} \left[1 + \frac{3}{8\bar{\eta}} - \frac{15}{128\bar{\eta}^2} + \frac{105}{1024\bar{\eta}^3} + \cdots \right], \\
 R_0^{(2)}(\bar{\eta}) &= I_0(\bar{\eta}) \sim \sqrt{\frac{1}{2\pi\bar{\eta}}} e^{\bar{\eta}} \left[1 + \frac{1}{8\bar{\eta}} + \frac{9}{128\bar{\eta}^2} + \frac{75}{1024\bar{\eta}^3} + \cdots \right], \\
 R_1^{(2)}(\bar{\eta}) &= I_1(\bar{\eta}) \sim \sqrt{\frac{1}{2\pi\bar{\eta}}} e^{\bar{\eta}} \left[1 - \frac{3}{8\bar{\eta}} - \frac{15}{128\bar{\eta}^2} - \frac{105}{1024\bar{\eta}^3} + \cdots \right],
 \end{aligned}$$

as $\bar{\eta} \rightarrow \infty$. (2.80)

For $r \neq 0$, one has the following asymptotic expansions for the modified Bessel functions as $\bar{\eta} \rightarrow \infty$:

$$\begin{aligned}
 R_0^{(1)}(\bar{\eta}r) &= K_0(\bar{\eta}r) \sim \sqrt{\frac{\pi}{2\bar{\eta}r}} e^{-\bar{\eta}r} \left[1 - \frac{1}{8\bar{\eta}r} + \frac{9}{128(\bar{\eta}r)^2} - \frac{75}{1024(\bar{\eta}r)^3} + \cdots \right], \\
 R_1^{(1)}(\bar{\eta}r) &= K_1(\bar{\eta}r) \sim \sqrt{\frac{\pi}{2\bar{\eta}r}} e^{-\bar{\eta}r} \left[1 + \frac{3}{8\bar{\eta}r} - \frac{15}{128(\bar{\eta}r)^2} + \frac{105}{1024(\bar{\eta}r)^3} + \cdots \right], \\
 R_0^{(2)}(\bar{\eta}r) &= I_0(\bar{\eta}r) \sim \sqrt{\frac{1}{2\pi\bar{\eta}r}} e^{\bar{\eta}r} \left[1 + \frac{1}{8\bar{\eta}r} + \frac{9}{128(\bar{\eta}r)^2} + \frac{75}{1024(\bar{\eta}r)^3} + \cdots \right], \\
 R_1^{(2)}(\bar{\eta}r) &= I_1(\bar{\eta}r) \sim \sqrt{\frac{1}{2\pi\bar{\eta}r}} e^{\bar{\eta}r} \left[1 - \frac{3}{8\bar{\eta}r} - \frac{15}{128(\bar{\eta}r)^2} - \frac{105}{1024(\bar{\eta}r)^3} + \cdots \right],
 \end{aligned}$$

as $\bar{\eta} \rightarrow \infty$. (2.81)

As $\bar{\eta} \rightarrow 0^+$, the asymptotic expansions for the modified Bessel functions of the first kind and the second kind are the follows have the following asymptotic expansions (Zayed, 1996):

$$R_0^{(1)}(\bar{\eta}) = K_0(\bar{\eta}) \sim -\ln\bar{\eta},$$

$$R_1^{(1)}(\bar{\eta}) = K_1(\bar{\eta}) \sim \frac{1}{\bar{\eta}},$$

$$R_0^{(2)}(\bar{\eta}) = I_0(\bar{\eta}) \sim 1,$$

$$R_1^{(2)}(\bar{\eta}) = I_1(\bar{\eta}) \sim \frac{\bar{\eta}}{2},$$

$$\text{as } \bar{\eta} \rightarrow 0^+. \tag{2.82}$$

For $\eta = 0$, the modified Bessel functions of the first kinds take the following values:

$$R_0^{(2)}(0) = I_0(0) = 1,$$

$$R_1^{(2)}(0) = I_1(0) = 0. \tag{2.83}$$

CHAPTER 3. “PERFECT BONDING RIGID FIBER” MODEL

The interaction over the interface between the different constituents associated with phase transformation in the SMA fiber is one of the most important subjects for the studies and applications of SMA fiber reinforced composites. The interaction depends not only on the mechanical properties of the constituents, but also on the bonding conditions. For analytic study, the assumption of perfect bonding between fiber and matrix describes a fundamental and the simplest bonding condition. In the case that the fiber is much stronger than the matrix, the phase transformation in the fiber exerts significant influence on the deformation of the matrix through the perfect bonding condition. However, the influence of matrix on the fiber is relative small and can be ignored. In this chapter, we focus our attention on the situation that the fiber is much stronger than the matrix and the fiber and the matrix are perfectly bonded.

3.1 Boundary Conditions

Assume that the fiber and the matrix are perfectly bonded. Also assume that after the phase transformation, the radial displacement in the fiber is negligible compared to the axial one. Due to the interaction between the fiber and the matrix, the deformation of the fiber consists of two parts: the deformation from the phase transformation and the elastic deformation imposed by the constraint of the matrix. Since the transformation strain is generally much larger than the elastic strains, the former is the dominant strain in the SMA fiber. In what follows, we will model the SMA fiber as a “rigid fiber” in the sense that after the phase transformation, the matrix exerts no effect on the fiber and the radial displacement of the fiber is ignored. The only deformation considered in the fiber is that of the phase transformation. In this setting, we only need to study the deformation of the matrix. The problem

turns out to be an axisymmetric one of a hollow cylindrical region as discussed in Chapter 2. The boundary conditions on the inter surface are expressed as

$$u_r^{(1)}(a, z) = 0, \quad u_z^{(1)}(a, z) = u^*(z), \quad (3.1)$$

where $u^*(z)$ is the displacement phase transformation characteristic function given by (2.65). The stresses satisfy the following restriction conditions at infinity:

$$\sigma_{rr}^{(1)} = o(1), \quad \sigma_{\theta\theta}^{(1)} = o(1), \quad \sigma_{zz}^{(1)} = o(1), \quad \sigma_{rz}^{(1)} = o(1) \quad \text{as } r^2 + z^2 \rightarrow \infty. \quad (3.2)$$

3.2 Exact Solutions

Because the deformation of the matrix is axisymmetric, the general solutions can be obtained from Section 2.7 in Chapter 2. Bearing in mind of the restriction conditions (3.2) and using results (2.60), one arrives at the general solutions to the displacements in the Fourier transformed space

$$\begin{aligned} \tilde{u}_r^{(1)}(r; \eta) &= -i \frac{1 + \nu^{(1)}}{E^{(1)}} \eta |\eta| \left\{ K_1^{(1)}(|\eta|r) A^{(1)}(\eta) + |\eta|r K_0^{(1)}(|\eta|r) B^{(1)}(\eta) \right\}, \\ \tilde{u}_z^{(1)}(r; \eta) &= \frac{1 + \nu^{(1)}}{E^{(1)}} \eta^2 \left\{ K_0^{(1)}(|\eta|r) A^{(1)}(\eta) + \left[-4(1 - \nu^{(1)}) K_0^{(1)}(|\eta|r) \right. \right. \\ &\quad \left. \left. + |\eta|r K_1^{(1)}(|\eta|r) \right] B^{(1)}(\eta) \right\} \quad \text{on } \tilde{\Omega}^{(1)}. \end{aligned} \quad (3.3)$$

In order to get the exact solution of the problem considered, we transform the boundary conditions (3.1) to the Fourier transformed domain. Generally, the function $u^*(z)$ in the boundary conditions belongs to S^* but is not absolutely integrable. For such functions, we use the generalized Fourier transform. Consequently, the boundary conditions (3.1) after generalized Fourier transform become

$$\tilde{u}_r^{(1)}(a; \eta) = 0, \quad \tilde{u}_z^{(1)}(a; \eta) \equiv \tilde{u}^*(\eta) = i \frac{1}{\eta} \tilde{\gamma}^*(\eta), \quad -\infty < \eta < \infty. \quad (3.4)$$

Setting $r = a$ in (3.3) and substituting them into (3.4), one arrives at the algebraic equations of the boundary conditions:

$$|\eta|K_1(|\eta|a)A^{(1)}(\eta) + \eta^2 a K_0(|\eta|a)B^{(1)}(\eta) = 0,$$

$$K_0(|\eta|a)A^{(1)}(\eta) - [4(1 - \nu^{(1)})K_0(|\eta|a) - |\eta|aK_1(|\eta|a)]B^{(1)}(\eta) = i \frac{E^{(1)}}{(1 + \nu^{(1)})\eta^3} \tilde{\gamma}^*(\eta),$$

$$-\infty < \eta < \infty. \quad (3.5)$$

Then, one can solve for the unknown functions $A^{(1)}(\eta)$ and $B^{(1)}(\eta)$ as

$$A^{(1)}(\eta) = -i \frac{E^{(1)}}{1 + \nu^{(1)}} \frac{|\eta|aK_0(|\eta|a)}{\Delta\eta^3} \tilde{\gamma}^*(\eta),$$

$$B^{(1)}(\eta) = i \frac{E^{(1)}}{1 + \nu^{(1)}} \frac{K_1(|\eta|a)}{\Delta\eta^3} \tilde{\gamma}^*(\eta),$$

$$-\infty < \eta < \infty, \quad (3.6)$$

where $\Delta = \Delta(\eta)$ is given by

$$\Delta(\eta) = -|\eta|aK_0^2(|\eta|a) - 4(1 - \nu^{(1)})K_0(|\eta|a)K_1(|\eta|a) + |\eta|aK_1^2(|\eta|a),$$

$$-\infty < \eta < \infty. \quad (3.7)$$

Substituting (3.6) into (2.52) with $n = 1$, one obtains the Fourier transformed Love's stress function for the matrix :

$$\begin{aligned} \frac{\tilde{\Phi}^{(1)}}{\tilde{\gamma}^*} = i \frac{E^{(1)}}{(1 + \nu^{(1)})} \frac{1}{\Delta\eta^3} \left\{ -|\eta|aK_0(|\eta|a)K_0(|\eta|r) \right. \\ \left. + |\eta|rK_1(|\eta|a)K_1(|\eta|r) \right\} \text{ on } \tilde{\Omega}^{(1)}. \end{aligned} \quad (3.8)$$

Likewise, substituting (3.6) into (2.58), (2.59), and (2.60) with $n = 1$, one obtains the Fourier transformed stresses, strains, and displacements for the matrix.

The Fourier transformed stresses for the matrix are

$$\frac{\tilde{\sigma}_{rr}^{(1)}}{\tilde{\gamma}^*} = \frac{E^{(1)}}{(1 + \nu^{(1)})} \frac{1}{\Delta} \left\{ \left[a|\eta|K_0(a|\eta|) + (1 - 2\nu^{(1)})K_1(a|\eta|) \right] K_0(|\eta|r) \right.$$

$$\begin{aligned}
& + \left[\frac{a}{r} K_0(a|\eta|) - |\eta|r K_1(a|\eta|) \right] K_1(|\eta|r) \Big\}, \\
\frac{\tilde{\sigma}_{\theta\theta}^{(1)}}{\tilde{\gamma}^*} &= \frac{E^{(1)}}{(1 + \nu^{(1)})} \frac{1}{\Delta} \left\{ (1 - 2\nu^{(1)}) K_1(a|\eta|) K_0(|\eta|r) \right. \\
& \left. - \frac{a}{r} K_0(a|\eta|) K_1(|\eta|r) \right\}, \\
\frac{\tilde{\sigma}_{zz}^{(1)}}{\tilde{\gamma}^*} &= \frac{E^{(1)}}{(1 + \nu^{(1)})} \frac{1}{\Delta} \left\{ \left[-a|\eta| K_0(a|\eta|) - 2(2 - \nu^{(1)}) K_1(a|\eta|) \right] K_0(|\eta|r) \right. \\
& \left. + |\eta|r K_1(a|\eta|) K_1(|\eta|r) \right\}, \\
\frac{\tilde{\sigma}_{rz}^{(1)}}{\tilde{\gamma}^*} &= i \frac{E^{(1)}}{(1 + \nu^{(1)})} \frac{\text{sign}(\eta)}{\Delta} \left\{ -|\eta|r K_1(a|\eta|) K_0(|\eta|r) + \left[a|\eta| K_0(a|\eta|) \right. \right. \\
& \left. \left. + 2(1 - \nu^{(1)}) K_1(a|\eta|) \right] K_1(|\eta|r) \right\} \quad \text{on } \tilde{\Omega}^{(1)}. \tag{3.9}
\end{aligned}$$

The Fourier transformed strains for the matrix are

$$\begin{aligned}
\frac{\tilde{\gamma}_{rr}^{(1)}}{\tilde{\gamma}^*} &= \frac{1}{\Delta} \left\{ \left[a|\eta| K_0(a|\eta|) + K_1(a|\eta|) \right] K_0(|\eta|r) \right. \\
& \left. + \left[\frac{a}{r} K_0(a|\eta|) - |\eta|r K_1(a|\eta|) \right] K_1(|\eta|r) \right\}, \\
\frac{\tilde{\gamma}_{\theta\theta}^{(1)}}{\tilde{\gamma}^*} &= \frac{1}{\Delta} \left\{ K_1(a|\eta|) K_0(|\eta|r) - \frac{a}{r} K_0(a|\eta|) K_1(|\eta|r) \right\}, \\
\frac{\tilde{\gamma}_{zz}^{(1)}}{\tilde{\gamma}^*} &= \frac{1}{\Delta} \left\{ - \left[a|\eta| K_0(a|\eta|) + 4(1 - \nu^{(1)}) K_1(a|\eta|) \right] K_0(|\eta|r) \right. \\
& \left. + |\eta|r K_1(a|\eta|) K_1(|\eta|r) \right\}, \\
\frac{\tilde{\gamma}_{rz}^{(1)}}{\tilde{\gamma}^*} &= i \frac{\text{sign}(\eta)}{\Delta} \left\{ -|\eta|r K_1(a|\eta|) K_0(|\eta|r) + \left[a|\eta| K_0(a|\eta|) \right. \right. \\
& \left. \left. + 2(1 - \nu^{(1)}) K_1(a|\eta|) \right] K_1(|\eta|r) \right\} \quad \text{on } \Omega^{(1)}. \tag{3.10}
\end{aligned}$$

The Fourier transformed displacements for the matrix are

$$\begin{aligned}\frac{\tilde{u}_r^{(1)}}{\tilde{\gamma}^*} &= \frac{1}{\Delta|\eta|} \left\{ \frac{r}{a} K_1(a|\eta|) K_0(|\eta|r) - K_0(a|\eta|) K_1(|\eta|r) \right\}, \\ \frac{\tilde{u}_z^{(1)}}{\tilde{\gamma}^*} &= -i \frac{1}{\Delta\eta} \left\{ \left[a|\eta| K_0(a|\eta|) + 4(1 - \nu^{(1)}) K_1(a|\eta|) \right] K_0(|\eta|r) \right. \\ &\quad \left. - |\eta|r K_1(a|\eta|) K_1(|\eta|r) \right\} \quad \text{on } \Omega^{(1)}.\end{aligned}\quad (3.11)$$

For fixed r , all these ratios given in (3.8), (3.9), (3.10), and (3.11) are functions of the material properties of the matrix and independent of the phase transformation in the fiber. If we consider the phase transformation in the fiber as input or excitation and the Love's stress function, stresses, strains, and displacements in the matrix as outputs or responses, these ratios give the corresponding transfer functions, respectively. Theoretically, if we know the phase transformation characteristic function of the fiber, we can find the Love's stress function and the distributions of stress, strain, displacement in the matrix through these ratios.

Multiplying these ratios (3.8), (3.9), (3.10), and (3.11) by $\tilde{\gamma}^*$ and performing inverse Fourier transform, one obtains the Love's stress function, stresses, strains, and displacements of the matrix in the original physical domain $\mathcal{R}^{(1)}$. The Love's stress function is

$$\begin{aligned}\Phi^{(1)}(r, z) &= i \frac{E^{(1)}}{2\pi(1 + \nu^{(1)})} \int_{-\infty}^{\infty} \frac{1}{\Delta\eta^3} \left\{ -|\eta| a K_0(|\eta|a) K_0(|\eta|r) \right. \\ &\quad \left. + |\eta|r K_1(|\eta|a) K_1(|\eta|r) \right\} \tilde{\gamma}^*(\eta) e^{-i\eta z} d\eta \quad \text{on } \Omega^{(1)}.\end{aligned}\quad (3.12)$$

The stresses have the following forms:

$$\begin{aligned}\sigma_{rr}^{(1)}(r, z) &= \frac{E^{(1)}}{2\pi(1 + \nu^{(1)})} \int_{-\infty}^{\infty} \frac{1}{\Delta} \left\{ \left[a|\eta| K_0(a|\eta|) + (1 - 2\nu^{(1)}) K_1(a|\eta|) \right] K_0(|\eta|r) \right. \\ &\quad \left. + \left[\frac{a}{r} K_0(a|\eta|) - |\eta|r K_1(a|\eta|) \right] K_1(|\eta|r) \right\} \tilde{\gamma}^*(\eta) e^{-i\eta z} d\eta,\end{aligned}$$

$$\begin{aligned}
\sigma_{\theta\theta}^{(1)}(r, z) &= \frac{E^{(1)}}{2\pi(1+\nu^{(1)})} \int_{-\infty}^{\infty} \frac{1}{\Delta} \left\{ (1-2\nu^{(1)})K_1(a|\eta|)K_0(|\eta|r) \right. \\
&\quad \left. - \frac{a}{r}K_0(a|\eta|)K_1(|\eta|r) \right\} \tilde{\gamma}^*(\eta)e^{-i\eta z} d\eta, \\
\sigma_{zz}^{(1)}(r, z) &= \frac{E^{(1)}}{2\pi(1+\nu^{(1)})} \int_{-\infty}^{\infty} \frac{1}{\Delta} \left\{ \left[-a|\eta|K_0(a|\eta|) - 2(2-\nu^{(1)})K_1(a|\eta|) \right] K_0(|\eta|r) \right. \\
&\quad \left. + |\eta|rK_1(a|\eta|)K_1(|\eta|r) \right\} \tilde{\gamma}^*(\eta)e^{-i\eta z} d\eta, \\
\sigma_{rz}^{(1)}(r, z) &= i \frac{E^{(1)}}{2\pi(1+\nu^{(1)})} \int_{-\infty}^{\infty} \frac{\text{sign}(\eta)}{\Delta} \left\{ -|\eta|rK_1(a|\eta|)K_0(|\eta|r) + \left[a|\eta|K_0(a|\eta|) \right. \right. \\
&\quad \left. \left. + 2(1-\nu^{(1)})K_1(a|\eta|) \right] K_1(|\eta|r) \right\} \tilde{\gamma}^*(\eta)e^{-i\eta z} d\eta \quad \text{on } \Omega^{(1)}. \quad (3.13)
\end{aligned}$$

The strain components can be written as

$$\begin{aligned}
\gamma_{rr}^{(1)}(r, z) &= \frac{1}{2\pi} \int_{-\infty}^{\infty} \frac{1}{\Delta} \left\{ \left[a|\eta|K_0(a|\eta|) + K_1(a|\eta|) \right] K_0(|\eta|r) \right. \\
&\quad \left. + \left[\frac{a}{r}K_0(a|\eta|) - |\eta|rK_1(a|\eta|) \right] K_1(|\eta|r) \right\} \tilde{\gamma}^*(\eta)e^{-i\eta z} d\eta, \\
\gamma_{\theta\theta}^{(1)}(r, z) &= \frac{1}{2\pi} \int_{-\infty}^{\infty} \frac{1}{\Delta} \left\{ K_1(a|\eta|)K_0(|\eta|r) \right. \\
&\quad \left. - \frac{a}{r}K_0(a|\eta|)K_1(|\eta|r) \right\} \tilde{\gamma}^*(\eta)e^{-i\eta z} d\eta, \\
\gamma_{zz}^{(1)}(r, z) &= \frac{1}{2\pi} \int_{-\infty}^{\infty} \frac{1}{\Delta} \left\{ - \left[a|\eta|K_0(a|\eta|) + 4(1-\nu^{(1)})K_1(a|\eta|) \right] K_0(|\eta|r) \right. \\
&\quad \left. + |\eta|rK_1(a|\eta|)K_1(|\eta|r) \right\} \tilde{\gamma}^*(\eta)e^{-i\eta z} d\eta, \\
\gamma_{rz}^{(1)}(r, z) &= i \frac{1}{2\pi} \int_{-\infty}^{\infty} \frac{\text{sign}(\eta)}{\Delta} \left\{ -|\eta|rK_1(a|\eta|)K_0(|\eta|r) + \left[a|\eta|K_0(a|\eta|) \right. \right.
\end{aligned}$$

$$+2(1 - \nu^{(1)})K_1(a|\eta|) \Big] K_1(|\eta|r) \Big\} \tilde{\gamma}^*(\eta) e^{-i\eta z} d\eta \quad \text{on } \Omega^{(1)}. \quad (3.14)$$

The displacement components are

$$\begin{aligned} u_r^{(1)}(r, z) &= \frac{1}{2\pi} \int_{-\infty}^{\infty} \frac{1}{\Delta|\eta|} \left\{ \frac{r}{a} K_1(a|\eta|) K_0(|\eta|r) \right. \\ &\quad \left. - K_0(a|\eta|) K_1(|\eta|r) \right\} \tilde{\gamma}^*(\eta) e^{-i\eta z} d\eta, \\ u_z^{(1)}(r, z) &= -i \frac{1}{2\pi} \int_{-\infty}^{\infty} \frac{1}{\Delta\eta} \left\{ [a|\eta| K_0(a|\eta|) + 4(1 - \nu^{(1)}) K_1(a|\eta|)] K_0(|\eta|r) \right. \\ &\quad \left. - |\eta|r K_1(a|\eta|) K_1(|\eta|r) \right\} \tilde{\gamma}^*(\eta) e^{-i\eta z} d\eta \quad \text{on } \Omega^{(1)}. \end{aligned} \quad (3.15)$$

Alternatively, the (3.12), (3.13), (3.14) and (3.15) can also be obtained by directly substituting (3.6) and (3.7) into (2.61), (2.62), (2.63), and (2.64) with $n = 1$.

3.3 Single Finite Segment Transformation

Now, we focus our attention on the case that only a single finite segment of length $2L$ of the fiber undergoes phase transformation. Assume the phase transformation is uniform with a constant normal transformation strain γ^T along the axial direction of the fiber. After the phase transformation, the length of this segment becomes $2L(1 + \gamma^T)$. Therefore, the displacement phase transformation characteristic function is given by (2.67):

$$u^*(z) = \begin{cases} \gamma^T L & z > L, \\ \gamma^T z & |z| \leq L, \\ -\gamma^T L & z < -L. \end{cases} \quad (3.16)$$

The (strain) phase transformation characteristic function is given by (2.66):

$$\gamma^*(z) = \begin{cases} \gamma^T & |z| \leq L, \\ 0 & |z| > L. \end{cases} \quad (3.17)$$

Applying Fourier transform on (3.17) and using the result in (2.21), one has

$$\tilde{\gamma}^* = \tilde{\gamma}^*(\eta) = \frac{2\gamma^T}{\eta} \sin(L\eta). \quad (3.18)$$

Substituting (3.18) into (3.6), the unknown functions $A^{(1)}(\eta)$ and $B^{(1)}(\eta)$ are

$$\begin{aligned} A^{(1)}(\eta) &= -i \frac{2E^{(1)}\gamma^T}{1+\nu^{(1)}} \frac{|\eta|aK_0(|\eta|a)}{\Delta\eta^4} \sin(L\eta), \\ B^{(1)}(\eta) &= i \frac{2E^{(1)}\gamma^T}{1+\nu^{(1)}} \frac{K_1(|\eta|a)}{\Delta\eta^4} \sin(L\eta), \\ &-\infty < \eta < \infty. \end{aligned} \quad (3.19)$$

For this case, it is convenient to use normalized variables defined by (2.68) and (2.69). In the normalized coordinates (\bar{r}, \bar{z}) , one has

$$\begin{aligned} \bar{A}^{(1)}(\bar{\eta}) &= A^{(1)}(\eta)|_{\eta=\bar{\eta}/a} = -i \frac{2a^4 E^{(1)}\gamma^T}{1+\nu^{(1)}} \frac{|\bar{\eta}|K_0(|\bar{\eta}|)}{\bar{\Delta}\bar{\eta}^4} \sin(\alpha\bar{\eta}), \\ \bar{B}^{(1)}(\bar{\eta}) &= B^{(1)}(\eta)|_{\eta=\bar{\eta}/a} = i \frac{2a^4 E^{(1)}\gamma^T}{1+\nu^{(1)}} \frac{K_1(|\bar{\eta}|)}{\bar{\Delta}\bar{\eta}^4} \sin(\alpha\bar{\eta}), \\ &-\infty < \bar{\eta} < \infty, \end{aligned} \quad (3.20)$$

where $\bar{\Delta} = \bar{\Delta}(\bar{\eta})$ is given by

$$\begin{aligned} \bar{\Delta}(\bar{\eta}) &= \Delta(\eta)|_{\eta=\bar{\eta}/a} = -|\bar{\eta}|K_0^2(|\bar{\eta}|) - 4(1-\nu^{(1)})K_0(|\bar{\eta}|)K_1(|\bar{\eta}|) + |\bar{\eta}|K_1^2(|\bar{\eta}|), \\ &-\infty < \bar{\eta} < \infty. \end{aligned} \quad (3.21)$$

Substituting (3.20) and (3.21) into (2.71) with $n = 1$, one obtains the Love's stress function for the matrix. Note that the imaginary part of the integrand is odd

function of $\bar{\eta}$. The Love's stress function can be written as the following forms in the normalized coordinates

$$\begin{aligned} \bar{\Phi}^{(1)}(\bar{r}, \bar{z}) = \frac{\alpha^3 E^{(1)} \gamma^T}{\pi(1 + \nu^{(1)})} \int_{-\infty}^{\infty} \frac{1}{\Delta \bar{\eta}^4} \left\{ -|\bar{\eta}| K_0(|\bar{\eta}|) K_0(|\bar{\eta}| \bar{r}) \right. \\ \left. + |\bar{\eta}| \bar{r} K_1(|\bar{\eta}|) K_1(|\bar{\eta}| \bar{r}) \right\} \sin(\alpha \bar{\eta}) \sin(\alpha \bar{z} \bar{\eta}) d\bar{\eta} \quad \text{on } \bar{\Omega}^{(1)}. \end{aligned} \quad (3.22)$$

Similarly, substituting (3.20) and (3.21) into (2.75), (2.76), and (2.78), Also noticing that the imaginary parts of the integrands are odd functions of $\bar{\eta}$, one obtains the fields of stress, strain, and displacement in the normalized coordinates.

The stresses can be written as the following forms in the normalized coordinates

$$\begin{aligned} \bar{\sigma}_{rr}^{(1)}(\bar{r}, \bar{z}) = \frac{E^{(1)} \gamma^T}{(1 + \nu^{(1)}) \pi} \int_{-\infty}^{\infty} \frac{1}{\Delta \bar{\eta}} \left\{ \left[|\bar{\eta}| K_0(|\bar{\eta}|) + (1 - 2\nu^{(1)}) K_1(|\bar{\eta}|) \right] K_0(|\bar{\eta}| \bar{r}) \right. \\ \left. + \left[\frac{1}{\bar{r}} K_0(|\bar{\eta}|) - |\bar{\eta}| \bar{r} K_1(|\bar{\eta}|) \right] K_1(|\bar{\eta}| \bar{r}) \right\} \sin(\alpha \bar{\eta}) \cos(\alpha \bar{z} \bar{\eta}) d\bar{\eta}, \\ \bar{\sigma}_{\theta\theta}^{(1)}(\bar{r}, \bar{z}) = \frac{E^{(1)} \gamma^T}{(1 + \nu^{(1)}) \pi} \int_{-\infty}^{\infty} \frac{1}{\Delta \bar{\eta}} \left\{ (1 - 2\nu^{(1)}) K_1(|\bar{\eta}|) K_0(|\bar{\eta}| \bar{r}) \right. \\ \left. - \frac{1}{\bar{r}} K_0(|\bar{\eta}|) K_1(|\bar{\eta}| \bar{r}) \right\} \sin(\alpha \bar{\eta}) \cos(\alpha \bar{z} \bar{\eta}) d\bar{\eta}, \\ \bar{\sigma}_{zz}^{(1)}(\bar{r}, \bar{z}) = \frac{E^{(1)} \gamma^T}{(1 + \nu^{(1)}) \pi} \int_{-\infty}^{\infty} \frac{1}{\Delta \bar{\eta}} \left\{ \left[-|\bar{\eta}| K_0(|\bar{\eta}|) - 2(2 - \nu^{(1)}) K_1(|\bar{\eta}|) \right] K_0(|\bar{\eta}| \bar{r}) \right. \\ \left. + |\bar{\eta}| \bar{r} K_1(|\bar{\eta}|) K_1(|\bar{\eta}| \bar{r}) \right\} \sin(\alpha \bar{\eta}) \cos(\alpha \bar{z} \bar{\eta}) d\bar{\eta}, \\ \bar{\sigma}_{rz}^{(1)}(\bar{r}, \bar{z}) = \frac{E^{(1)} \gamma^T}{(1 + \nu^{(1)}) \pi} \int_{-\infty}^{\infty} \frac{1}{\Delta |\bar{\eta}|} \left\{ -|\bar{\eta}| \bar{r} K_1(|\bar{\eta}|) K_0(|\bar{\eta}| \bar{r}) + \left[|\bar{\eta}| K_0(|\bar{\eta}|) \right. \right. \\ \left. \left. + 2(1 - \nu^{(1)}) K_1(|\bar{\eta}|) \right] K_1(|\bar{\eta}| \bar{r}) \right\} \sin(\alpha \bar{\eta}) \sin(\alpha \bar{z} \bar{\eta}) d\bar{\eta} \\ \text{on } \bar{\Omega}^{(1)}. \end{aligned} \quad (3.23)$$

The strain components can be written in terms of normalized coordinates as

$$\begin{aligned}
\bar{\gamma}_{rr}^{(1)}(\bar{r}, \bar{z}) &= \frac{\gamma^T}{\pi} \int_{-\infty}^{\infty} \frac{1}{\Delta\bar{\eta}} \left\{ \left[|\bar{\eta}|K_0(|\bar{\eta}|) + K_1(|\bar{\eta}|) \right] K_0(|\bar{\eta}|\bar{r}) \right. \\
&\quad \left. + \left[\frac{1}{\bar{r}}K_0(|\bar{\eta}|) - |\bar{\eta}|\bar{r}K_1(|\bar{\eta}|) \right] K_1(|\bar{\eta}|\bar{r}) \right\} \sin(\alpha\bar{\eta})\cos(\alpha\bar{z}\bar{\eta})d\bar{\eta}, \\
\bar{\gamma}_{\theta\theta}^{(1)}(\bar{r}, \bar{z}) &= \frac{\gamma^T}{\pi} \int_{-\infty}^{\infty} \frac{1}{\Delta\bar{\eta}} \left\{ K_1(|\bar{\eta}|)K_0(|\bar{\eta}|\bar{r}) \right. \\
&\quad \left. - \frac{1}{\bar{r}}K_0(|\bar{\eta}|)K_1(|\bar{\eta}|\bar{r}) \right\} \sin(\alpha\bar{\eta})\cos(\alpha\bar{z}\bar{\eta})d\bar{\eta}, \\
\bar{\gamma}_{zz}^{(1)}(\bar{r}, \bar{z}) &= \frac{\gamma^T}{\pi} \int_{-\infty}^{\infty} \frac{1}{\Delta\bar{\eta}} \left\{ - \left[|\bar{\eta}|K_0(|\bar{\eta}|) + 4(1 - \nu^{(1)})K_1(|\bar{\eta}|) \right] K_0(|\bar{\eta}|\bar{r}) \right. \\
&\quad \left. + |\bar{\eta}|\bar{r}K_1(|\bar{\eta}|)K_1(|\bar{\eta}|\bar{r}) \right\} \sin(\alpha\bar{\eta})\cos(\alpha\bar{z}\bar{\eta})d\bar{\eta}, \\
\bar{\gamma}_{rz}^{(1)}(\bar{r}, \bar{z}) &= \frac{\gamma^T}{\pi} \int_{-\infty}^{\infty} \frac{1}{\Delta|\bar{\eta}|} \left\{ - |\bar{\eta}|\bar{r}K_1(|\bar{\eta}|)K_0(|\bar{\eta}|\bar{r}) + \left[|\bar{\eta}|K_0(|\bar{\eta}|) \right. \right. \\
&\quad \left. \left. + 2(1 - \nu^{(1)})K_1(|\bar{\eta}|) \right] K_1(|\bar{\eta}|\bar{r}) \right\} \sin(\alpha\bar{\eta})\sin(\alpha\bar{z}\bar{\eta})d\bar{\eta} \\
&\quad \text{on } \bar{\Omega}^{(1)}. \tag{3.24}
\end{aligned}$$

The displacement components, in terms of \bar{r} and \bar{z} , are

$$\begin{aligned}
\bar{u}_r^{(1)}(\bar{r}, \bar{z}) &= \frac{a\gamma^T}{\pi} \int_{-\infty}^{\infty} \frac{1}{\Delta\bar{\eta}} \left\{ \bar{r}K_1(|\bar{\eta}|)K_0(|\bar{\eta}|\bar{r}) \right. \\
&\quad \left. - K_0(|\bar{\eta}|)K_1(|\bar{\eta}|\bar{r}) \right\} \sin(\alpha\bar{\eta})\cos(\alpha\bar{z}\bar{\eta})d\bar{\eta}, \\
\bar{u}_z^{(1)}(\bar{r}, \bar{z}) &= -\frac{a\gamma^T}{\pi} \int_{-\infty}^{\infty} \frac{1}{\Delta\bar{\eta}^2} \left\{ \left[|\bar{\eta}|K_0(|\bar{\eta}|) + 4(1 - \nu^{(1)})K_1(|\bar{\eta}|) \right] K_0(|\bar{\eta}|\bar{r}) \right. \\
&\quad \left. - |\bar{\eta}|\bar{r}K_1(|\bar{\eta}|)K_1(|\bar{\eta}|\bar{r}) \right\} \sin(\alpha\bar{\eta})\sin(\alpha\bar{z}\bar{\eta})d\bar{\eta} \quad \text{on } \bar{\Omega}^{(1)}. \tag{3.25}
\end{aligned}$$

These results can also be obtained by substituting (3.18) into (3.12), (3.13), (3.14), and (3.15), and normalizing them with (2.68) and (2.69).

As shown in (3.23), (3.24), and (3.25), it is clear that all the components of stress, strain, and displacement are proportional to the transformation strain γ^T .

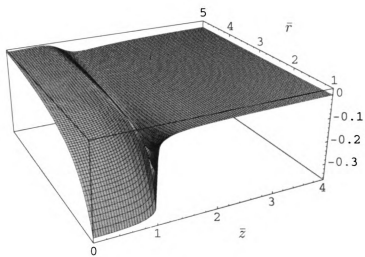
3.4 Numerical Evaluation

In this section, we present the numerical evaluation of the exact solutions (3.23), (3.24), and (3.25), which are for single finite segment of fiber undergoing phase transformation. The calculation is performed using Mathematica with Poisson's ratio $\nu^{(1)} = 0.25$. Noticing that all the integrands are even functions of $\bar{\eta}$, one only needs to calculate the integration over the interval $(0, \infty)$.

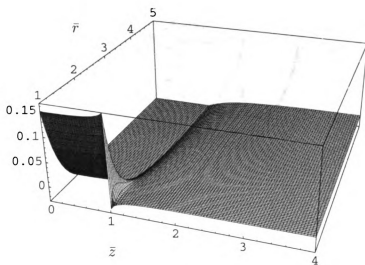
Figures 3.1 – 3.3 show the 3D plots of stress distributions, the strain distributions, and the displacements for the case of $\alpha = 10$, respectively.

Figure 3.4 displays the distributions of the stresses on the interface with the fiber for $\alpha = 10$. It is shown that across the phase boundary ($\bar{z} = 1$), the normal stresses have finite jumps, whereas the shear stress seems to approach infinity. Outside the transformed region, the normal stresses are very small in magnitude compared to the shear stress $\bar{\sigma}_{rz}$.

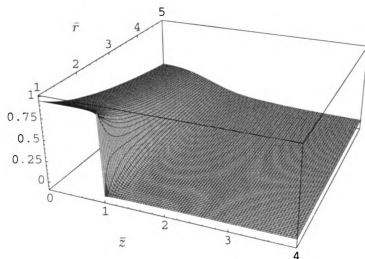
Figure 3.5 shows the shear stress distributions on the interface with the fiber for $\alpha = 1, 5, 10$, and 20 , respectively. It shows that the shear stress increases with the aspect ratio α .



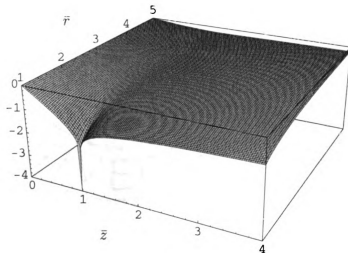
(a) $\frac{\bar{\sigma}_{rr}^{(1)}}{E^{(1)}\gamma^T}$



(b) $\frac{\bar{\sigma}_{\theta\theta}^{(1)}}{E^{(1)}\gamma^T}$



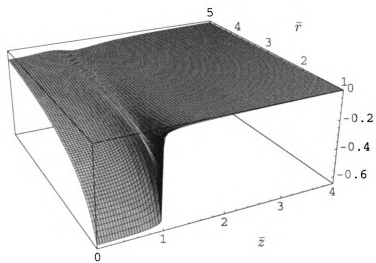
(c) $\frac{\bar{\sigma}_{zz}^{(1)}}{E^{(1)}\gamma T}$



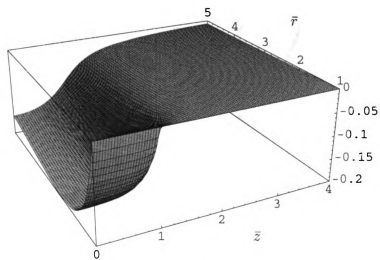
(d) $\frac{\bar{\sigma}_{rz}^{(1)}}{E^{(1)}\gamma T}$

Figure 3.1. The 3D plots of stress distributions for $\nu^{(1)} = 0.25$ and $\alpha = 10$.

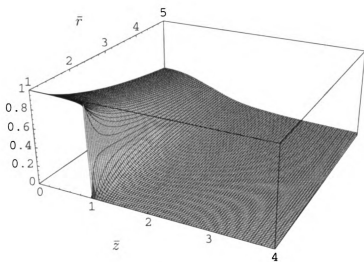
(a) $\frac{\bar{\sigma}_{rr}^{(1)}}{E^{(1)}\gamma T}$, (b) $\frac{\bar{\sigma}_{\theta\theta}^{(1)}}{E^{(1)}\gamma T}$, (c) $\frac{\bar{\sigma}_{zz}^{(1)}}{E^{(1)}\gamma T}$, and (d) $\frac{\bar{\sigma}_{rz}^{(1)}}{E^{(1)}\gamma T}$.



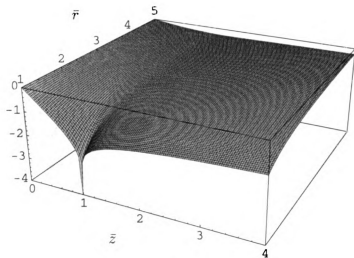
(a) $\frac{\bar{r}r^{(1)}}{\gamma T}$



(b) $\frac{\bar{r}q^{(1)}}{\gamma T}$



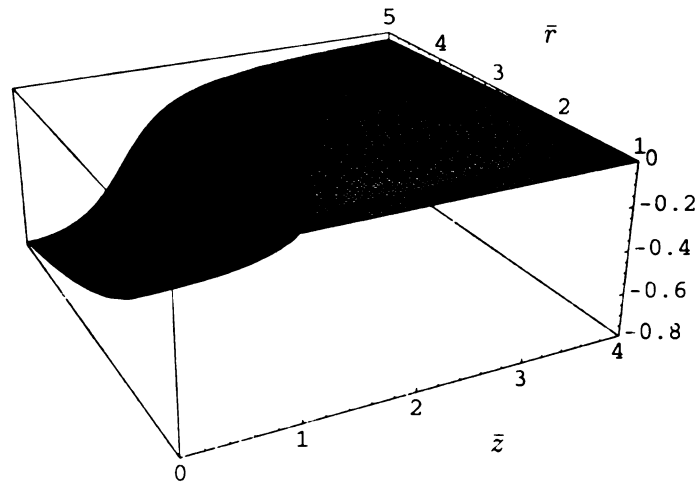
(c) $\frac{\bar{\gamma}_{\bar{x}\bar{z}}^{(1)}}{\gamma_{\bar{z}}}$



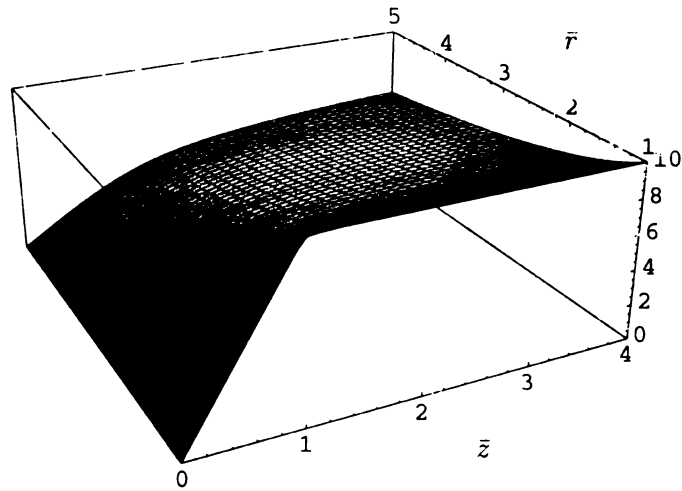
(d) $\frac{\bar{\gamma}_{\bar{x}\bar{z}}^{(1)}}{\gamma_{\bar{z}}}$

Figure 3.2. The 3D plots of strain distributions for $\nu^{(1)} = 0.25$ and $\alpha = 10$.

(a) $\frac{\bar{\gamma}_{\bar{r}\bar{r}}^{(1)}}{\gamma_{\bar{r}}}$, (b) $\frac{\bar{\gamma}_{\bar{\theta}\bar{\theta}}^{(1)}}{\gamma_{\bar{r}}}$, (c) $\frac{\bar{\gamma}_{\bar{x}\bar{z}}^{(1)}}{\gamma_{\bar{z}}}$, and (d) $\frac{\bar{\gamma}_{\bar{x}\bar{z}}^{(1)}}{\gamma_{\bar{z}}}$.



(a) $\frac{\bar{u}_r^{(1)}}{a\gamma T}$



(b) $\frac{\bar{u}_z^{(1)}}{a\gamma T}$

Figure 3.3. The 3D plots of displacements for $\nu^{(1)} = 0.25$ and $\alpha = 10$. (a) $\frac{\bar{u}_r^{(1)}}{a\gamma T}$, and (b) $\frac{\bar{u}_z^{(1)}}{a\gamma T}$.

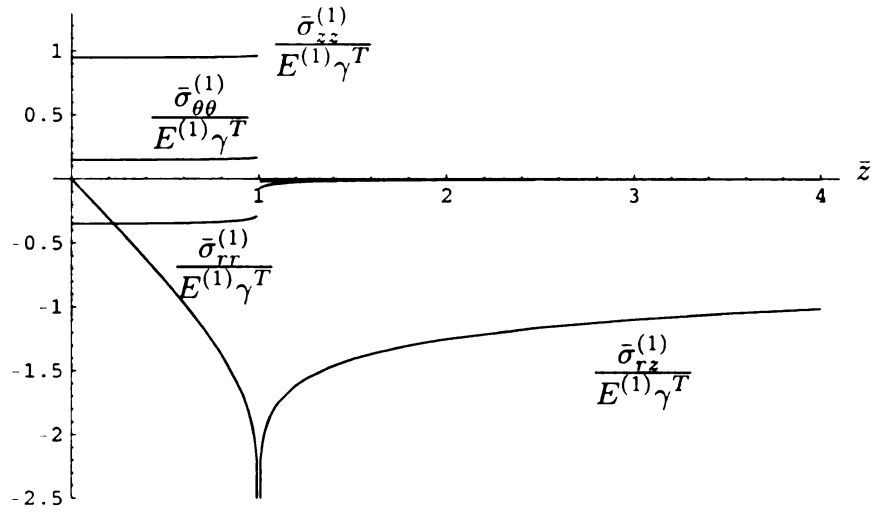


Figure 3.4. The distributions of the stresses on the fiber-matrix interface for $\nu^{(1)} = 0.25$ and $\alpha = 10$.

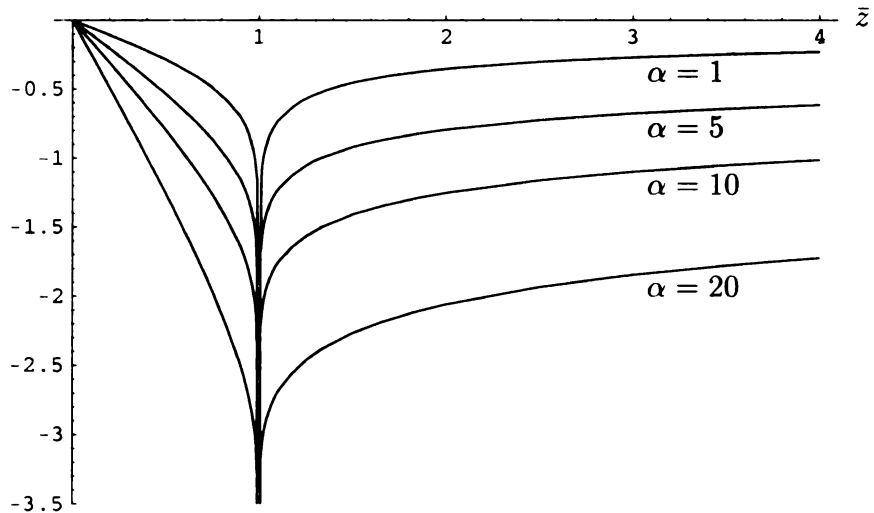


Figure 3.5. The shear stress distributions, $\frac{\bar{\sigma}_{rz}^{(1)}}{E^{(1)}\gamma^T}$, on the fiber-matrix interface for $\nu^{(1)} = 0.25$ and $\alpha = 1, 5, 10,$ and 20 , respectively.

3.5 Analysis of Singularities

For SMA fiber reinforced composites, the stresses are induced by the phase transformation in the SMA fiber. The stress concentration in the matrix usually occurs near the interface with the fiber, especially at the location near the phases boundary in the fiber. In this section, we develop approximate expressions for the stress distributions at the interface with emphasis on the possible singularities near the phase boundary ($|\bar{z}| = 1$).

By setting $\bar{r} = 1$ in (3.23) and considering that the integrands are even functions, the stress components at the interface with the fiber are given by

$$\begin{aligned}
 \bar{\sigma}_{rr}^{(1)}(1, \bar{z}) &= \frac{2E^{(1)}\gamma^T}{\pi(1 + \nu^{(1)})} \int_0^\infty \frac{\bar{\Delta}_{rr}^{(1)}}{\bar{\Delta}\bar{\eta}} \sin(\alpha\bar{\eta}) \cos(\alpha\bar{z}\bar{\eta}) d\bar{\eta}, \\
 \bar{\sigma}_{\theta\theta}^{(1)}(1, \bar{z}) &= \frac{2E^{(1)}\gamma^T}{\pi(1 + \nu^{(1)})} \int_0^\infty \frac{\bar{\Delta}_{\theta\theta}^{(1)}}{\bar{\Delta}\bar{\eta}} \sin(\alpha\bar{\eta}) \cos(\alpha\bar{z}\bar{\eta}) d\bar{\eta}, \\
 \bar{\sigma}_{zz}^{(1)}(1, \bar{z}) &= \frac{2E^{(1)}\gamma^T}{\pi(1 + \nu^{(1)})} \int_0^\infty \frac{\bar{\Delta}_{zz}^{(1)}}{\bar{\Delta}\bar{\eta}} \sin(\alpha\bar{\eta}) \cos(\alpha\bar{z}\bar{\eta}) d\bar{\eta}, \\
 \bar{\sigma}_{rz}^{(1)}(1, \bar{z}) &= \frac{2E^{(1)}\gamma^T}{\pi(1 + \nu^{(1)})} \int_0^\infty \frac{\bar{\Delta}_{rz}^{(1)}}{\bar{\Delta}\bar{\eta}} \sin(\alpha\bar{\eta}) \sin(\alpha\bar{z}\bar{\eta}) d\bar{\eta}, \\
 &-\infty < \bar{z} < \infty,
 \end{aligned} \tag{3.26}$$

where $\bar{\Delta}_{rr}^{(1)}$, $\bar{\Delta}_{\theta\theta}^{(1)}$, $\bar{\Delta}_{zz}^{(1)}$, and $\bar{\Delta}_{rz}^{(1)}$ denote, in this chapter, the following functions of $\bar{\eta}$:

$$\begin{aligned}
 \bar{\Delta}_{rr}(\bar{\eta}) &= \bar{\eta}K_0^2(\bar{\eta}) + 2(1 - \nu^{(1)})K_0(\bar{\eta})K_1(\bar{\eta}) - \bar{\eta}K_1^2(\bar{\eta}), \\
 \bar{\Delta}_{\theta\theta}(\bar{\eta}) &= -2\nu^{(1)}K_0(\bar{\eta})K_1(\bar{\eta}), \\
 \bar{\Delta}_{zz}(\bar{\eta}) &= -\bar{\eta}K_0^2(\bar{\eta}) - 2(2 - \nu^{(1)})K_0(\bar{\eta})K_1(\bar{\eta}) + \bar{\eta}K_1^2(\bar{\eta}), \\
 \bar{\Delta}_{rz}(\bar{\eta}) &= 2(1 - \nu^{(1)})\bar{\eta}K_1^2(\bar{\eta}),
 \end{aligned}$$

$$0 < \bar{\eta} < \infty. \tag{3.27}$$

With the aid of the asymptotic expansions (2.80), one finds the following asymptotic expansions:

$$\begin{aligned}
\frac{\bar{\Delta}_{rr}}{\bar{\Delta}} &\sim -\frac{1-2\nu^{(1)}}{3-4\nu^{(1)}} - \frac{1-\nu^{(1)}}{(3-4\nu^{(1)})^2} \frac{1}{\bar{\eta}}, \\
\frac{\bar{\Delta}_{\theta\theta}}{\bar{\Delta}} &\sim \frac{2\nu^{(1)}}{3-4\nu^{(1)}} - \frac{\nu^{(1)}}{(3-4\nu^{(1)})^2} \frac{1}{\bar{\eta}}, \\
\frac{\bar{\Delta}_{zz}}{\bar{\Delta}} &\sim \frac{3-2\nu^{(1)}}{3-4\nu^{(1)}} - \frac{\nu^{(1)}}{(3-4\nu^{(1)})^2} \frac{1}{\bar{\eta}}, \\
\frac{\bar{\Delta}_{rz}}{\bar{\eta}\bar{\Delta}} &\sim -\frac{2(1-\nu^{(1)})}{3-4\nu^{(1)}} + \frac{(1-\nu^{(1)})(11-4\nu^{(1)})}{2(3-4\nu^{(1)})^2} \frac{1}{\bar{\eta}},
\end{aligned}
\tag{3.28}$$

as $\bar{\eta} \rightarrow \infty$.

The leading (zero order) terms play a major role in the behavior of the stresses near the phase boundary which will be made clear as follows. Utilizing (3.28), one can separate the stress components into two parts

$$\begin{aligned}
\bar{\sigma}_{rr}(1, \bar{z}) &= \frac{2E^{(1)}\gamma^T}{(1+\nu^{(1)})\pi} \left\{ -\frac{1-2\nu^{(1)}}{3-4\nu^{(1)}} \int_0^\infty \frac{\sin(\alpha\bar{\eta})\cos(\alpha\bar{z}\bar{\eta})}{\bar{\eta}} d\bar{\eta} \right. \\
&\quad \left. + \int_0^\infty \left[\frac{\bar{\Delta}_{rr}}{\bar{\Delta}} + \frac{1-2\nu^{(1)}}{3-4\nu^{(1)}} \right] \frac{\sin(\alpha\bar{\eta})\cos(\alpha\bar{z}\bar{\eta})}{\bar{\eta}} d\bar{\eta} \right\}, \\
\bar{\sigma}_{\theta\theta}(1, \bar{z}) &= \frac{2E^{(1)}\gamma^T}{(1+\nu^{(1)})\pi} \left\{ \frac{2\nu^{(1)}}{3-4\nu^{(1)}} \int_0^\infty \frac{\sin(\alpha\bar{\eta})\cos(\alpha\bar{z}\bar{\eta})}{\bar{\eta}} d\bar{\eta} \right. \\
&\quad \left. + \int_0^\infty \left[\frac{\bar{\Delta}_{\theta\theta}}{\bar{\Delta}} - \frac{2\nu^{(1)}}{3-4\nu^{(1)}} \right] \frac{\sin(\alpha\bar{\eta})\cos(\alpha\bar{z}\bar{\eta})}{\bar{\eta}} d\bar{\eta} \right\}, \\
\bar{\sigma}_{zz}(1, \bar{z}) &= \frac{2E^{(1)}\gamma^T}{(1+\nu^{(1)})\pi} \left\{ \frac{3-2\nu^{(1)}}{3-4\nu^{(1)}} \int_0^\infty \frac{\sin(\alpha\bar{\eta})\cos(\alpha\bar{z}\bar{\eta})}{\bar{\eta}} d\bar{\eta} \right. \\
&\quad \left. + \int_0^\infty \left[\frac{\bar{\Delta}_{zz}}{\bar{\Delta}} - \frac{3-2\nu^{(1)}}{3-4\nu^{(1)}} \right] \frac{\sin(\alpha\bar{\eta})\cos(\alpha\bar{z}\bar{\eta})}{\bar{\eta}} d\bar{\eta} \right\}, \\
\bar{\sigma}_{rz}(1, \bar{z}) &= \frac{2E^{(1)}\gamma^T}{(1+\nu^{(1)})\pi} \left\{ -\frac{2(1-\nu^{(1)})}{3-4\nu^{(1)}} \int_0^\infty \frac{\sin(\alpha\bar{\eta})\sin(\alpha\bar{z}\bar{\eta})}{\bar{\eta}} d\bar{\eta} \right. \\
&\quad \left. + \int_0^\infty \left[\frac{\bar{\Delta}_{rz}}{\bar{\Delta}\bar{\eta}} + \frac{2(1-\nu^{(1)})}{3-4\nu^{(1)}} \right] \frac{\sin(\alpha\bar{\eta})\sin(\alpha\bar{z}\bar{\eta})}{\bar{\eta}} d\bar{\eta} \right\},
\end{aligned}$$

$$-\infty < \bar{z} < \infty. \quad (3.29)$$

The second integrals can be further decomposed into two parts by dividing the interval of integration into $(0, s)$ and (s, ∞) , for some $s > 0$. Hence, we have

$$\begin{aligned} \bar{\sigma}_{rr}(1, \bar{z}) &= \frac{2E^{(1)}\gamma^T}{(1+\nu^{(1)})\pi} \left\{ -\frac{1-2\nu^{(1)}}{3-4\nu^{(1)}} \int_0^\infty \frac{\sin(\alpha\bar{\eta})\cos(\alpha\bar{z}\bar{\eta})}{\bar{\eta}} d\bar{\eta} \right. \\ &\quad + \int_0^s \left[\frac{\bar{\Delta}_{rr}}{\bar{\Delta}} + \frac{1-2\nu^{(1)}}{3-4\nu^{(1)}} \right] \frac{\sin(\alpha\bar{\eta})\cos(\alpha\bar{z}\bar{\eta})}{\bar{\eta}} d\bar{\eta} \\ &\quad \left. + \int_s^\infty \left[\frac{\bar{\Delta}_{rr}}{\bar{\Delta}} + \frac{1-2\nu^{(1)}}{3-4\nu^{(1)}} \right] \frac{\sin(\alpha\bar{\eta})\cos(\alpha\bar{z}\bar{\eta})}{\bar{\eta}} d\bar{\eta} \right\}, \\ \bar{\sigma}_{\theta\theta}(1, \bar{z}) &= \frac{2E^{(1)}\gamma^T}{(1+\nu^{(1)})\pi} \left\{ \frac{2\nu^{(1)}}{3-4\nu^{(1)}} \int_0^\infty \frac{\sin(\alpha\bar{\eta})\cos(\alpha\bar{z}\bar{\eta})}{\bar{\eta}} d\bar{\eta} \right. \\ &\quad + \int_0^s \left[\frac{\bar{\Delta}_{\theta\theta}}{\bar{\Delta}} - \frac{2\nu^{(1)}}{3-4\nu^{(1)}} \right] \frac{\sin(\alpha\bar{\eta})\cos(\alpha\bar{z}\bar{\eta})}{\bar{\eta}} d\bar{\eta} \\ &\quad \left. + \int_s^\infty \left[\frac{\bar{\Delta}_{\theta\theta}}{\bar{\Delta}} - \frac{2\nu^{(1)}}{3-4\nu^{(1)}} \right] \frac{\sin(\alpha\bar{\eta})\cos(\alpha\bar{z}\bar{\eta})}{\bar{\eta}} d\bar{\eta} \right\}, \\ \bar{\sigma}_{zz}(1, \bar{z}) &= \frac{2E^{(1)}\gamma^T}{(1+\nu^{(1)})\pi} \left\{ \frac{3-2\nu^{(1)}}{3-4\nu^{(1)}} \int_0^\infty \frac{\sin(\alpha\bar{\eta})\cos(\alpha\bar{z}\bar{\eta})}{\bar{\eta}} d\bar{\eta} \right. \\ &\quad + \int_0^s \left[\frac{\bar{\Delta}_{zz}}{\bar{\Delta}} - \frac{3-2\nu^{(1)}}{3-4\nu^{(1)}} \right] \frac{\sin(\alpha\bar{\eta})\cos(\alpha\bar{z}\bar{\eta})}{\bar{\eta}} d\bar{\eta} \\ &\quad \left. + \int_s^\infty \left[\frac{\bar{\Delta}_{zz}}{\bar{\Delta}} - \frac{3-2\nu^{(1)}}{3-4\nu^{(1)}} \right] \frac{\sin(\alpha\bar{\eta})\cos(\alpha\bar{z}\bar{\eta})}{\bar{\eta}} d\bar{\eta} \right\}, \\ \bar{\sigma}_{rz}(1, \bar{z}) &= \frac{2E^{(1)}\gamma^T}{(1+\nu^{(1)})\pi} \left\{ -\frac{2(1-\nu^{(1)})}{3-4\nu^{(1)}} \int_0^\infty \frac{\sin(\alpha\bar{\eta})\sin(\alpha\bar{z}\bar{\eta})}{\bar{\eta}} d\bar{\eta} \right. \\ &\quad + \int_0^s \left[\frac{\bar{\Delta}_{rz}}{\bar{\Delta}\bar{\eta}} + \frac{2(1-\nu^{(1)})}{3-4\nu^{(1)}} \right] \frac{\sin(\alpha\bar{\eta})\sin(\alpha\bar{z}\bar{\eta})}{\bar{\eta}} d\bar{\eta} \\ &\quad \left. + \int_s^\infty \left[\frac{\bar{\Delta}_{rz}}{\bar{\Delta}\bar{\eta}} + \frac{2(1-\nu^{(1)})}{3-4\nu^{(1)}} \right] \frac{\sin(\alpha\bar{\eta})\sin(\alpha\bar{z}\bar{\eta})}{\bar{\eta}} d\bar{\eta} \right\}, \end{aligned}$$

$$-\infty < \bar{z} < \infty. \quad (3.30)$$

Note that for positive s , one has

$$\int_s^\infty \frac{\sin(\alpha\bar{\eta})\cos(\alpha\bar{z}\bar{\eta})}{\bar{\eta}^2} d\bar{\eta} \leq \int_s^\infty \left| \frac{\sin(\alpha\bar{\eta})\cos(\alpha\bar{z}\bar{\eta})}{\bar{\eta}^2} \right| d\bar{\eta} \leq \int_s^\infty \frac{1}{\bar{\eta}^2} d\bar{\eta} = \frac{1}{s}. \quad (3.31)$$

Hence, for sufficiently large s , the third integrals in (3.30) are small and then we have the approximations

$$\begin{aligned} \bar{\sigma}_{rr}(1, \bar{z}) &\simeq \frac{2E^{(1)}\gamma^T}{(1+\nu^{(1)})\pi} \left\{ -\frac{1-2\nu^{(1)}}{3-4\nu^{(1)}} \int_0^\infty \frac{\sin(\alpha\bar{\eta})\cos(\alpha\bar{z}\bar{\eta})}{\bar{\eta}} d\bar{\eta} \right. \\ &\quad \left. + \int_0^s \left[\frac{\bar{\Delta}_{rr}}{\bar{\Delta}} + \frac{1-2\nu^{(1)}}{3-4\nu^{(1)}} \right] \frac{\sin(\alpha\bar{\eta})\cos(\alpha\bar{z}\bar{\eta})}{\bar{\eta}} d\bar{\eta} \right\}, \\ \bar{\sigma}_{\theta\theta}(1, \bar{z}) &\simeq \frac{2E^{(1)}\gamma^T}{(1+\nu^{(1)})\pi} \left\{ \frac{2\nu^{(1)}}{3-4\nu^{(1)}} \int_0^\infty \frac{\sin(\alpha\bar{\eta})\cos(\alpha\bar{z}\bar{\eta})}{\bar{\eta}} d\bar{\eta} \right. \\ &\quad \left. + \int_0^s \left[\frac{\bar{\Delta}_{\theta\theta}}{\bar{\Delta}} - \frac{2\nu^{(1)}}{3-4\nu^{(1)}} \right] \frac{\sin(\alpha\bar{\eta})\cos(\alpha\bar{z}\bar{\eta})}{\bar{\eta}} d\bar{\eta}, \right. \\ \bar{\sigma}_{zz}(1, \bar{z}) &\simeq \frac{2E^{(1)}\gamma^T}{(1+\nu^{(1)})\pi} \left\{ \frac{3-2\nu^{(1)}}{3-4\nu^{(1)}} \int_0^\infty \frac{\sin(\alpha\bar{\eta})\cos(\alpha\bar{z}\bar{\eta})}{\bar{\eta}} d\bar{\eta} \right. \\ &\quad \left. + \int_0^s \left[\frac{\bar{\Delta}_{zz}}{\bar{\Delta}} - \frac{3-2\nu^{(1)}}{3-4\nu^{(1)}} \right] \frac{\sin(\alpha\bar{\eta})\cos(\alpha\bar{z}\bar{\eta})}{\bar{\eta}} d\bar{\eta}, \right. \\ \bar{\sigma}_{rz}(1, \bar{z}) &\simeq \frac{2E^{(1)}\gamma^T}{(1+\nu^{(1)})\pi} \left\{ -\frac{2(1-\nu^{(1)})}{3-4\nu^{(1)}} \int_0^\infty \frac{\sin(\alpha\bar{\eta})\sin(\alpha\bar{z}\bar{\eta})}{\bar{\eta}} d\bar{\eta} \right. \\ &\quad \left. + \int_0^s \left[\frac{\bar{\Delta}_{rz}}{\bar{\Delta}\bar{\eta}} + \frac{2(1-\nu^{(1)})}{3-4\nu^{(1)}} \right] \frac{\sin(\alpha\bar{\eta})\sin(\alpha\bar{z}\bar{\eta})}{\bar{\eta}} d\bar{\eta} \right\}, \\ &\quad -\infty < \bar{z} < \infty. \end{aligned} \quad (3.32)$$

Now, notice that the integrands in the second integrals of (3.32) involve K_0 and K_1 , which are possibly singular only at 0. To show the behaviors of these integrands near 0, we consider the asymptotic expansions of K_0 and K_1 as $\bar{\eta} \rightarrow 0^+$. Using (2.82), one finds

$$\frac{\bar{\Delta}_{rr}}{\bar{\Delta}} \sim \frac{(\bar{\eta}\ln\bar{\eta})^2 - 2(1-\nu^{(1)})\ln\bar{\eta} - 1}{-(\bar{\eta}\ln\bar{\eta})^2 + 4(1-\nu^{(1)})\ln\bar{\eta} + 1} \rightarrow -\frac{1}{2}, \quad (\bar{\eta} \rightarrow 0^+),$$

$$\begin{aligned}
\frac{\bar{\Delta}_{\theta\theta}}{\bar{\Delta}} &\sim \frac{2\nu^{(1)}\ln\bar{\eta}}{-(\bar{\eta}\ln\bar{\eta})^2 + 4(1 - \nu^{(1)})\ln\bar{\eta} + 1} \rightarrow \frac{\nu^{(1)}}{2(1 - \nu^{(1)})}, \quad (\bar{\eta} \rightarrow 0^+), \\
\frac{\bar{\Delta}_{zz}}{\bar{\Delta}} &\sim \frac{-(\bar{\eta}\ln\bar{\eta})^2 + 2(2 - \nu^{(1)})\ln\bar{\eta} + 1}{-(\bar{\eta}\ln\bar{\eta})^2 + 4(1 - \nu^{(1)})\ln\bar{\eta} + 1} \rightarrow -\frac{2 - \nu^{(1)}}{2(1 - \nu^{(1)})}, \quad (\bar{\eta} \rightarrow 0^+), \\
\frac{\bar{\Delta}_{rz}}{\bar{\Delta}} &\sim \frac{2(1 - \nu^{(1)})}{-(\bar{\eta}\ln\bar{\eta})^2 + 4(1 - \nu^{(1)})\ln\bar{\eta} + 1} \rightarrow 0, \quad (\bar{\eta} \rightarrow 0^+). \tag{3.33}
\end{aligned}$$

Therefore, noticing $(\sin\bar{\eta}/\bar{\eta}) \rightarrow 1$ as $\bar{\eta} \rightarrow 0^+$, one concludes that all the second integrands in (3.32) are finite at 0. It follows that all the second integrals of (3.32) are finite and continuous in \bar{z} . For the first parts of (3.32), they can be evaluated explicitly by the Dirichlet's discontinuous factor (Courant and Hilbert, 1989, p.81)

$$\int_0^\infty \frac{\sin(\alpha\bar{\eta})\cos(\alpha\bar{z}\bar{\eta})}{\bar{\eta}} d\bar{\eta} = \begin{cases} \pi/2 & |\bar{z}| < 1, \\ \pi/4 & |\bar{z}| = 1, \\ 0 & |\bar{z}| > 1, \end{cases} \tag{3.34}$$

which has a finite jump at $|\bar{z}| = 1$, and

$$\int_0^\infty \frac{\sin(\alpha\bar{\eta})\sin(\alpha\bar{z}\bar{\eta})}{\bar{\eta}} d\bar{\eta} = \frac{1}{2} \ln \left| \frac{1 + \bar{z}}{1 - \bar{z}} \right|, \tag{3.35}$$

which is singular at $|\bar{z}| = 1$.

In consequence, the singularities of all stress components near the phase boundary are isolated in the first integrals of (3.32). It is found that the normal stresses suffer finite jumps at $|\bar{z}| = 1$. On the other hand, the shear stress blows up at $|\bar{z}| = 1$ with the singularity characterized by the function $\frac{1}{2} \ln|(1 + \bar{z})/(1 - \bar{z})|$. Specifically, the jumps of the normal stresses across the phase boundary $|\bar{z}| = 1$ are given by

$$\llbracket \bar{\sigma}_{rr}(1, z) \rrbracket_{z=1} = \lim_{\epsilon \rightarrow 0} [\bar{\sigma}_{rr}(1, 1 + \epsilon) - \bar{\sigma}_{rr}(1, 1 - \epsilon)] = \frac{(1 - 2\nu^{(1)})E^{(1)}\gamma^T}{(1 + \nu^{(1)})(3 - 4\nu^{(1)})},$$

$$\llbracket \bar{\sigma}_{\theta\theta}(1, z) \rrbracket_{z=1} = \lim_{\epsilon \rightarrow 0} [\bar{\sigma}_{\theta\theta}(1, 1 + \epsilon) - \bar{\sigma}_{\theta\theta}(1, 1 - \epsilon)] = -\frac{2\nu^{(1)}E^{(1)}\gamma^T}{(1 + \nu^{(1)})(3 - 4\nu^{(1)})},$$

$$\llbracket \bar{\sigma}_{zz}(1, z) \rrbracket_{z=1} = \lim_{\epsilon \rightarrow 0} [\bar{\sigma}_{zz}(1, 1 + \epsilon) - \bar{\sigma}_{zz}(1, 1 - \epsilon)] = -\frac{(3 - 2\nu^{(1)})E^{(1)}\gamma^T}{(1 + \nu^{(1)})(3 - 4\nu^{(1)})}. \quad (3.36)$$

Whereas, the shear stress approaches infinity with the intensity

$$\bar{\sigma}_{rz}(1, \bar{z}) \sim \frac{2(1 - \nu^{(1)})E^{(1)}\gamma^T}{(1 + \nu^{(1)})(3 - 4\nu^{(1)})\pi} \ln \left| \frac{1 + \bar{z}}{1 - \bar{z}} \right|, \quad (|\bar{z}| \rightarrow 1). \quad (3.37)$$

The above results indicate that, across the phase boundary of the fiber $|\bar{z}| = 1$, the jumps of the normal stresses and the intensity of singularity of the shear stress are entirely determined by the Young's modulus $E^{(1)}$, the Poisson's ratio $\nu^{(1)}$ and the transformation strain γ^T . They are independent of the aspect ratio α . In other words, the jumps of the normal stresses and the intensity of singularity of the shear stress are determined by the material properties of the matrix but are independent of the geometry of the transformed region. In addition, the magnitude of the jumps of the normal stresses are directly proportional to the Young's modulus of the fiber $E^{(1)}$ and the transformation strain γ^T . The numerical results obtained earlier are consistent with (3.36) and (3.37). The singularity of $\bar{\sigma}_{rz}$ at $|\bar{z}| = 1$ indicates severe stress concentration.

3.6 Remarks

In the study on the “perfect bonding rigid fiber” model of a SMA fiber reinforced composite, the exact solutions to the distributions of stress, strain, and displacement are obtained for general phase transformation pattern. Particularly, the situation that only a single finite segment of the fiber undergoes phase transformation is further discussed. The normalized forms of the solutions are given for this situation. The numerical evaluation is performed and it shows that across the phase boundary, the normal stresses have finite jumps, whereas the shear stress approach

infinity. Further, by using asymptotic expansion technique, the singularities of the stresses are isolated. It is found that the jumps of the normal stresses and the intensity of singularity for the shear stress are determined by the material properties $(E^{(1)}, \nu^{(1)})$ and transformation strain γ^T , and are independent of the aspect ratio α . The singularity in shear stress indicates a severe stress concentration near the phase boundary.

CHAPTER 4. “PERFECT BONDING ELASTIC FIBER” MODEL

In the “perfect bonding rigid fiber” model developed in the previous chapter, the influence of matrix on fiber is ignored. The phase transformation in the fiber is considered to be constraint free. Under perfectly bonding condition, the constraint free phase transformation in the fiber directly gives rise to the boundary condition for determining the deformation of the matrix. The solution provides a good approximation to the case that the fiber is much stronger than the matrix. In more general cases, however, the matrix exerts a significant influence on the deformation of the fiber, even constrains the phase transformation in the fiber. The deformation of the fiber must be considered together with those of the matrix. The interaction between fiber and matrix is determined by the bonding conditions. In this chapter, we consider the general case that the fiber and the matrix are perfectly bonded. Instead of considering the deformation of the matrix only as in the “rigid fiber” model in the previous chapter, we will also investigate the deformation of the fiber to see the influence of matrix on the phase transformation in the fiber.

4.1 Bonding Conditions

Assume the fiber and the matrix are bonded perfectly. Across the fiber-matrix interface, the displacements are continuous. In addition, the equilibrium requires that the traction is also continuous across the fiber-matrix interface. Thus, the system, with perfect bond between fiber and matrix, obeys the following bonding conditions across the fiber-matrix interface:

$$[[\sigma_{rr}]]_{\mathcal{P}} = [[\sigma_{rz}]]_{\mathcal{P}} = [[u_r]]_{\mathcal{P}} = [[u_z]]_{\mathcal{P}} = 0, \quad (4.1)$$

where \mathcal{P} is the fiber-matrix interface given by (2.40) and the notation $[[\circ]]_{\mathcal{P}}$ defines the jump discontinuity by

$$[[\circ]]_{\mathcal{P}} \equiv [\circ^{(1)} - \circ^{(2)}] \Big|_{(r,\theta,z) \in \mathcal{P}}. \quad (4.2)$$

Moreover, in the absence of any loads at infinity and for regularity in the center of the fiber, the stresses are required to satisfy the restriction conditions (2.47) and (2.48).

By applying Fourier transformation on (4.1), the bonding conditions in the Fourier transformed domain become

$$[[\tilde{\sigma}_{rr}]]_{r=a} = [[\tilde{\sigma}_{rz}]]_{r=a} = [[\tilde{u}_r]]_{r=a} = [[\tilde{u}_z]]_{r=a} = 0, \quad -\infty < \eta < \infty, \quad (4.3)$$

where $[[\tilde{\circ}]]_{r=a}$ defined by

$$[[\tilde{\circ}]]_{r=a} \equiv [\tilde{\circ}^{(1)} - \tilde{\circ}^{(2)}]_{|_{r=a}}. \quad (4.4)$$

4.2 Exact Solutions

In this section, we first consider the general situation that the phase transformation characteristic function $\gamma^*(z)$ is given by (2.43). In the Fourier transformed domain, the general solutions to the system are given in Chapter 2 by (2.52), (2.58), (2.59), and (2.60). Setting $r = a$ in (2.58) and (2.60) and substituting them into (4.3), one arrives at the linear algebraic equations for the bonding conditions:

$$\begin{aligned} q_1^{(1)} A^{(1)} + q_2^{(1)} B^{(1)} - q_1^{(2)} A^{(2)} - q_2^{(2)} B^{(2)} &= 0, \\ q_3^{(1)} A^{(1)} + q_4^{(1)} B^{(1)} - q_3^{(2)} A^{(2)} - q_4^{(2)} B^{(2)} &= 0, \\ q_5^{(1)} A^{(1)} + q_6^{(1)} B^{(1)} + wq_5^{(2)} A^{(2)} + wq_6^{(2)} B^{(2)} &= 0, \\ q_7^{(1)} A^{(1)} + q_8^{(1)} B^{(1)} - wq_7^{(2)} A^{(2)} - wq_8^{(2)} B^{(2)} &= i \frac{E^{(1)}}{(1 + \nu^{(1)})\eta^3} \tilde{\gamma}^*, \\ -\infty < \eta < \infty, & \end{aligned} \quad (4.5)$$

where we denote

$$q_1^{(n)} = q_1^{(n)}(\eta) = R_0^{(n)}(|\eta|a) - \frac{(-1)^n}{|\eta|a} R_1^{(n)}(|\eta|a),$$

$$q_2^{(n)} = q_2^{(n)}(\eta) = (-1)^n(1 - 2\nu^{(n)})R_0^{(n)}(|\eta|a) + |\eta|aR_1^{(n)}(|\eta|a),$$

$$q_3^{(n)} = q_3^{(n)}(\eta) = (-1)^n R_1^{(n)}(|\eta|a),$$

$$q_4^{(n)} = q_4^{(n)}(\eta) = (-1)^n |\eta|a R_0^{(n)}(|\eta|a) + 2(1 - \nu^{(n)})R_1^{(n)}(|\eta|a),$$

$$q_5^{(n)} = q_5^{(n)}(\eta) = R_1^{(n)}(|\eta|a),$$

$$q_6^{(n)} = q_6^{(n)}(\eta) = |\eta|a R_0^{(n)}(|\eta|a),$$

$$q_7^{(n)} = q_7^{(n)}(\eta) = R_0^{(n)}(|\eta|a),$$

$$q_8^{(n)} = q_8^{(n)}(\eta) = (-1)^n 4(1 - \nu^{(n)})R_0^{(n)}(|\eta|a) + |\eta|a R_1^{(n)}(|\eta|a),$$

$$-\infty < \eta < \infty. \quad (4.6)$$

The constant w denotes the ratio of the shear modulus of the matrix $G^{(1)}$ to the shear modulus of the fiber $G^{(2)}$:

$$w = \frac{G^{(1)}}{G^{(2)}} = \frac{(1 + \nu^{(2)})E^{(1)}}{(1 + \nu^{(1)})E^{(2)}}. \quad (4.7)$$

The function $\tilde{\gamma}^* = \tilde{\gamma}^*(\eta)$ is the Fourier transform of phase transformation characteristic function $\gamma^* = \gamma^*(z)$.

Solving (4.5), one finds the unknown functions $A^{(n)}$ and $B^{(n)}$ as

$$A^{(n)} = A^{(n)}(\eta) = -i \frac{E^{(1)}}{1 + \nu^{(1)}} \frac{\Delta_A^{(n)}}{\eta^3 \Delta} \tilde{\gamma}^*$$

$$B^{(n)} = B^{(n)}(\eta) = i \frac{E^{(1)}}{1 + \nu^{(1)}} \frac{\Delta_B^{(n)}}{\eta^3 \Delta} \tilde{\gamma}^*$$

$$-\infty < \eta < \infty, \quad (4.8)$$

where $\Delta = \Delta(\eta)$ is given by the fourth order determinant

$$\Delta(\eta) = \begin{vmatrix} q_1^{(1)} & q_2^{(1)} & -q_1^{(2)} & -q_2^{(2)} \\ q_3^{(1)} & q_4^{(1)} & -q_3^{(2)} & -q_4^{(2)} \\ q_5^{(1)} & q_6^{(1)} & wq_5^{(2)} & wq_6^{(2)} \\ q_7^{(1)} & q_8^{(1)} & -wq_7^{(2)} & -wq_8^{(2)} \end{vmatrix},$$

$$-\infty < \eta < \infty, \quad (4.9)$$

and $\Delta_A^{(n)} = \Delta_A^{(n)}(\eta)$ and $\Delta_B^{(n)} = \Delta_B^{(n)}(\eta)$ are given by the third order determinants

$$\Delta_A^{(1)}(\eta) = \begin{vmatrix} q_2^{(1)} & -q_1^{(2)} & -q_2^{(2)} \\ q_4^{(1)} & -q_3^{(2)} & -q_4^{(2)} \\ q_6^{(1)} & wq_5^{(2)} & wq_6^{(2)} \end{vmatrix},$$

$$\Delta_B^{(1)}(\eta) = \begin{vmatrix} q_1^{(1)} & -q_1^{(2)} & -q_2^{(2)} \\ q_3^{(1)} & -q_3^{(2)} & -q_4^{(2)} \\ q_5^{(1)} & wq_5^{(2)} & wq_6^{(2)} \end{vmatrix},$$

$$\Delta_A^{(2)}(\eta) = \begin{vmatrix} q_1^{(1)} & q_2^{(1)} & -q_2^{(2)} \\ q_3^{(1)} & q_4^{(1)} & -q_4^{(2)} \\ q_5^{(1)} & q_6^{(1)} & wq_6^{(2)} \end{vmatrix},$$

$$\Delta_B^{(2)}(\eta) = \begin{vmatrix} q_1^{(1)} & q_2^{(1)} & -q_1^{(2)} \\ q_3^{(1)} & q_4^{(1)} & -q_3^{(2)} \\ q_5^{(1)} & q_6^{(1)} & wq_5^{(2)} \end{vmatrix},$$

$$-\infty < \eta < \infty. \quad (4.10)$$

Substituting (4.8) into (2.52), one obtains the Fourier transformed Love's stress functions for the matrix and the fiber:

$$\frac{\tilde{\Phi}^{(n)}}{\tilde{\gamma}^*} = i \frac{E^{(1)}}{(1 + \nu^{(1)})} \frac{1}{\eta^3 \Delta} \left[-\Delta_A^{(n)} R_0^{(n)}(|\eta|r) \right]$$

$$+\Delta_B^{(n)}|\eta|rR_1^{(n)}(|\eta|r)] \quad \text{on } \tilde{\Omega}^{(n)}. \quad (4.11)$$

Similarly, substituting (4.8) into (2.58), (2.59), and (2.60), one obtains the Fourier transformed stresses, strains, and displacements for the matrix and the fiber. The Fourier transformed stresses for the matrix and the fiber are

$$\begin{aligned} \frac{\tilde{\sigma}_{rr}^{(n)}}{\tilde{\gamma}^*} &= i \frac{E^{(1)}}{(1+\nu^{(1)})} \frac{1}{\Delta} \left\{ \left[R_0^{(n)}(|\eta|r) - \frac{(-1)^n}{|\eta|r} R_1^{(n)}(|\eta|r) \right] \Delta_A^{(n)} \right. \\ &\quad \left. - \left[(-1)^n(1-2\nu^{(n)})R_0^{(n)}(|\eta|r) + |\eta|rR_1^{(n)}(|\eta|r) \right] \Delta_B^{(n)} \right\}, \\ \frac{\tilde{\sigma}_{\theta\theta}^{(n)}}{\tilde{\gamma}^*} &= \frac{E^{(1)}}{(1+\nu^{(1)})} \frac{(-1)^n}{\Delta} \left\{ \frac{1}{|\eta|r} R_1^{(n)}(|\eta|r) \Delta_A^{(n)} \right. \\ &\quad \left. - (1-2\nu^{(n)})R_0^{(n)}(|\eta|r) \Delta_B^{(n)} \right\}, \\ \frac{\tilde{\sigma}_{zz}^{(n)}}{\tilde{\gamma}^*} &= \frac{E^{(1)}}{(1+\nu^{(1)})} \frac{1}{\Delta} \left\{ -R_0^{(n)}(|\eta|r) \Delta_A^{(n)} \right. \\ &\quad \left. + \left[(-1)^n 2(2-\nu^{(1)})R_0^{(n)}(|\eta|r) + |\eta|rR_1^{(n)}(|\eta|r) \right] \Delta_B^{(n)} \right\}, \\ \frac{\tilde{\sigma}_{rz}^{(n)}}{\tilde{\gamma}^*} &= i \frac{E^{(1)}}{(1+\nu^{(1)})} \frac{\text{sign}(\eta)}{\Delta} \left\{ (-1)^{n+1} R_1^{(n)}(|\eta|r) \Delta_A^{(n)} \right. \\ &\quad \left. + \left[(-1)^n |\eta|r R_0^{(n)}(|\eta|r) + 2(1-\nu^{(1)})R_1^{(n)}(|\eta|r) \right] \Delta_B^{(n)} \right\} \\ &\quad \text{on } \tilde{\Omega}^{(n)}. \quad (4.12) \end{aligned}$$

The Fourier transformed strains for the matrix and the fiber are

$$\begin{aligned} \frac{\tilde{\gamma}_{rr}^{(n)}}{\tilde{\gamma}^*} &= w^{n-1} \frac{1}{\Delta} \left\{ \left[R_0^{(n)}(|\eta|r) - \frac{(-1)^n}{|\eta|r} R_1^{(n)}(|\eta|r) \right] \Delta_A^{(n)} \right. \\ &\quad \left. - \left[(-1)^n R_0^{(n)}(|\eta|r) + |\eta|r R_1^{(n)}(|\eta|r) \right] \Delta_B^{(n)} \right\}, \\ \frac{\tilde{\gamma}_{\theta\theta}^{(n)}}{\tilde{\gamma}^*} &= (-1)^n w^{n-1} \frac{1}{\Delta} \left\{ \frac{1}{|\eta|r} R_1^{(n)}(|\eta|r) \Delta_A^{(n)} \right. \end{aligned}$$

$$\begin{aligned}
& -R_0^{(n)}(|\eta|r)\Delta_B^{(n)} \Big\}, \\
\frac{\tilde{\gamma}_{zz}^{(n)}}{\tilde{\gamma}^*} &= w^{n-1} \frac{1}{\Delta} \Big\{ -R_0^{(n)}(|\eta|r)\Delta_A^{(n)} \\
& + \left[(-1)^n 4(1 - \nu^{(n)})R_0^{(n)}(|\eta|r) \right. \\
& \left. + |\eta|r R_1^{(n)}(|\eta|r) \right] \Delta_B^{(n)} \Big\} + \delta_{n2}, \\
\frac{\tilde{\gamma}_{rz}^{(n)}}{\tilde{\gamma}^*} &= iw^{n-1} \frac{\text{sign}(\eta)}{\Delta} \Big\{ (-1)^{n+1} R_1^{(n)}(|\eta|r)\Delta_A^{(n)} \\
& + \left[(-1)^n |\eta|r R_0^{(n)}(|\eta|r) + 2(1 - \nu^{(n)})R_1^{(n)}(|\eta|r) \right] \Delta_B^{(n)} \Big\} \\
& \text{on } \tilde{\Omega}^{(n)}. \tag{4.13}
\end{aligned}$$

The Fourier transformed stresses for the matrix and the fiber are

$$\begin{aligned}
\frac{\tilde{u}_r^{(n)}}{\tilde{\gamma}^*} &= (-1)^n w^{n-1} \frac{1}{|\eta|\Delta} \Big\{ R_1^{(n)}(|\eta|r)\Delta_A^{(n)} \\
& - |\eta|r R_0^{(n)}(|\eta|r)\Delta_B^{(n)} \Big\}, \\
\frac{\tilde{u}_z^{(n)}}{\tilde{\gamma}^*} &= iw^{n-1} \frac{1}{\eta\Delta} \Big\{ -R_0^{(n)}(|\eta|r)\Delta_A^{(n)} \\
& + \left[(-1)^n 4(1 - \nu^{(n)})R_0^{(n)}(|\eta|r) \right. \\
& \left. + |\eta|r R_1^{(n)}(|\eta|r) \right] \Delta_B^{(n)} \Big\} + i\delta_{n2} \frac{1}{\eta} \\
& \text{on } \tilde{\Omega}^{(n)}. \tag{4.14}
\end{aligned}$$

For fixed r , all these ratios given in (4.11), (4.12), (4.13), and (4.14) are functions of the material properties of the matrix and the fiber as well as the geometry

parameter of the fiber through the radius a , but independent of the phase transformation in the fiber. If we consider the phase transformation in the fiber as input or excitation and the Love's stress function, stresses, strains, and displacements in the matrix and the fiber as outputs or responses, these ratios give the corresponding transfer functions, respectively. Theoretically, if we know the phase transformation characteristic function in the fiber, we can find the distributions of stress, strain, displacement in the matrix and the fiber through these ratios.

Multiplying these ratios (4.11), (4.12), (4.13), and (4.14) by $\tilde{\gamma}^*$ and performing inverse Fourier transform, one obtains the Love's stress functions, stresses, strains, and displacements of the matrix and the fiber in the original physical domains $\mathcal{R}^{(n)}$. The Love's stress functions are

$$\begin{aligned} \Phi^{(n)}(r, z) = & i \frac{E^{(1)}}{2\pi(1 + \nu^{(1)})} \int_{-\infty}^{\infty} \frac{1}{\eta^3 \Delta} \left[-\Delta_A^{(n)} R_0^{(n)}(|\eta|r) \right. \\ & \left. + \Delta_B^{(n)} |\eta|r R_1^{(n)}(|\eta|r) \right] \tilde{\gamma}^*(\eta) e^{-iz\eta} d\eta \quad \text{on } \Omega^{(n)}. \end{aligned} \quad (4.15)$$

The stresses can be written as the following forms

$$\begin{aligned} \sigma_{rr}^{(n)}(r, z) = & i \frac{E^{(1)}}{2\pi(1 + \nu^{(1)})} \int_{-\infty}^{\infty} \frac{1}{\Delta} \left\{ \left[R_0^{(n)}(|\eta|r) - \frac{(-1)^n}{|\eta|r} R_1^{(n)}(|\eta|r) \right] \Delta_A^{(n)} \right. \\ & \left. - \left[(-1)^n (1 - 2\nu^{(n)}) R_0^{(n)}(|\eta|r) + |\eta|r R_1^{(n)}(|\eta|r) \right] \Delta_B^{(n)} \right\} \tilde{\gamma}^*(\eta) e^{-iz\eta} d\eta, \\ \sigma_{\theta\theta}^{(n)}(r, z) = & \frac{E^{(1)}}{2\pi(1 + \nu^{(1)})} \int_{-\infty}^{\infty} \frac{(-1)^n}{\Delta} \left\{ \frac{1}{|\eta|r} R_1^{(n)}(|\eta|r) \Delta_A^{(n)} \right. \\ & \left. - (1 - 2\nu^{(n)}) R_0^{(n)}(|\eta|r) \Delta_B^{(n)} \right\} \tilde{\gamma}^*(\eta) e^{-iz\eta} d\eta, \\ \sigma_{zz}^{(n)}(r, z) = & \frac{E^{(1)}}{2\pi(1 + \nu^{(1)})} \int_{-\infty}^{\infty} \frac{1}{\Delta} \left\{ -R_0^{(n)}(|\eta|r) \Delta_A^{(n)} \right. \\ & \left. + \left[(-1)^n 2(2 - \nu^{(1)}) R_0^{(n)}(|\eta|r) + |\eta|r R_1^{(n)}(|\eta|r) \right] \Delta_B^{(n)} \right\} \tilde{\gamma}^*(\eta) e^{-iz\eta} d\eta, \end{aligned}$$

$$\begin{aligned}
\sigma_{rz}^{(n)}(r, z) &= i \frac{E^{(1)}}{2\pi(1+\nu^{(1)})} \int_{-\infty}^{\infty} \frac{\text{sign}(\eta)}{\Delta} \left\{ (-1)^{n+1} R_1^{(n)}(|\eta|r) \Delta_A^{(n)} \right. \\
&\quad \left. + \left[(-1)^n |\eta|r R_0^{(n)}(|\eta|r) + 2(1-\nu^{(1)}) R_1^{(n)}(|\eta|r) \right] \Delta_B^{(n)} \right\} \tilde{\gamma}^*(\eta) e^{-iz\eta} d\eta \\
&\quad \text{on } \Omega^{(n)}. \tag{4.16}
\end{aligned}$$

The strain components can be written as

$$\begin{aligned}
\gamma_{rr}^{(n)}(r, z) &= \frac{w^{n-1}}{2\pi} \int_{-\infty}^{\infty} \frac{1}{\Delta} \left\{ \left[R_0^{(n)}(|\eta|r) - \frac{(-1)^n}{|\eta|r} R_1^{(n)}(|\eta|r) \right] \Delta_A^{(n)} \right. \\
&\quad \left. - \left[(-1)^n R_0^{(n)}(|\eta|r) + |\eta|r R_1^{(n)}(|\eta|r) \right] \Delta_B^{(n)} \right\} \tilde{\gamma}^*(\eta) e^{-iz\eta} d\eta, \\
\gamma_{\theta\theta}^{(n)}(r, z) &= (-1)^n \frac{w^{n-1}}{2\pi} \int_{-\infty}^{\infty} \frac{1}{\Delta} \left\{ \frac{1}{|\eta|r} R_1^{(n)}(|\eta|r) \Delta_A^{(n)} \right. \\
&\quad \left. - R_0^{(n)}(|\eta|r) \Delta_B^{(n)} \right\} \tilde{\gamma}^*(\eta) e^{-iz\eta} d\eta, \\
\gamma_{zz}^{(n)}(r, z) &= \frac{w^{n-1}}{2\pi} \int_{-\infty}^{\infty} \frac{1}{\Delta} \left\{ -R_0^{(n)}(|\eta|r) \Delta_A^{(n)} \right. \\
&\quad \left. + \left[(-1)^n 4(1-\nu^{(n)}) R_0^{(n)}(|\eta|r) \right. \right. \\
&\quad \left. \left. + |\eta|r R_1^{(n)}(|\eta|r) \right] \Delta_B^{(n)} \right\} \tilde{\gamma}^*(\eta) e^{-iz\eta} d\eta + \delta_{n2} \gamma^*(z), \\
\gamma_{rz}^{(n)}(r, z) &= i \frac{w^{n-1}}{2\pi} \int_{-\infty}^{\infty} \frac{\text{sign}(\eta)}{\Delta} \left\{ (-1)^{n+1} R_1^{(n)}(|\eta|r) \Delta_A^{(n)} \right. \\
&\quad \left. + \left[(-1)^n |\eta|r R_0^{(n)}(|\eta|r) + 2(1-\nu^{(n)}) R_1^{(n)}(|\eta|r) \right] \Delta_B^{(n)} \right\} \tilde{\gamma}^*(\eta) e^{-iz\eta} d\eta \\
&\quad \text{on } \Omega^{(n)}. \tag{4.17}
\end{aligned}$$

The displacement components are

$$u_r^{(n)}(r, z) = (-1)^n \frac{w^{n-1}}{2\pi} \int_{-\infty}^{\infty} \frac{1}{|\eta|\Delta} \left\{ R_1^{(n)}(|\eta|r) \Delta_A^{(n)} \right.$$

where

direct

4.3 S

U

for g

(4.16)

only

form

the a

funct

In th

$$\begin{aligned}
& -|\eta|rR_0^{(n)}(|\eta|r)\Delta_B^{(n)}\} \tilde{\gamma}^*(\eta)e^{-iz\eta}d\eta, \\
u_z^{(n)}(r, z) = & i\frac{w^{n-1}}{2\pi} \int_{-\infty}^{\infty} \frac{1}{\eta\Delta} \left\{ -R_0^{(n)}(|\eta|r)\Delta_A^{(n)} \right. \\
& + \left[(-1)^n 4(1 - \nu^{(n)})R_0^{(n)}(|\eta|r) \right. \\
& \left. \left. + |\eta|rR_1^{(n)}(|\eta|r) \right] \Delta_B^{(n)} \right\} \tilde{\gamma}^*(\eta)e^{-iz\eta}d\eta + \delta_{n2}u^*(z) \\
& \text{on } \Omega^{(n)}, \tag{4.18}
\end{aligned}$$

where $u^*(z)$ is the displacement phase transformation function (2.65)

$$u^*(z) = \int_{z_0}^z \gamma^*(s)ds. \tag{4.19}$$

Alternatively, the (4.15), (4.16), (4.17), and (4.18) can also be obtained by directly substituting (4.8), (4.9), and (4.10) into (2.61), (2.62), (2.63), and (2.64).

4.3 Single Finite Segment Transformation

Under perfect bonding condition between fiber and matrix, the exact solutions for general phase transformation characteristic function γ^* are given by (4.15), (4.16), (4.17), and (4.18). In this section, we will look at the situation in which only a single finite segment of the fiber undergoes phase transformation.

Assuming only a single finite segment of length $2L$ of the fiber undergoes uniform phase transformation with a constant normal transformation strain γ^T along the axial direction of the fiber, i.e., $\Lambda = [-L, L]$, the transformation characteristic function is give by

$$\gamma^* = \gamma^*(z) \equiv \begin{cases} \gamma^T & |z| \leq L, \\ 0 & |z| > L. \end{cases} \tag{4.20}$$

In the Fourier transformed domain, one has from (2.21) that

$$\tilde{\gamma}^* = \tilde{\gamma}^*(\eta) = \frac{2\gamma^T}{\eta} \sin(L\eta). \tag{4.21}$$

Substituting (4.21) into (4.8), one has

$$\begin{aligned}
A^{(n)}(\eta) &= -i \frac{2E^{(1)}\gamma^T}{1 + \nu^{(1)}} \frac{\Delta_A^{(n)}}{\eta^4 \Delta} \sin(L\eta), \\
B^{(n)}(\eta) &= i \frac{2E^{(1)}\gamma^T}{1 + \nu^{(1)}} \frac{\Delta_B^{(n)}}{\eta^4 \Delta} \sin(L\eta), \\
-\infty &< \eta < \infty.
\end{aligned} \tag{4.22}$$

Using the normalized coordinates (\bar{r}, \bar{z}) and aspect ratio α defined by (2.68) and (2.69), one has

$$\begin{aligned}
\bar{A}^{(n)}(\bar{\eta}) &= A^{(n)}(\eta) \Big|_{\eta=\bar{\eta}/\alpha} = -i \frac{2E^{(1)}\gamma^T}{1 + \nu^{(1)}} \frac{\bar{\Delta}_A^{(n)}(\bar{\eta})}{\bar{\eta}^4 \bar{\Delta}(\bar{\eta})} \sin(\alpha\bar{\eta}), \\
\bar{B}^{(n)}(\bar{\eta}) &= B^{(n)}(\eta) \Big|_{\eta=\bar{\eta}/\alpha} = i \frac{2E^{(1)}\gamma^T}{1 + \nu^{(1)}} \frac{\bar{\Delta}_B^{(n)}(\bar{\eta})}{\bar{\eta}^4 \bar{\Delta}(\bar{\eta})} \sin(\alpha\bar{\eta}), \\
-\infty &< \bar{\eta} < \infty,
\end{aligned} \tag{4.23}$$

where $\bar{\Delta} = \bar{\Delta}(\bar{\eta}) = \Delta(\eta) \Big|_{\eta=\bar{\eta}/\alpha}$ is given by the determinant

$$\bar{\Delta}(\bar{\eta}) = \begin{vmatrix} \bar{q}_1^{(1)} & \bar{q}_2^{(1)} & -\bar{q}_1^{(2)} & -\bar{q}_2^{(2)} \\ \bar{q}_3^{(1)} & \bar{q}_4^{(1)} & -\bar{q}_3^{(2)} & -\bar{q}_4^{(2)} \\ \bar{q}_5^{(1)} & \bar{q}_6^{(1)} & w\bar{q}_5^{(2)} & w\bar{q}_6^{(2)} \\ \bar{q}_7^{(1)} & \bar{q}_8^{(1)} & -w\bar{q}_7^{(2)} & -w\bar{q}_8^{(2)} \end{vmatrix}, \tag{4.24}$$

$$-\infty < \bar{\eta} < \infty,$$

and $\bar{\Delta}_A^{(n)} = \bar{\Delta}_A^{(n)}(\bar{\eta}) = \Delta_A^{(n)}(\eta) \Big|_{\eta=\bar{\eta}/\alpha}$ and $\bar{\Delta}_B^{(n)} = \bar{\Delta}_B^{(n)}(\bar{\eta}) = \Delta_B^{(n)}(\eta) \Big|_{\eta=\bar{\eta}/\alpha}$ are given by

$$\bar{\Delta}_A^{(1)}(\bar{\eta}) = \begin{vmatrix} \bar{q}_2^{(1)} & -\bar{q}_1^{(2)} & -\bar{q}_2^{(2)} \\ \bar{q}_4^{(1)} & -\bar{q}_3^{(2)} & -\bar{q}_4^{(2)} \\ \bar{q}_6^{(1)} & w\bar{q}_5^{(2)} & w\bar{q}_6^{(2)} \end{vmatrix},$$

$$\bar{\Delta}_B^{(1)}(\bar{\eta}) = \begin{vmatrix} \bar{q}_1^{(1)} & -\bar{q}_1^{(2)} & -\bar{q}_2^{(2)} \\ \bar{q}_3^{(1)} & -\bar{q}_3^{(2)} & -\bar{q}_4^{(2)} \\ \bar{q}_5^{(1)} & w\bar{q}_5^{(2)} & w\bar{q}_6^{(2)} \end{vmatrix},$$

$$\bar{\Delta}_A^{(2)}(\bar{\eta}) = \begin{vmatrix} \bar{q}_1^{(1)} & \bar{q}_2^{(1)} & -\bar{q}_2^{(2)} \\ \bar{q}_3^{(1)} & \bar{q}_4^{(1)} & -\bar{q}_4^{(2)} \\ \bar{q}_5^{(1)} & \bar{q}_6^{(1)} & w\bar{q}_6^{(2)} \end{vmatrix},$$

$$\bar{\Delta}_B^{(2)}(\bar{\eta}) = \begin{vmatrix} \bar{q}_1^{(1)} & \bar{q}_2^{(1)} & -\bar{q}_1^{(2)} \\ \bar{q}_3^{(1)} & \bar{q}_4^{(1)} & -\bar{q}_3^{(2)} \\ \bar{q}_5^{(1)} & \bar{q}_6^{(1)} & w\bar{q}_5^{(2)} \end{vmatrix},$$

$$-\infty < \bar{\eta} < \infty. \quad (4.25)$$

And $\bar{q}_j^{(n)} = \bar{q}_j^{(n)}(\bar{\eta}) = q_j^{(n)}(\eta)|_{\eta=\bar{\eta}/a}$, $j = 1, 2, \dots, 8$, are

$$\bar{q}_1^{(n)}(\bar{\eta}) = R_0^{(n)}(|\bar{\eta}|) - \frac{(-1)^n}{|\bar{\eta}|} R_1^{(n)}(|\bar{\eta}|),$$

$$\bar{q}_2^{(n)}(\bar{\eta}) = (-1)^n(1 - 2\nu^{(n)})R_0^{(n)}(|\bar{\eta}|) + |\bar{\eta}|R_1^{(n)}(|\bar{\eta}|),$$

$$\bar{q}_3^{(n)}(\bar{\eta}) = (-1)^n R_1^{(n)}(|\bar{\eta}|),$$

$$\bar{q}_4^{(n)}(\bar{\eta}) = (-1)^n |\bar{\eta}| R_0^{(n)}(|\bar{\eta}|) + 2(1 - \nu^{(n)})R_1^{(n)}(|\bar{\eta}|),$$

$$\bar{q}_5^{(n)}(\bar{\eta}) = R_1^{(n)}(|\bar{\eta}|),$$

$$\bar{q}_6^{(n)}(\bar{\eta}) = |\bar{\eta}| R_0^{(n)}(|\bar{\eta}|),$$

$$\bar{q}_7^{(n)}(\bar{\eta}) = R_0^{(n)}(|\bar{\eta}|),$$

$$\begin{aligned} \bar{q}_8^{(n)}(\bar{\eta}) &= (-1)^n 4(1 - \nu^{(n)}) R_0^{(n)}(|\bar{\eta}|) + |\bar{\eta}| R_1^{(n)}(|\bar{\eta}|), \\ -\infty &< \bar{\eta} < \infty. \end{aligned} \quad (4.26)$$

Substituting (4.21) into (4.15), and then normalizing by (2.68) and (2.69), or directly substituting (4.22) into (2.71), one obtains the Love's stress functions in the normalized coordinates. Noticing that the imaginary parts of the integrands are odd functions of $\bar{\eta}$, the Love's stress functions, in the normalized coordinate, have the following forms

$$\begin{aligned} \bar{\Phi}^{(n)}(\bar{r}, \bar{z}) &= \frac{E^{(1)} \gamma^T a^3}{\pi(1 + \nu^{(1)})} \int_{-\infty}^{\infty} \frac{1}{\bar{\eta}^4 \bar{\Delta}} \left[-\bar{\Delta}_A^{(n)} R_0^{(n)}(|\bar{\eta}| \bar{r}) \right. \\ &\quad \left. + \bar{\Delta}_B^{(n)} |\bar{\eta}| \bar{r} R_1^{(n)}(|\bar{\eta}| \bar{r}) \right] \sin(\alpha \bar{\eta}) \sin(\alpha \bar{z} \bar{\eta}) d\bar{\eta} \quad \text{on } \Omega^{(n)}. \end{aligned} \quad (4.27)$$

Similarly, substituting (4.22) into (2.75), (2.76), and (2.78), and considering that the imaginary parts of the integrands are odd functions of $\bar{\eta}$, one has distributions of stress, strain, and displacement in the normalized coordinates. The stresses, in the normalized coordinates, are

$$\begin{aligned} \bar{\sigma}_{\bar{r}\bar{r}}^{(n)}(\bar{r}, \bar{z}) &= \frac{E^{(1)} \gamma^T}{(1 + \nu^{(1)}) \pi} \int_{-\infty}^{\infty} \frac{1}{\bar{\eta} \bar{\Delta}} \left\{ \left[R_0^{(n)}(|\bar{\eta}| \bar{r}) \right. \right. \\ &\quad \left. \left. - \frac{(-1)^n}{|\bar{\eta}| \bar{r}} R_1^{(n)}(|\bar{\eta}| \bar{r}) \right] \bar{\Delta}_A^{(n)} - \left[(-1)^n (1 - 2\nu^{(n)}) R_0^{(n)}(|\bar{\eta}| \bar{r}) \right. \right. \\ &\quad \left. \left. + |\bar{\eta}| \bar{r} R_1^{(n)}(|\bar{\eta}| \bar{r}) \right] \bar{\Delta}_B^{(n)} \right\} \sin(\alpha \bar{\eta}) \cos(\alpha \bar{z} \bar{\eta}) d\bar{\eta}, \\ \bar{\sigma}_{\bar{\theta}\bar{\theta}}^{(n)}(\bar{r}, \bar{z}) &= \frac{E^{(1)} \gamma^T}{(1 + \nu^{(1)}) \pi} \int_{-\infty}^{\infty} \frac{(-1)^n}{\bar{\eta} \bar{\Delta}} \left\{ \frac{1}{|\bar{\eta}| \bar{r}} R_1^{(n)}(|\bar{\eta}| \bar{r}) \bar{\Delta}_A^{(n)} \right. \\ &\quad \left. - (1 - 2\nu^{(n)}) R_0^{(n)}(|\bar{\eta}| \bar{r}) \bar{\Delta}_B^{(n)} \right\} \sin(\alpha \bar{\eta}) \cos(\alpha \bar{z} \bar{\eta}) d\bar{\eta}, \end{aligned}$$

$$\begin{aligned}
\bar{\sigma}_{zz}^{(n)}(\bar{r}, \bar{z}) &= \frac{E^{(1)}\gamma^T}{(1+\nu^{(1)})\pi} \int_{-\infty}^{\infty} \frac{1}{\bar{\eta}\bar{\Delta}} \left\{ -R_0^{(n)}(|\bar{\eta}|\bar{r})\bar{\Delta}_A^{(n)} \right. \\
&\quad + \left[(-1)^n 2(2-\nu^{(1)})R_0^{(n)}(|\bar{\eta}|\bar{r}) \right. \\
&\quad \left. \left. + |\bar{\eta}|\bar{r}R_1^{(n)}(|\bar{\eta}|\bar{r}) \right] \bar{\Delta}_B^{(n)} \right\} \sin(\alpha\bar{\eta})\cos(\alpha\bar{z}\bar{\eta})d\bar{\eta}, \\
\bar{\sigma}_{rz}^{(n)}(\bar{r}, \bar{z}) &= \frac{E^{(1)}\gamma^T}{(1+\nu^{(1)})\pi} \int_{-\infty}^{\infty} \frac{1}{|\bar{\eta}|\bar{\Delta}} \left\{ (-1)^{n+1}R_1^{(n)}(|\bar{\eta}|\bar{r})\bar{\Delta}_A^{(n)} \right. \\
&\quad + \left[(-1)^n |\bar{\eta}|\bar{r}R_0^{(n)}(|\bar{\eta}|\bar{r}) \right. \\
&\quad \left. \left. + 2(1-\nu^{(1)})R_1^{(n)}(|\bar{\eta}|\bar{r}) \right] \bar{\Delta}_B^{(n)} \right\} \sin(\alpha\bar{\eta})\sin(\alpha\bar{z}\bar{\eta})d\bar{\eta} \\
&\quad \text{on } \bar{\Omega}^{(n)}. \tag{4.28}
\end{aligned}$$

The strain components, in terms of normalized coordinates, are

$$\begin{aligned}
\bar{\gamma}_{rr}^{(n)}(\bar{r}, \bar{z}) &= \frac{\gamma^T w^{n-1}}{\pi} \int_{-\infty}^{\infty} \frac{1}{\bar{\eta}\bar{\Delta}} \left\{ \left[R_0^{(n)}(|\bar{\eta}|\bar{r}) \right. \right. \\
&\quad \left. \left. - \frac{(-1)^n}{|\bar{\eta}|\bar{r}} R_1^{(n)}(|\bar{\eta}|\bar{r}) \right] \bar{\Delta}_A^{(n)} - \left[(-1)^n R_0^{(n)}(|\bar{\eta}|\bar{r}) \right. \right. \\
&\quad \left. \left. + |\bar{\eta}|\bar{r}R_1^{(n)}(|\bar{\eta}|\bar{r}) \right] \bar{\Delta}_B^{(n)} \right\} \sin(\alpha\bar{\eta})\cos(\alpha\bar{z}\bar{\eta})d\bar{\eta}, \\
\bar{\gamma}_{\theta\theta}^{(n)}(\bar{r}, \bar{z}) &= (-1)^n \frac{\gamma^T w^{n-1}}{\pi} \int_{-\infty}^{\infty} \frac{1}{\bar{\eta}\bar{\Delta}} \left\{ \frac{1}{|\bar{\eta}|\bar{r}} R_1^{(n)}(|\bar{\eta}|\bar{r})\bar{\Delta}_A^{(n)} \right. \\
&\quad \left. - R_0^{(n)}(|\bar{\eta}|\bar{r})\bar{\Delta}_B^{(n)} \right\} \sin(\alpha\bar{\eta})\cos(\alpha\bar{z}\bar{\eta})d\bar{\eta}, \\
\bar{\gamma}_{zz}^{(n)}(\bar{r}, \bar{z}) &= \frac{\gamma^T w^{n-1}}{\pi} \int_{-\infty}^{\infty} \frac{1}{\bar{\eta}\bar{\Delta}} \left\{ -R_0^{(n)}(|\bar{\eta}|\bar{r})\bar{\Delta}_A^{(n)} \right. \\
&\quad + \left[(-1)^n 4(1-\nu^{(n)})R_0^{(n)}(|\bar{\eta}|\bar{r}) \right. \\
&\quad \left. \left. + |\bar{\eta}|\bar{r}R_1^{(n)}(|\bar{\eta}|\bar{r}) \right] \bar{\Delta}_B^{(n)} \right\} \sin(\alpha\bar{\eta})\cos(\alpha\bar{z}\bar{\eta})d\bar{\eta} + \delta_{n2}\bar{\gamma}^*,
\end{aligned}$$

$$\begin{aligned}
\bar{\gamma}_{rz}^{(n)}(\bar{r}, \bar{z}) &= \frac{\gamma^T w^{n-1}}{\pi} \int_{-\infty}^{\infty} \frac{1}{|\bar{\eta}| \bar{\Delta}} \left\{ (-1)^{n+1} R_1^{(n)}(|\bar{\eta}| \bar{r}) \bar{\Delta}_A^{(n)} \right. \\
&\quad + \left[(-1)^n |\bar{\eta}| \bar{r} R_0^{(n)}(|\bar{\eta}| \bar{r}) \right. \\
&\quad \left. \left. + 2(1 - \nu^{(n)}) R_1^{(n)}(|\bar{\eta}| \bar{r}) \right] \bar{\Delta}_B^{(n)} \right\} \sin(\alpha \bar{\eta}) \sin(\alpha \bar{z} \bar{\eta}) d\bar{\eta} \\
&\quad \text{on } \bar{\Omega}^{(n)}, \tag{4.29}
\end{aligned}$$

where

$$\bar{\gamma}^* = \bar{\gamma}^*(\bar{z}) \equiv \begin{cases} \gamma^T & |\bar{z}| \leq 1, \\ 0 & |\bar{z}| > 1. \end{cases} \tag{4.30}$$

The displacement components, in terms of \bar{r} and \bar{z} , are

$$\begin{aligned}
\bar{u}_r^{(n)}(\bar{r}, \bar{z}) &= (-1)^n \frac{\alpha \gamma^T w^{n-1}}{\pi} \int_{-\infty}^{\infty} \frac{1}{\bar{\eta} |\bar{\eta}| \bar{\Delta}} \left\{ R_1^{(n)}(|\bar{\eta}| \bar{r}) \bar{\Delta}_A^{(n)} \right. \\
&\quad \left. - |\bar{\eta}| \bar{r} R_0^{(n)}(|\bar{\eta}| \bar{r}) \bar{\Delta}_B^{(n)} \right\} \sin(\alpha \bar{\eta}) \cos(\alpha \bar{z} \bar{\eta}) d\bar{\eta}, \\
\bar{u}_z^{(n)}(\bar{r}, \bar{z}) &= \frac{\alpha \gamma^T w^{n-1}}{\pi} \int_{-\infty}^{\infty} \frac{1}{\bar{\eta}^2 \bar{\Delta}} \left\{ -R_0^{(n)}(|\bar{\eta}| \bar{r}) \bar{\Delta}_A^{(n)} \right. \\
&\quad + \left[(-1)^n 4(1 - \nu^{(n)}) R_0^{(n)}(|\bar{\eta}| \bar{r}) \right. \\
&\quad \left. \left. + |\bar{\eta}| \bar{r} R_1^{(n)}(|\bar{\eta}| \bar{r}) \right] \bar{\Delta}_B^{(n)} \right\} \sin(\alpha \bar{\eta}) \sin(\alpha \bar{z} \bar{\eta}) d\bar{\eta} + \delta_{n2} \bar{u}^* \\
&\quad \text{on } \bar{\Omega}^{(n)}. \tag{4.31}
\end{aligned}$$

where

$$\bar{u}^* = \bar{u}^*(z) \equiv \begin{cases} \gamma^T L & \bar{z} > 1, \\ \gamma^T L \bar{z} & |\bar{z}| \leq 1, \\ -\gamma^T L & \bar{z} < -1. \end{cases} \tag{4.32}$$

4.4 Numerical Evaluation

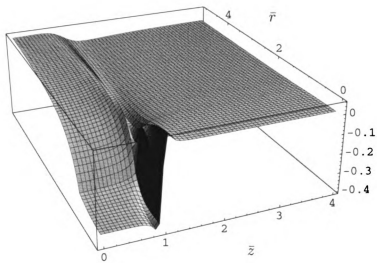
In order to illustrate the results obtained, we present the numerical evaluation for the case that a single finite segment of the fiber undergoes phase transformation. The calculations are performed using Mathematica. In the calculation, we take the ratio as $w = 0.000096$, the Poisson's ratios $\nu^{(1)} = 0.35$ and $\nu^{(2)} = 0.29$.

Figures 4.1 – 4.3 show the 3D plots of the stress distributions, the strain distributions, and the displacement fields for the case that the aspect ratio $\alpha = 10$.

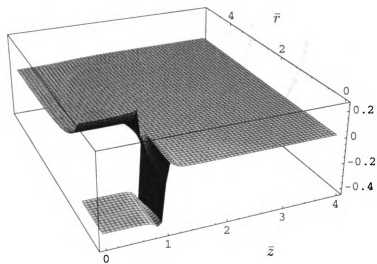
Figure 4.4 displays the distributions of the stresses of the matrix on the fiber-matrix interface for $\alpha = 10$. It is shown that across the phase boundary ($\bar{z} = 1$), as in the “rigid fiber” model, the normal stresses have finite jumps, whereas the shear stress seems to approach infinity. Outside of the transformed region, the normal stresses are very small compared with the shear stress.

Figure 4.5 displays the distributions of the stresses of the fiber on the fiber-matrix interface for $\alpha = 10$. The same as the matrix, across the phase boundary ($\bar{z} = 1$), the normal stresses of the fiber have finite jumps, whereas the shear stress seems approach to infinity. Unlike the matrix, on the other hand, the longitudinal normal stress $\sigma_{zz}^{(2)}$ is the dominant component of stress in whole fiber, except near phase boundary ($\bar{z} = 1$) where the shear stress $\sigma_{rz}^{(2)}$ has an infinity singularity.

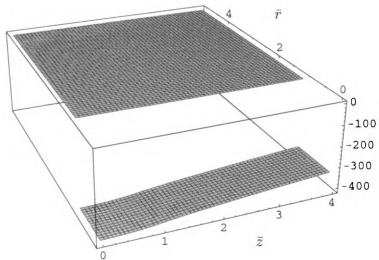
The dominant compress stress in the fiber comes from the resistance of the matrix to the relative move of the fiber induced by the phase transformation. As the result of the compress stress, the phase transformation in the fiber is constrained. The constrained (elastic) strain of the fiber in the phase transformed segment is $\bar{\gamma}_{zz}^{(2)} - \gamma^T$, which reaches the maximum value at the middle of the fiber-matrix interface of phase transformed region in the fiber, i.e., at $(\bar{r}, \bar{z}) = (1, 0)$. Figure 4.6 plots the relation between the maximum constrained strain in the fiber and the logarithm ratio w for $\alpha = 1, 10, \text{ and } 100$, with $\nu^{(1)} = \nu^{(2)} = 0.3$. It is shown that the maximum constrained strain in the fiber increases with the increase of either w



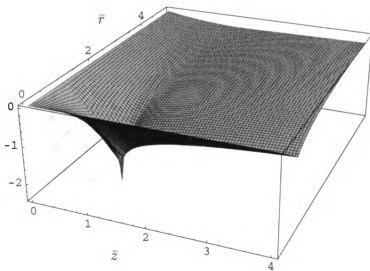
(a) $\frac{\bar{\sigma}_{rr}}{E^{(1)}\gamma T}$



(b) $\frac{\bar{\sigma}_{\theta\theta}}{E^{(1)}\gamma T}$

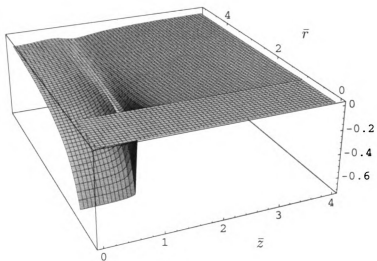


(c) $\frac{\bar{\sigma}_{zz}}{E^{(1)}\gamma T}$

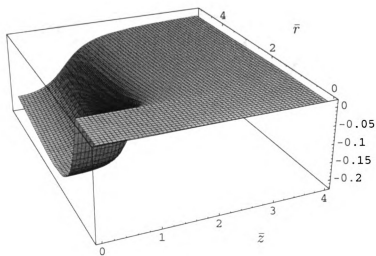


(d) $\frac{\bar{\sigma}_{rz}}{E^{(1)}\gamma T}$

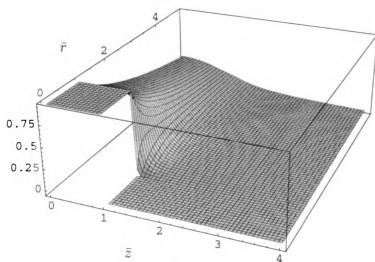
Figure 4.1. The 3D plots of stress distributions for $w = 0.000096$, $\nu^{(1)} = 0.35$, $\nu^{(2)} = 0.29$, and $\alpha = 10$. (a) $\frac{\bar{\sigma}_{rr}}{E^{(1)}\gamma T}$, (b) $\frac{\bar{\sigma}_{\theta\theta}}{E^{(1)}\gamma T}$, (c) $\frac{\bar{\sigma}_{zz}}{E^{(1)}\gamma T}$, and (d) $\frac{\bar{\sigma}_{rz}}{E^{(1)}\gamma T}$.



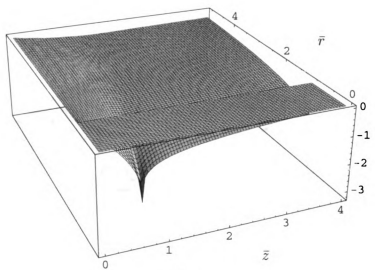
(a) $\frac{\bar{v}_r}{\gamma T}$



(b) $\frac{\bar{v}_\theta}{\gamma T}$

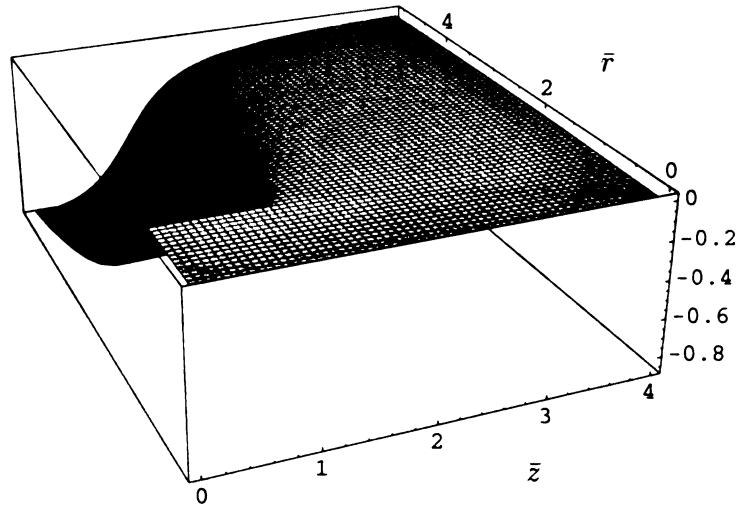


(c) $\frac{\tilde{\gamma}_{z\bar{z}}}{\gamma_T}$

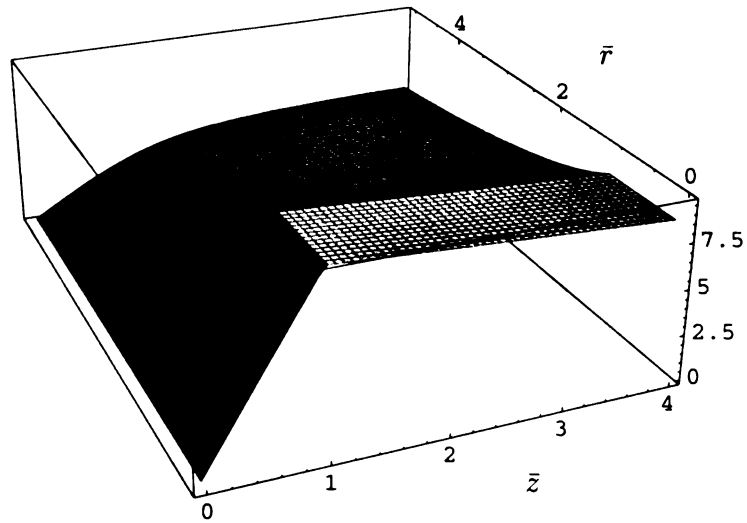


(d) $\frac{\tilde{\gamma}_{r\bar{r}}}{\gamma_T}$

Figure 4.2. The 3D plots of strain distributions for $w = 0.000096$, $\nu^{(1)} = 0.35$, $\nu^{(2)} = 0.29$, and $\alpha = 10$. (a) $\frac{\tilde{\gamma}_{r\bar{r}}}{\gamma_T}$, (b) $\frac{\tilde{\gamma}_{\theta\bar{\theta}}}{\gamma_T}$, (c) $\frac{\tilde{\gamma}_{z\bar{z}}}{\gamma_T}$, and (d) $\frac{\tilde{\gamma}_{r\bar{r}}}{\gamma_T}$.



(a) $\frac{\bar{u}_r}{a\gamma T}$



(b) $\frac{\bar{u}_z}{a\gamma T}$

Figure 4.3. The 3D plots of displacements for $w = 0.000096$, $\nu^{(1)} = 0.35$, $\nu^{(2)} = 0.29$, and $\alpha = 10$. (a) $\frac{\bar{u}_r}{a\gamma T}$, and (b) $\frac{\bar{u}_z}{a\gamma T}$.

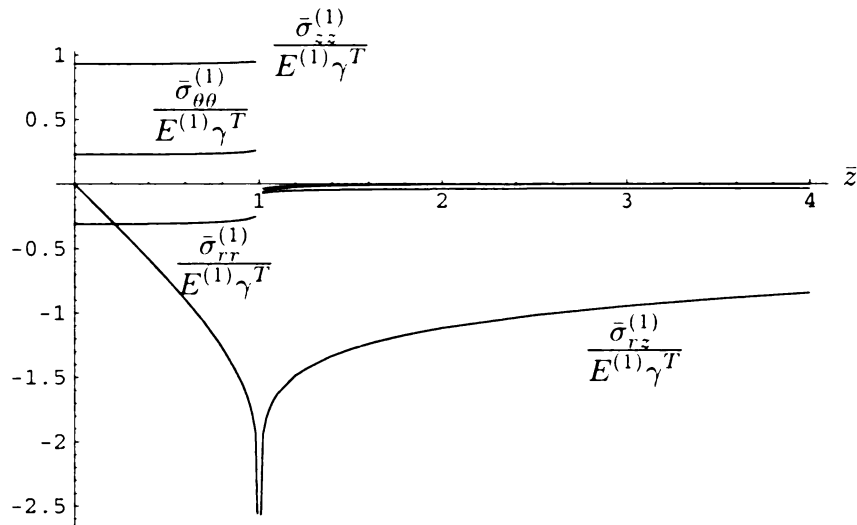


Figure 4.4. The stress distributions of the matrix on the fiber-matrix interface for $w = 0.000096$, $\nu^{(1)} = 0.35$, $\nu^{(2)} = 0.29$, and $\alpha = 10$.

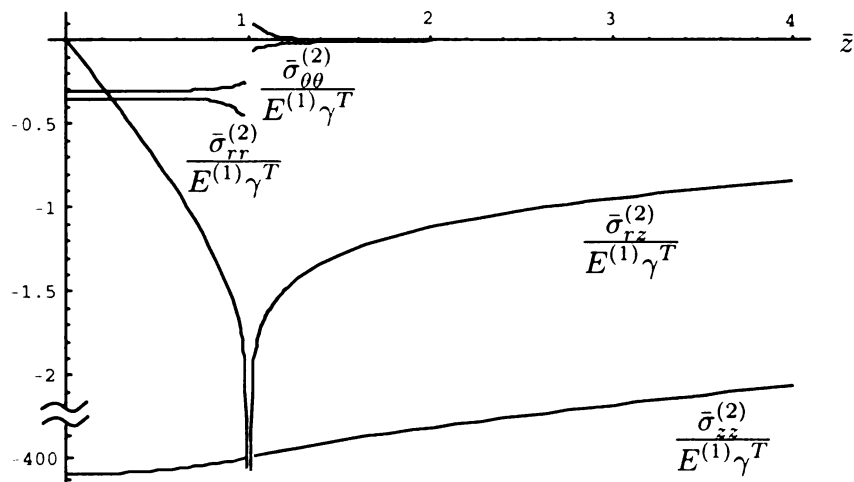


Figure 4.5. The stress distributions of the fiber on the fiber-matrix interface for $w = 0.000096$, $\nu^{(1)} = 0.35$, $\nu^{(2)} = 0.29$, and $\alpha = 10$.

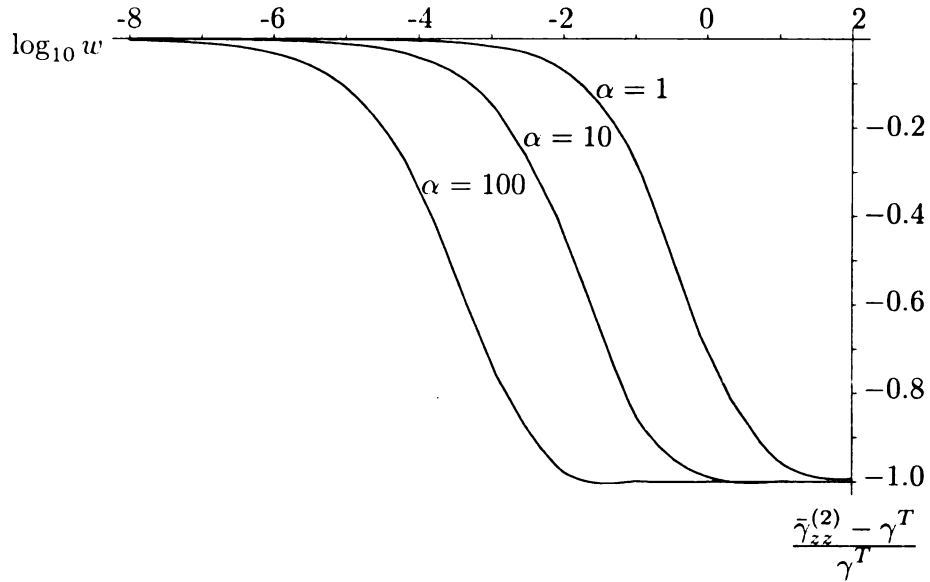


Figure 4.6. The maximum constrained strain in the fiber, $\frac{\bar{\gamma}_{zz}^{(2)} - \gamma^T}{\gamma^T}$, against the logarithm of w for $\alpha = 1, 10,$ and 100 , with $\nu^{(1)} = \nu^{(2)} = 0.3$. Here, w is the ratio of the shear modulus of the fiber $G^{(1)}$ to the shear modulus of the matrix $G^{(2)}$:

$$w = \frac{G^{(1)}}{G^{(2)}} = \frac{(1 + \nu^{(2)})E^{(1)}}{(1 + \nu^{(1)})E^{(2)}}.$$

or α . The fact that the maximum constrained strain in the fiber increases with w means that stiffer matrix exerts greater constraint on the phase transformation of the fiber. On the other hand, the fact that the maximum constrained strain in the fiber increases with α could conclude that, in the setting of composite, the phase transformation in the fiber prefers a configuration with multi-piece small transformed segments to keep small α instead of a large transformed segment to avoid greater constraint from the matrix.

4.5 Reduction to the Perfect Bonding Rigid Fiber Model

For the situation that the SMA fiber is much stronger than the matrix, one has $w \rightarrow 0$ from (4.7). For the fiber ($n = 2$), this is equivalent to that $E^{(2)}$ is finite and $E^{(1)} \rightarrow 0$. From (4.17), (4.18), and (4.16), one has the constraint free deformation in the fiber:

$$\gamma_{rr}^{(2)} = \gamma_{\theta\theta}^{(2)} = \gamma_{rz}^{(2)} = 0, \quad \gamma_{zz}^{(2)} = \gamma^* \quad \text{on } \Omega^{(2)}, \quad (4.33)$$

$$u_r^{(2)} = 0, \quad u_z^{(2)} = u^* \quad \text{on } \Omega^{(2)}, \quad (4.34)$$

and

$$\sigma_{rr}^{(2)} = \sigma_{\theta\theta}^{(2)} = \sigma_{zz}^{(2)} = \sigma_{rz}^{(2)} = 0, \quad \text{on } \Omega^{(2)}. \quad (4.35)$$

For the matrix ($n = 1$), the condition that $w \rightarrow 0$ is equivalent to that $E^{(1)}$ is finite and $E^{(2)} \rightarrow \infty$. Notice that as $w = 0$, (4.9) and (4.10) lead to the relations

$$\begin{aligned} \Delta(\eta) &= \Delta^{(1)}(\eta) \cdot \Delta^{(2)}(\eta), \\ \Delta_A^{(1)}(\eta) &= |\eta| a K_0(|\eta| a) \cdot \Delta^{(2)}(\eta), \\ \Delta_B^{(1)}(\eta) &= K_1(|\eta| a) \cdot \Delta^{(2)}(\eta), \end{aligned} \quad (4.36)$$

where

$$\Delta^{(2)}(\eta) = \begin{vmatrix} q_1^{(2)} & q_2^{(2)} \\ q_3^{(2)} & q_4^{(2)} \end{vmatrix},$$

$$\Delta^{(1)}(\eta) = -|\eta|aK_0^2(|\eta|a) - 4(1 - \nu^{(1)})K_0(|\eta|a)K_1(|\eta|a) + |\eta|aK_1^2(|\eta|a). \quad (4.37)$$

Substituting the above (4.36) and (4.37) into (4.15), (4.16), (4.17), and (4.18), and canceling $\Delta^{(2)}$, the results are consistent with (3.12), (3.13), (3.14), and (3.15), respectively, for the “perfect bonding rigid fiber” model discussed in the previous chapter.

Similarly, for the case of single finite segment transform with the normalized transformation characteristic function $\bar{\gamma}^*$ given by (4.30), it shows that as $w \rightarrow 0$, the results (4.27), (4.28), (4.29), and (4.31) reduce to (3.22), (3.23), (3.24), and (3.25), respectively.

4.6 Approximations of the Stress Distributions

In order to further observe the behavior of the exact solution for stresses, we develop the approximate expressions. Our attention is focused on (4.28) for the case that a single finite segment of fiber undergoes phase transformation. For simple, we introduce the following notations in this chapter:

$$\begin{aligned} \bar{\Delta}_{rr}^{(n)}(\bar{r}; \bar{\eta}) &= \left[R_0^{(n)}(|\bar{\eta}|\bar{r}) - \frac{(-1)^n}{|\bar{\eta}|\bar{r}} R_1^{(n)}(|\bar{\eta}|\bar{r}) \right] \bar{\Delta}_A^{(n)} \\ &\quad - \left[(-1)^n (1 - 2\nu^{(n)}) R_0^{(n)}(|\bar{\eta}|\bar{r}) + |\bar{\eta}|\bar{r} R_1^{(n)}(|\bar{\eta}|\bar{r}) \right] \bar{\Delta}_B^{(n)}, \\ \bar{\Delta}_{\theta\theta}^{(n)}(\bar{r}; \bar{\eta}) &= (-1)^n \left[\frac{1}{|\bar{\eta}|\bar{r}} R_1^{(n)}(|\bar{\eta}|\bar{r}) \bar{\Delta}_A^{(n)} - (1 - 2\nu^{(n)}) R_0^{(n)}(|\bar{\eta}|\bar{r}) \bar{\Delta}_B^{(n)} \right], \\ \bar{\Delta}_{zz}^{(n)}(\bar{r}; \bar{\eta}) &= -R_0^{(n)}(|\bar{\eta}|\bar{r}) \bar{\Delta}_A^{(n)} + \left[(-1)^n 2(2 - \nu^{(n)}) R_0^{(n)}(|\bar{\eta}|\bar{r}) \right. \\ &\quad \left. + |\bar{\eta}|\bar{r} R_1^{(n)}(|\bar{\eta}|\bar{r}) \right] \bar{\Delta}_B^{(n)}, \\ \bar{\Delta}_{rz}^{(n)}(\bar{r}; \bar{\eta}) &= -(-1)^n R_1^{(n)}(|\bar{\eta}|\bar{r}) \bar{\Delta}_A^{(n)} + \left[(-1)^n |\bar{\eta}|\bar{r} R_0^{(n)}(|\bar{\eta}|\bar{r}) \right. \end{aligned}$$

$$+2(1 - \nu^{(n)})R_1^{(n)}(|\bar{\eta}|\bar{r})\bar{\Delta}_B^{(n)} \quad \text{on } \bar{\Omega}^{(n)}. \quad (4.38)$$

Noting that the integrands in (4.28) are even functions about $\bar{\eta}$ and using notations (4.38), the stress components can be written as

$$\begin{aligned} \bar{\sigma}_{rr}^{(n)}(\bar{r}, \bar{z}) &= \frac{2E^{(1)}\gamma^T}{\pi(1 + \nu^{(1)})} \int_0^\infty \frac{\bar{\Delta}_{rr}^{(n)}(\bar{r}, \bar{\eta})}{\bar{\eta}\bar{\Delta}(\bar{\eta})} \sin(\alpha\bar{\eta})\cos(\alpha\bar{z}\bar{\eta})d\bar{\eta}, \\ \bar{\sigma}_{\theta\theta}^{(n)}(\bar{r}, \bar{z}) &= \frac{2E^{(1)}\gamma^T}{\pi(1 + \nu^{(1)})} \int_0^\infty \frac{\bar{\Delta}_{\theta\theta}^{(n)}(\bar{r}, \bar{\eta})}{\bar{\eta}\bar{\Delta}(\bar{\eta})} \sin(\alpha\bar{\eta})\cos(\alpha\bar{z}\bar{\eta})d\bar{\eta}, \\ \bar{\sigma}_{zz}^{(n)}(\bar{r}, \bar{z}) &= \frac{2E^{(1)}\gamma^T}{\pi(1 + \nu^{(1)})} \int_0^\infty \frac{\bar{\Delta}_{zz}^{(n)}(\bar{r}, \bar{\eta})}{\bar{\eta}\bar{\Delta}(\bar{\eta})} \sin(\alpha\bar{\eta})\cos(\alpha\bar{z}\bar{\eta})d\bar{\eta}, \\ \bar{\sigma}_{rz}^{(n)}(\bar{r}, \bar{z}) &= \frac{2E^{(1)}\gamma^T}{\pi(1 + \nu^{(1)})} \int_0^\infty \frac{\bar{\Delta}_{rz}^{(n)}(\bar{r}, \bar{\eta})}{\bar{\eta}\bar{\Delta}(\bar{\eta})} \sin(\alpha\bar{\eta})\sin(\alpha\bar{z}\bar{\eta})d\bar{\eta} \quad \text{on } \bar{\Omega}^{(n)}. \end{aligned} \quad (4.39)$$

Decomposing the integrals into two parts by dividing the interval of integration into $(0, s)$ and (s, ∞) for some $s > 0$, one has

$$\begin{aligned} \bar{\sigma}_{rr}^{(n)}(\bar{r}, \bar{z}) &= \frac{2E^{(1)}\gamma^T}{\pi(1 + \nu^{(1)})} \int_0^s \frac{\bar{\Delta}_{rr}^{(n)}(\bar{r}, \bar{\eta})}{\bar{\eta}\bar{\Delta}(\bar{\eta})} \sin(\alpha\bar{\eta})\cos(\alpha\bar{z}\bar{\eta})d\bar{\eta} \\ &\quad + \frac{2E^{(1)}\gamma^T}{\pi(1 + \nu^{(1)})} \int_s^\infty \frac{\bar{\Delta}_{rr}^{(n)}(\bar{r}, \bar{\eta})}{\bar{\eta}\bar{\Delta}(\bar{\eta})} \sin(\alpha\bar{\eta})\cos(\alpha\bar{z}\bar{\eta})d\bar{\eta}, \\ \bar{\sigma}_{\theta\theta}^{(n)}(\bar{r}, \bar{z}) &= \frac{2E^{(1)}\gamma^T}{\pi(1 + \nu^{(1)})} \int_0^s \frac{\bar{\Delta}_{\theta\theta}^{(n)}(\bar{r}, \bar{\eta})}{\bar{\eta}\bar{\Delta}(\bar{\eta})} \sin(\alpha\bar{\eta})\cos(\alpha\bar{z}\bar{\eta})d\bar{\eta} \\ &\quad + \frac{2E^{(1)}\gamma^T}{\pi(1 + \nu^{(1)})} \int_s^\infty \frac{\bar{\Delta}_{\theta\theta}^{(n)}(\bar{r}, \bar{\eta})}{\bar{\eta}\bar{\Delta}(\bar{\eta})} \sin(\alpha\bar{\eta})\cos(\alpha\bar{z}\bar{\eta})d\bar{\eta}, \\ \bar{\sigma}_{zz}^{(n)}(\bar{r}, \bar{z}) &= \frac{2E^{(1)}\gamma^T}{\pi(1 + \nu^{(1)})} \int_0^s \frac{\bar{\Delta}_{zz}^{(n)}(\bar{r}, \bar{\eta})}{\bar{\eta}\bar{\Delta}(\bar{\eta})} \sin(\alpha\bar{\eta})\cos(\alpha\bar{z}\bar{\eta})d\bar{\eta} \\ &\quad + \frac{2E^{(1)}\gamma^T}{\pi(1 + \nu^{(1)})} \int_s^\infty \frac{\bar{\Delta}_{zz}^{(n)}(\bar{r}, \bar{\eta})}{\bar{\eta}\bar{\Delta}(\bar{\eta})} \sin(\alpha\bar{\eta})\cos(\alpha\bar{z}\bar{\eta})d\bar{\eta}, \\ \bar{\sigma}_{rz}^{(n)}(\bar{r}, \bar{z}) &= \frac{2E^{(1)}\gamma^T}{\pi(1 + \nu^{(1)})} \int_0^s \frac{\bar{\Delta}_{rz}^{(n)}(\bar{r}, \bar{\eta})}{\bar{\eta}\bar{\Delta}(\bar{\eta})} \sin(\alpha\bar{\eta})\sin(\alpha\bar{z}\bar{\eta})d\bar{\eta} \end{aligned}$$

$$\begin{aligned}
& + \frac{2E^{(1)}\gamma^T}{\pi(1+\nu^{(1)})} \int_s^\infty \frac{\bar{\Delta}_{rz}^{(n)}(\bar{r}, \bar{\eta})}{\bar{\eta}\bar{\Delta}(\bar{\eta})} \sin(\alpha\bar{\eta})\sin(\alpha\bar{z}\bar{\eta})d\bar{\eta} \\
& \text{on } \bar{\Omega}^{(n)}. \tag{4.40}
\end{aligned}$$

First, we consider the second integrals in (4.40). To develop approximate expressions, we use the asymptotic expansions (2.81) for the modified Bessel functions as $\bar{\eta} \rightarrow \infty$. Substituting (2.81) into (4.26), one has the asymptotic expansions for $\bar{q}_k^{(n)}(\bar{\eta})$, $k = 1, 2, \dots, 8$,

$$q_1^{(n)}(\bar{\eta}) \sim \sqrt{\frac{1}{2\pi(-1)^n\bar{\eta}}} e^{(-1)^n\bar{\eta}} \left[1 - (-1)^n \frac{7}{8\bar{\eta}} + \frac{57}{128\bar{\eta}^2} + (-1)^n \frac{195}{1024\bar{\eta}^3} + \dots \right],$$

$$\begin{aligned}
q_2^{(n)}(\bar{\eta}) \sim & \sqrt{\frac{1}{2\pi(-1)^n\bar{\eta}}} e^{(-1)^n\bar{\eta}} \left[\bar{\eta} + (-1)^n \frac{5 - 16\nu^{(n)}}{8} + \frac{1 - 32\nu^{(n)}}{128\bar{\eta}} \right. \\
& \left. + (-1)^n \frac{-33 - 144\nu^{(n)}}{1024\bar{\eta}^2} + \dots \right],
\end{aligned}$$

$$q_3^{(n)}(\bar{\eta}) \sim \sqrt{\frac{1}{2\pi(-1)^n\bar{\eta}}} e^{(-1)^n\bar{\eta}} \left[(-1)^n - \frac{3}{8\bar{\eta}} - (-1)^n \frac{15}{128\bar{\eta}^2} - \frac{105}{1024\bar{\eta}^3} + \dots \right],$$

$$\begin{aligned}
q_4^{(n)}(\bar{\eta}) \sim & \sqrt{\frac{1}{2\pi(-1)^n\bar{\eta}}} e^{(-1)^n\bar{\eta}} \left[(-1)^n\bar{\eta} + \frac{17 - 16\nu^{(n)}}{8} - (-1)^n \frac{87 - 96\nu^{(n)}}{128\bar{\eta}} \right. \\
& \left. - \frac{165 - 240\nu^{(n)}}{1024\bar{\eta}^2} + \dots \right],
\end{aligned}$$

$$q_5^{(n)}(\bar{\eta}) \sim \sqrt{\frac{1}{2\pi(-1)^n\bar{\eta}}} e^{(-1)^n\bar{\eta}} \left[1 + (-1)^n \frac{3}{8\bar{\eta}} - \frac{15}{128\bar{\eta}^2} - (-1)^n \frac{105}{1024\bar{\eta}^3} + \dots \right],$$

$$q_6^{(n)}(\bar{\eta}) \sim \sqrt{\frac{1}{2\pi(-1)^n\bar{\eta}}} e^{(-1)^n\bar{\eta}} \left[\bar{\eta} + (-1)^n \frac{1}{8} + \frac{9}{128\bar{\eta}} + (-1)^n \frac{75}{1024\bar{\eta}^2} + \dots \right],$$

$$q_7^{(n)}(\bar{\eta}) \sim \sqrt{\frac{1}{2\pi(-1)^n\bar{\eta}}} e^{(-1)^n\bar{\eta}} \left[1 + (-1)^n \frac{1}{8\bar{\eta}} + \frac{9}{128\bar{\eta}^2} + (-1)^n \frac{75}{1024\bar{\eta}^3} + \dots \right],$$

$$q_8^{(n)}(\bar{\eta}) \sim \sqrt{\frac{1}{2\pi(-1)^n \bar{\eta}}} e^{(-1)^n \bar{\eta}} \left[\bar{\eta} + (-1)^n \frac{29 - 32\nu^{(n)}}{8} + \frac{49 - 64\nu^{(n)}}{128\bar{\eta}} \right. \\ \left. + (-1)^n \frac{183 - 288\nu^{(n)}}{1024\bar{\eta}^2} + \dots \right],$$

$$\text{as } \bar{\eta} \rightarrow \infty. \quad (4.41)$$

Substituting (4.41) into (4.25), the asymptotic expansions for $\bar{\Delta}_A^{(n)}(\bar{\eta})$ and $\bar{\Delta}_B^{(n)}(\bar{\eta})$ as $\bar{\eta} \rightarrow \infty$ are

$$\bar{\Delta}_A^{(1)}(\bar{\eta}) \sim \sqrt{\frac{1}{8\pi\bar{\eta}^3}} e^{\bar{\eta}} \left\{ \left[1 + (3 - 4\nu^{(2)})w \right] \bar{\eta} + \left[-\frac{15}{8} + 2\nu^{(2)} \right. \right. \\ \left. \left. - \left(\frac{45}{8} - 6\nu^{(1)} - \frac{15}{2}\nu^{(2)} + 8\nu^{(1)}\nu^{(2)} \right) w \right] + \left[\frac{265}{128} - \frac{7}{4}\nu^{(2)} \right. \right. \\ \left. \left. + \left(\frac{155}{128} - \frac{17}{4}\nu^{(1)} - \frac{9}{32}\nu^{(2)} + 3\nu^{(1)}\nu^{(2)} \right) w \right] \frac{1}{\bar{\eta}} + \dots \right\},$$

$$\bar{\Delta}_B^{(1)}(\bar{\eta}) \sim \sqrt{\frac{1}{8\pi\bar{\eta}^3}} e^{\bar{\eta}} \left\{ \left[1 + (3 - 4\nu^{(2)})w \right] + \left[-\frac{11}{8} + 2\nu^{(2)} - \left(\frac{1}{8} + \frac{1}{2}\nu^{(2)} \right) w \right] \frac{1}{\bar{\eta}} \right. \\ \left. + \left[\frac{129}{128} - \frac{3}{4}\nu^{(2)} - \left(\frac{189}{128} - \frac{39}{32}\nu^{(2)} \right) w \right] \frac{1}{\bar{\eta}^2} + \dots \right\},$$

$$\bar{\Delta}_A^{(2)}(\bar{\eta}) \sim \sqrt{\frac{\pi}{8\bar{\eta}^3}} e^{-\bar{\eta}} \left\{ \left[3 - 4\nu^{(1)} + w \right] \bar{\eta} + \left[\frac{45}{8} - \frac{15}{2}\nu^{(1)} - 6\nu^{(2)} + 8\nu^{(1)}\nu^{(2)} \right. \right. \\ \left. \left. + \left(\frac{15}{8} - 2\nu^{(1)} \right) w \right] + \left[\frac{155}{128} - \frac{9}{32}\nu^{(1)} - \frac{17}{4}\nu^{(2)} + 3\nu^{(1)}\nu^{(2)} \right. \right. \\ \left. \left. + \left(\frac{265}{128} - \frac{7}{4}\nu^{(1)} \right) w \right] \frac{1}{\bar{\eta}} + \dots \right\},$$

$$\bar{\Delta}_B^{(2)}(\bar{\eta}) \sim \sqrt{\frac{\pi}{8\bar{\eta}^3}} e^{-\bar{\eta}} \left\{ 3 - 4\nu^{(1)} + w + \left[\frac{1}{8} + \frac{1}{2}\nu^{(1)} + \left(\frac{11}{8} - 2\nu^{(1)} \right) w \right] \frac{1}{\bar{\eta}} \right. \\ \left. + \left[-\frac{189}{128} + \frac{39}{32}\nu^{(1)} + \left(\frac{129}{128} - \frac{3}{4}\nu^{(1)} \right) w \right] \frac{1}{\bar{\eta}^2} + \dots \right\},$$

$$\text{as } \bar{\eta} \rightarrow \infty. \quad (4.42)$$

The asymptotic expansion for $\bar{\Delta}$ is

$$\begin{aligned} \bar{\Delta}(\bar{\eta}) &= -\bar{q}_7^{(1)} \bar{\Delta}_A^{(1)} + \bar{q}_8^{(1)} \bar{\Delta}_B^{(1)} + w \bar{q}_7^{(2)} \bar{\Delta}_A^{(2)} - w \bar{q}_8^{(2)} \bar{\Delta}_B^{(2)} \\ &\sim \frac{1}{4\bar{\eta}^2} \left\{ \left[-3 + 4\nu^{(1)} - 2\left(5 - 6\nu^{(1)} - 6\nu^{(2)} + 8\nu^{(1)}\nu^{(2)}\right)w - \left(3 - 4\nu^{(2)}\right)w^2 \right] \right. \\ &\quad \left. + \left[2\left(2 - 3\nu^{(1)} - 3\nu^{(2)} + 4\nu^{(1)}\nu^{(2)}\right)\left(1 - w^2\right) \right] \frac{1}{\bar{\eta}} + \dots \right\}, \\ &\text{as } \bar{\eta} \rightarrow \infty, \end{aligned} \quad (4.43)$$

or, simply denoted as

$$\bar{\Delta}(\bar{\eta}) \sim \frac{1}{4\bar{\eta}^2} \left\{ \Delta_0 + \Delta_1 \frac{1}{\bar{\eta}} + \dots \right\} \text{ as } \bar{\eta} \rightarrow \infty, \quad (4.44)$$

where

$$\begin{aligned} \Delta_0 &= -3 + 4\nu^{(1)} - 2\left(5 - 6\nu^{(1)} - 6\nu^{(2)} + 8\nu^{(1)}\nu^{(2)}\right)w - \left(3 - 4\nu^{(2)}\right)w^2, \\ \Delta_1 &= 2\left(2 - 3\nu^{(1)} - 3\nu^{(2)} + 4\nu^{(1)}\nu^{(2)}\right)\left(1 - w^2\right). \end{aligned} \quad (4.45)$$

For matrix, i.e., $n = 1$ and $1 \leq \bar{r} < \infty$, replacing $\bar{\eta}$ with $\bar{\eta}\bar{r}$ in (2.80), one has the asymptotic expansions (2.81) for the modified Bessel functions of the second kinds as $\bar{\eta} \rightarrow \infty$:

$$\begin{aligned} R_0^{(1)}(\bar{\eta}\bar{r}) &= K_0(\bar{\eta}\bar{r}) \sim \sqrt{\frac{\pi}{2\bar{\eta}\bar{r}}} e^{-\bar{\eta}\bar{r}} \left[1 - \frac{1}{8\bar{\eta}\bar{r}} + \frac{9}{128(\bar{\eta}\bar{r})^2} - \frac{75}{1024(\bar{\eta}\bar{r})^3} + \dots \right], \\ R_1^{(1)}(\bar{\eta}\bar{r}) &= K_1(\bar{\eta}\bar{r}) \sim \sqrt{\frac{\pi}{2\bar{\eta}\bar{r}}} e^{-\bar{\eta}\bar{r}} \left[1 + \frac{3}{8\bar{\eta}\bar{r}} - \frac{15}{128(\bar{\eta}\bar{r})^2} + \frac{105}{1024(\bar{\eta}\bar{r})^3} + \dots \right]. \end{aligned}$$

$$\text{as } \bar{\eta} \rightarrow \infty. \quad (4.46)$$

Substituting (4.42) and (4.46) into (4.38), one finds the asymptotic expressions for $\bar{\Delta}_{rr}^{(1)}(\bar{r}; \bar{\eta})$, $\bar{\Delta}_{\theta\theta}^{(1)}(\bar{r}; \bar{\eta})$, $\bar{\Delta}_{zz}^{(1)}(\bar{r}; \bar{\eta})$, and $\bar{\Delta}_{rz}^{(1)}(\bar{r}; \bar{\eta})$ for $1 \leq \bar{r} < \infty$ as $\bar{\eta} \rightarrow \infty$:

$$\begin{aligned} \bar{\Delta}_{rr}^{(1)}(\bar{r}; \bar{\eta}) &\sim \frac{1}{4\bar{\eta}^2\sqrt{\bar{r}}} e^{(1-\bar{r})\bar{\eta}} \left\{ (1-\bar{r})(1+3w-4\nu^{(2)}w)\bar{\eta} \right. \\ &\quad + \left[-\frac{5}{4} + \frac{7}{8\bar{r}} + \frac{11\bar{r}}{8} - 2\nu^{(1)} + 2\nu^{(2)} - 2\bar{r}\nu^{(2)} \right. \\ &\quad \left. \left. - \left(\frac{15}{4} - \frac{21}{8\bar{r}} - \frac{\bar{r}}{8} - 5\nu^{(2)} + \frac{7}{2\bar{r}}\nu^{(2)} - \frac{\bar{r}}{2}\bar{\nu}^{(2)} \right) w \right] + \dots \right\}, \\ \bar{\Delta}_{\theta\theta}^{(1)}(\bar{r}; \bar{\eta}) &\sim \frac{1}{4\bar{\eta}^2\sqrt{\bar{r}}} e^{(1-\bar{r})\bar{\eta}} \left\{ \left(1 - \frac{1}{\bar{r}} - 2\nu^{(1)} \right) (1+3w-4\nu^{(2)}w) \right. \\ &\quad + \left[-\frac{1}{8}(1-2\nu^{(1)})(11-16\nu^{(2)}) \right. \\ &\quad + \frac{1}{4}(7+\nu^{(1)}-8\nu^{(2)})\frac{1}{\bar{r}} - \frac{3}{8\bar{r}^2} - \frac{1}{8}\left((1-2\nu^{(1)})(1+4\nu^{(2)}) \right. \\ &\quad \left. \left. - 14(1-\nu^{(1)})(3-4\nu^{(2)})\frac{1}{\bar{r}} + (9-12\nu^{(2)})\frac{1}{\bar{r}^2} \right) w \right] \frac{1}{\bar{\eta}} + \dots \right\}, \\ \bar{\Delta}_{zz}^{(1)}(\bar{r}; \bar{\eta}) &\sim \frac{1}{4\bar{\eta}^2\sqrt{\bar{r}}} e^{(1-\bar{r})\bar{\eta}} \left\{ -(1-\bar{r})(1+3w-4\nu^{(2)}w)\bar{\eta} \right. \\ &\quad + \left[-\frac{7}{4} + 2(\nu^{(1)}-\nu^{(2)}) + \frac{1}{8\bar{r}} + \left(-\frac{11}{8} + 2\nu^{(2)} \right) \bar{r} \right. \\ &\quad \left. \left. - \left(\frac{21}{4} - 7\nu^{(2)} + \frac{-3+4\nu^{(2)}}{8\bar{r}} + \frac{1}{8}(1+4\nu^{(2)})\bar{r} \right) w \right] + \dots \right\}, \\ \bar{\Delta}_{rz}^{(1)}(\bar{r}; \bar{\eta}) &\sim \frac{1}{4\bar{\eta}^2\sqrt{\bar{r}}} e^{(1-\bar{r})\bar{\eta}} \left\{ (1-\bar{r})(1+3w-4\nu^{(2)}w)\bar{\eta} \right. \\ &\quad + \left[\frac{1}{4} - 2(\nu^{(1)}-\nu^{(2)}) + \frac{3}{8\bar{r}} + \frac{1}{8}(11-4\nu^{(2)})\bar{r} \right. \end{aligned}$$

$$-\frac{1}{8} \left(-6 + 8\nu^{(2)} - (9 - 12\nu^{(2)})\frac{1}{\bar{r}} - (1 + 4\nu^{(2)})\bar{r} \right) w \Big] + \dots \Big\},$$

$$\text{as } \bar{\eta} \rightarrow \infty. \quad (4.47)$$

Therefore, from (4.47) and (4.44), one has the following asymptotic expressions

as $\bar{\eta} \rightarrow \infty$:

$$\begin{aligned} \frac{\bar{\Delta}_{rr}^{(1)}(\bar{r}; \bar{\eta})}{\bar{\eta}\bar{\Delta}(\bar{\eta})} &\sim \frac{1}{\sqrt{\bar{r}}} e^{(1-\bar{r})\bar{\eta}} \left\{ b_{rr}^{(1)} + c_{rr}^{(1)} \frac{1}{\bar{\eta}} \right\}, \\ \frac{\bar{\Delta}_{\theta\theta}^{(1)}(\bar{r}; \bar{\eta})}{\bar{\eta}\bar{\Delta}(\bar{\eta})} &\sim \frac{1}{\sqrt{\bar{r}}} e^{(1-\bar{r})\bar{\eta}} \left\{ c_{\theta\theta}^{(1)} \frac{1}{\bar{\eta}} + d_{\theta\theta}^{(1)} \frac{1}{\bar{\eta}^2} \right\}, \\ \frac{\bar{\Delta}_{zz}^{(1)}(\bar{r}; \bar{\eta})}{\bar{\eta}\bar{\Delta}(\bar{\eta})} &\sim \frac{1}{\sqrt{\bar{r}}} e^{(1-\bar{r})\bar{\eta}} \left\{ b_{zz}^{(1)} + c_{zz}^{(1)} \frac{1}{\bar{\eta}} \right\}, \\ \frac{\bar{\Delta}_{rz}^{(1)}(\bar{r}; \bar{\eta})}{\bar{\eta}\bar{\Delta}(\bar{\eta})} &\sim \frac{1}{\sqrt{\bar{r}}} e^{(1-\bar{r})\bar{\eta}} \left\{ b_{rz}^{(1)} + c_{rz}^{(1)} \frac{1}{\bar{\eta}} \right\}, \end{aligned}$$

$$\text{as } \bar{\eta} \rightarrow \infty, \quad (4.48)$$

In the above expressions, each is decomposed as product of an exponential function of $\bar{\eta}$ and a fractional function of $\bar{\eta}$. The coefficients in (4.48) are independent of the integration variable $\bar{\eta}$:

$$b_{rr}^{(1)} = (1 - \bar{r})(1 + 3w - 4\nu^{(2)}w) / \Delta_0,$$

$$\begin{aligned} c_{rr}^{(1)} = &\left\{ \left[-\frac{5}{4} + \frac{7}{8\bar{r}} + \frac{11\bar{r}}{8} - 2\nu^{(1)} + 2\nu^{(2)} - 2\bar{r}\nu^{(2)} \right. \right. \\ &\left. \left. - \left(\frac{15}{4} - \frac{21}{8\bar{r}} - \frac{\bar{r}}{8} - 5\nu^{(2)} + \frac{7}{2\bar{r}}\nu^{(2)} - \frac{\bar{r}}{2}\bar{\nu}^{(2)} \right) w \right] \Delta_0 \right. \\ &\left. - (1 - \bar{r})(1 + 3w - 4\nu^{(2)}w) \right\} / \Delta_0^2, \end{aligned}$$

$$c_{\theta\theta}^{(1)} = \left(1 - \frac{1}{\bar{r}} - 2\nu^{(1)} \right) (1 + 3w - 4\nu^{(2)}w) / \Delta_0,$$

$$d_{\theta\theta}^{(1)} = \left\{ \left[-\frac{1}{8}(1 - 2\nu^{(1)})(11 - 16\nu^{(2)}) + \frac{1}{4}(7 + \nu^{(1)} - 8\nu^{(2)})\frac{1}{\bar{r}} \right. \right.$$

$$\begin{aligned}
& -\frac{3}{8\bar{r}^2} - \frac{1}{8} \left((1 - 2\nu^{(1)})(1 + 4\nu^{(2)}) \right. \\
& \left. - 14(1 - \nu^{(1)})(3 - 4\nu^{(2)})\frac{1}{\bar{r}} + (9 - 12\nu^{(2)})\frac{1}{\bar{r}^2} \right) w \Big] \Delta_0 \\
& - \left(1 - \frac{1}{\bar{r}} - 2\nu^{(1)} \right) \left(1 + 3w - 4\nu^{(2)}w \right) \Delta_1 \Big\} / \Delta_0^2, \\
b_{zz}^{(1)} &= -(1 - \bar{r})(1 + 3w - 4\nu^{(2)}w) / \Delta_0, \\
c_{zz}^{(1)} &= \left\{ \left[-\frac{7}{4} + 2(\nu^{(1)} - \nu^{(2)}) + \frac{1}{8\bar{r}} + \left(-\frac{11}{8} + 2\nu^{(2)}\right)\bar{r} \right. \right. \\
& \left. \left. - \left(\frac{21}{4} - 7\nu^{(2)} + \frac{-3 + 4\nu^{(2)}}{8\bar{r}} + \frac{1}{8}(1 + 4\nu^{(2)})\bar{r}\right) w \right] \Delta_0 \right. \\
& \left. + (1 - \bar{r})(1 + 3w - 4\nu^{(2)}w) \right\} / \Delta_0^2, \\
b_{rz}^{(1)} &= (1 - \bar{r})(1 + 3w - 4\nu^{(2)}w) / \Delta_0, \\
c_{rz}^{(1)} &= \left\{ \left[\frac{1}{4} - 2(\nu^{(1)} - \nu^{(2)}) + \frac{3}{8\bar{r}} + \frac{1}{8}(11 - 4\nu^{(2)})\bar{r} \right. \right. \\
& \left. \left. - \frac{1}{8} \left(-6 + 8\nu^{(2)} - (9 - 12\nu^{(2)})\frac{1}{\bar{r}} - (1 + 4\nu^{(2)})\bar{r} \right) w \right] \Delta_0 \right. \\
& \left. - (1 - \bar{r})(1 + 3w - 4\nu^{(2)}w) \right\} / \Delta_0^2, \tag{4.49}
\end{aligned}$$

where Δ_0 and Δ_1 are constants given by (4.45).

The similar asymptotic expansions for the fiber ($n = 2$) can be found by following the same procedure. Since $a = 0$ at the center of the fiber, we will deal with it in two separate cases: $0 < \bar{r} \leq 1$ and $\bar{r} = 0$. For $0 < \bar{r} \leq 1$, replacing $\bar{\eta}$ with $\bar{\eta}\bar{r} (\neq 0)$ in (2.80), one has the asymptotic expansions (2.81) for the modified Bessel functions of the first kinds as $\bar{\eta} \rightarrow \infty$:

$$R_0^{(2)}(\bar{\eta}\bar{r}) = I_0(\bar{\eta}\bar{r}) \sim \sqrt{\frac{\pi}{2\bar{\eta}\bar{r}}} e^{-\bar{\eta}\bar{r}} \left[1 + \frac{1}{8\bar{\eta}\bar{r}} + \frac{9}{128(\bar{\eta}\bar{r})^2} + \frac{75}{1024(\bar{\eta}\bar{r})^3} + \dots \right],$$

$$R_1^{(2)}(\bar{\eta}\bar{r}) = I_1(\bar{\eta}\bar{r}) \sim \sqrt{\frac{\pi}{2\bar{\eta}\bar{r}}} e^{-\bar{\eta}\bar{r}} \left[1 - \frac{3}{8\bar{\eta}\bar{r}} - \frac{15}{128(\bar{\eta}\bar{r})^2} - \frac{105}{1024(\bar{\eta}\bar{r})^3} + \dots \right],$$

as $\bar{\eta} \rightarrow \infty$. (4.50)

Substituting (4.50) and (4.42) into (4.38) and then together with (4.44), one arrives at the asymptotic expressions for $0 < \bar{r} \leq 1$:

$$\begin{aligned} \frac{\bar{\Delta}_{rr}^{(2)}(\bar{r}; \bar{\eta})}{\bar{\eta}\bar{\Delta}(\bar{\eta})} &\sim \frac{1}{\sqrt{\bar{r}}} e^{-(1-\bar{r})\bar{\eta}} \left\{ b_{rr}^{(2)} + c_{rr}^{(2)} \frac{1}{\bar{\eta}} \right\}, \\ \frac{\bar{\Delta}_{\theta\theta}^{(2)}(\bar{r}; \bar{\eta})}{\bar{\eta}\bar{\Delta}(\bar{\eta})} &\sim \frac{1}{\sqrt{\bar{r}}} e^{-(1-\bar{r})\bar{\eta}} \left\{ c_{\theta\theta}^{(2)} \frac{1}{\bar{\eta}} + d_{\theta\theta}^{(2)} \frac{1}{\bar{\eta}^2} \right\}, \\ \frac{\bar{\Delta}_{zz}^{(2)}(\bar{r}; \bar{\eta})}{\bar{\eta}\bar{\Delta}(\bar{\eta})} &\sim \frac{1}{\sqrt{\bar{r}}} e^{-(1-\bar{r})\bar{\eta}} \left\{ b_{zz}^{(2)} + c_{zz}^{(2)} \frac{1}{\bar{\eta}} \right\}, \\ \frac{\bar{\Delta}_{rz}^{(2)}(\bar{r}; \bar{\eta})}{\bar{\eta}\bar{\Delta}(\bar{\eta})} &\sim \frac{1}{\sqrt{\bar{r}}} e^{-(1-\bar{r})\bar{\eta}} \left\{ b_{rz}^{(2)} + c_{rz}^{(2)} \frac{1}{\bar{\eta}} \right\}, \end{aligned}$$

as $\bar{\eta} \rightarrow \infty$. (4.51)

Similar to (4.48), each expression above is a product of an exponential function of $\bar{\eta}$ and a fractional function of $\bar{\eta}$. The coefficients in (4.51) are independent of the integration variable $\bar{\eta}$:

$$\begin{aligned} b_{rr}^{(2)} = -b_{zz}^{(2)} = -b_{rz}^{(2)} &= (1 - \bar{r})(3 - 4\nu^{(1)} + w) / \Delta_0, \\ c_{\theta\theta}^{(2)} &= \left(\frac{1}{\bar{r}} - 1 + 2\nu^{(2)} \right) (3 - 4\nu^{(1)} + w) / \Delta_0, \\ c_{rr}^{(2)} &= \left\{ \left[\frac{15}{4} - \frac{21}{8\bar{r}} - \frac{\bar{r}}{8} - 5\nu^{(1)} + \frac{7}{2\bar{r}}\nu^{(1)} - \frac{\bar{r}}{2}\nu^{(1)} \right. \right. \\ &\quad \left. \left. + \left(\frac{5}{4} - \frac{7}{8\bar{r}} - \frac{11\bar{r}}{8} - 2\nu^{(1)} + 2\bar{r}\nu^{(1)} + 2\bar{\nu}^{(2)} \right) w \right] \Delta_0 \right. \\ &\quad \left. - (1 - \bar{r})(3 - 4\nu^{(1)} + w) \right\} / \Delta_0^2, \end{aligned}$$

$$\begin{aligned}
d_{\theta\theta}^{(2)} &= \left\{ \left[-\frac{1}{8} - \frac{9}{8\bar{r}^2} + \frac{21}{4\bar{r}} - \frac{1}{2}\nu^{(1)} + \frac{3}{2\bar{r}^2}\nu^{(1)} - \frac{7}{\bar{r}}\nu^{(1)} + \frac{1}{4}\nu^{(2)} \right. \right. \\
&\quad \left. \left. - \frac{21}{4\bar{r}}\nu^{(2)} + \nu^{(1)}\nu^{(2)} + \frac{7}{\bar{r}}\nu^{(1)}\nu^{(2)} - \left(\frac{11}{8} + \frac{3}{8\bar{r}^2} - \frac{7}{4\bar{r}} \right. \right. \right. \\
&\quad \left. \left. - 2\nu^{(1)} + \frac{2}{\bar{r}}\nu^{(1)} - \frac{11}{4}\nu^{(2)} - \frac{1}{4\bar{r}}\nu^{(2)} + 4\nu^{(1)}\nu^{(2)} \right) w \right] \Delta_0 \\
&\quad \left. - \left(\frac{1}{\bar{r}} - 1 + 2\nu^{(2)} \right) (3 - 4\nu^{(1)} - w) \Delta_1 \right\} / \Delta_0^2, \\
c_{zz}^{(2)} &= \left\{ \left[\frac{21}{4} - \frac{3}{8\bar{r}} + \frac{\bar{r}}{8} - 7\nu^{(1)} + \frac{1}{2\bar{r}}\nu^{(1)} + \frac{\bar{r}}{2}\nu^{(1)} \right. \right. \\
&\quad \left. \left. + \left(\frac{7}{4} - \frac{1}{8\bar{r}} + \frac{11\bar{r}}{8} + 2\nu^{(1)} - 2\bar{r}\nu^{(1)} - 2\nu^{(2)} \right) w \right] \Delta_0 \right. \\
&\quad \left. + (1 - \bar{r})(3 - 4\nu^{(1)} + w) \right\} / \Delta_0^2, \\
c_{rz}^{(2)} &= \left\{ \left[\frac{3}{4} + \frac{9}{8\bar{r}} + \frac{\bar{r}}{8} - \nu^{(1)} - \frac{3}{2\bar{r}}\nu^{(1)} + \frac{\bar{r}}{2}\nu^{(1)} \right. \right. \\
&\quad \left. \left. + \left(\frac{1}{4} + \frac{3}{8\bar{r}} + \frac{11\bar{r}}{8} + 2\nu^{(1)} - 2\bar{r}\nu^{(1)} - 2\nu^{(2)} \right) w \right] \Delta_0 \right. \\
&\quad \left. + (1 - \bar{r})(3 - 4\nu^{(1)} + w) \right\} / \Delta_0^2, \tag{4.52}
\end{aligned}$$

where Δ_0 and Δ_1 are constants given by (4.45).

At the center of the fiber, $\bar{r} = 0$, we notice that the modified Bessel functions of the first kinds take the following values at 0:

$$\begin{aligned}
R_0^{(2)}(0) &= I_0(0) = 1, \\
R_1^{(2)}(0) &= I_1(0) = 0. \tag{4.53}
\end{aligned}$$

As $\eta \rightarrow 0^+$, one has asymptotic expansion

$$\frac{R_1^{(2)}(\eta)}{\eta} = \frac{I_1(\eta)}{\eta} \rightarrow \frac{1}{2}, \quad \text{as } \eta \rightarrow 0^+. \tag{4.54}$$

Substituting (4.53), (4.54) and (4.42) into (4.38) and then together with (4.44), one arrives at the asymptotic expressions for $\bar{r} = 0$:

$$\begin{aligned}\frac{\bar{\Delta}_{rr}^{(2)}(0; \bar{\eta})}{\bar{\eta}\bar{\Delta}(\bar{\eta})} &= \frac{\bar{\Delta}_{\theta\theta}^{(2)}(0; \bar{\eta})}{\bar{\eta}\bar{\Delta}(\bar{\eta})} \sim \sqrt{2\pi\bar{\eta}}e^{-\bar{\eta}} \left\{ b_{rr} + c_{rr} \frac{1}{\bar{\eta}} \right\}, \\ \frac{\bar{\Delta}_{zz}^{(2)}(0; \bar{\eta})}{\bar{\eta}\bar{\Delta}(\bar{\eta})} &\sim \sqrt{2\pi\bar{\eta}}e^{-\bar{\eta}} \left\{ b_{zz} + c_{zz} \frac{1}{\bar{\eta}} \right\}, \\ \frac{\bar{\Delta}_{rz}^{(2)}(0; \bar{\eta})}{\bar{\eta}\bar{\Delta}(\bar{\eta})} &= 0,\end{aligned}$$

as $\bar{\eta} \rightarrow \infty$. (4.55)

The coefficients in (4.55) are independent of the integration variable $\bar{\eta}$:

$$\begin{aligned}b_{rr} &= \frac{1}{2} \left[3 - 4\nu^{(1)} + w \right] / \Delta_0, \\ c_{rr} &= \left\{ \left[-\frac{3}{16} + \frac{1}{4}\nu^{(1)} + 3\nu^{(2)} - 4\nu^{(1)}\nu^{(2)} \right. \right. \\ &\quad \left. \left. + \left(-\frac{1}{16} - \nu^{(1)} + 2\nu^{(2)} \right) w \right] \Delta_0 \right. \\ &\quad \left. - \frac{1}{2} \left[3 - 4\nu^{(1)} + w \right] \Delta_1 \right\} / \Delta_0^2, \\ b_{zz} &= \left[-3 + 4\nu^{(1)} - w \right] / \Delta_0, \\ c_{zz} &= \left\{ \left[\frac{51}{8} - \frac{17}{2}\nu^{(1)} + \left(\frac{17}{8} + 2\nu^{(1)} - 2\nu^{(2)} \right) w \right] \Delta_0 \right. \\ &\quad \left. - \left[-3 + 4\nu^{(1)} - w \right] \Delta_1 \right\} / \Delta_0^2,\end{aligned}$$

(4.56)

where Δ_0 and Δ_1 are constants given by (4.45).

Now, let $M(\eta)$ be a bonded function in $[1, \infty)$ with $M_0 = \max_{\eta \in [1, \infty)} |M(\eta)|$.

Then, for $\lambda > 0$ and $s \geq 1$, one has

$$\int_s^\infty M(\eta)e^{-\lambda\eta}d\eta \leq \int_s^\infty |M(\eta)|e^{-\lambda\eta}d\eta$$

$$\begin{aligned}
&\leq M_0 \int_s^\infty e^{-\lambda\eta} d\eta \\
&= M_0 \frac{1}{\lambda} e^{-\lambda s} \\
&\rightarrow 0 \quad \text{as } s \rightarrow \infty.
\end{aligned} \tag{4.57}$$

Substituting (4.48), (4.51), and (4.55) into the second terms of (4.40), the second integrals in (4.40) can be written in the forms as (4.57) with $M(\eta)$ given by

$$\left(a_0 + a_1 \frac{1}{\eta} + a_2 \frac{1}{\eta^2} \right) \sin(\alpha\eta) \cos(\alpha z\eta)$$

or

$$\left(a_0 + a_1 \frac{1}{\eta} + a_2 \frac{1}{\eta^2} \right) \sin(\alpha\eta) \sin(\alpha z\eta) \tag{4.58}$$

for certain constants a_0 , a_1 , and a_2 . These functions of $\bar{\eta}$ are bonded in $[1, \infty)$. For the matrix ($n = 1$), let $\lambda = \bar{r} - 1$, while for the fiber ($n = 2$), let $\lambda = 1 - \bar{r}$. Inside both the matrix and the fiber ($\bar{r} \neq 1$), one has $\lambda > 0$. Therefore, the second integrals in (4.40) are small for sufficiently large s . Thus, away from the fiber-matrix interface, one has the approximations of stresses of the matrix and fiber, which are true for certain sufficiently large s :

$$\begin{aligned}
\bar{\sigma}_{rr}^{(n)}(\bar{r}, \bar{z}) &\simeq \frac{2E^{(1)}\gamma^T}{\pi(1+\nu^{(1)})} \int_0^s \frac{\bar{\Delta}_{rr}^{(n)}(\bar{r}, \bar{\eta})}{\bar{\eta}\bar{\Delta}(\bar{\eta})} \sin(\alpha\bar{\eta}) \cos(\alpha\bar{z}\bar{\eta}) d\bar{\eta}, \\
\bar{\sigma}_{\theta\theta}^{(n)}(\bar{r}, \bar{z}) &\simeq \frac{2E^{(1)}\gamma^T}{\pi(1+\nu^{(1)})} \int_0^s \frac{\bar{\Delta}_{\theta\theta}^{(n)}(\bar{r}, \bar{\eta})}{\bar{\eta}\bar{\Delta}(\bar{\eta})} \sin(\alpha\bar{\eta}) \cos(\alpha\bar{z}\bar{\eta}) d\bar{\eta}, \\
\bar{\sigma}_{zz}^{(n)}(\bar{r}, \bar{z}) &\simeq \frac{2E^{(1)}\gamma^T}{\pi(1+\nu^{(1)})} \int_0^s \frac{\bar{\Delta}_{zz}^{(n)}(\bar{r}, \bar{\eta})}{\bar{\eta}\bar{\Delta}(\bar{\eta})} \sin(\alpha\bar{\eta}) \cos(\alpha\bar{z}\bar{\eta}) d\bar{\eta}, \\
\bar{\sigma}_{rz}^{(n)}(\bar{r}, \bar{z}) &\simeq \frac{2E^{(1)}\gamma^T}{\pi(1+\nu^{(1)})} \int_0^s \frac{\bar{\Delta}_{rz}^{(n)}(\bar{r}, \bar{\eta})}{\bar{\eta}\bar{\Delta}(\bar{\eta})} \sin(\alpha\bar{\eta}) \sin(\alpha\bar{z}\bar{\eta}) d\bar{\eta} \quad \text{on } \bar{\Omega}^{(n)}.
\end{aligned} \tag{4.59}$$

Now, notice that the integrands in the above integrals involve $R_0^1 = K_0$ and $R_1^1 = K_1$, which are possibly singular only at 0. To show the behaviors of these

integrands for $\bar{\eta}$ near 0, we consider the asymptotic expansions of $R_0^{(n)}$ and $R_1^{(n)}$ as $\bar{\eta} \rightarrow 0^+$ (Zayed, 1996):

$$R_0^{(1)}(\bar{\eta}) = K_0(\bar{\eta}) \sim -\ln\bar{\eta},$$

$$R_1^{(1)}(\bar{\eta}) = K_1(\bar{\eta}) \sim \frac{1}{\bar{\eta}},$$

$$R_0^{(2)}(\bar{\eta}) = I_0(\bar{\eta}) \sim 1,$$

$$R_1^{(2)}(\bar{\eta}) = I_1(\bar{\eta}) \sim \frac{\bar{\eta}}{2},$$

$$\text{as } \bar{\eta} \rightarrow 0^+. \quad (4.60)$$

Substituting (4.60) into (4.26) one has the asymptotic expansions for $\bar{q}_k^{(1)}(\bar{\eta})$, $k = 1, 2, \dots, 8$,

$$\bar{q}_1^{(1)}(\bar{\eta}) \sim \frac{1}{\bar{\eta}^2} - \ln\bar{\eta},$$

$$\bar{q}_2^{(1)}(\bar{\eta}) \sim 1 + (1 - 2\nu^{(1)})\ln\bar{\eta},$$

$$\bar{q}_3^{(1)}(\bar{\eta}) \sim -\frac{1}{\bar{\eta}},$$

$$\bar{q}_4^{(1)}(\bar{\eta}) \sim \frac{2(1 - \nu^{(1)})}{\bar{\eta}} + \bar{\eta}\ln\bar{\eta},$$

$$\bar{q}_5^{(1)}(\bar{\eta}) \sim \frac{1}{\bar{\eta}},$$

$$\bar{q}_6^{(1)}(\bar{\eta}) \sim -\bar{\eta}\ln\bar{\eta},$$

$$\bar{q}_7^{(1)}(\bar{\eta}) \sim -\ln\bar{\eta},$$

$$\bar{q}_8^{(1)}(\bar{\eta}) \sim 1 + 4(1 - \nu^{(1)})\ln\bar{\eta},$$

$$\text{as } \bar{\eta} \rightarrow 0^+, \quad (4.61)$$

and the asymptotic expansions for $\bar{q}_k^{(2)}(\bar{\eta})$, $k = 1, 2, \dots, 8$,

$$\bar{q}_1^{(2)}(\bar{\eta}) \sim \frac{1}{2},$$

$$\bar{q}_2^{(2)}(\bar{\eta}) \sim 1 - 2\nu^{(2)} + \frac{\bar{\eta}^2}{2},$$

$$\bar{q}_3^{(2)}(\bar{\eta}) \sim \frac{\bar{\eta}}{2},$$

$$\bar{q}_4^{(2)}(\bar{\eta}) \sim (2 - \nu^{(2)})\bar{\eta},$$

$$\bar{q}_5^{(2)}(\bar{\eta}) \sim \frac{\bar{\eta}}{2},$$

$$\bar{q}_6^{(2)}(\bar{\eta}) \sim \bar{\eta},$$

$$\bar{q}_7^{(2)}(\bar{\eta}) \sim 1,$$

$$\bar{q}_8^{(2)}(\bar{\eta}) \sim 4(1 - \nu^{(2)}) + \frac{\bar{\eta}^2}{2},$$

$$\text{as } \bar{\eta} \rightarrow 0^+. \quad (4.62)$$

The asymptotic expansions for $\bar{\Delta}_A^{(n)}$ and $\bar{\Delta}_B^{(n)}$ are

$$\begin{aligned} \bar{\Delta}_A^{(1)}(\bar{\eta}) \sim & 2(1 - \nu^{(1)})\nu^{(2)}w + \frac{1}{2} \left[-1 - \nu^{(2)} + (1 - 2\nu^{(1)} + \nu^{(2)} \right. \\ & \left. + 2\nu^{(1)}\nu^{(2)})w \right] \bar{\eta}^2 \ln \bar{\eta} + \frac{1}{2}(\nu^{(1)} - \nu^{(2)})w\bar{\eta}^2, \end{aligned}$$

$$\begin{aligned} \bar{\Delta}_B^{(1)}(\bar{\eta}) \sim & \frac{1}{2} \left[1 + \nu^{(2)} + w - 3\nu^{(2)}w \right] \\ & + \frac{1}{2}(-1 + \nu^{(2)})w\bar{\eta}^2 \ln \bar{\eta} + \frac{1}{4}(-1 + w)\bar{\eta}^2, \end{aligned}$$

$$\bar{\Delta}_A^{(2)}(\bar{\eta}) \sim 2(1 - \nu^{(1)})(1 - 2\nu^{(2)} + w)\frac{1}{\bar{\eta}^2} - 2(1 - \nu^{(1)})(2 - \nu^{(2)})\ln \bar{\eta}$$

$$-1 - \nu^{(1)} + \nu^{(2)} + w,$$

$$\bar{\Delta}_B^{(2)}(\bar{\eta}) \sim (1 - \nu^{(1)})(1 + w)\frac{1}{\bar{\eta}^2} - (1 - \nu^{(1)})\ln\bar{\eta} - \frac{1}{2}(1 - w),$$

$$\text{as } \bar{\eta} \rightarrow 0^+. \quad (4.63)$$

The asymptotic expansions for $\bar{\Delta}$ is

$$\bar{\Delta}(\bar{\eta}) = -\bar{q}_7^{(1)}\bar{\Delta}_A^{(1)} + \bar{q}_8^{(1)}\bar{\Delta}_B^{(1)} + w\bar{q}_7^{(2)}\bar{\Delta}_A^{(2)} - w\bar{q}_8^{(2)}\bar{\Delta}_B^{(2)}$$

$$\sim -2(1 - \nu^{(1)})w(1 + w - 2\nu^{(2)}w)\frac{1}{\bar{\eta}^2}$$

$$+2(1 - \nu^{(1)})(1 + \nu^{(2)} + w - 3\nu^{(2)}w)\ln\bar{\eta}$$

$$+\frac{1}{2}(1 - w)\left[1 + \nu^{(2)} + (3 - \nu^{(1)} - 4\nu^{(2)})w\right],$$

$$\text{as } \bar{\eta} \rightarrow 0^+. \quad (4.64)$$

For the matrix, one has the asymptotic expansions for $\bar{\Delta}_{rr}^{(1)}$, $\bar{\Delta}_\theta^{(1)}$, $\bar{\Delta}_{zz}^{(1)}$, and $\bar{\Delta}_{rz}^{(1)}$:

$$\bar{\Delta}_{rr}^{(1)}(\bar{r}; \bar{\eta}) \sim 2(1 - \nu^{(1)})\nu^{(2)}w\frac{1}{(\bar{r}\bar{\eta})^2} - \frac{1}{2\bar{r}^2}\left[1 + \nu^{(2)} - (1 - 2\nu^{(1)}\right.$$

$$\left. + \nu^{(2)} + 2\nu^{(1)}\nu^{(2)}\right)w\ln\bar{\eta} - \frac{1}{2}\left[(1 - 2\nu^{(1)})(1 + \nu^{(2)})\right.$$

$$\left. + (1 - 2\nu^{(1)} + \nu^{(2)} + 2\nu^{(1)}\nu^{(2)})w\right]\ln(\bar{r}\bar{\eta})$$

$$\bar{\Delta}_{\theta\theta}^{(1)}(\bar{r}; \bar{\eta}) \sim -2(1 - \nu^{(1)})\nu^{(2)}w\frac{1}{(\bar{r}\bar{\eta})^2} - \frac{1}{2\bar{r}^2}\left[1 + \nu^{(2)} - (1 - 2\nu^{(1)}\right.$$

$$\left. + \nu^{(2)} + 2\nu^{(1)}\nu^{(2)}\right)w\ln\bar{\eta} - \frac{1}{2}\left[1 - 2\nu^{(1)} + \nu^{(2)}\right.$$

$$\left. - 2\nu^{(1)}\nu^{(2)} + (1 - 2\nu^{(1)})(1 - 3\nu^{(2)})w\right]\ln(\bar{r}\bar{\eta})$$

$$\begin{aligned}
\bar{\Delta}_{zz}^{(1)}(\bar{r}; \bar{\eta}) &\sim \left[2 - \nu^{(1)} + 2\nu^{(2)} - \nu^{(1)}\nu^{(2)} + (2 - \nu^{(1)} - 4\nu^{(2)} \right. \\
&\quad \left. + \nu^{(1)}\nu^{(2)}w \right] \ln(\bar{r}\bar{\eta}) + \frac{1}{2}(1 + \nu^{(2)} + w - 3\nu^{(2)}w) \\
\bar{\Delta}_{rz}^{(1)}(\bar{r}; \bar{\eta}) &\sim (1 - \nu^{(1)})(1 + \nu^{(2)} + w - \nu^{(2)}w) \frac{1}{\bar{r}\bar{\eta}} - \frac{1}{2\bar{r}}(1 + \nu^{(2)} + w \\
&\quad - 3\nu^{(2)}w)\bar{\eta} \ln \bar{\eta} + \frac{\bar{r}}{2}(1 + \nu^{(2)} + w - 3\nu^{(2)}w)\bar{\eta} \ln(\bar{r}\bar{\eta}) \\
&\quad \text{as } \bar{\eta} \rightarrow 0^+. \tag{4.65}
\end{aligned}$$

Therefore, from the asymptotic expansions (4.65) and (4.64), one arrives the limitations:

$$\begin{aligned}
\frac{\bar{\Delta}_{rr}^{(1)}(\bar{r}; \bar{\eta})}{\bar{\Delta}} &\rightarrow \frac{-\nu^{(2)}}{(1 + w - 2\nu^{(2)}w)\bar{r}^2}, \\
\frac{\bar{\Delta}_{\theta\theta}^{(1)}(\bar{r}; \bar{\eta})}{\bar{\Delta}} &\rightarrow \frac{\nu^{(2)}}{(1 + w - 2\nu^{(2)}w)\bar{r}^2}, \\
\frac{\bar{\Delta}_{zz}^{(1)}(\bar{r}; \bar{\eta})}{\bar{\Delta}} &\rightarrow 0, \\
\frac{\bar{\Delta}_{rz}^{(1)}(\bar{r}; \bar{\eta})}{\bar{\Delta}} &\rightarrow 0, \\
&\quad \text{as } \bar{\eta} \rightarrow 0^+. \tag{4.66}
\end{aligned}$$

Similarly, for the fiber, one has the limitations:

$$\begin{aligned}
\frac{\bar{\Delta}_{rr}^{(2)}(\bar{r}; \bar{\eta})}{\bar{\Delta}} &\rightarrow \frac{-\nu^{(2)}}{1 + w - 2\nu^{(2)}w}, \\
\frac{\bar{\Delta}_{\theta\theta}^{(2)}(\bar{r}; \bar{\eta})}{\bar{\Delta}} &\rightarrow \frac{-\nu^{(2)}}{1 + w - 2\nu^{(2)}w}, \\
\frac{\bar{\Delta}_{zz}^{(2)}(\bar{r}; \bar{\eta})}{\bar{\Delta}} &\rightarrow -\frac{1 + \nu^{(2)} + w - \nu^{(2)}w}{w(1 + w - 2\nu^{(2)}w)},
\end{aligned}$$

$$\frac{\bar{\Delta}_{rz}^{(2)}(\bar{r}; \bar{\eta})}{\bar{\Delta}} \rightarrow 0,$$

$$\text{as } \bar{\eta} \rightarrow 0^+. \quad (4.67)$$

According to (4.66) and (4.67), the integrands of (4.59) are finite as $\bar{\eta} \rightarrow 0^+$. Since the interval of integration in (4.59) is $[0, s]$, which is finite, after integration, all the stresses are finite and continuous inside the matrix and the fiber ($\bar{r} \neq 1$).

4.7 Analysis of Singularities

Now, we further investigate the stress distributions at the fiber-matrix interface with emphasis on the possible singularities near the phase boundary ($|\bar{z}| = 1$). Setting $\bar{r} = 1$ in (4.39), the stress components at the interface are given by

$$\begin{aligned} \bar{\sigma}_{rr}^{(n)}(1, \bar{z}) &= \frac{2E^{(1)}\gamma^T}{\pi(1 + \nu^{(1)})} \int_0^\infty \frac{\bar{\Delta}_{rr}^{(n)}(1, \bar{z})}{\bar{\eta}\bar{\Delta}(\bar{\eta})} \sin(\alpha\bar{\eta}) \cos(\alpha\bar{z}\bar{\eta}) d\bar{\eta}, \\ \bar{\sigma}_{\theta\theta}^{(n)}(1, \bar{z}) &= \frac{2E^{(1)}\gamma^T}{\pi(1 + \nu^{(1)})} \int_0^\infty \frac{\bar{\Delta}_{\theta\theta}^{(n)}(1, \bar{z})}{\bar{\eta}\bar{\Delta}(\bar{\eta})} \sin(\alpha\bar{\eta}) \cos(\alpha\bar{z}\bar{\eta}) d\bar{\eta}, \\ \bar{\sigma}_{zz}^{(n)}(1, \bar{z}) &= \frac{2E^{(1)}\gamma^T}{\pi(1 + \nu^{(1)})} \int_0^\infty \frac{\bar{\Delta}_{zz}^{(n)}(1, \bar{z})}{\bar{\eta}\bar{\Delta}(\bar{\eta})} \sin(\alpha\bar{\eta}) \cos(\alpha\bar{z}\bar{\eta}) d\bar{\eta}, \\ \bar{\sigma}_{rz}^{(n)}(1, \bar{z}) &= \frac{2E^{(1)}\gamma^T}{\pi(1 + \nu^{(1)})} \int_0^\infty \frac{\bar{\Delta}_{rz}^{(n)}(1, \bar{z})}{\bar{\eta}\bar{\Delta}(\bar{\eta})} \sin(\alpha\bar{\eta}) \sin(\alpha\bar{z}\bar{\eta}) d\bar{\eta} \end{aligned}$$

$$-\infty < \bar{z} < \infty. \quad (4.68)$$

where $\bar{\Delta}_{rr}^{(n)}(1, \bar{z})$, $\bar{\Delta}_{\theta\theta}^{(n)}(1, \bar{z})$, $\bar{\Delta}_{zz}^{(n)}(1, \bar{z})$, and $\bar{\Delta}_{rz}^{(n)}(1, \bar{z})$ is obtained from (4.38):

$$\begin{aligned} \bar{\Delta}_{rr}^{(n)}(1; \bar{\eta}) &= \left[R_0^{(n)}(\bar{\eta}) - \frac{(-1)^n}{\bar{\eta}} R_1^{(n)}(\bar{\eta}) \right] \bar{\Delta}_A^{(n)}(\bar{\eta}) \\ &\quad - \left[(-1)^n (1 - 2\nu^{(n)}) R_0^{(n)}(\bar{\eta}) + \bar{\eta} R_1^{(n)}(\bar{\eta}) \right] \bar{\Delta}_B^{(n)}(\bar{\eta}), \\ \bar{\Delta}_{\theta\theta}^{(n)}(1; \bar{\eta}) &= (-1)^n \left[\frac{1}{\bar{\eta}} R_1^{(n)}(\bar{\eta}) \bar{\Delta}_A^{(n)}(\bar{\eta}) - (1 - 2\nu^{(n)}) R_0^{(n)}(\bar{\eta}) \bar{\Delta}_B^{(n)}(\bar{\eta}) \right], \end{aligned}$$

$$\begin{aligned}
\bar{\Delta}_{zz}^{(n)}(1; \bar{\eta}) &= -R_0^{(n)}(\bar{\eta})\bar{\Delta}_A^{(n)}(\bar{\eta}) \\
&\quad + \left[(-1)^n 2(2 - \nu^{(n)})R_0^{(n)}(\bar{\eta}) + \bar{\eta}R_1^{(n)}(\bar{\eta}) \right] \bar{\Delta}_B^{(n)}(\bar{\eta}), \\
\bar{\Delta}_{rz}^{(n)}(1; \bar{\eta}) &= (-1)^{n+1} R_1^{(n)}(\bar{\eta})\bar{\Delta}_A^{(n)}(\bar{\eta}) \\
&\quad + \left[(-1)^n \bar{\eta}R_0^{(n)}(\bar{\eta}) + 2(1 - \nu^{(n)})R_1^{(n)}(\bar{\eta}) \right] \bar{\Delta}_B^{(n)}(\bar{\eta}), \\
&\quad -\infty < \bar{\eta} < \infty, \tag{4.69}
\end{aligned}$$

Setting $\bar{r} = 1$ in (4.48) and (4.51) and including the terms of $(1/\bar{\eta}^2)$, one has the asymptotic expressions of the ratios for the matrix and the fiber

$$\begin{aligned}
\frac{\bar{\Delta}_{rr}^{(n)}(1; \bar{\eta})}{\bar{\eta}\bar{\Delta}} &\sim C_{rr}^{(n)} \frac{1}{\bar{\eta}} + D_{rr}^{(n)} \frac{1}{\bar{\eta}^2}, \\
\frac{\bar{\Delta}_{\theta\theta}^{(n)}(1; \bar{\eta})}{\bar{\eta}\bar{\Delta}} &\sim C_{\theta\theta}^{(n)} \frac{1}{\bar{\eta}} + D_{\theta\theta}^{(n)} \frac{1}{\bar{\eta}^2}, \\
\frac{\bar{\Delta}_{zz}^{(n)}(1; \bar{\eta})}{\bar{\eta}\bar{\Delta}} &\sim C_{zz}^{(n)} \frac{1}{\bar{\eta}} + D_{zz}^{(n)} \frac{1}{\bar{\eta}^2}, \\
\frac{\bar{\Delta}_{rz}^{(n)}(1; \bar{\eta})}{\bar{\eta}\bar{\Delta}} &\sim C_{rz}^{(n)} \frac{1}{\bar{\eta}} + D_{rz}^{(n)} \frac{1}{\bar{\eta}^2}, \\
&\quad \text{as } \bar{\eta} \rightarrow \infty, \tag{4.70}
\end{aligned}$$

where

$$\begin{aligned}
C_{rr}^{(n)} &= \left[1 - 2\nu^{(1)} - (1 - 2\nu^{(2)})w \right] / \Delta_0, \\
D_{rr}^{(n)} &= \left\{ \left[-1 + 3\nu^{(1)} + 2\nu^{(2)} - 4\nu^{(1)}\nu^{(2)} - (1 - 2\nu^{(1)} - 3\nu^{(2)} \right. \right. \\
&\quad \left. \left. + 4\nu^{(1)}\nu^{(2)})w \right] \Delta_0 - \left[1 - 2\nu^{(1)} - (1 - 2\nu^{(2)})w \right] \Delta_1 \right\} / \Delta_0^2, \\
C_{\theta\theta}^{(1)} &= -2\nu^{(1)} \left[1 + (3 - 4\nu^{(2)})w \right] / \Delta_0,
\end{aligned}$$

$$\begin{aligned}
C_{\theta\theta}^{(2)} &= 2\nu^{(2)}(3 - 4\nu^{(1)} + w) / \Delta_0, \\
D_{\theta\theta}^{(1)} &= \left\{ \left[3\nu^{(1)} - 4\nu^{(1)}\nu^{(2)} + (4 - 5\nu^{(1)} - 6\nu^{(2)} + 8\nu^{(1)}\nu^{(2)})w \right] \Delta_0 \right. \\
&\quad \left. + 2\nu^{(1)} \left[1 + (3 - 4\nu^{(2)})w \right] \Delta_1 \right\} / \Delta_0^2, \\
D_{\theta\theta}^{(2)} &= \left\{ \left[4 - 6\nu^{(1)} - 5\nu^{(2)} + 8\nu^{(1)}\nu^{(2)} + (3\nu^{(2)} - 4\nu^{(1)}\nu^{(2)})w \right] \Delta_0 \right. \\
&\quad \left. - 2\nu^{(2)}(3 - 4\nu^{(1)} + w)\Delta_1 \right\} / \Delta_0^2, \\
C_{zz}^{(1)} &= \left[-3 + 2\nu^{(1)} - (5 - 6\nu^{(2)})w \right] / \Delta_0, \\
C_{zz}^{(2)} &= \left[5 - 6\nu^{(1)} + (3 - 2\nu^{(2)})w \right] / \Delta_0, \\
D_{zz}^{(1)} &= \left\{ \left[4 - 3\nu^{(1)} - 6\nu^{(2)} + 4\nu^{(1)}\nu^{(2)} - (2 - 4\nu^{(1)} - 3\nu^{(2)} \right. \right. \\
&\quad \left. \left. + 4\nu^{(1)}\nu^{(2)})w \right] \Delta_0 + \left[3 - 2\nu^{(1)} + (5 - 6\nu^{(2)})w \right] \Delta_1 \right\} / \Delta_0^2, \\
D_{zz}^{(2)} &= \left\{ \left[-2 + 3\nu^{(1)} + 4\nu^{(2)} - 4\nu^{(1)}\nu^{(2)} + (4 - 6\nu^{(1)} - 3\nu^{(2)} \right. \right. \\
&\quad \left. \left. + 4\nu^{(1)}\nu^{(2)})w \right] \Delta_0 - \left[5 - 6\nu^{(1)} + (3 - 2\nu^{(2)})w \right] \Delta_1 \right\} / \Delta_0^2, \\
C_{rz}^{(n)} &= 2 \left[1 - \nu^{(1)} + (1 - \nu^{(2)})w \right] / \Delta_0, \\
D_{rz}^{(n)} &= \left\{ -2 \left[(1 - \nu^{(1)})(1 - 2\nu^{(2)}) - (1 - 2\nu^{(1)})(1 - \nu^{(2)})w \right] \Delta_0 \right. \\
&\quad \left. - 2 \left[1 - \nu^{(1)} + (1 - \nu^{(2)})w \right] \Delta_1 \right\} / \Delta_0^2, \tag{4.71}
\end{aligned}$$

and

$$\Delta_0 = -3 + 4\nu^{(1)} - 2 \left(5 - 6\nu^{(1)} - 6\nu^{(2)} + 8\nu^{(1)}\nu^{(2)} \right) w - \left(3 - 4\nu^{(2)} \right) w^2,$$

$$\Delta_1 = 2\left(2 - 3\nu^{(1)} - 3\nu^{(2)} + 4\nu^{(1)}\nu^{(2)}\right)\left(1 - w^2\right). \quad (4.72)$$

It is worthy to notice the difference between the asymptotic expansions: Insider the matrix ($1 < \bar{r} < \infty$) and the fiber ($0 \leq \bar{r} < 1$), the asymptotic expansions in (4.48), (4.51), and (4.55) have exponentially convergence factor $e^{-\lambda\bar{\eta}}$ as $\bar{\eta} \rightarrow \infty$, while on the fiber-matrix interface, the expressions in (4.48) and (4.51) have not. We will show, in the following, that this difference leads to totally different behavior of stress distributions on the fiber-matrix interface from those inside the matrix and the fiber.

The leading terms as $\bar{\eta} \rightarrow \infty$ in (4.70) have coefficients $C_{rr}^{(n)}$, $C_{\theta\theta}^{(n)}$, $C_{zz}^{(n)}$, and $C_{rz}^{(n)}$, respectively. These leading terms play a major rule in the behavior of the stresses near the phase boundary as illustrated as follows. Utilizing these leading terms, one can separate the stress components into two parts

$$\begin{aligned} \bar{\sigma}_{rr}^{(n)}(1, \bar{z}) &= \frac{2E^{(1)}\gamma^T}{(1 + \nu^{(1)})\pi} \left\{ C_{rr}^{(n)} \int_0^\infty \frac{\sin(\alpha\bar{\eta})\cos(\alpha\bar{z}\bar{\eta})}{\bar{\eta}} d\bar{\eta} \right. \\ &\quad \left. + \int_0^\infty \left[\frac{\bar{\Delta}_{rr}}{\bar{\Delta}} - C_{rr}^{(n)} \right] \frac{\sin(\alpha\bar{\eta})\cos(\alpha\bar{z}\bar{\eta})}{\bar{\eta}} d\bar{\eta} \right\}, \\ \bar{\sigma}_{\theta\theta}^{(n)}(1, \bar{z}) &= \frac{2E^{(1)}\gamma^T}{(1 + \nu^{(1)})\pi} \left\{ C_{\theta\theta}^{(n)} \int_0^\infty \frac{\sin(\alpha\bar{\eta})\cos(\alpha\bar{r}\bar{\eta})}{\bar{\eta}} d\bar{\eta} \right. \\ &\quad \left. + \int_0^\infty \left[\frac{\bar{\Delta}_{\theta\theta}}{\bar{\Delta}} - C_{\theta\theta}^{(n)} \right] \frac{\sin(\alpha\bar{\eta})\cos(\alpha\bar{r}\bar{\eta})}{\bar{\eta}} d\bar{\eta} \right\}, \\ \bar{\sigma}_{zz}^{(n)}(1, \bar{z}) &= \frac{2E^{(1)}\gamma^T}{(1 + \nu^{(1)})\pi} \left\{ C_{zz}^{(n)} \int_0^\infty \frac{\sin(\alpha\bar{\eta})\cos(\alpha\bar{r}\bar{\eta})}{\bar{\eta}} d\bar{\eta} \right. \\ &\quad \left. + \int_0^\infty \left[\frac{\bar{\Delta}_{zz}}{\bar{\Delta}} - C_{zz}^{(n)} \right] \frac{\sin(\alpha\bar{\eta})\cos(\alpha\bar{r}\bar{\eta})}{\bar{\eta}} d\bar{\eta} \right\}, \\ \bar{\sigma}_{rz}^{(n)}(1, \bar{z}) &= \frac{2E^{(1)}\gamma^T}{(1 + \nu^{(1)})\pi} \left\{ C_{rz}^{(n)} \int_0^\infty \frac{\sin(\alpha\bar{\eta})\sin(\alpha\bar{r}\bar{\eta})}{\bar{\eta}} d\bar{\eta} \right. \\ &\quad \left. + \int_0^\infty \left[\frac{\bar{\Delta}_{rz}}{\bar{\Delta}} - C_{rz}^{(n)} \right] \frac{\sin(\alpha\bar{\eta})\sin(\alpha\bar{r}\bar{\eta})}{\bar{\eta}} d\bar{\eta} \right\}, \end{aligned}$$

$$-\infty < \bar{z} < \infty. \quad (4.73)$$

The second integrals can be further decomposed into two parts by dividing the integral interval $(0, \infty)$ into $(0, s)$ and (s, ∞) for some $s > 0$. Hence, we have

$$\begin{aligned} \bar{\sigma}_{rr}^{(n)}(1, \bar{z}) &= \frac{2E^{(1)}\gamma^T}{(1 + \nu^{(1)})\pi} \left\{ C_{rr}^{(n)} \int_0^\infty \frac{\sin(\alpha\bar{\eta})\cos(\alpha\bar{z}\bar{\eta})}{\bar{\eta}} d\bar{\eta} \right. \\ &\quad \left. + \int_0^s \left[\frac{\bar{\Delta}_{rr}}{\bar{\Delta}} - C_{rr}^{(n)} \right] \frac{\sin(\alpha\bar{\eta})\cos(\alpha\bar{z}\bar{\eta})}{\bar{\eta}} d\bar{\eta} \right\} \\ &\quad \left. + \int_s^\infty \left[\frac{\bar{\Delta}_{rr}}{\bar{\Delta}} - C_{rr}^{(n)} \right] \frac{\sin(\alpha\bar{\eta})\cos(\alpha\bar{z}\bar{\eta})}{\bar{\eta}} d\bar{\eta} \right\}, \\ \bar{\sigma}_{\theta\theta}^{(n)}(1, \bar{z}) &= \frac{2E^{(1)}\gamma^T}{(1 + \nu^{(1)})\pi} \left\{ C_{\theta\theta}^{(n)} \int_0^\infty \frac{\sin(\alpha\bar{\eta})\cos(\alpha\bar{z}\bar{\eta})}{\bar{\eta}} d\bar{\eta} \right. \\ &\quad \left. + \int_0^s \left[\frac{\bar{\Delta}_{\theta\theta}}{\bar{\Delta}} - C_{\theta\theta}^{(n)} \right] \frac{\sin(\alpha\bar{\eta})\cos(\alpha\bar{z}\bar{\eta})}{\bar{\eta}} d\bar{\eta} \right\} \\ &\quad \left. + \int_s^\infty \left[\frac{\bar{\Delta}_{\theta\theta}}{\bar{\Delta}} - C_{\theta\theta}^{(n)} \right] \frac{\sin(\alpha\bar{\eta})\cos(\alpha\bar{z}\bar{\eta})}{\bar{\eta}} d\bar{\eta} \right\}, \\ \bar{\sigma}_{zz}^{(n)}(1, \bar{z}) &= \frac{2E^{(1)}\gamma^T}{(1 + \nu^{(1)})\pi} \left\{ C_{zz}^{(n)} \int_0^\infty \frac{\sin(\alpha\bar{\eta})\cos(\alpha\bar{z}\bar{\eta})}{\bar{\eta}} d\bar{\eta} \right. \\ &\quad \left. + \int_0^s \left[\frac{\bar{\Delta}_{zz}}{\bar{\Delta}} - C_{zz}^{(n)} \right] \frac{\sin(\alpha\bar{\eta})\cos(\alpha\bar{z}\bar{\eta})}{\bar{\eta}} d\bar{\eta} \right\} \\ &\quad \left. + \int_s^\infty \left[\frac{\bar{\Delta}_{zz}}{\bar{\Delta}} - C_{zz}^{(n)} \right] \frac{\sin(\alpha\bar{\eta})\cos(\alpha\bar{z}\bar{\eta})}{\bar{\eta}} d\bar{\eta} \right\}, \\ \bar{\sigma}_{rz}^{(n)}(1, \bar{z}) &= \frac{2E^{(1)}\gamma^T}{(1 + \nu^{(1)})\pi} \left\{ C_{rz}^{(n)} \int_0^\infty \frac{\sin(\alpha\bar{\eta})\sin(\alpha\bar{z}\bar{\eta})}{\bar{\eta}} d\bar{\eta} \right. \\ &\quad \left. + \int_0^s \left[\frac{\bar{\Delta}_{rz}}{\bar{\Delta}} - C_{rz}^{(n)} \right] \frac{\sin(\alpha\bar{\eta})\sin(\alpha\bar{z}\bar{\eta})}{\bar{\eta}} d\bar{\eta} \right\} \\ &\quad \left. + \int_s^\infty \left[\frac{\bar{\Delta}_{rz}}{\bar{\Delta}} - C_{rz}^{(n)} \right] \frac{\sin(\alpha\bar{\eta})\sin(\alpha\bar{z}\bar{\eta})}{\bar{\eta}} d\bar{\eta} \right\}, \end{aligned}$$

$$-\infty < \bar{z} < \infty. \quad (4.74)$$

Noting that for positive s , one has

$$\int_s^\infty \frac{\sin(\alpha\bar{\eta})\cos(\alpha\bar{z}\bar{\eta})}{\bar{\eta}^2} d\bar{\eta} \leq \int_s^\infty \left| \frac{\sin(\alpha\bar{\eta})\cos(\alpha\bar{z}\bar{\eta})}{\bar{\eta}^2} \right| d\bar{\eta} \leq \int_s^\infty \frac{1}{\bar{\eta}^2} d\bar{\eta} = \frac{1}{s},$$

$$\int_s^\infty \frac{\sin(\alpha\bar{\eta})\sin(\alpha\bar{z}\bar{\eta})}{\bar{\eta}^2} d\bar{\eta} \leq \int_s^\infty \left| \frac{\sin(\alpha\bar{\eta})\sin(\alpha\bar{z}\bar{\eta})}{\bar{\eta}^2} \right| d\bar{\eta} \leq \int_s^\infty \frac{1}{\bar{\eta}^2} d\bar{\eta} = \frac{1}{s}. \quad (4.75)$$

For sufficiently large s , in view of (4.70) and (4.75), the third integrals in (4.74) are very small and can be ignored. Hence, we have the approximations

$$\begin{aligned} \bar{\sigma}_{rr}^{(n)}(1, \bar{z}) &\simeq \frac{2E^{(1)}\gamma^T}{(1+\nu^{(1)})\pi} \left\{ C_{rr}^{(n)} \int_0^\infty \frac{\sin(\alpha\bar{\eta})\cos(\alpha\bar{z}\bar{\eta})}{\bar{\eta}} d\bar{\eta} \right. \\ &\quad \left. + \int_0^s \left[\frac{\bar{\Delta}_{rr}}{\bar{\Delta}} - C_{rr}^{(n)} \right] \frac{\sin(\alpha\bar{\eta})\cos(\alpha\bar{z}\bar{\eta})}{\bar{\eta}} d\bar{\eta} \right\}, \\ \bar{\sigma}_{\theta\theta}^{(n)}(1, \bar{z}) &\simeq \frac{2E^{(1)}\gamma^T}{(1+\nu^{(1)})\pi} \left\{ C_{\theta\theta}^{(n)} \int_0^\infty \frac{\sin(\alpha\bar{\eta})\cos(\alpha\bar{z}\bar{\eta})}{\bar{\eta}} d\bar{\eta} \right. \\ &\quad \left. + \int_0^s \left[\frac{\bar{\Delta}_{\theta\theta}}{\bar{\Delta}} - C_{\theta\theta}^{(n)} \right] \frac{\sin(\alpha\bar{\eta})\cos(\alpha\bar{z}\bar{\eta})}{\bar{\eta}} d\bar{\eta} \right\}, \\ \bar{\sigma}_{zz}^{(n)}(1, \bar{z}) &\simeq \frac{2E^{(1)}\gamma^T}{(1+\nu^{(1)})\pi} \left\{ C_{zz}^{(n)} \int_0^\infty \frac{\sin(\alpha\bar{\eta})\cos(\alpha\bar{z}\bar{\eta})}{\bar{\eta}} d\bar{\eta} \right. \\ &\quad \left. + \int_0^s \left[\frac{\bar{\Delta}_{zz}}{\bar{\Delta}} - C_{zz}^{(n)} \right] \frac{\sin(\alpha\bar{\eta})\cos(\alpha\bar{z}\bar{\eta})}{\bar{\eta}} d\bar{\eta} \right\}, \\ \bar{\sigma}_{rz}^{(n)}(1, \bar{z}) &\simeq \frac{2E^{(1)}\gamma^T}{(1+\nu^{(1)})\pi} \left\{ C_{rz}^{(n)} \int_0^\infty \frac{\sin(\alpha\bar{\eta})\sin(\alpha\bar{z}\bar{\eta})}{\bar{\eta}} d\bar{\eta} \right. \\ &\quad \left. + \int_0^s \left[\frac{\bar{\Delta}_{rz}}{\bar{\Delta}} - C_{rz}^{(n)} \right] \frac{\sin(\alpha\bar{\eta})\sin(\alpha\bar{z}\bar{\eta})}{\bar{\eta}} d\bar{\eta} \right\}, \\ &\quad -\infty < \bar{z} < \infty. \end{aligned} \quad (4.76)$$

Now, notice that the second integrals of (4.76) involve K_0 , K_1 , I_0 , and I_1 . Only K_0 and K_1 have singularity at 0. Hence, the possible singularities of the integrands are only at 0. To show the behaviors of these integrands near 0, we consider the

asymptotic expansions of the second integrands as $\bar{\eta} \rightarrow 0^+$. Let $\bar{r} = 1$ in (4.66) and (4.67), one has

$$\begin{aligned}
\frac{\bar{\Delta}_{rr}^{(1)}(1; \bar{\eta})}{\bar{\Delta}} &\rightarrow \frac{-\nu^{(2)}}{1+w-2\nu^{(2)}w}, \\
\frac{\bar{\Delta}_{\theta\theta}^{(1)}(1; \bar{\eta})}{\bar{\Delta}} &\rightarrow \frac{\nu^{(2)}}{1+w-2\nu^{(2)}w}, \\
\frac{\bar{\Delta}_{zz}^{(1)}(1; \bar{\eta})}{\bar{\Delta}} &\rightarrow 0, \\
\frac{\bar{\Delta}_{rz}^{(1)}(1; \bar{\eta})}{\bar{\Delta}} &\rightarrow 0,
\end{aligned}$$

as $\bar{\eta} \rightarrow 0^+$, (4.77)

and

$$\begin{aligned}
\frac{\bar{\Delta}_{rr}^{(2)}(1; \bar{\eta})}{\bar{\Delta}} &\rightarrow \frac{-\nu^{(2)}}{1+w-2\nu^{(2)}w}, \\
\frac{\bar{\Delta}_{\theta\theta}^{(2)}(1; \bar{\eta})}{\bar{\Delta}} &\rightarrow \frac{-\nu^{(2)}}{1+w-2\nu^{(2)}w}, \\
\frac{\bar{\Delta}_{zz}^{(2)}(1; \bar{\eta})}{\bar{\Delta}} &\rightarrow -\frac{1+\nu^{(2)}+w-\nu^{(2)}w}{w(1+w-2\nu^{(2)}w)}, \\
\frac{\bar{\Delta}_{rz}^{(2)}(1; \bar{\eta})}{\bar{\Delta}} &\rightarrow 0,
\end{aligned}$$

as $\bar{\eta} \rightarrow 0^+$. (4.78)

Therefore, noticing $(\sin\bar{\eta}/\bar{\eta}) \rightarrow 1$ as $\bar{\eta} \rightarrow 0^+$, one conclude that all the second integrands in (4.76) are finite at 0. It follows that all the second integrals of (4.76) are finite and continuous in \bar{z} . For the first parts of (4.76), they can be evaluated explicitly by the identities

$$\int_0^\infty \frac{\sin(\alpha\bar{\eta})\cos(\alpha\bar{z}\bar{\eta})}{\bar{\eta}} d\bar{\eta} = \begin{cases} \pi/2 & |\bar{z}| < 1, \\ \pi/4 & |\bar{z}| = 1, \\ 0 & |\bar{z}| > 1, \end{cases} \quad (4.79)$$

which has jumps at $|\bar{z}| = 1$, and

$$\int_0^\infty \frac{\sin(\alpha\bar{\eta})\sin(\alpha\bar{z}\bar{\eta})}{\bar{\eta}} d\bar{\eta} = \frac{1}{2} \ln \left| \frac{1+\bar{z}}{1-\bar{z}} \right|, \quad (4.80)$$

which includes singularities at $|\bar{z}| = 1$.

In consequence, the singularities of all stress components near the phase boundary are isolated in the first integrals of (4.76). It is found that the normal stresses suffer finite jumps at $|\bar{z}| = 1$. On the other hand, the shear stress blows up at $|\bar{z}| = 1$ with the singularity characterized by function $\frac{1}{2} \ln|(1+\bar{z})/(1-\bar{z})|$. Specially, the jumps of the normal stresses across the phase boundary $|\bar{z}| = 1$ are

$$\begin{aligned} \llbracket \bar{\sigma}_{rr}^{(n)} \rrbracket_{(1,1)} &= \frac{E^{(1)}\gamma^T}{1+\nu^{(1)}} C_{rr}^{(n)}, \\ \llbracket \bar{\sigma}_{\theta\theta}^{(n)} \rrbracket_{(1,1)} &= \frac{E^{(1)}\gamma^T}{1+\nu^{(1)}} C_{\theta\theta}^{(n)}, \\ \llbracket \bar{\sigma}_{zz}^{(n)} \rrbracket_{(1,1)} &= \frac{E^{(1)}\gamma^T}{1+\nu^{(1)}} C_{zz}^{(n)}, \end{aligned} \quad (4.81)$$

whereas the shear stress approaches infinity with the intensity

$$\bar{\sigma}_{rz}^{(n)}(1, \bar{z}) \sim \frac{E^{(1)}\gamma^T}{(1+\nu^{(1)})\pi} C_{rz}^{(n)} \ln \left| \frac{1+\bar{z}}{1-\bar{z}} \right|, \quad (|\bar{z}| \rightarrow 1). \quad (4.82)$$

The results show that, across the phase boundary of the fiber $|\bar{z}| = 1$, the jumps of the normal stresses and the intensity of singularity of the shear stress are determined by the Young's modulus $E^{(n)}$, the Poisson's ratio $\nu^{(n)}$, and the transformation strain γ^T , but are independent of the aspect ratio α . In other word, the jumps of the normal stresses and the intensity of singularity of the shear stress are determined by the material properties of the matrix and fiber but are independent of the geometry property of the transformed region. The numerical results are consistent with (4.81) and (4.82). The singularity of $\bar{\sigma}_{rz}^{(n)}$ at $|\bar{z}| = 1$ indicates severe stress concentration.

4.8 Remarks

In this chapter, we further investigated the mechanical behavior of SMA fiber reinforced composite associate with phase transformation in the fiber. To take the influence of the matrix on the deformation of the fiber into account, we studied the “perfect bonding elastic fiber” model, which considers the deformation of the fiber also. In this model, the fiber and the matrix are assumed perfectly bonded. The elastostatic problem turns out to be axisymmetric with two separate cylindrical regions, which are connected by perfect bonding conditions. The exact solutions for stresses, strains, and displacements in both the fiber and the matrix are obtained for general phase transformation characteristic function.

Particularly, the case that only one single finite segment of the fiber undergoing phase transformation is further investigated in detail. The results are presented in normalized variables corresponding to the geometry of phase transformed region. By principle of superposition, the properties to this case describe the fundamental behaviors of general linear deformation. By asymptotic analysis, the approximations of the solutions are derived. It is shown that inside the matrix and the fiber all stress components are finite and continuous. However, on the fiber-matrix interface, all stress components have singularities across the phase boundary. The singularities are isolated. The numerical evaluation are also performed. All the results in the “perfect bonding elastic fiber” model are similar to the “perfect bonding rigid fiber” model. As w approaches ∞ , i.e., the fiber is very strong compared with matrix, the results reduce to those of the “perfect bonding rigid fiber” model.

As for the influence of the matrix on the deformation and the phase transformation in the fiber, it is shown that the constraint on the fiber increases with the increase of either w or α . The stiffer matrix exerts greater constraint on the phase transformation of the fiber. On the other hand, in the setting of composite, the phase transformation in the fiber prefers a configuration with multi-piece small

transformed segments to keep small α instead of a large transformed segment to avoid greater constraint from the matrix.

It should notice that both “perfect bonding rigid fiber” and “perfect bonding elastic fiber” models have singularities in stresses at the intersection of the fiber-matrix interface and the phase boundary of the fiber. We suspect that it is a result of the perfect bonding assumption so that some features associated with phase transformation in the SMA fiber, especially near the fiber-matrix interface, are not properly modeled. In the next chapter, we will study another model without perfect bonding assumption.

CHAPTER 5. “SPRING BONDING” MODEL

Previous studies in the Chapter 3 and Chapter 4 indicate that, under the assumption of perfect bonding condition between the fiber and the matrix, the shear stress is singular at the intersection between the fiber-matrix interface and the phase boundary in the fiber. To achieve more reasonable results, we propose a model that relaxes the perfect bonding condition to allow for displacement discontinuity across the fiber-matrix interface. Such a displacement jump results in a shear stress with magnitude proportional to the magnitude of the jump. We will call it a “spring bonding” model. We envision a transition region near the interface within which the morphology of the phase mixture is complicated and 3-dimensional in nature. The collect effect of this transition region is modeled as a linear “shear spring”.

5.1 Bonding Conditions

Assume that the matrix and the fiber are bonded with an elastic “glue”, which maintains perfect bonding in radial direction while resists the relative slip with a linear “shear spring” in axial direction. The relative slip results in a shear stress on the fiber-matrix interface with magnitude proportional to the magnitude of the jump of axial displacement across the interface. The equilibrium still requires that the stress components σ_{rr} and σ_{rz} are continuous accros the fiber-matrix interface. Thus, the system obeys the bonding conditions:

$$[[\sigma_{rr}]]_{\mathcal{P}} = [[u_r]]_{\mathcal{P}} = 0, \quad \sigma_{rz}^{(n)}|_{\mathcal{P}} = k[[u_z]]_{\mathcal{P}}, \quad (5.1)$$

or

$$[[\sigma_{rr}]]_{\mathcal{P}} = [[\sigma_{rz}]]_{\mathcal{P}} = [[u_r]]_{\mathcal{P}} = 0, \quad \sigma_{rz}^{(1)}|_{\mathcal{P}} = k[[u_z]]_{\mathcal{P}}, \quad (5.2)$$

where k is the stiffness of the “shear spring”, \mathcal{P} is the fiber-matrix interface given

by (2.40), and the notation $[[\circ]]_{\mathcal{P}}$ defines the jump discontinuity by

$$[[\circ]]_{\mathcal{P}} \equiv [\circ^{(1)} - \circ^{(2)}] \Big|_{(r,\theta,z) \in \mathcal{P}}. \quad (5.3)$$

After Fourier transform, the bonding conditions (5.2) become

$$[[\tilde{\sigma}_{rr}]]_{r=a} = [[\tilde{\sigma}_{rz}]]_{r=a} = [[\tilde{u}_r]]_{r=a} = 0, \quad \tilde{\sigma}_{rz}^{(1)} = k[[\tilde{u}_z]]_{r=a}, \quad -\infty < \eta < \infty, \quad (5.4)$$

where $[[\tilde{\circ}]]_{r=a}$ defined by

$$[[\tilde{\circ}]]_{r=a} \equiv [\tilde{\circ}^{(1)} - \tilde{\circ}^{(2)}] \Big|_{r=a}. \quad (5.5)$$

5.2 Exact Solutions

Now, we consider the general situation that the phase transformation characteristic function $\gamma^*(z)$ is given by (2.43). In the Fourier transformed domain, the general solutions to the system are given in Chapter 2 by (2.52), (2.58), (2.59), and (2.60). Setting $r = a$ in (2.58) and (2.60) and substituting them into (5.4), one arrives at the algebraic equations for the bonding conditions:

$$q_1^{(1)} A^{(1)} + q_2^{(1)} B^{(1)} - q_1^{(2)} A^{(2)} - q_2^{(2)} B^{(2)} = 0,$$

$$q_3^{(1)} A^{(1)} + q_4^{(1)} B^{(1)} - q_3^{(2)} A^{(2)} - q_4^{(2)} B^{(2)} = 0,$$

$$q_5^{(1)} A^{(1)} + q_6^{(1)} B^{(1)} + wq_5^{(2)} A^{(2)} + wq_6^{(2)} B^{(2)} = 0,$$

$$\left[q_7^{(1)} - \frac{E^{(1)}}{1 + \nu^{(1)}} \frac{|\eta|}{k} q_3^{(1)} \right] A^{(1)} + \left[q_8^{(1)} - \frac{E^{(1)}}{1 + \nu^{(1)}} \frac{|\eta|}{k} q_4^{(1)} \right] B^{(1)}$$

$$-wq_7^{(2)} A^{(2)} - wq_8^{(2)} B^{(2)} = i \frac{E^{(1)}}{1 + \nu^{(1)}} \frac{1}{\eta^3} \tilde{\gamma}^*,$$

$$-\infty < \eta < \infty, \quad (5.6)$$

where, for simple, we denote

$$\begin{aligned}
q_1^{(n)} &= q_1^{(n)}(\eta) = R_0^{(n)}(|\eta|a) - \frac{(-1)^n}{|\eta|a} R_1^{(n)}(|\eta|a), \\
q_2^{(n)} &= q_2^{(n)}(\eta) = (-1)^n(1 - 2\nu^{(n)})R_0^{(n)}(|\eta|a) + |\eta|aR_1^{(n)}(|\eta|a), \\
q_3^{(n)} &= q_3^{(n)}(\eta) = (-1)^n R_1^{(n)}(|\eta|a), \\
q_4^{(n)} &= q_4^{(n)}(\eta) = (-1)^n|\eta|aR_0^{(n)}(|\eta|a) + 2(1 - \nu^{(n)})R_1^{(n)}(|\eta|a), \\
q_5^{(n)} &= q_5^{(n)}(\eta) = R_1^{(n)}(|\eta|a), \\
q_6^{(n)} &= q_6^{(n)}(\eta) = |\eta|aR_0^{(n)}(|\eta|a), \\
q_7^{(n)} &= q_7^{(n)}(\eta) = R_0^{(n)}(|\eta|a), \\
q_8^{(n)} &= q_8^{(n)}(\eta) = (-1)^n4(1 - \nu^{(n)})R_0^{(n)}(|\eta|a) + |\eta|aR_1^{(n)}(|\eta|a), \\
&-\infty < \eta < \infty. \tag{5.7}
\end{aligned}$$

The constant w denotes the ratio of the shear modulus of the matrix $G^{(1)}$ to the shear modulus of the fiber $G^{(2)}$:

$$w = \frac{G^{(1)}}{G^{(2)}} = \frac{(1 + \nu^{(2)})E^{(1)}}{(1 + \nu^{(1)})E^{(2)}}. \tag{5.8}$$

The function $\tilde{\gamma}^* = \tilde{\gamma}^*(\eta)$ is the Fourier transform of phase transformation characteristic function $\gamma^* = \gamma^*(z)$. Here, $q_j^{(n)}$, $j = 1, 2, \dots, 8$, in (5.7) and w in (5.8) are the same as those in (4.6) and (4.7) for the “perfect bonding elastic fiber” model, respectively.

Solving (5.6), one finds the unknown functions $A^{(n)}(\eta)$ and $B^{(n)}(\eta)$ as

$$A^{(n)} = A^{(n)}(\eta) = -i \frac{E^{(1)}}{1 + \nu^{(1)}} \frac{\Delta_A^{(n)}}{\eta^3 \Delta} \tilde{\gamma}^*$$

$$B^{(n)} = B^{(n)}(\eta) = i \frac{E^{(1)}}{1 + \nu^{(1)}} \frac{\Delta_B^{(n)}}{\eta^3 \Delta} \tilde{\gamma}^*,$$

$$-\infty < \eta < \infty, \quad (5.9)$$

where $\Delta = \Delta(\eta)$ is given by the fourth order determinant

$$\Delta(\eta) = \begin{vmatrix} q_1^{(1)} & q_2^{(1)} & -q_1^{(2)} & -q_2^{(2)} \\ q_3^{(1)} & q_4^{(1)} & -q_3^{(2)} & -q_4^{(2)} \\ q_5^{(1)} & q_6^{(1)} & wq_5^{(2)} & wq_6^{(2)} \\ q_7^{(1)} - \frac{E^{(1)}}{1+\nu^{(1)}} \frac{|\eta|}{k} q_3^{(1)} & q_8^{(1)} - \frac{E^{(1)}}{1+\nu^{(1)}} \frac{|\eta|}{k} q_4^{(1)} & -wq_7^{(2)} & -wq_8^{(2)} \end{vmatrix},$$

$$-\infty < \eta < \infty, \quad (5.10)$$

and $\Delta_A^{(n)} = \Delta_A^{(n)}(\eta)$ and $\Delta_B^{(n)} = \Delta_B^{(n)}(\eta)$ are given by the third order determinants

$$\Delta_A^{(1)}(\eta) = \begin{vmatrix} q_2^{(1)} & -q_1^{(2)} & -q_2^{(2)} \\ q_4^{(1)} & -q_3^{(2)} & -q_4^{(2)} \\ q_6^{(1)} & wq_5^{(2)} & wq_6^{(2)} \end{vmatrix},$$

$$\Delta_B^{(1)}(\eta) = \begin{vmatrix} q_1^{(1)} & -q_1^{(2)} & -q_2^{(2)} \\ q_3^{(1)} & -q_3^{(2)} & -q_4^{(2)} \\ q_5^{(1)} & wq_5^{(2)} & wq_6^{(2)} \end{vmatrix},$$

$$\Delta_A^{(2)}(\eta) = \begin{vmatrix} q_1^{(1)} & q_2^{(1)} & -q_2^{(2)} \\ q_3^{(1)} & q_4^{(1)} & -q_4^{(2)} \\ q_5^{(1)} & q_6^{(1)} & wq_6^{(2)} \end{vmatrix},$$

$$\Delta_B^{(2)}(\eta) = \begin{vmatrix} q_1^{(1)} & q_2^{(1)} & -q_1^{(2)} \\ q_3^{(1)} & q_4^{(1)} & -q_3^{(2)} \\ q_5^{(1)} & q_6^{(1)} & wq_5^{(2)} \end{vmatrix},$$

$$-\infty < \eta < \infty. \quad (5.11)$$

Notice that $\Delta_A^{(n)}$ and $\Delta_B^{(n)}$ in (5.11) are the same as those in the “perfect bonding elastic fiber” model (4.10), while Δ in (5.10) is different from that in (4.9). Here, the Δ in (5.10) has extra terms including k . Although $A^{(n)}$ and $B^{(n)}$ in (5.9) have the same forms as those in (4.8) for the “perfect bonding elastic fiber” model, they are different in nature because Δ in (5.10) is different from that in (4.9). For the determinant Δ in (5.10), only two terms involve k . Using the linearity of determinant, one can separate the determinant Δ into two determinants:

$$\begin{aligned} \Delta(\eta) = & \begin{vmatrix} q_1^{(1)} & q_2^{(1)} & -q_1^{(2)} & -q_2^{(2)} \\ q_3^{(1)} & q_4^{(1)} & -q_3^{(2)} & -q_4^{(2)} \\ q_5^{(1)} & q_6^{(1)} & wq_5^{(2)} & wq_6^{(2)} \\ q_7^{(1)} & q_8^{(1)} & -wq_7^{(2)} & -wq_8^{(2)} \end{vmatrix} \\ & + \begin{vmatrix} q_1^{(1)} & q_2^{(1)} & -q_1^{(2)} & -q_2^{(2)} \\ q_3^{(1)} & q_4^{(1)} & -q_3^{(2)} & -q_4^{(2)} \\ q_5^{(1)} & q_6^{(1)} & wq_5^{(2)} & wq_6^{(2)} \\ -\frac{E^{(1)}}{1+\nu^{(1)}} \frac{|\eta|}{k} q_3^{(1)} & -\frac{E^{(1)}}{1+\nu^{(1)}} \frac{|\eta|}{k} q_4^{(1)} & 0 & 0 \end{vmatrix}, \\ & -\infty < \eta < \infty. \end{aligned} \quad (5.12)$$

Expanding the second determinant according to the 4th row, one has

$$\Delta(\eta) = \begin{vmatrix} q_1^{(1)} & q_2^{(1)} & -q_1^{(2)} & -q_2^{(2)} \\ q_3^{(1)} & q_4^{(1)} & -q_3^{(2)} & -q_4^{(2)} \\ q_5^{(1)} & q_6^{(1)} & wq_5^{(2)} & wq_6^{(2)} \\ q_7^{(1)} & q_8^{(1)} & -wq_7^{(2)} & -wq_8^{(2)} \end{vmatrix} + \frac{E^{(1)}}{1+\nu^{(1)}} \frac{|\eta|}{k} \left(q_3^{(1)} \Delta_A^{(1)} - q_4^{(1)} \Delta_B^{(1)} \right),$$

$$-\infty < \eta < \infty. \quad (5.13)$$

Here, the first term of Δ is the same as that in the “perfect bonding elastic fiber” model (4.9) and the effect of the spring k comes only from the second term.

Substituting (5.9) into (2.52), one obtains the Fourier transformed Love’s stress functions for the matrix and the fiber:

$$\begin{aligned} \frac{\tilde{\Phi}^{(n)}}{\tilde{\gamma}^*} = & i \frac{E^{(1)}}{(1 + \nu^{(1)})} \frac{1}{\eta^3 \Delta} \left[-\Delta_A^{(n)} R_0^{(n)}(|\eta|r) \right. \\ & \left. + \Delta_B^{(n)} |\eta|r R_1^{(n)}(|\eta|r) \right] \quad \text{on } \tilde{\Omega}^{(n)}. \end{aligned} \quad (5.14)$$

Similarly, substituting (5.9) into (2.58), (2.59), and (2.60), one obtains the Fourier transformed stresses, strains, and displacements for the matrix and the fiber, respectively. The Fourier transformed stresses for the matrix and the fiber are

$$\begin{aligned} \frac{\tilde{\sigma}_{rr}^{(n)}}{\tilde{\gamma}^*} = & i \frac{E^{(1)}}{(1 + \nu^{(1)})} \frac{1}{\Delta} \left\{ \left[R_0^{(n)}(|\eta|r) - \frac{(-1)^n}{|\eta|r} R_1^{(n)}(|\eta|r) \right] \Delta_A^{(n)} \right. \\ & \left. - \left[(-1)^n (1 - 2\nu^{(n)}) R_0^{(n)}(|\eta|r) + |\eta|r R_1^{(n)}(|\eta|r) \right] \Delta_B^{(n)} \right\}, \\ \frac{\tilde{\sigma}_{\theta\theta}^{(n)}}{\tilde{\gamma}^*} = & \frac{E^{(1)}}{(1 + \nu^{(1)})} \frac{(-1)^n}{\Delta} \left\{ \frac{1}{|\eta|r} R_1^{(n)}(|\eta|r) \Delta_A^{(n)} \right. \\ & \left. - (1 - 2\nu^{(n)}) R_0^{(n)}(|\eta|r) \Delta_B^{(n)} \right\}, \\ \frac{\tilde{\sigma}_{zz}^{(n)}}{\tilde{\gamma}^*} = & \frac{E^{(1)}}{(1 + \nu^{(1)})} \frac{1}{\Delta} \left\{ -R_0^{(n)}(|\eta|r) \Delta_A^{(n)} \right. \\ & \left. + \left[(-1)^n 2(2 - \nu^{(1)}) R_0^{(n)}(|\eta|r) + |\eta|r R_1^{(n)}(|\eta|r) \right] \Delta_B^{(n)} \right\}, \\ \frac{\tilde{\sigma}_{rz}^{(n)}}{\tilde{\gamma}^*} = & i \frac{E^{(1)}}{(1 + \nu^{(1)})} \frac{\text{sign}(\eta)}{\Delta} \left\{ (-1)^{n+1} R_1^{(n)}(|\eta|r) \Delta_A^{(n)} \right. \\ & \left. + \left[(-1)^n |\eta|r R_0^{(n)}(|\eta|r) + 2(1 - \nu^{(1)}) R_1^{(n)}(|\eta|r) \right] \Delta_B^{(n)} \right\} \end{aligned}$$

$$\text{on } \tilde{\Omega}^{(n)}. \quad (5.15)$$

The Fourier transformed strains for the matrix and the fiber are

$$\begin{aligned} \frac{\tilde{\gamma}_{rr}^{(n)}}{\tilde{\gamma}^*} &= w^{n-1} \frac{1}{\Delta} \left\{ \left[R_0^{(n)}(|\eta|r) - \frac{(-1)^n}{|\eta|r} R_1^{(n)}(|\eta|r) \right] \Delta_A^{(n)} \right. \\ &\quad \left. - \left[(-1)^n R_0^{(n)}(|\eta|r) + |\eta|r R_1^{(n)}(|\eta|r) \right] \Delta_B^{(n)} \right\}, \\ \frac{\tilde{\gamma}_{\theta\theta}^{(n)}}{\tilde{\gamma}^*} &= (-1)^n w^{n-1} \frac{1}{\Delta} \left\{ \frac{1}{|\eta|r} R_1^{(n)}(|\eta|r) \Delta_A^{(n)} \right. \\ &\quad \left. - R_0^{(n)}(|\eta|r) \Delta_B^{(n)} \right\}, \\ \frac{\tilde{\gamma}_{zz}^{(n)}}{\tilde{\gamma}^*} &= w^{n-1} \frac{1}{\Delta} \left\{ -R_0^{(n)}(|\eta|r) \Delta_A^{(n)} \right. \\ &\quad \left. + \left[(-1)^n 4(1 - \nu^{(n)}) R_0^{(n)}(|\eta|r) \right. \right. \\ &\quad \left. \left. + |\eta|r R_1^{(n)}(|\eta|r) \right] \Delta_B^{(n)} \right\} + \delta_{n2}, \\ \frac{\tilde{\gamma}_{rz}^{(n)}}{\tilde{\gamma}^*} &= iw^{n-1} \frac{\text{sign}(\eta)}{\Delta} \left\{ (-1)^{n+1} R_1^{(n)}(|\eta|r) \Delta_A^{(n)} \right. \\ &\quad \left. + \left[(-1)^n |\eta|r R_0^{(n)}(|\eta|r) + 2(1 - \nu^{(n)}) R_1^{(n)}(|\eta|r) \right] \Delta_B^{(n)} \right\} \end{aligned}$$

$$\text{on } \tilde{\Omega}^{(n)}. \quad (5.16)$$

The Fourier transformed stresses for the matrix and the fiber are

$$\begin{aligned} \frac{\tilde{u}_r^{(n)}}{\tilde{\gamma}^*} &= (-1)^n w^{n-1} \frac{1}{|\eta|\Delta} \left\{ R_1^{(n)}(|\eta|r) \Delta_A^{(n)} \right. \\ &\quad \left. - |\eta|r R_0^{(n)}(|\eta|r) \Delta_B^{(n)} \right\}, \\ \frac{\tilde{u}_z^{(n)}}{\tilde{\gamma}^*} &= iw^{n-1} \frac{1}{\eta\Delta} \left\{ -R_0^{(n)}(|\eta|r) \Delta_A^{(n)} \right. \end{aligned}$$

$$\begin{aligned}
& + \left[(-1)^n 4(1 - \nu^{(n)}) R_0^{(n)}(|\eta|r) \right. \\
& \left. + |\eta|r R_1^{(n)}(|\eta|r) \right] \Delta_B^{(n)} \Big\} + i\delta_{n2} \frac{1}{\eta} \\
& \text{on } \tilde{\Omega}^{(n)}. \tag{5.17}
\end{aligned}$$

For fixed r , all these ratios given in (5.14), (5.15), (5.16), and (5.17) are functions of the material properties of the matrix and the fiber as well as the geometry parameter of the fiber through the radius a of the fiber, but independent of the phase transformation in the fiber. If consider the phase transformation in the fiber as input or excitation and the Love's stress function, stresses, strains, and displacements in the matrix as outputs or responses, these ratios give the corresponding transfer functions, respectively. Theoretically, these ratios characterize all the behavior of the composite associate with the phase transformation in the fiber. For given materials of fiber and matrix, these ratios are completely determined by the corresponding material properties and the radius of the fiber. Then, for a given phase transformation pattern, the distributions of stress, strain, displacement in the matrix and the fiber can be found through the phase transformation characteristic function of the fiber together with these ratios.

Multiplying these ratios in (5.14), (5.15), (5.16), and (5.17) by the phase transformation characteristic function of the fiber $\tilde{\gamma}^*$ and performing inverse Fourier transform, one obtains the Love's stress functions, stresses, strains, and displacements of the matrix and the fiber in the original physical domains $\mathcal{R}^{(n)}$, respectively.

The Love's stress functions are

$$\begin{aligned}
\Phi^{(n)}(r, z) = & i \frac{E^{(1)}}{2\pi(1 + \nu^{(1)})} \int_{-\infty}^{\infty} \frac{1}{\eta^3 \Delta} \left[-\Delta_A^{(n)} R_0^{(n)}(|\eta|r) \right. \\
& \left. + \Delta_B^{(n)} |\eta|r R_1^{(n)}(|\eta|r) \right] \tilde{\gamma}^*(\eta) e^{-iz\eta} d\eta \quad \text{on } \Omega^{(n)}. \tag{5.18}
\end{aligned}$$

The stresses can be written as the following forms

$$\begin{aligned}
\sigma_{rr}^{(n)}(r, z) &= i \frac{E^{(1)}}{2\pi(1+\nu^{(1)})} \int_{-\infty}^{\infty} \frac{1}{\Delta} \left\{ \left[R_0^{(n)}(|\eta|r) - \frac{(-1)^n}{|\eta|r} R_1^{(n)}(|\eta|r) \right] \Delta_A^{(n)} \right. \\
&\quad \left. - \left[(-1)^n (1 - 2\nu^{(n)}) R_0^{(n)}(|\eta|r) + |\eta|r R_1^{(n)}(|\eta|r) \right] \Delta_B^{(n)} \right\} \tilde{\gamma}^*(\eta) e^{-iz\eta} d\eta, \\
\sigma_{\theta\theta}^{(n)}(r, z) &= \frac{E^{(1)}}{2\pi(1+\nu^{(1)})} \int_{-\infty}^{\infty} \frac{(-1)^n}{\Delta} \left\{ \frac{1}{|\eta|r} R_1^{(n)}(|\eta|r) \Delta_A^{(n)} \right. \\
&\quad \left. - (1 - 2\nu^{(n)}) R_0^{(n)}(|\eta|r) \Delta_B^{(n)} \right\} \tilde{\gamma}^*(\eta) e^{-iz\eta} d\eta, \\
\sigma_{zz}^{(n)}(r, z) &= \frac{E^{(1)}}{2\pi(1+\nu^{(1)})} \int_{-\infty}^{\infty} \frac{1}{\Delta} \left\{ -R_0^{(n)}(|\eta|r) \Delta_A^{(n)} \right. \\
&\quad \left. + \left[(-1)^n 2(2 - \nu^{(1)}) R_0^{(n)}(|\eta|r) + |\eta|r R_1^{(n)}(|\eta|r) \right] \Delta_B^{(n)} \right\} \tilde{\gamma}^*(\eta) e^{-iz\eta} d\eta, \\
\sigma_{rz}^{(n)}(r, z) &= i \frac{E^{(1)}}{2\pi(1+\nu^{(1)})} \int_{-\infty}^{\infty} \frac{\text{sign}(\eta)}{\Delta} \left\{ (-1)^{n+1} R_1^{(n)}(|\eta|r) \Delta_A^{(n)} \right. \\
&\quad \left. + \left[(-1)^n |\eta|r R_0^{(n)}(|\eta|r) + 2(1 - \nu^{(1)}) R_1^{(n)}(|\eta|r) \right] \Delta_B^{(n)} \right\} \tilde{\gamma}^*(\eta) e^{-iz\eta} d\eta
\end{aligned}$$

on $\Omega^{(n)}$. (5.19)

The strain components can be written as

$$\begin{aligned}
\gamma_{rr}^{(n)}(r, z) &= \frac{w^{n-1}}{2\pi} \int_{-\infty}^{\infty} \frac{1}{\Delta} \left\{ \left[R_0^{(n)}(|\eta|r) - \frac{(-1)^n}{|\eta|r} R_1^{(n)}(|\eta|r) \right] \Delta_A^{(n)} \right. \\
&\quad \left. - \left[(-1)^n R_0^{(n)}(|\eta|r) + |\eta|r R_1^{(n)}(|\eta|r) \right] \Delta_B^{(n)} \right\} \tilde{\gamma}^*(\eta) e^{-iz\eta} d\eta, \\
\gamma_{\theta\theta}^{(n)}(r, z) &= (-1)^n \frac{w^{n-1}}{2\pi} \int_{-\infty}^{\infty} \frac{1}{\Delta} \left\{ \frac{1}{|\eta|r} R_1^{(n)}(|\eta|r) \Delta_A^{(n)} \right. \\
&\quad \left. - R_0^{(n)}(|\eta|r) \Delta_B^{(n)} \right\} \tilde{\gamma}^*(\eta) e^{-iz\eta} d\eta,
\end{aligned}$$

$$\begin{aligned}
\gamma_{zz}^{(n)}(r, z) &= \frac{w^{n-1}}{2\pi} \int_{-\infty}^{\infty} \frac{1}{\Delta} \left\{ -R_0^{(n)}(|\eta|r)\Delta_A^{(n)} \right. \\
&\quad + \left[(-1)^n 4(1 - \nu^{(n)})R_0^{(n)}(|\eta|r) \right. \\
&\quad \left. \left. + |\eta|rR_1^{(n)}(|\eta|r) \right] \Delta_B^{(n)} \right\} \tilde{\gamma}^*(\eta) e^{-iz\eta} d\eta + \delta_{n2}\gamma^*(z), \\
\gamma_{rz}^{(n)}(r, z) &= i \frac{w^{n-1}}{2\pi} \int_{-\infty}^{\infty} \frac{\text{sign}(\eta)}{\Delta} \left\{ (-1)^{n+1} R_1^{(n)}(|\eta|r)\Delta_A^{(n)} \right. \\
&\quad \left. + \left[(-1)^n |\eta|rR_0^{(n)}(|\eta|r) + 2(1 - \nu^{(n)})R_1^{(n)}(|\eta|r) \right] \Delta_B^{(n)} \right\} \tilde{\gamma}^*(\eta) e^{-iz\eta} d\eta \\
&\quad \text{on } \Omega^{(n)}. \tag{5.20}
\end{aligned}$$

The displacement components are

$$\begin{aligned}
u_r^{(n)}(r, z) &= (-1)^n \frac{w^{n-1}}{2\pi} \int_{-\infty}^{\infty} \frac{1}{|\eta|\Delta} \left\{ R_1^{(n)}(|\eta|r)\Delta_A^{(n)} \right. \\
&\quad \left. - |\eta|rR_0^{(n)}(|\eta|r)\Delta_B^{(n)} \right\} \tilde{\gamma}^*(\eta) e^{-iz\eta} d\eta, \\
u_z^{(n)}(r, z) &= i \frac{w^{n-1}}{2\pi} \int_{-\infty}^{\infty} \frac{1}{\eta\Delta} \left\{ -R_0^{(n)}(|\eta|r)\Delta_A^{(n)} \right. \\
&\quad + \left[(-1)^n 4(1 - \nu^{(n)})R_0^{(n)}(|\eta|r) \right. \\
&\quad \left. \left. + |\eta|rR_1^{(n)}(|\eta|r) \right] \Delta_B^{(n)} \right\} \tilde{\gamma}^*(\eta) e^{-iz\eta} d\eta + \delta_{n2}u^*(z) \\
&\quad \text{on } \Omega^{(n)}, \tag{5.21}
\end{aligned}$$

where $u^*(z)$ is the displacement phase transformation function as in (2.64)

$$u^*(z) = \int_{z_0}^z \gamma^*(s) ds. \tag{5.22}$$

Alternatively, the (5.18), (5.19), (5.20), and (5.21) can also be obtained by directly substituting (5.9), (5.10), and (5.11) into (2.61), (2.62), (2.63), and (2.64), respectively.

Here, although the forms of (5.18), (5.19), (5.20), and (5.21) are the same as those of (4.15), (4.16), (4.17), and (4.18) for the “perfect bonding elastic fiber” model, they are different since the Δ is different in these two cases in which Δ are given by (4.9) and (5.13), respectively.

5.3 Single Finite Segment Transformation

Now, we look at the situation that only a single finite segment of the fiber undergoes phase transformation. Assuming only a single finite segment of length $2L$ of the fiber undergoes a uniform phase transformation with a constant normal transformation strain γ^T along the axial direction of the fiber, i.e., $\Lambda = [-L, L]$, the transformation characteristic function is give by

$$\gamma^* = \gamma^*(z) \equiv \begin{cases} \gamma^T & |z| \leq L, \\ 0 & |z| > L. \end{cases} \quad (5.23)$$

In the Fourier transformed domain, one has from (2.21) that

$$\tilde{\gamma}^* = \tilde{\gamma}^*(\eta) = \frac{2\gamma^T}{\eta} \sin(L\eta). \quad (5.24)$$

Substituting (5.24) into (5.9), one has

$$\begin{aligned} A^{(n)}(\eta) &= -i \frac{2E^{(1)}\gamma^T}{1 + \nu^{(1)}} \frac{\Delta_A^{(n)}}{\eta^4 \Delta} \sin(L\eta), \\ B^{(n)}(\eta) &= i \frac{2E^{(1)}\gamma^T}{1 + \nu^{(1)}} \frac{\Delta_B^{(n)}}{\eta^4 \Delta} \sin(L\eta), \\ &-\infty < \eta < \infty. \end{aligned} \quad (5.25)$$

For this special case, it is convenient to introduce the normalized coordinates (\bar{r}, \bar{z}) and aspect ratio α defined by (2.68) and (2.69), respectively. As for the spring,

we define the normalized stiffness \bar{k} by

$$\bar{k} = \frac{ak}{E^{(2)}}. \quad (5.26)$$

In terms of these normalized or dimensionless variables, one has

$$\begin{aligned} \bar{A}^{(n)}(\bar{\eta}) &= A^{(n)}(\eta) \Big|_{\eta=\bar{\eta}/a} = -i \frac{2E^{(1)}\gamma^T}{1+\nu^{(1)}} \frac{\bar{\Delta}_A^{(n)}}{\bar{\eta}^4 \bar{\Delta}} \sin(\alpha\bar{\eta}), \\ \bar{B}^{(n)}(\bar{\eta}) &= B^{(n)}(\eta) \Big|_{\eta=\bar{\eta}/a} = i \frac{2E^{(1)}\gamma^T}{1+\nu^{(1)}} \frac{\bar{\Delta}_B^{(n)}}{\bar{\eta}^4 \bar{\Delta}} \sin(\alpha\bar{\eta}), \\ &-\infty < \bar{\eta} < \infty, \end{aligned} \quad (5.27)$$

where $\bar{\Delta} = \bar{\Delta}(\bar{\eta}) = \Delta^{(n)}(\eta) \Big|_{\eta=\bar{\eta}/a}$ is given by determinant

$$\bar{\Delta}(\bar{\eta}) = \begin{vmatrix} \bar{q}_1^{(1)} & \bar{q}_2^{(1)} & -\bar{q}_1^{(2)} & -\bar{q}_2^{(2)} \\ \bar{q}_3^{(1)} & \bar{q}_4^{(1)} & -\bar{q}_3^{(2)} & -\bar{q}_4^{(2)} \\ \bar{q}_5^{(1)} & \bar{q}_6^{(1)} & w\bar{q}_5^{(2)} & w\bar{q}_6^{(2)} \\ \bar{q}_7^{(1)} & \bar{q}_8^{(1)} & -w\bar{q}_7^{(2)} & -w\bar{q}_8^{(2)} \end{vmatrix} + \frac{w}{1+\nu^{(2)}} \frac{|\bar{\eta}|}{\bar{k}} \left(\bar{q}_3^{(1)} \bar{\Delta}_A^{(1)} - \bar{q}_4^{(1)} \bar{\Delta}_B^{(1)} \right), \quad (5.28)$$

and $\bar{\Delta}_A^{(n)} = \bar{\Delta}_A^{(n)}(\bar{\eta}) = \Delta_A^{(n)}(\eta) \Big|_{\eta=\bar{\eta}/a}$ and $\bar{\Delta}_B^{(n)} = \bar{\Delta}_B^{(n)}(\bar{\eta}) = \Delta_B^{(n)}(\eta) \Big|_{\eta=\bar{\eta}/a}$ are given by

$$\bar{\Delta}_A^{(1)}(\bar{\eta}) = \begin{vmatrix} \bar{q}_2^{(1)} & -\bar{q}_1^{(2)} & -\bar{q}_2^{(2)} \\ \bar{q}_4^{(1)} & -\bar{q}_3^{(2)} & -\bar{q}_4^{(2)} \\ \bar{q}_6^{(1)} & w\bar{q}_5^{(2)} & w\bar{q}_6^{(2)} \end{vmatrix},$$

$$\bar{\Delta}_B^{(1)}(\bar{\eta}) = \begin{vmatrix} \bar{q}_1^{(1)} & -\bar{q}_1^{(2)} & -\bar{q}_2^{(2)} \\ \bar{q}_3^{(1)} & -\bar{q}_3^{(2)} & -\bar{q}_4^{(2)} \\ \bar{q}_5^{(1)} & w\bar{q}_5^{(2)} & w\bar{q}_6^{(2)} \end{vmatrix},$$

$$\bar{\Delta}_A^{(2)}(\bar{\eta}) = \begin{vmatrix} \bar{q}_1^{(1)} & \bar{q}_2^{(1)} & -\bar{q}_2^{(2)} \\ \bar{q}_3^{(1)} & \bar{q}_4^{(1)} & -\bar{q}_4^{(2)} \\ \bar{q}_5^{(1)} & \bar{q}_6^{(1)} & w\bar{q}_6^{(2)} \end{vmatrix},$$

$$\bar{\Delta}_B^{(2)}(\bar{\eta}) = \begin{vmatrix} \bar{q}_1^{(1)} & \bar{q}_2^{(1)} & -\bar{q}_1^{(2)} \\ \bar{q}_3^{(1)} & \bar{q}_4^{(1)} & -\bar{q}_3^{(2)} \\ \bar{q}_5^{(1)} & \bar{q}_6^{(1)} & w\bar{q}_5^{(2)} \end{vmatrix},$$

$$-\infty < \bar{\eta} < \infty. \quad (5.29)$$

Here, $\bar{q}_j^{(n)} = \bar{q}_j^{(n)}(\bar{\eta}) = q_j^{(n)}(\eta)|_{\eta=\bar{\eta}/a}$, $j = 1, 2, \dots, 8$, are

$$\bar{q}_1^{(n)}(\bar{\eta}) = R_0^{(n)}(|\bar{\eta}|) - \frac{(-1)^n}{|\bar{\eta}|} R_1^{(n)}(|\bar{\eta}|),$$

$$\bar{q}_2^{(n)}(\bar{\eta}) = (-1)^n(1 - 2\nu^{(n)})R_0^{(n)}(|\bar{\eta}|) + |\bar{\eta}|R_1^{(n)}(|\bar{\eta}|),$$

$$\bar{q}_3^{(n)}(\bar{\eta}) = (-1)^n R_1^{(n)}(|\bar{\eta}|),$$

$$\bar{q}_4^{(n)}(\bar{\eta}) = (-1)^n |\bar{\eta}| R_0^{(n)}(|\bar{\eta}|) + 2(1 - \nu^{(n)})R_1^{(n)}(|\bar{\eta}|),$$

$$\bar{q}_5^{(n)}(\bar{\eta}) = R_1^{(n)}(|\bar{\eta}|),$$

$$\bar{q}_6^{(n)}(\bar{\eta}) = |\bar{\eta}| R_0^{(n)}(|\bar{\eta}|),$$

$$\bar{q}_7^{(n)}(\bar{\eta}) = R_0^{(n)}(|\bar{\eta}|),$$

$$\bar{q}_8^{(n)}(\bar{\eta}) = (-1)^n 4(1 - \nu^{(n)})R_0^{(n)}(|\bar{\eta}|) + |\bar{\eta}|R_1^{(n)}(|\bar{\eta}|),$$

$$-\infty < \bar{\eta} < \infty. \quad (5.30)$$

Notice that $\bar{q}_j^{(n)}(\bar{\eta})$, $j = 1, 2, \dots, 8$, in (5.30) and $\bar{\Delta}_A^{(n)}(\bar{\eta})$ and $\bar{\Delta}_B^{(n)}(\bar{\eta})$ in (5.29) are the same as those in (4.26) and (4.25) for the “elastic fiber” model, respectively. However, $\bar{\Delta}(\bar{\eta})$ in (5.28), which has an extra term including \bar{k} , is differ from that in (4.24) for the “elastic fiber” model. Therefore, even though $\bar{A}^{(n)}(\bar{\eta})$ and $\bar{B}^{(n)}(\bar{\eta})$

have the same form in (5.27) and (4.22), they are different because $\bar{\Delta}(\bar{\eta})$ is not the same.

Substituting (5.23) into (5.18), and then normalize them by using (2.68), (2.69), and (5.26), or directly substituting (5.27) into (2.71), one obtains the Love's stress function in the normalized coordinates. Noticing that the imaginary parts of the integrands are odd functions of $\bar{\eta}$, the Love's stress functions, in the normalized coordinate, have the following forms

$$\begin{aligned} \bar{\Phi}^{(n)}(\bar{r}, \bar{z}) = & \frac{E^{(1)}\gamma^T a^3}{\pi(1+\nu^{(1)})} \int_{-\infty}^{\infty} \frac{1}{\bar{\eta}^4 \bar{\Delta}} \left[-\bar{\Delta}_A^{(n)} R_0^{(n)}(|\bar{\eta}|\bar{r}) \right. \\ & \left. + \bar{\Delta}_B^{(n)} |\bar{\eta}|\bar{r} R_1^{(n)}(|\bar{\eta}|\bar{r}) \right] \sin(\alpha\bar{\eta}) \sin(\alpha\bar{z}\bar{\eta}) d\bar{\eta} \quad \text{on } \Omega^{(n)}. \end{aligned} \quad (5.31)$$

Similarly, substituting (5.27) into (2.75), (2.76), and (2.78), and considering that the imaginary parts of the integrands are odd functions of $\bar{\eta}$, one has distributions of stress, strain, and displacement in the normalized coordinates. The stresses, in the normalized coordinates, are

$$\begin{aligned} \bar{\sigma}_{rr}^{(n)}(\bar{r}, \bar{z}) = & \frac{E^{(1)}\gamma^T}{(1+\nu^{(1)})\pi} \int_{-\infty}^{\infty} \frac{1}{\bar{\eta}\bar{\Delta}} \left\{ \left[R_0^{(n)}(|\bar{\eta}|\bar{r}) \right. \right. \\ & \left. \left. - \frac{(-1)^n}{|\bar{\eta}|\bar{r}} R_1^{(n)}(|\bar{\eta}|\bar{r}) \right] \bar{\Delta}_A^{(n)} - \left[(-1)^n (1-2\nu^{(n)}) R_0^{(n)}(|\bar{\eta}|\bar{r}) \right. \right. \\ & \left. \left. + |\bar{\eta}|\bar{r} R_1^{(n)}(|\bar{\eta}|\bar{r}) \right] \bar{\Delta}_B^{(n)} \right\} \sin(\alpha\bar{\eta}) \cos(\alpha\bar{z}\bar{\eta}) d\bar{\eta}, \\ \bar{\sigma}_{\theta\theta}^{(n)}(\bar{r}, \bar{z}) = & \frac{E^{(1)}\gamma^T}{(1+\nu^{(1)})\pi} \int_{-\infty}^{\infty} \frac{(-1)^n}{\bar{\eta}\bar{\Delta}} \left\{ \frac{1}{|\bar{\eta}|\bar{r}} R_1^{(n)}(|\bar{\eta}|\bar{r}) \bar{\Delta}_A^{(n)} \right. \\ & \left. - (1-2\nu^{(n)}) R_0^{(n)}(|\bar{\eta}|\bar{r}) \bar{\Delta}_B^{(n)} \right\} \sin(\alpha\bar{\eta}) \cos(\alpha\bar{z}\bar{\eta}) d\bar{\eta}, \\ \bar{\sigma}_{zz}^{(n)}(\bar{r}, \bar{z}) = & \frac{E^{(1)}\gamma^T}{(1+\nu^{(1)})\pi} \int_{-\infty}^{\infty} \frac{1}{\bar{\eta}\bar{\Delta}} \left\{ -R_0^{(n)}(|\bar{\eta}|\bar{r}) \bar{\Delta}_A^{(n)} \right. \\ & \left. + \left[(-1)^n 2(2-\nu^{(1)}) R_0^{(n)}(|\bar{\eta}|\bar{r}) \right. \right. \end{aligned}$$

$$\begin{aligned}
& +|\bar{\eta}|\bar{r}R_1^{(n)}(|\bar{\eta}|\bar{r})\left]\bar{\Delta}_B^{(n)}\right\}\sin(\alpha\bar{\eta})\cos(\alpha\bar{z}\bar{\eta})d\bar{\eta}, \\
\bar{\sigma}_{rz}^{(n)}(\bar{r}, \bar{z}) &= \frac{E^{(1)}\gamma^T}{(1+\nu^{(1)})\pi} \int_{-\infty}^{\infty} \frac{1}{|\bar{\eta}|\bar{\Delta}} \left\{ (-1)^{n+1}R_1^{(n)}(|\bar{\eta}|\bar{r})\bar{\Delta}_A^{(n)} \right. \\
& + \left[(-1)^n|\bar{\eta}|\bar{r}R_0^{(n)}(|\bar{\eta}|\bar{r}) \right. \\
& \left. \left. + 2(1-\nu^{(1)})R_1^{(n)}(|\bar{\eta}|\bar{r})\right]\bar{\Delta}_B^{(n)} \right\} \sin(\alpha\bar{\eta})\sin(\alpha\bar{z}\bar{\eta})d\bar{\eta} \\
& \text{on } \bar{\Omega}^{(n)}. \tag{5.32}
\end{aligned}$$

The strain components, in terms of normalized coordinates, are

$$\begin{aligned}
\bar{\gamma}_{rr}^{(n)}(\bar{r}, \bar{z}) &= \frac{\gamma^T w^{n-1}}{\pi} \int_{-\infty}^{\infty} \frac{1}{\bar{\eta}\bar{\Delta}} \left\{ \left[R_0^{(n)}(|\bar{\eta}|\bar{r}) \right. \right. \\
& - \frac{(-1)^n}{|\bar{\eta}|\bar{r}} R_1^{(n)}(|\bar{\eta}|\bar{r})\left]\bar{\Delta}_A^{(n)} - \left[(-1)^n R_0^{(n)}(|\bar{\eta}|\bar{r}) \right. \right. \\
& \left. \left. + |\bar{\eta}|\bar{r}R_1^{(n)}(|\bar{\eta}|\bar{r})\right]\bar{\Delta}_B^{(n)} \right\} \sin(\alpha\bar{\eta})\cos(\alpha\bar{z}\bar{\eta})d\bar{\eta}, \\
\bar{\gamma}_{\theta\theta}^{(n)}(\bar{r}, \bar{z}) &= (-1)^n \frac{\gamma^T w^{n-1}}{\pi} \int_{-\infty}^{\infty} \frac{1}{\bar{\eta}\bar{\Delta}} \left\{ \frac{1}{|\bar{\eta}|\bar{r}} R_1^{(n)}(|\bar{\eta}|\bar{r})\bar{\Delta}_A^{(n)} \right. \\
& \left. - R_0^{(n)}(|\bar{\eta}|\bar{r})\bar{\Delta}_B^{(n)} \right\} \sin(\alpha\bar{\eta})\cos(\alpha\bar{z}\bar{\eta})d\bar{\eta}, \\
\bar{\gamma}_{zz}^{(n)}(\bar{r}, \bar{z}) &= \frac{\gamma^T w^{n-1}}{\pi} \int_{-\infty}^{\infty} \frac{1}{\bar{\eta}\bar{\Delta}} \left\{ -R_0^{(n)}(|\bar{\eta}|\bar{r})\bar{\Delta}_A^{(n)} \right. \\
& + \left[(-1)^n 4(1-\nu^{(n)})R_0^{(n)}(|\bar{\eta}|\bar{r}) \right. \\
& \left. \left. + |\bar{\eta}|\bar{r}R_1^{(n)}(|\bar{\eta}|\bar{r})\right]\bar{\Delta}_B^{(n)} \right\} \sin(\alpha\bar{\eta})\cos(\alpha\bar{z}\bar{\eta})d\bar{\eta} + \delta_{n2}\bar{\gamma}^* \\
\bar{\gamma}_{rz}^{(n)}(\bar{r}, \bar{z}) &= \frac{\gamma^T w^{n-1}}{\pi} \int_{-\infty}^{\infty} \frac{1}{|\bar{\eta}|\bar{\Delta}} \left\{ (-1)^{n+1}R_1^{(n)}(|\bar{\eta}|\bar{r})\bar{\Delta}_A^{(n)} \right. \\
& \left. + \left[(-1)^n|\bar{\eta}|\bar{r}R_0^{(n)}(|\bar{\eta}|\bar{r}) \right. \right.
\end{aligned}$$

$$\begin{aligned}
& +2(1 - \nu^{(n)})R_1^{(n)}(|\bar{\eta}|\bar{r}) \left] \bar{\Delta}_B^{(n)} \right\} \sin(\alpha\bar{\eta})\sin(\alpha\bar{z}\bar{\eta})d\bar{\eta} \\
& \text{on } \bar{\Omega}^{(n)}, \tag{5.33}
\end{aligned}$$

where

$$\bar{\gamma}^* = \bar{\gamma}^*(\bar{z}) \equiv \begin{cases} \gamma^T & |\bar{z}| \leq 1, \\ 0 & |\bar{z}| > 1. \end{cases} \tag{5.34}$$

The displacement components, in terms of \bar{r} and \bar{z} , are

$$\begin{aligned}
\bar{u}_r^{(n)}(\bar{r}, \bar{z}) &= (-1)^n \frac{a\gamma^T w^{n-1}}{\pi} \int_{-\infty}^{\infty} \frac{1}{\bar{\eta}|\bar{\eta}|\bar{\Delta}} \left\{ R_1^{(n)}(|\bar{\eta}|\bar{r})\bar{\Delta}_A^{(n)} \right. \\
& \quad \left. - |\bar{\eta}|\bar{r}R_0^{(n)}(|\bar{\eta}|\bar{r})\bar{\Delta}_B^{(n)} \right\} \sin(\alpha\bar{\eta})\cos(\alpha\bar{z}\bar{\eta})d\bar{\eta}, \\
\bar{u}_z^{(n)}(\bar{r}, \bar{z}) &= \frac{a\gamma^T w^{n-1}}{\pi} \int_{-\infty}^{\infty} \frac{1}{\bar{\eta}^2\bar{\Delta}} \left\{ -R_0^{(n)}(|\bar{\eta}|\bar{r})\bar{\Delta}_A^{(n)} \right. \\
& \quad + \left[(-1)^n 4(1 - \nu^{(n)})R_0^{(n)}(|\bar{\eta}|\bar{r}) \right. \\
& \quad \left. \left. + |\bar{\eta}|\bar{r}R_1^{(n)}(|\bar{\eta}|\bar{r}) \right] \bar{\Delta}_B^{(n)} \right\} \sin(\alpha\bar{\eta})\sin(\alpha\bar{z}\bar{\eta})d\bar{\eta} + \delta_{n2}\bar{u}^* \\
& \text{on } \bar{\Omega}^{(n)}. \tag{5.35}
\end{aligned}$$

where

$$\bar{u}^* = \bar{u}^*(z) \equiv \begin{cases} \gamma^T L & \bar{z} > 1, \\ \gamma^T L \bar{z} & |\bar{z}| \leq 1, \\ -\gamma^T L & \bar{z} < -1. \end{cases} \tag{5.36}$$

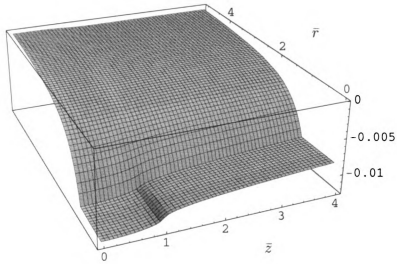
All the results (5.31), (5.32), (5.33), and (5.35) possess the same forms as those in (4.27), (4.28), (4.29), and (4.31) for the “perfect bonding elastic fiber” model, respectively, except that $\bar{\Delta}$ is given by (5.28), which includes an extra term involving \bar{k} , instead of by (4.24).

5.4 Numerical Evaluation

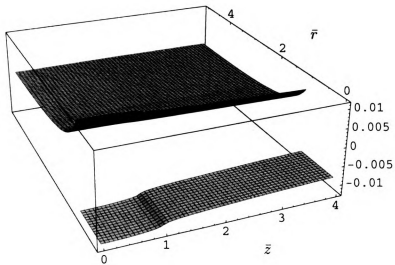
In this section, we present the numerical evaluation of the exact solutions for the case that a single finite segment of the fiber undergoes phase transformation. The calculation is performed using Mathematica. In the calculation, the matrix is assumed with Young's modulus $E^{(1)} = 1\text{GPa}$ and Poisson's ratio $\nu^{(1)} = 0.3$, and the fiber with Young's modulus $E^{(2)} = 100\text{GPa}$ and Poisson's ratio $\nu^{(2)} = 0.3$, respectively. The normalized stiffness of the "spring" is taken to be $\bar{k} = 10^{-5}$, and the aspect ratio be $\alpha = 10$. Noticing that all the integrands are even functions of $\bar{\eta}$, one only needs to calculate the integration over the interval $(0, \infty)$.

Figure 5.1–5.3 show the 3D plots of the stress distributions, the strain distributions, and the displacements, respectively, for the case of $\alpha = 10$.

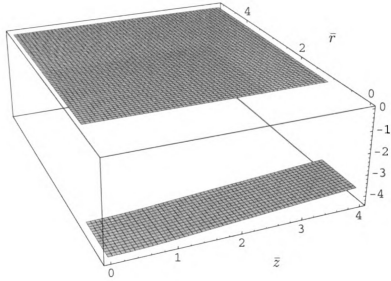
The distributions of the stresses on the fiber-matrix interface for $\alpha = 10$ are shown in Figure 5.4 for matrix and in Figure 5.5 for fiber. It is shown that all the stress components are finite and continuous in \bar{z} on the interface. It also shows that the shear stress component $\bar{\sigma}_{rz}$ has maximum magnitude near the phase boundary ($|\bar{z}| = 1$), while the normal stresses, $\bar{\sigma}_{rr}$, $\bar{\sigma}_{\theta\theta}$, and $\bar{\sigma}_{zz}$, reach maximum magnitudes at the middle of the phase transformed region in the fiber ($|\bar{z}| = 0$).



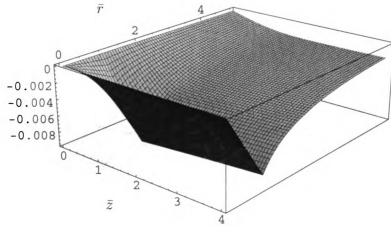
(a) $\frac{\bar{\sigma}_{rr}}{E^{(1)}\gamma T}$



(b) $\frac{\bar{\sigma}_{\theta\theta}}{E^{(1)}\gamma T}$

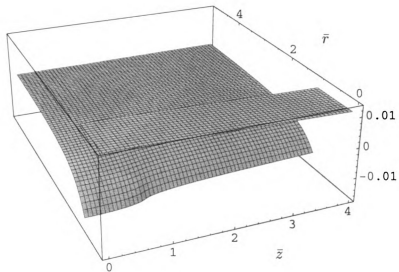


(c) $\frac{\bar{\sigma}_{zz}}{E^{(1)}\gamma T}$

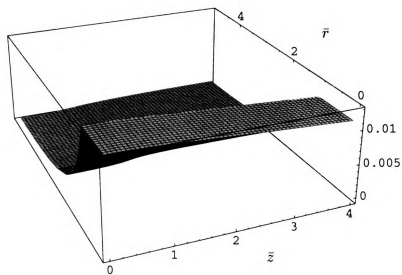


(d) $\frac{\bar{\sigma}_{rz}}{E^{(1)}\gamma T}$

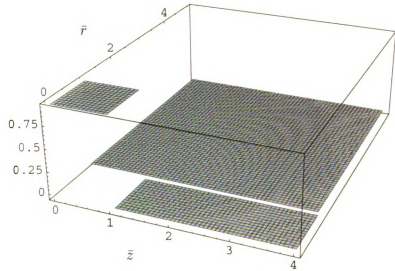
Figure 5.1. The 3D plots of stress distributions for $E^{(1)} = 1\text{GPa}$, $E^{(2)} = 100\text{GPa}$, $\nu^{(1)} = \nu^{(2)} = 0.3$, $\bar{k} = 10^{-5}$, and $\alpha = 10$. (a) $\frac{\bar{\sigma}_{rr}}{E^{(1)}\gamma T}$, (b) $\frac{\bar{\sigma}_{\theta\theta}}{E^{(1)}\gamma T}$, (c) $\frac{\bar{\sigma}_{zz}}{E^{(1)}\gamma T}$, and (d) $\frac{\bar{\sigma}_{rz}}{E^{(1)}\gamma T}$.



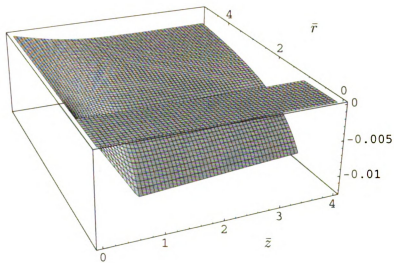
(a) $\frac{\bar{\sigma}_{rr}}{\gamma T}$



(b) $\frac{\bar{\sigma}_{\theta\theta}}{\gamma T}$

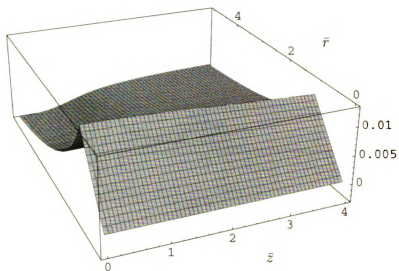


(c) $\frac{\tilde{\gamma}_{z\bar{r}}}{\gamma_T}$

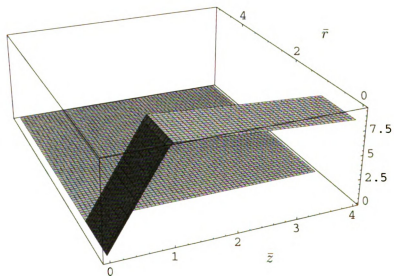


(d) $\frac{\tilde{\gamma}_{r\bar{r}}}{\gamma_T}$

Figure 5.2. The 3D plots of strain distributions for $E^{(1)} = 1\text{GPa}$, $E^{(2)} = 100\text{GPa}$, $\nu^{(1)} = \nu^{(2)} = 0.3$, $\bar{k} = 10^{-5}$, and $\alpha = 10$. (a) $\frac{\tilde{\gamma}_{r\bar{r}}}{\gamma_T}$, (b) $\frac{\tilde{\gamma}_{\theta\theta}}{\gamma_T}$, (c) $\frac{\tilde{\gamma}_{z\bar{r}}}{\gamma_T}$, and (d) $\frac{\tilde{\gamma}_{r\bar{r}}}{\gamma_T}$.



(a) $\frac{\bar{u}_r}{a\gamma T}$



(b) $\frac{\bar{u}_z}{a\gamma T}$

Figure 5.3. The 3D plots of displacements for $E^{(1)} = 1\text{GPa}$, $E^{(2)} = 100\text{GPa}$, $\nu^{(1)} = \nu^{(2)} = 0.3$, $\bar{k} = 10^{-5}$, and $\alpha = 10$. (a) $\frac{\bar{u}_r}{a\gamma T}$, and (b) $\frac{\bar{u}_z}{a\gamma T}$.

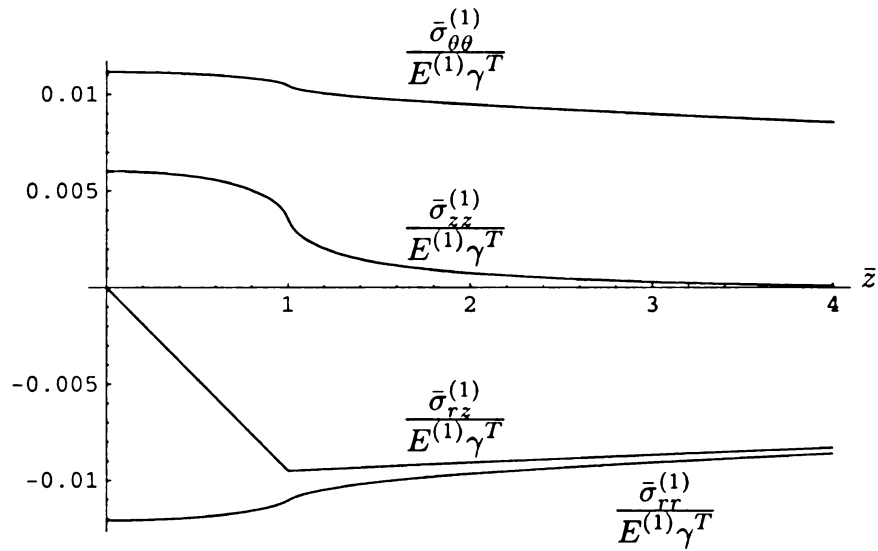


Figure 5.4. The stress distributions of matrix on the fiber-matrix interface for $E^{(1)} = 1\text{GPa}$, $E^{(2)} = 100\text{GPa}$, $\nu^{(1)} = \nu^{(2)} = 0.3$, $\bar{k} = 10^{-5}$, and $\alpha = 10$.

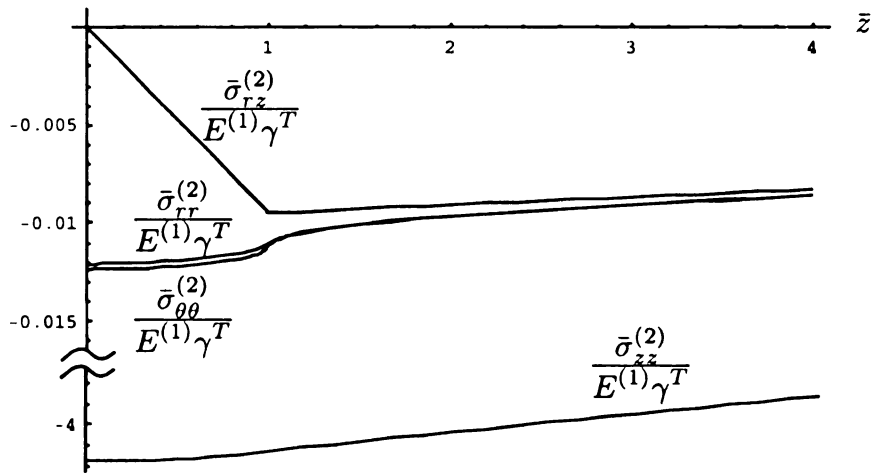


Figure 5.5. The stress distributions of fiber on the fiber-matrix interface for $E^{(1)} = 1\text{GPa}$, $E^{(2)} = 100\text{GPa}$, $\nu^{(1)} = \nu^{(2)} = 0.3$, $\bar{k} = 10^{-5}$, and $\alpha = 10$.

5.5 Reduction to the Spring Bonding Rigid Fiber Model

For the situation that the SMA fiber is much stronger than the matrix, one has $w \rightarrow 0$ by (5.8). For the fiber ($n = 2$), this is equivalent to that $E^{(2)}$ is finite and $E^{(1)} \rightarrow 0$. From (5.19), (5.20), and (5.21), one has the constraint free deformation in the fiber:

$$\gamma_{rr}^{(2)} = \gamma_{\theta\theta}^{(2)} = \gamma_{rz}^{(2)} = 0, \quad \gamma_{zz}^{(2)} = \gamma^* \quad \text{on } \Omega^{(2)}, \quad (5.37)$$

$$u_r^{(2)} = 0, \quad u_z^{(2)} = u^* \quad \text{on } \Omega^{(2)}, \quad (5.38)$$

and

$$\sigma_{rr}^{(2)} = \sigma_{\theta\theta}^{(2)} = \sigma_{zz}^{(2)} = \sigma_{rz}^{(2)} = 0, \quad \text{on } \Omega^{(2)}. \quad (5.39)$$

For the matrix ($n = 1$), however, the condition that $w \rightarrow 0$ is equivalent to that $E^{(1)}$ is finite and $E^{(2)} \rightarrow \infty$. Notice that as $w = 0$, (5.13) and (5.11) lead to the relations

$$\Delta(\eta) = \Delta^{(1)}(\eta) \cdot \Delta^{(2)}(\eta),$$

$$\Delta_A^{(1)}(\eta) = |\eta| a K_0(|\eta| a) \cdot \Delta^{(2)}(\eta),$$

$$\Delta_B^{(1)}(\eta) = K_1(|\eta| a) \cdot \Delta^{(2)}(\eta), \quad (5.40)$$

where

$$\Delta^{(2)}(\eta) = \begin{vmatrix} q_1^{(2)} & q_2^{(2)} \\ q_3^{(2)} & q_4^{(2)} \end{vmatrix},$$

$$\Delta^{(1)}(\eta) = \begin{vmatrix} q_5^{(1)} & q_6^{(1)} \\ q_7^{(1)} & q_8^{(1)} \end{vmatrix} + \frac{E^{(1)}}{1 + \nu^{(1)}} \frac{|\eta|}{k} \begin{vmatrix} q_3^{(1)} & q_4^{(1)} \\ q_5^{(1)} & q_6^{(1)} \end{vmatrix}$$

$$= -|\eta| a K_0^2(|\eta| a) - 4(1 - \nu^{(1)}) K_0(|\eta| a) K_1(|\eta| a)$$

$$\begin{aligned}
& + \left[1 - \frac{2(1 - \nu^{(1)})E^{(1)}}{a(1 + \nu^{(2)})k} \right] |\eta| a K_1^2(|\eta|a), \\
& -\infty < \bar{\eta} < \infty.
\end{aligned} \tag{5.41}$$

For the general phase transformation characteristic function $\gamma^*(z)$, substituting the above (5.40) and (5.41) into (5.18), (5.19), (5.20), and (5.21) with $n = 1$, and canceling $\Delta^{(2)}$, one obtains the Love's stress function, stresses, strains, and displacements for the "rigid fiber" with "spring bonding" model. The Love's stress function for the matrix is

$$\begin{aligned}
\Phi^{(1)}(r, z) = & i \frac{E^{(1)}}{2\pi(1 + \nu^{(1)})} \int_{-\infty}^{\infty} \frac{1}{\eta^3 \Delta^{(1)}} \left\{ -|\eta| a K_0(|\eta|a) K_0(|\eta|r) \right. \\
& \left. + |\eta| r K_1(|\eta|a) K_1(|\eta|r) \right\} \tilde{\gamma}^*(\eta) e^{-i\eta z} d\eta \quad \text{on } \Omega^{(1)}.
\end{aligned} \tag{5.42}$$

The stresses in the matrix reduce to the following forms:

$$\begin{aligned}
\sigma_{rr}^{(1)}(r, z) = & \frac{E^{(1)}}{2\pi(1 + \nu^{(1)})} \int_{-\infty}^{\infty} \frac{1}{\Delta^{(1)}} \left\{ \left[a|\eta| K_0(a|\eta|) + (1 - 2\nu^{(1)}) K_1(a|\eta|) \right] K_0(|\eta|r) \right. \\
& \left. + \left[\frac{a}{r} K_0(a|\eta|) - |\eta| r K_1(a|\eta|) \right] K_1(|\eta|r) \right\} \tilde{\gamma}^*(\eta) e^{-i\eta z} d\eta, \\
\sigma_{\theta\theta}^{(1)}(r, z) = & \frac{E^{(1)}}{2\pi(1 + \nu^{(1)})} \int_{-\infty}^{\infty} \frac{1}{\Delta^{(1)}} \left\{ (1 - 2\nu^{(1)}) K_1(a|\eta|) K_0(|\eta|r) \right. \\
& \left. - \frac{a}{r} K_0(a|\eta|) K_1(|\eta|r) \right\} \tilde{\gamma}^*(\eta) e^{-i\eta z} d\eta, \\
\sigma_{zz}^{(1)}(r, z) = & \frac{E^{(1)}}{2\pi(1 + \nu^{(1)})} \int_{-\infty}^{\infty} \frac{1}{\Delta^{(1)}} \left\{ \left[-a|\eta| K_0(a|\eta|) - 2(2 - \nu^{(1)}) K_1(a|\eta|) \right] K_0(|\eta|r) \right. \\
& \left. + |\eta| r K_1(a|\eta|) K_1(|\eta|r) \right\} \tilde{\gamma}^*(\eta) e^{-i\eta z} d\eta, \\
\sigma_{rz}^{(1)}(r, z) = & i \frac{E^{(1)}}{2\pi(1 + \nu^{(1)})} \int_{-\infty}^{\infty} \frac{\text{sign}(\eta)}{\Delta^{(1)}} \left\{ -|\eta| r K_1(a|\eta|) K_0(|\eta|r) + \left[a|\eta| K_0(a|\eta|) \right. \right.
\end{aligned}$$

$$+2(1 - \nu^{(1)})K_1(a|\eta|)]K_1(|\eta|r)\} \tilde{\gamma}^*(\eta)e^{-i\eta z} d\eta \quad \text{on } \Omega^{(1)}. \quad (5.43)$$

The strain components in the matrix can be written as

$$\begin{aligned} \gamma_{rr}^{(1)}(r, z) &= \frac{1}{2\pi} \int_{-\infty}^{\infty} \frac{1}{\Delta^{(1)}} \left\{ \left[a|\eta|K_0(a|\eta|) + K_1(a|\eta|) \right] K_0(|\eta|r) \right. \\ &\quad \left. + \left[\frac{a}{r}K_0(a|\eta|) - |\eta|rK_1(a|\eta|) \right] K_1(|\eta|r) \right\} \tilde{\gamma}^*(\eta)e^{-i\eta z} d\eta, \\ \gamma_{\theta\theta}^{(1)}(r, z) &= \frac{1}{2\pi} \int_{-\infty}^{\infty} \frac{1}{\Delta^{(1)}} \left\{ K_1(a|\eta|)K_0(|\eta|r) \right. \\ &\quad \left. - \frac{a}{r}K_0(a|\eta|)K_1(|\eta|r) \right\} \tilde{\gamma}^*(\eta)e^{-i\eta z} d\eta, \\ \gamma_{zz}^{(1)}(r, z) &= \frac{1}{2\pi} \int_{-\infty}^{\infty} \frac{1}{\Delta^{(1)}} \left\{ - \left[a|\eta|K_0(a|\eta|) + 4(1 - \nu^{(1)})K_1(a|\eta|) \right] K_0(|\eta|r) \right. \\ &\quad \left. + |\eta|rK_1(a|\eta|)K_1(|\eta|r) \right\} \tilde{\gamma}^*(\eta)e^{-i\eta z} d\eta, \\ \gamma_{rz}^{(1)}(r, z) &= i \frac{1}{2\pi} \int_{-\infty}^{\infty} \frac{\text{sign}(\eta)}{\Delta^{(1)}} \left\{ - |\eta|rK_1(a|\eta|)K_0(|\eta|r) + \left[a|\eta|K_0(a|\eta|) \right. \right. \\ &\quad \left. \left. + 2(1 - \nu^{(1)})K_1(a|\eta|) \right] K_1(|\eta|r) \right\} \tilde{\gamma}^*(\eta)e^{-i\eta z} d\eta \quad \text{on } \Omega^{(1)}. \quad (5.44) \end{aligned}$$

The displacement components in the matrix are

$$\begin{aligned} u_r^{(1)}(r, z) &= \frac{1}{2\pi} \int_{-\infty}^{\infty} \frac{1}{|\eta|\Delta^{(1)}} \left\{ \frac{r}{a}K_1(a|\eta|)K_0(|\eta|r) \right. \\ &\quad \left. - K_0(a|\eta|)K_1(|\eta|r) \right\} \tilde{\gamma}^*(\eta)e^{-i\eta z} d\eta, \\ u_z^{(1)}(r, z) &= -i \frac{1}{2\pi} \int_{-\infty}^{\infty} \frac{1}{\eta\Delta^{(1)}} \left\{ \left[a|\eta|K_0(a|\eta|) + 4(1 - \nu^{(1)})K_1(a|\eta|) \right] K_0(|\eta|r) \right. \end{aligned}$$

$$-|\eta|rK_1(a|\eta|)K_1(|\eta|r)\} \tilde{\gamma}^*(\eta)e^{-i\eta z}d\eta \quad \text{on } \Omega^{(1)}. \quad (5.45)$$

Similarly, one can obtain the results of strong fiber (as $w \rightarrow 0$) for the case of single finite segment of the fiber transform with the normalized transformation characteristic function $\tilde{\gamma}^*$ given by (5.23). In the fiber, the deformation is constraint free. In the matrix, the Love's stress function, in terms of normalized variables, is

$$\begin{aligned} \bar{\Phi}^{(1)}(\bar{r}, \bar{z}) = & \frac{a^3 E^{(1)} \gamma^T}{\pi(1 + \nu^{(1)})} \int_{-\infty}^{\infty} \frac{1}{\bar{\Delta}^{(1)} \bar{\eta}^4} \left\{ -|\bar{\eta}|K_0(|\bar{\eta}|)K_0(|\bar{\eta}|\bar{r}) \right. \\ & \left. + |\bar{\eta}|\bar{r}K_1(|\bar{\eta}|)K_1(|\bar{\eta}|\bar{r}) \right\} \sin(\alpha\bar{\eta})\sin(\alpha\bar{\eta}\bar{z})d\bar{\eta} \quad \text{on } \bar{\Omega}^{(1)}, \end{aligned} \quad (5.46)$$

where

$$\begin{aligned} \bar{\Delta}^{(1)}(\bar{\eta}) = & \begin{vmatrix} \bar{q}_5^{(1)} & \bar{q}_6^{(1)} \\ \bar{q}_7^{(1)} & \bar{q}_8^{(1)} \end{vmatrix} + \frac{w}{1 + \nu^{(2)}} \frac{|\bar{\eta}|}{\bar{k}} \begin{vmatrix} \bar{q}_3^{(1)} & \bar{q}_4^{(1)} \\ \bar{q}_5^{(1)} & \bar{q}_6^{(1)} \end{vmatrix} \\ = & -|\bar{\eta}|K_0^2(|\bar{\eta}|) - 4(1 - \nu^{(1)})K_0(|\bar{\eta}|)K_1(|\bar{\eta}|) \\ & + \left[1 - \frac{2(1 - \nu^{(1)})w}{(1 + \nu^{(2)})\bar{k}} \right] |\bar{\eta}|K_1^2(|\bar{\eta}|), \\ & -\infty < \bar{\eta} < \infty. \end{aligned} \quad (5.47)$$

The stresses of the matrix, in terms of normalized variables, are

$$\begin{aligned} \bar{\sigma}_{rr}^{(1)}(\bar{r}, \bar{z}) = & \frac{E^{(1)} \gamma^T}{(1 + \nu^{(1)})\pi} \int_{-\infty}^{\infty} \frac{1}{\bar{\Delta}^{(1)} \bar{\eta}} \left\{ \left[|\bar{\eta}|K_0(|\bar{\eta}|) + (1 - 2\nu^{(1)})K_1(|\bar{\eta}|) \right] K_0(|\bar{\eta}|\bar{r}) \right. \\ & \left. + \left[\frac{1}{\bar{r}}K_0(|\bar{\eta}|) - |\bar{\eta}|\bar{r}K_1(|\bar{\eta}|) \right] K_1(|\bar{\eta}|\bar{r}) \right\} \sin(\alpha\bar{\eta})\cos(\alpha\bar{z}\bar{\eta})d\bar{\eta}, \\ \bar{\sigma}_{\theta\theta}^{(1)}(\bar{r}, \bar{z}) = & \frac{E^{(1)} \gamma^T}{(1 + \nu^{(1)})\pi} \int_{-\infty}^{\infty} \frac{1}{\bar{\Delta}^{(1)} \bar{\eta}} \left\{ (1 - 2\nu^{(1)})K_1(|\bar{\eta}|)K_0(|\bar{\eta}|\bar{r}) \right. \end{aligned}$$

$$\begin{aligned}
& -\frac{1}{\bar{r}}K_0(|\bar{\eta}|)K_1(|\bar{\eta}|\bar{r}) \Big\} \sin(\alpha\bar{\eta})\cos(\alpha\bar{z}\bar{\eta})d\bar{\eta}, \\
\bar{\sigma}_{zz}^{(1)}(\bar{r}, \bar{z}) &= \frac{E^{(1)}\gamma^T}{(1+\nu^{(1)})\pi} \int_{-\infty}^{\infty} \frac{1}{\bar{\Delta}^{(1)}\bar{\eta}} \left\{ \left[-|\bar{\eta}|K_0(|\bar{\eta}|) - 2(2-\nu^{(1)})K_1(|\bar{\eta}|) \right] K_0(|\bar{\eta}|\bar{r}) \right. \\
& \quad \left. + |\bar{\eta}|\bar{r}K_1(|\bar{\eta}|)K_1(|\bar{\eta}|\bar{r}) \right\} \sin(\alpha\bar{\eta})\cos(\alpha\bar{z}\bar{\eta})d\bar{\eta}, \\
\bar{\sigma}_{rz}^{(1)}(\bar{r}, \bar{z}) &= \frac{E^{(1)}\gamma^T}{(1+\nu^{(1)})\pi} \int_{-\infty}^{\infty} \frac{1}{\bar{\Delta}^{(1)}|\bar{\eta}|} \left\{ -|\bar{\eta}|\bar{r}K_1(|\bar{\eta}|)K_0(|\bar{\eta}|\bar{r}) + \left[|\bar{\eta}|K_0(|\bar{\eta}|) \right. \right. \\
& \quad \left. \left. + 2(1-\nu^{(1)})K_1(|\bar{\eta}|) \right] K_1(|\bar{\eta}|\bar{r}) \right\} \sin(\alpha\bar{\eta})\sin(\alpha\bar{z}\bar{\eta})d\bar{\eta} \\
& \qquad \qquad \qquad \text{on } \bar{\Omega}^{(1)}. \tag{5.48}
\end{aligned}$$

The strain components of the matrix can be written in terms of normalized coordinates as

$$\begin{aligned}
\bar{\gamma}_{rr}^{(1)}(\bar{r}, \bar{z}) &= \frac{\gamma^T}{\pi} \int_{-\infty}^{\infty} \frac{1}{\bar{\Delta}^{(1)}\bar{\eta}} \left\{ \left[|\bar{\eta}|K_0(|\bar{\eta}|) + K_1(|\bar{\eta}|) \right] K_0(|\bar{\eta}|\bar{r}) \right. \\
& \quad \left. + \left[\frac{1}{\bar{r}}K_0(|\bar{\eta}|) - |\bar{\eta}|\bar{r}K_1(|\bar{\eta}|) \right] K_1(|\bar{\eta}|\bar{r}) \right\} \sin(\alpha\bar{\eta})\cos(\alpha\bar{z}\bar{\eta})d\bar{\eta}, \\
\bar{\gamma}_{\theta\theta}^{(1)}(\bar{r}, \bar{z}) &= \frac{\gamma^T}{\pi} \int_{-\infty}^{\infty} \frac{1}{\bar{\Delta}^{(1)}\bar{\eta}} \left\{ K_1(|\bar{\eta}|)K_0(|\bar{\eta}|\bar{r}) \right. \\
& \quad \left. - \frac{1}{\bar{r}}K_0(|\bar{\eta}|)K_1(|\bar{\eta}|\bar{r}) \right\} \sin(\alpha\bar{\eta})\cos(\alpha\bar{z}\bar{\eta})d\bar{\eta}, \\
\bar{\gamma}_{zz}^{(1)}(\bar{r}, \bar{z}) &= \frac{\gamma^T}{\pi} \int_{-\infty}^{\infty} \frac{1}{\bar{\Delta}^{(1)}\bar{\eta}} \left\{ - \left[|\bar{\eta}|K_0(|\bar{\eta}|) + 4(1-\nu^{(1)})K_1(|\bar{\eta}|) \right] K_0(|\bar{\eta}|\bar{r}) \right. \\
& \quad \left. + |\bar{\eta}|\bar{r}K_1(|\bar{\eta}|)K_1(|\bar{\eta}|\bar{r}) \right\} \sin(\alpha\bar{\eta})\cos(\alpha\bar{z}\bar{\eta})d\bar{\eta}, \\
\bar{\gamma}_{rz}^{(1)}(\bar{r}, \bar{z}) &= \frac{\gamma^T}{\pi} \int_{-\infty}^{\infty} \frac{1}{\bar{\Delta}^{(1)}|\bar{\eta}|} \left\{ -|\bar{\eta}|\bar{r}K_1(|\bar{\eta}|)K_0(|\bar{\eta}|\bar{r}) + \left[|\bar{\eta}|K_0(|\bar{\eta}|) \right. \right.
\end{aligned}$$

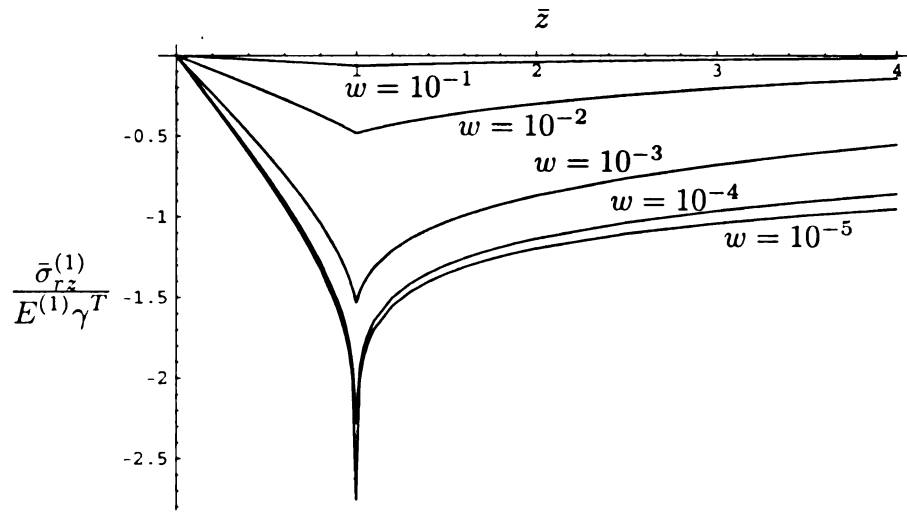
$$\begin{aligned}
& +2(1 - \nu^{(1)})K_1(|\bar{\eta}|) \left] K_1(|\bar{\eta}|\bar{r}) \right\} \sin(\alpha\bar{\eta})\sin(\alpha\bar{z}\bar{\eta})d\bar{\eta} \\
& \text{on } \bar{\Omega}^{(1)}. \tag{5.49}
\end{aligned}$$

The displacement components of the matrix, in terms of normalized coordinates, are

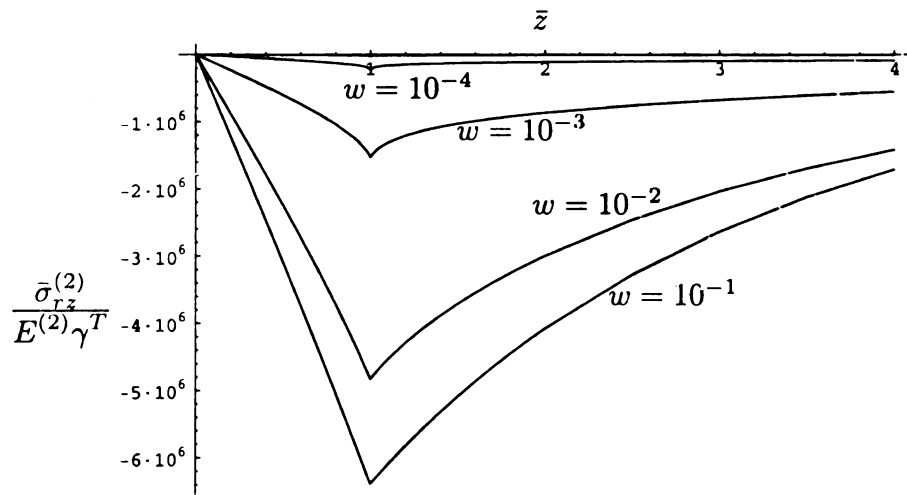
$$\begin{aligned}
\bar{u}_r^{(1)}(\bar{r}, \bar{z}) &= \frac{a\gamma^T}{\pi} \int_{-\infty}^{\infty} \frac{1}{\bar{\Delta}^{(1)}\bar{\eta}} \left\{ \bar{r}K_1(|\bar{\eta}|)K_0(|\bar{\eta}|\bar{r}) \right. \\
& \quad \left. - K_0(|\bar{\eta}|)K_1(|\bar{\eta}|\bar{r}) \right\} \sin(\alpha\bar{\eta})\cos(\alpha\bar{z}\bar{\eta})d\bar{\eta}, \\
\bar{u}_z^{(1)}(\bar{r}, \bar{z}) &= -\frac{a\gamma^T}{\pi} \int_{-\infty}^{\infty} \frac{1}{\bar{\Delta}^{(1)}\bar{\eta}^2} \left\{ \left[|\bar{\eta}|K_0(|\bar{\eta}|) + 4(1 - \nu^{(1)})K_1(|\bar{\eta}|) \right] K_0(|\bar{\eta}|\bar{r}) \right. \\
& \quad \left. - |\bar{\eta}|\bar{r}K_1(|\bar{\eta}|)K_1(|\bar{\eta}|\bar{r}) \right\} \sin(\alpha\bar{\eta})\sin(\alpha\bar{z}\bar{\eta})d\bar{\eta} \quad \text{on } \bar{\Omega}^{(1)}. \tag{5.50}
\end{aligned}$$

Comparing the results for the spring bonded rigid fiber model (5.42) – (5.46) and (5.48) – (5.50) with those for the perfectly bonded rigid fiber model (3.12) – (3.15) and (3.22) – (3.25), one found that the only difference is that in the spring bonding model there exists a extra term involving k or \bar{k} in $\Delta^{(1)}$ or $\bar{\Delta}^{(1)}$.

Figure 5.6 displays the distributions of shear stress $\bar{\sigma}_{rz}^{(n)}$ over $E^{(n)}\gamma^T$ on the fiber-matrix interface for the case of single finite segment undergoing phase transformation. The distributions are plotted for various values for the ratio of shear modulus of fiber to that of matrix: $w = 10^{-5}, 10^{-4}, 10^{-3}, 10^{-2}$, and 10^{-1} , respectively. Figure 5.6(a) is for matrix and Figure 5.6(b) for fiber. The distributions reach their maximum at phase boundary for both matrix and fiber. It shows that for fixed $E^{(1)}$, the shear stress of the matrix on the fiber-matrix interface increases as w decreases. In fiber for fixed $E^{(2)}$, on the other hand, the shear stress decreases with w decreases. This means stiffer fiber generates larger shear stress in the matrix while softer matrix generates less in the fiber when fiber undergoes phase transformation.



(a)



(b)

Figure 5.6. The shear stress distributions $\frac{\bar{\sigma}_{rz}^{(n)}}{E^{(n)}\gamma^T}$ on the fiber-matrix interface for $\nu^{(1)} = \nu^{(2)} = 0.3$, $\alpha = 10$, $\bar{k} = 10^{-3}$, and various ratios of shear modulus of fiber to that of matrix: $w = 10^{-5}, 10^{-4}, 10^{-3}, 10^{-2}$, and 10^{-1} . (a) For matrix, and (b) for fiber.

5.6 Reduction to the Perfect Bonding (Elastic Fiber) Model

As the stiffness k increase, the relative axial displacement between fiber and matrix decrease. Let $k \rightarrow \infty$, one has

$$\Delta(\eta) = \begin{pmatrix} q_1^{(1)} & q_2^{(1)} & -q_1^{(2)} & -q_2^{(2)} \\ q_3^{(1)} & q_4^{(1)} & -q_3^{(2)} & -q_4^{(2)} \\ q_5^{(1)} & q_6^{(1)} & wq_5^{(2)} & wq_6^{(2)} \\ q_7^{(1)} & q_8^{(1)} & -wq_7^{(2)} & -wq_8^{(2)} \end{pmatrix},$$

$$-\infty < \eta < \infty. \quad (5.51)$$

It reduce to the results for the case of elastic fiber with perfect bonding.

Figure 5.7 and Figure 5.8 display the distributions of displacement components $\bar{u}_z^{(n)}$ over $a\gamma^T$ and of shear stress $\bar{\sigma}_{rz}^{(n)}$ over $E^{(1)}\gamma^T$ on the fiber-matrix interface for the case of single finite segment undergoing phase transformation, respectively. To show the effect of stiffness, distributions are plotted for various stiffness values, $\bar{k} = 0, 10^{-5}, 10^{-4}, 10^{-3}, 10^{-2}$, and 10^{-1} , respectively. In Figure 5.7, the solid curves are for the distributions of fiber while the dash ones for those of matrix. For the case that $\bar{k} = 0$, the fiber and matrix are completely debonded. The fiber undergoes free phase transformation and there is no deformation in the matrix (Figure 5.7). Although the difference between longitudinal displacement of the fiber and the matrix reaches its maximum, there is no shear stress generated on the fiber-matrix interface because $\bar{k} = 0$ (Figure 5.8). As \bar{k} increase, the relative longitudinal displacement between fiber and matrix decreases, while the shear stress increases. Finally, for $\bar{k} \rightarrow \infty$, the longitudinal displacement of the matrix coincides with that of the fiber, but the shear stress blows up across the phase boundary. This reduces to the perfect bonding situation.

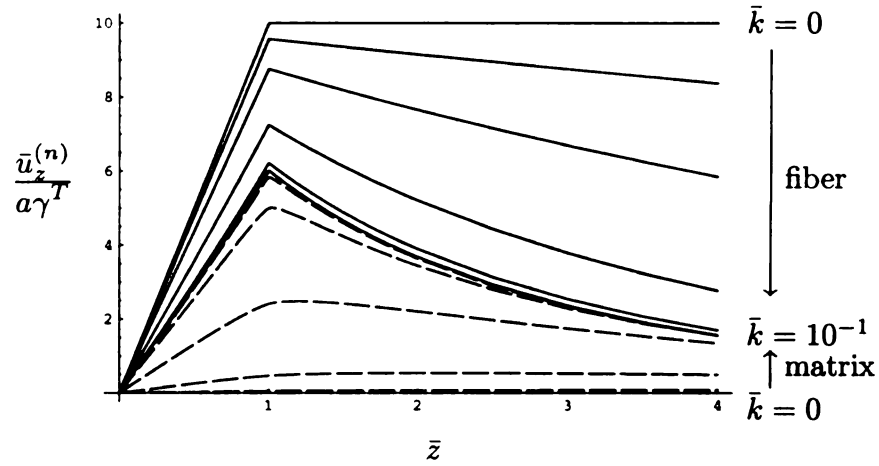


Figure 5.7. The displacement distributions $\frac{\bar{u}_z^{(n)}}{a\gamma^T}$ on the fiber-matrix interface for $E^{(1)} = 1\text{GPa}$, $E^{(2)} = 100\text{GPa}$, $\nu^{(1)} = \nu^{(2)} = 0.3$, and $\alpha = 10$, and various stiffnesses ($\bar{k} = 0, 10^{-5}, 10^{-4}, 10^{-3}, 10^{-2}$, and 10^{-1}). The solid curves are for fiber and dashed ones for matrix.

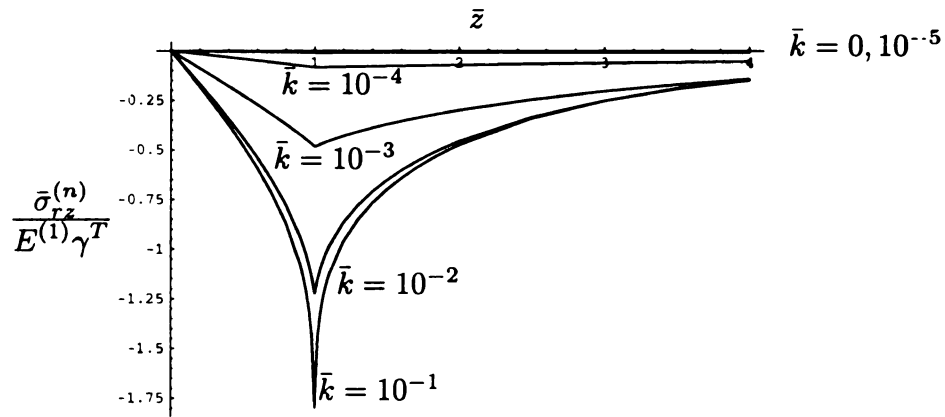


Figure 5.8. The shear stress distributions $\frac{\bar{\sigma}_{rz}^{(n)}}{E^{(1)}\gamma^T}$ on the fiber-matrix interface for $E^{(1)} = 1\text{GPa}$, $E^{(2)} = 100\text{GPa}$, $\nu^{(1)} = \nu^{(2)} = 0.3$, and $\alpha = 10$, and various stiffnesses ($\bar{k} = 0, 10^{-5}, 10^{-4}, 10^{-3}, 10^{-2}$, and 10^{-1}).

5.7 Boundedness of the Stress Distributions on the Interface

Setting $\bar{r} = 1$ in (5.32) and considering that the integrands are even functions, the stress components at the interface are given by

$$\begin{aligned}
\bar{\sigma}_{rr}^{(n)}(1, \bar{z}) &= \frac{2E^{(1)}\gamma^T}{\pi(1+\nu^{(1)})} \int_0^\infty \frac{\bar{\Delta}_{rr}^{(n)}(1; \bar{\eta})}{\bar{\eta}\bar{\Delta}(\bar{\eta})} \sin(\alpha\bar{\eta}) \cos(\alpha\bar{z}\bar{\eta}) d\bar{\eta}, \\
\bar{\sigma}_{\theta\theta}^{(n)}(1, \bar{z}) &= \frac{2E^{(1)}\gamma^T}{\pi(1+\nu^{(1)})} \int_0^\infty \frac{\bar{\Delta}_{\theta\theta}^{(n)}(1; \bar{\eta})}{\bar{\eta}\bar{\Delta}(\bar{\eta})} \sin(\alpha\bar{\eta}) \cos(\alpha\bar{z}\bar{\eta}) d\bar{\eta}, \\
\bar{\sigma}_{zz}^{(n)}(1, \bar{z}) &= \frac{2E^{(1)}\gamma^T}{\pi(1+\nu^{(1)})} \int_0^\infty \frac{\bar{\Delta}_{zz}^{(n)}(1; \bar{\eta})}{\bar{\eta}\bar{\Delta}(\bar{\eta})} \sin(\alpha\bar{\eta}) \cos(\alpha\bar{z}\bar{\eta}) d\bar{\eta}, \\
\bar{\sigma}_{rz}^{(n)}(1, \bar{z}) &= \frac{2E^{(1)}\gamma^T}{\pi(1+\nu^{(1)})} \int_0^\infty \frac{\bar{\Delta}_{rz}^{(n)}(1; \bar{\eta})}{\bar{\eta}\bar{\Delta}(\bar{\eta})} \sin(\alpha\bar{\eta}) \sin(\alpha\bar{z}\bar{\eta}) d\bar{\eta}, \\
&-\infty < \bar{\eta} < \infty,
\end{aligned} \tag{5.52}$$

where $\bar{\Delta}_{rr}^{(n)}(1; \bar{\eta})$, $\bar{\Delta}_{\theta\theta}^{(n)}(1; \bar{\eta})$, $\bar{\Delta}_{zz}^{(n)}(1; \bar{\eta})$, and $\bar{\Delta}_{rz}^{(n)}(1; \bar{\eta})$ are functions of $\bar{\eta}$:

$$\begin{aligned}
\bar{\Delta}_{rr}^{(n)}(1; \bar{\eta}) &= \left[R_0^{(n)}(\bar{\eta}) - \frac{(-1)^n}{\bar{\eta}} R_1^{(n)}(\bar{\eta}) \right] \bar{\Delta}_A^{(n)}(\bar{\eta}) \\
&\quad - \left[(-1)^n (1 - 2\nu^{(n)}) R_0^{(n)}(\bar{\eta}) + \bar{\eta} R_1^{(n)}(\bar{\eta}) \right] \bar{\Delta}_B^{(n)}(\bar{\eta}), \\
\bar{\Delta}_{\theta\theta}^{(n)}(1; \bar{\eta}) &= (-1)^n \left[\frac{1}{\bar{\eta}} R_1^{(n)}(\bar{\eta}) \bar{\Delta}_A^{(n)}(\bar{\eta}) - (1 - 2\nu^{(n)}) R_0^{(n)}(\bar{\eta}) \bar{\Delta}_B^{(n)}(\bar{\eta}) \right], \\
\bar{\Delta}_{zz}^{(n)}(1; \bar{\eta}) &= -R_0^{(n)}(\bar{\eta}) \bar{\Delta}_A^{(n)}(\bar{\eta}) \\
&\quad + \left[(-1)^n 2(2 - \nu^{(n)}) R_0^{(n)}(\bar{\eta}) + \bar{\eta} R_1^{(n)}(\bar{\eta}) \right] \bar{\Delta}_B^{(n)}(\bar{\eta}), \\
\bar{\Delta}_{rz}^{(n)}(1; \bar{\eta}) &= (-1)^{n+1} R_1^{(n)}(\bar{\eta}) \bar{\Delta}_A^{(n)}(\bar{\eta}) \\
&\quad + \left[(-1)^n \bar{\eta} R_0^{(n)}(\bar{\eta}) + 2(1 - \nu^{(n)}) R_1^{(n)}(\bar{\eta}) \right] \bar{\Delta}_B^{(n)}(\bar{\eta}), \\
&-\infty < \bar{\eta} < \infty,
\end{aligned} \tag{5.53}$$

To develop approximate expressions, we use the following asymptotic expansions for the modified Bessel functions (Olver, 1974)

$$\begin{aligned}
R_0^{(1)}(\bar{\eta}) &= K_0(\bar{\eta}) \sim \sqrt{\frac{\pi}{2\bar{\eta}}} e^{-\bar{\eta}} \left[1 - \frac{1}{8\bar{\eta}} + \frac{9}{128\bar{\eta}^2} - \frac{75}{1024\bar{\eta}^3} + \dots \right], \\
R_1^{(1)}(\bar{\eta}) &= K_1(\bar{\eta}) \sim \sqrt{\frac{\pi}{2\bar{\eta}}} e^{-\bar{\eta}} \left[1 + \frac{3}{8\bar{\eta}} - \frac{15}{128\bar{\eta}^2} + \frac{105}{1024\bar{\eta}^3} + \dots \right], \\
R_0^{(2)}(\bar{\eta}) &= I_0(\bar{\eta}) \sim \sqrt{\frac{\pi}{2\bar{\eta}}} e^{-\bar{\eta}} \left[1 + \frac{1}{8\bar{\eta}} + \frac{9}{128\bar{\eta}^2} + \frac{75}{1024\bar{\eta}^3} + \dots \right], \\
R_1^{(2)}(\bar{\eta}) &= I_1(\bar{\eta}) \sim \sqrt{\frac{\pi}{2\bar{\eta}}} e^{-\bar{\eta}} \left[1 - \frac{3}{8\bar{\eta}} - \frac{15}{128\bar{\eta}^2} - \frac{105}{1024\bar{\eta}^3} + \dots \right],
\end{aligned}$$

as $\bar{\eta} \rightarrow \infty$. (5.54)

The asymptotic expansions of $\bar{\Delta}_A^{(n)}$ and $\bar{\Delta}_B^{(n)}$, $n = 1, 2$, are

$$\begin{aligned}
\bar{\Delta}_A^{(1)}(\bar{\eta}) &\sim \sqrt{\frac{1}{8\pi\bar{\eta}^3}} e^{\bar{\eta}} \left\{ \left[1 + (3 - 4\nu^{(2)})w \right] \bar{\eta} \right. \\
&\quad \left. - \frac{1}{8} \left[15 - 16\nu^{(2)} + (15 - 16\nu^{(1)})(3 - 4\nu^{(2)})w \right] + \dots \right\}, \\
\bar{\Delta}_B^{(1)}(\bar{\eta}) &\sim \sqrt{\frac{1}{8\pi\bar{\eta}^3}} e^{\bar{\eta}} \left\{ \left[1 + (3 - 4\nu^{(2)})w \right] \right. \\
&\quad \left. - \frac{1}{8} \left[11 - 16\nu^{(2)} + (1 + 4\nu^{(2)})w \right] \frac{1}{\bar{\eta}} + \dots \right\}, \\
\bar{\Delta}_A^{(2)}(\bar{\eta}) &\sim \sqrt{\frac{\pi}{8\bar{\eta}^3}} e^{-\bar{\eta}} \left\{ \left[3 - 4\nu^{(1)} + w \right] \bar{\eta} \right. \\
&\quad \left. + \frac{1}{8} \left[(3 - 4\nu^{(1)})(15 - 16\nu^{(2)}) + (15 - 16\nu^{(1)})w \right] + \dots \right\}, \\
\bar{\Delta}_B^{(2)}(\bar{\eta}) &\sim \sqrt{\frac{\pi}{8\bar{\eta}^3}} e^{-\bar{\eta}} \left\{ \left[3 - 4\nu^{(1)} + w \right] \right. \\
&\quad \left. + \frac{1}{8} \left[1 + 4\nu^{(1)} + (11 - 16\nu^{(1)})w \right] \frac{1}{\bar{\eta}} + \dots \right\},
\end{aligned}$$

$$(\bar{\eta} \rightarrow \infty). \quad (5.55)$$

The asymptotic expansion of $\bar{\Delta}$ is

$$\bar{\Delta}(\bar{\eta}) \sim \frac{1}{4\bar{\eta}^2} \left[\frac{w}{1+\nu^{(2)}} \frac{\bar{\eta}}{\bar{k}} \bar{\Delta}_k(\bar{\eta}) + \bar{\Delta}_0(\bar{\eta}) \right], \quad (\bar{\eta} \rightarrow \infty), \quad (5.56)$$

where

$$\begin{aligned} \bar{\Delta}_k(\bar{\eta}) &= -2 \left[1 - \nu^{(1)} + (1 - \nu^{(2)})w \right] \\ &\quad + 2 \left[(1 - \nu^{(1)})(1 - 2\nu^{(2)}) - (1 - 2\nu^{(1)})(1 - \nu^{(2)})w \right] \frac{1}{\bar{\eta}}, \\ \bar{\Delta}_0(\bar{\eta}) &= \left[-3 + 4\nu^{(1)} - 2(5 - 6\nu^{(1)} - 6\nu^{(2)} + 8\nu^{(1)}\nu^{(2)})w - (3 - 4\nu^{(2)})w^2 \right] \\ &\quad + 2 \left[2 - 3\nu^{(1)} - 3\nu^{(2)} + 4\nu^{(1)}\nu^{(2)} \right] (1 - w^2) \frac{1}{\bar{\eta}}. \end{aligned} \quad (5.57)$$

The asymptotic expansions of $\bar{\Delta}_{rr}^{(n)}(1; \bar{\eta})$, $\bar{\Delta}_{\theta\theta}^{(n)}(1; \bar{\eta})$, $\bar{\Delta}_{zz}^{(n)}(1; \bar{\eta})$, and $\bar{\Delta}_{rz}^{(n)}(1; \bar{\eta})$,

as $\bar{\eta} \rightarrow \infty$, are

$$\begin{aligned} \bar{\Delta}_{rr}^{(n)}(1; \bar{\eta}) &\sim \frac{1}{4\bar{\eta}^2} \left\{ \left[1 - 2\nu^{(1)} - (1 - 2\nu^{(2)})w \right] \right. \\ &\quad \left. - \left[1 - 3\nu^{(1)} - 2\nu^{(2)} + 4\nu^{(1)}\nu^{(2)} \right] \right. \\ &\quad \left. + (1 - 2\nu^{(1)} - 3\nu^{(2)} + 4\nu^{(1)}\nu^{(2)})w \right\} \frac{1}{\bar{\eta}}, \\ \bar{\Delta}_{\theta\theta}^{(1)}(1; \bar{\eta}) &\sim \frac{1}{4\bar{\eta}^2} \left\{ -2\nu^{(1)} \left[1 + (3 - 4\nu^{(2)})w \right] + \left[\nu^{(1)}(3 - 4\nu^{(2)} \right. \right. \\ &\quad \left. \left. + (4 - 5\nu^{(1)} - 6\nu^{(2)} + 8\nu^{(1)}\nu^{(2)})w \right] \right\} \frac{1}{\bar{\eta}}, \\ \bar{\Delta}_{\theta\theta}^{(2)}(1; \bar{\eta}) &\sim \frac{1}{4\bar{\eta}^2} \left\{ 2\nu^{(2)} \left[3 - 4\nu^{(1)} + w \right] + \left[4 - 6\nu^{(1)} - 5\nu^{(2)} \right. \right. \\ &\quad \left. \left. + 8\nu^{(1)}\nu^{(2)} + (3 - 4\nu^{(1)})\nu^{(2)}w \right] \right\} \frac{1}{\bar{\eta}}, \end{aligned}$$

$$\begin{aligned}
\bar{\Delta}_{zz}^{(1)}(1; \bar{\eta}) &\sim \frac{1}{4\bar{\eta}^2} \left\{ - \left[3 - 2\nu^{(1)} + (5 - 6\nu^{(2)})w \right] \right. \\
&\quad + \left[4 - 3\nu^{(1)} - 6\nu^{(2)} + 4\nu^{(1)}\nu^{(2)} \right. \\
&\quad \left. \left. - (2 - 4\nu^{(1)} - 3\nu^{(2)} + 4\nu^{(1)}\nu^{(2)})w \right] \frac{1}{\bar{\eta}} \right\}, \\
\bar{\Delta}_{zz}^{(2)}(1; \bar{\eta}) &\sim \frac{1}{4\bar{\eta}^2} \left\{ \left[5 - 6\nu^{(1)} + (3 - 2\nu^{(2)})w \right] \right. \\
&\quad + \left[-2 + 3\nu^{(1)} + 4\nu^{(2)} - 4\nu^{(1)}\nu^{(2)} \right. \\
&\quad \left. \left. + (4 - 6\nu^{(1)} - 3\nu^{(2)} + 4\nu^{(1)}\nu^{(2)})w \right] \frac{1}{\bar{\eta}} \right\}, \\
\bar{\Delta}_{rz}^{(n)}(1; \bar{\eta}) &\sim \frac{1}{4\bar{\eta}^2} \left\{ 2 \left[1 - \nu^{(1)} + (1 - \nu^{(2)})w \right] - 2 \left[(1 - \nu^{(1)})(1 - 2\nu^{(2)}) \right. \right. \\
&\quad \left. \left. - (1 - 2\nu^{(1)})(1 - \nu^{(2)})w \right] \frac{1}{\bar{\eta}} \right\}, \\
&\quad (\bar{\eta} \rightarrow \infty). \tag{5.58}
\end{aligned}$$

Therefore, if \bar{k} is finite and non-zero constant, one has

$$\begin{aligned}
\frac{\bar{\Delta}_{rr}^{(n)}(1; \bar{\eta})}{\bar{\Delta}} &\sim \frac{H_{rr}^{(n)}}{\bar{\eta}} = \frac{(1 + \nu^{(2)})\bar{k}}{w} \frac{1 - 2\nu^{(1)} - (1 - 2\nu^{(2)})w}{2 \left[-1 + \nu^{(1)} - (1 - \nu^{(2)})w \right]} \frac{1}{\bar{\eta}} \\
\frac{\bar{\Delta}_{\theta\theta}^{(1)}(1; \bar{\eta})}{\bar{\Delta}} &\sim \frac{H_{\theta\theta}^{(1)}}{\bar{\eta}} = - \frac{(1 + \nu^{(2)})\bar{k}}{w} \frac{\nu^{(1)} \left[1 + (3 - 4\nu^{(2)})w \right]}{\left[-1 + \nu^{(1)} - (1 - \nu^{(2)})w \right]} \frac{1}{\bar{\eta}} \\
\frac{\bar{\Delta}_{\theta\theta}^{(2)}(1; \bar{\eta})}{\bar{\Delta}} &\sim \frac{H_{\theta\theta}^{(2)}}{\bar{\eta}} = \frac{(1 + \nu^{(2)})\bar{k}}{w} \frac{2\nu^{(2)}(3 - 4\nu^{(1)} + w)}{2 \left[-1 + \nu^{(1)} - (1 - \nu^{(2)})w \right]} \frac{1}{\bar{\eta}} \\
\frac{\bar{\Delta}_{zz}^{(1)}(1; \bar{\eta})}{\bar{\Delta}} &\sim \frac{H_{zz}^{(1)}}{\bar{\eta}} = - \frac{(1 + \nu^{(2)})\bar{k}}{w} \frac{3 - 2\nu^{(1)} + (5 - 6\nu^{(2)})w}{2 \left[-1 + \nu^{(1)} - (1 - \nu^{(2)})w \right]} \frac{1}{\bar{\eta}}
\end{aligned}$$

$$\begin{aligned}\frac{\bar{\Delta}_{zz}^{(2)}(1; \bar{\eta})}{\bar{\Delta}} &\sim \frac{H_{zz}^{(2)}}{\bar{\eta}} = \frac{(1 + \nu^{(2)})\bar{k}}{w} \frac{5 - 6\nu^{(1)} + (3 - 2\nu^{(2)})w}{2[-1 + \nu^{(1)} - (1 - \nu^{(2)})w]} \frac{1}{\bar{\eta}} \\ \frac{\bar{\Delta}_{rz}^{(n)}(1; \bar{\eta})}{\bar{\Delta}} &\sim \frac{H_{rz}^{(n)}}{\bar{\eta}} = -\frac{(1 + \nu^{(2)})\bar{k}}{w} \frac{1}{\bar{\eta}} \\ &(\bar{\eta} \rightarrow \infty).\end{aligned}\tag{5.59}$$

The integrals in (5.52) can be decomposed into two parts by dividing the interval of integration into $(0, s)$ and (s, ∞) , for some $s > 0$. Utilizing (5.59), the integrals on the interval (s, ∞) can be approximated for sufficiently large $s > 0$. Hence, we have

$$\begin{aligned}\bar{\sigma}_{rr}^{(n)}(1, \bar{z}) &\simeq \frac{2E^{(1)}\gamma^T}{\pi(1 + \nu^{(1)})} \left[\int_0^s \frac{\bar{\Delta}_{rr}^{(1)}}{\bar{\Delta}\bar{\eta}} \sin(\alpha\bar{\eta}) \cos(\alpha\bar{z}\bar{\eta}) d\bar{\eta} \right. \\ &\quad \left. + H_{rr}^{(n)} \int_s^\infty \frac{\sin(\alpha\bar{\eta}) \cos(\alpha\bar{z}\bar{\eta})}{\bar{\eta}^2} d\bar{\eta} \right], \\ \bar{\sigma}_{\theta\theta}^{(n)}(1, \bar{z}) &\simeq \frac{2E^{(1)}\gamma^T}{\pi(1 + \nu^{(1)})} \left[\int_0^s \frac{\bar{\Delta}_{\theta\theta}^{(1)}}{\bar{\Delta}\bar{\eta}} \sin(\alpha\bar{\eta}) \cos(\alpha\bar{z}\bar{\eta}) d\bar{\eta} \right. \\ &\quad \left. + H_{\theta\theta}^{(n)} \int_s^\infty \frac{\sin(\alpha\bar{\eta}) \cos(\alpha\bar{z}\bar{\eta})}{\bar{\eta}^2} d\bar{\eta} \right], \\ \bar{\sigma}_{zz}^{(n)}(1, \bar{z}) &\simeq \frac{2E^{(1)}\gamma^T}{\pi(1 + \nu^{(1)})} \left[\int_0^s \frac{\bar{\Delta}_{zz}^{(1)}}{\bar{\Delta}\bar{\eta}} \sin(\alpha\bar{\eta}) \cos(\alpha\bar{z}\bar{\eta}) d\bar{\eta} \right. \\ &\quad \left. + H_{zz}^{(n)} \int_s^\infty \frac{\sin(\alpha\bar{\eta}) \cos(\alpha\bar{z}\bar{\eta})}{\bar{\eta}^2} d\bar{\eta} \right], \\ \bar{\sigma}_{rz}^{(n)}(1, \bar{z}) &\simeq \frac{2E^{(1)}\gamma^T}{\pi(1 + \nu^{(1)})} \left[\int_0^s \frac{\bar{\Delta}_{rz}^{(1)}}{\bar{\Delta}\bar{\eta}} \sin(\alpha\bar{\eta}) \sin(\alpha\bar{z}\bar{\eta}) d\bar{\eta} \right. \\ &\quad \left. + H_{rz}^{(n)} \int_s^\infty \frac{\sin(\alpha\bar{\eta}) \sin(\alpha\bar{z}\bar{\eta})}{\bar{\eta}^2} d\bar{\eta} \right], \\ &-\infty < \bar{z} < \infty.\end{aligned}\tag{5.60}$$

Note that for positive s , one has

$$\int_s^\infty \frac{\sin(\alpha\bar{\eta})\cos(\alpha\bar{z}\bar{\eta})}{\bar{\eta}^2} d\bar{\eta} \leq \int_s^\infty \left| \frac{\sin(\alpha\bar{\eta})\cos(\alpha\bar{z}\bar{\eta})}{\bar{\eta}^2} \right| d\bar{\eta} \leq \int_s^\infty \frac{1}{\bar{\eta}^2} d\bar{\eta} = \frac{1}{s}$$

$$\int_s^\infty \frac{\sin(\alpha\bar{\eta})\sin(\alpha\bar{z}\bar{\eta})}{\bar{\eta}^2} d\bar{\eta} \leq \int_s^\infty \left| \frac{\sin(\alpha\bar{\eta})\sin(\alpha\bar{z}\bar{\eta})}{\bar{\eta}^2} \right| d\bar{\eta} \leq \int_s^\infty \frac{1}{\bar{\eta}^2} d\bar{\eta} = \frac{1}{s}. \quad (5.61)$$

Therefore, for sufficiently large s , the second integrals in (5.60) are small and then we have the approximations

$$\begin{aligned} \bar{\sigma}_{rr}^{(n)}(1, \bar{z}) &\simeq \frac{2E^{(1)}\gamma^T}{\pi(1+\nu^{(1)})} \int_0^s \frac{\bar{\Delta}_{rr}^{(n)}}{\bar{\Delta}\bar{\eta}} \sin(\alpha\bar{\eta})\cos(\alpha\bar{z}\bar{\eta}) d\bar{\eta}, \\ \bar{\sigma}_{\theta\theta}^{(n)}(1, \bar{z}) &\simeq \frac{2E^{(1)}\gamma^T}{\pi(1+\nu^{(1)})} \int_0^s \frac{\bar{\Delta}_{\theta\theta}^{(n)}}{\bar{\Delta}\bar{\eta}} \sin(\alpha\bar{\eta})\cos(\alpha\bar{z}\bar{\eta}) d\bar{\eta}, \\ \bar{\sigma}_{zz}^{(n)}(1, \bar{z}) &\simeq \frac{2E^{(1)}\gamma^T}{\pi(1+\nu^{(1)})} \int_0^s \frac{\bar{\Delta}_{zz}^{(n)}}{\bar{\Delta}\bar{\eta}} \sin(\alpha\bar{\eta})\cos(\alpha\bar{z}\bar{\eta}) d\bar{\eta}, \\ \bar{\sigma}_{rz}^{(n)}(1, \bar{z}) &\simeq \frac{2E^{(1)}\gamma^T}{\pi(1+\nu^{(1)})} \int_0^s \frac{\bar{\Delta}_{rz}^{(n)}}{\bar{\Delta}\bar{\eta}} \sin(\alpha\bar{\eta})\sin(\alpha\bar{z}\bar{\eta}) d\bar{\eta}, \end{aligned}$$

$$-\infty < \bar{z} < \infty. \quad (5.62)$$

The integrals of (5.62) involve K_0 , K_1 , I_0 , and I_1 . Only K_0 and K_1 have singularity at 0. Hence, the possible singularities of the integrands are only at $\bar{\eta} = 0$. To show the behaviors of these integrands near $\bar{\eta} = 0$, we consider the asymptotic expansions of the modified Bessel functions (Zayed, 1996, p.66):

$$R_0^{(1)}(\bar{\eta}) = K_0(\bar{\eta}) \sim -\ln\bar{\eta},$$

$$R_1^{(1)}(\bar{\eta}) = K_1(\bar{\eta}) \sim \frac{1}{\bar{\eta}},$$

$$R_0^{(2)}(\bar{\eta}) = I_0(\bar{\eta}) \sim 1,$$

$$R_1^{(2)}(\bar{\eta}) = I_1(\bar{\eta}) \sim \frac{\bar{\eta}}{2},$$

$$\text{as } \bar{\eta} \rightarrow 0^+. \quad (5.63)$$

The asymptotic expansions of $\bar{\Delta}_A^{(n)}$ and $\bar{\Delta}_B^{(n)}$, $n = 1, 2$, are

$$\begin{aligned} \bar{\Delta}_A^{(1)}(\bar{\eta}) &\sim 2(1 - \nu^{(1)})\nu^{(2)}w + \frac{1}{2} \left[-1 - \nu^{(2)} + (1 - 2\nu^{(1)} + \nu^{(2)} \right. \\ &\quad \left. + 2\nu^{(1)}\nu^{(2)})w \right] \bar{\eta}^2 \ln \bar{\eta} + \frac{1}{2}(\nu^{(1)} - \nu^{(2)})w\bar{\eta}^2, \\ \bar{\Delta}_B^{(1)}(\bar{\eta}) &\sim \frac{1}{2} \left[1 + \nu^{(2)} + (1 - 3\nu^{(2)})w \right] \\ &\quad - \frac{1}{2}(1 - \nu^{(2)})w\bar{\eta}^2 \ln \bar{\eta} - \frac{1}{4}(1 - w)\bar{\eta}^2, \\ \bar{\Delta}_A^{(2)}(\bar{\eta}) &\sim 2(1 - \nu^{(1)})(1 - 2\nu^{(2)} + w)\frac{1}{\bar{\eta}^2} - 2(1 - \nu^{(1)})(2 - \nu^{(2)})\ln \bar{\eta} \\ &\quad - 1 - \nu^{(1)} + \nu^{(2)} + w, \\ \bar{\Delta}_B^{(2)}(\bar{\eta}) &\sim (1 - \nu^{(1)})(1 + w)\frac{1}{\bar{\eta}^2} - (1 - \nu^{(1)})\ln \bar{\eta} - \frac{1}{2}(1 - w), \end{aligned}$$

$$\text{as } \bar{\eta} \rightarrow 0^+. \quad (5.64)$$

The asymptotic expansion of $\bar{\Delta}$ is

$$\bar{\Delta}(\bar{\eta}) \sim \frac{w}{1 + \nu^{(2)}} \frac{\bar{\eta}}{k} \bar{\Delta}_k(\bar{\eta}) + \bar{\Delta}_0(\bar{\eta}), \quad \text{as } \bar{\eta} \rightarrow 0^+, \quad (5.65)$$

where

$$\begin{aligned} \bar{\Delta}_k(\bar{\eta}) &= -(1 - \nu^{(1)}) \left[1 + \nu^{(2)} + (1 - \nu^{(2)})w \right] \frac{1}{\bar{\eta}} \\ &\quad + \frac{1}{2} \left[1 - \nu^{(1)} - (1 - \nu^{(2)})w \right] \bar{\eta}, \\ \bar{\Delta}_0(\bar{\eta}) &= -2 \left[1 - \nu^{(1)} + (1 - \nu^{(1)} - 2\nu^{(2)} + 2\nu^{(1)}\nu^{(2)})w \right] w \frac{1}{\bar{\eta}^2} \end{aligned}$$

$$\begin{aligned}
& +2(1 - \nu^{(1)}) \left[1 + \nu^{(2)} + (1 - 3\nu^{(2)})w \right] \ln \bar{\eta} \\
& + \frac{1}{2} \left[1 + \nu^{(2)} + (2 - \nu^{(1)} - 5\nu^{(2)})w - (3 - \nu^{(1)} - 4\nu^{(2)})w^2 \right]. \quad (5.66)
\end{aligned}$$

The asymptotic expansions of $\bar{\Delta}_{rr}^{(n)}(1; \bar{\eta})$, $\bar{\Delta}_{\theta\theta}^{(n)}(1; \bar{\eta})$, $\bar{\Delta}_{zz}^{(n)}(1; \bar{\eta})$, and $\bar{\Delta}_{rz}^{(n)}(1; \bar{\eta})$ are

$$\begin{aligned}
\bar{\Delta}_{rr}^{(n)}(1; \bar{\eta}) & \sim 2(1 - \nu^{(1)})\nu^{(2)}w \frac{1}{\bar{\eta}^2} - (1 - \nu^{(1)})(1 + \nu^{(2)})\ln \bar{\eta} \\
& - \frac{1}{2} \left[1 + \nu^{(2)} + (1 - \nu^{(1)} - 2\nu^{(2)})w \right],
\end{aligned}$$

$$\begin{aligned}
\bar{\Delta}_{\theta\theta}^{(1)}(1; \bar{\eta}) & \sim -2(1 - \nu^{(1)})\nu^{(2)}w \frac{1}{\bar{\eta}^2} \\
& + \left[\nu^{(1)}(1 + \nu^{(2)}) - (1 - 2\nu^{(1)} - \nu^{(2)} + 4\nu^{(1)}\nu^{(2)}) \right] \ln \bar{\eta} \\
& - \frac{1}{2}(\nu^{(1)} - \nu^{(2)})w,
\end{aligned}$$

$$\begin{aligned}
\bar{\Delta}_{\theta\theta}^{(2)}(1; \bar{\eta}) & \sim 2(1 - \nu^{(1)})\nu^{(2)}w \frac{1}{\bar{\eta}^2} - (1 - \nu^{(1)})(1 + \nu^{(2)})\ln \bar{\eta} \\
& - \frac{1}{2} \left[\nu^{(1)} + \nu^{(2)} - 2\nu^{(2)}w \right],
\end{aligned}$$

$$\begin{aligned}
\bar{\Delta}_{zz}^{(1)}(1; \bar{\eta}) & \sim \left[(2 - \nu^{(1)})(1 + \nu^{(2)}) - (2 - \nu^{(1)} - 4\nu^{(2)} + \nu^{(1)}\nu^{(2)})w \right] \ln \bar{\eta} \\
& + \frac{1}{2} \left[1 + \nu^{(2)} + (1 - 3\nu^{(2)})w \right],
\end{aligned}$$

$$\begin{aligned}
\bar{\Delta}_{zz}^{(2)}(1; \bar{\eta}) & \sim 2(1 - \nu^{(1)}) \left[1 + \nu^{(2)} + (1 - \nu^{(2)})w \right] \frac{1}{\bar{\eta}^2} \\
& - \frac{1}{2} \left[1 - \nu^{(2)} - (3 - \nu^{(1)} - 2\nu^{(2)})w \right],
\end{aligned}$$

$$\bar{\Delta}_{rz}^{(n)}(1; \bar{\eta}) \sim (1 - \nu^{(1)}) \left[1 + \nu^{(2)} + (1 - \nu^{(2)})w \right] \frac{1}{\bar{\eta}}$$

$$-\frac{1}{2} \left[1 - \nu^{(1)} - (1 - \nu^{(2)})w \right],$$

$$\text{as } \bar{\eta} \rightarrow 0^+. \quad (5.67)$$

Therefore, if \bar{k} is a finite and non-zero constant, one has

$$\frac{\bar{\Delta}_{rr}^{(n)}(1; \bar{\eta})}{\bar{\Delta}} \rightarrow -\frac{(1 - \nu^{(1)})\nu^{(2)}}{1 - \nu^{(1)} + (1 - \nu^{(1)} - 2\nu^{(2)} + 2\nu^{(1)}\nu^{(2)})w},$$

$$\frac{\bar{\Delta}_{\theta\theta}^{(n)}(1; \bar{\eta})}{\bar{\Delta}} \rightarrow -\frac{(1 - \nu^{(1)})\nu^{(2)}}{1 - \nu^{(1)} + (1 - \nu^{(1)} - 2\nu^{(2)} + 2\nu^{(1)}\nu^{(2)})w},$$

$$\frac{\bar{\Delta}_{zz}^{(1)}(1; \bar{\eta})}{\bar{\Delta}} \rightarrow 0,$$

$$\frac{\bar{\Delta}_{zz}^{(2)}(1; \bar{\eta})}{\bar{\Delta}} \rightarrow -\frac{(1 - \nu^{(1)}) \left[1 + \nu^{(2)} + (1 - \nu^{(2)})w \right]}{\left[1 - \nu^{(1)} + (1 - \nu^{(1)} - 2\nu^{(2)} + 2\nu^{(1)}\nu^{(2)})w \right] w},$$

$$\frac{\bar{\Delta}_{rz}^{(n)}(1; \bar{\eta})}{\bar{\Delta}} \rightarrow 0$$

$$\text{as } \bar{\eta} \rightarrow 0^+. \quad (5.68)$$

Noticing $(\sin \bar{\eta} / \bar{\eta}) \rightarrow 1$ as $\bar{\eta} \rightarrow 0^+$, all the integrands in (5.62) are finite at $\bar{\eta} = 0$. One concludes that all the integrals in (5.62) are finite and continuous in \bar{z} . Consequently, all the stresses are finite in the fiber and the matrix.

5.8 Maximum shear stress

The shear stress distribution on the fiber-matrix interface plays a crucial role in the load transfer between components of the composite. An intensive shear stress on the interface will lead to debonding between fiber and matrix and degrade

the behavior of material, even result in the failure of material. Because phase transformation in the fiber, the shear stress concentrates at the intersection of fiber-matrix interface and phase boundary. Generally, the maximum shear stress depends on the properties of materials, bonding, and phase transformation. For fixed E^1 and ignoring Poisson's effect, the material properties could be described by the ratio of shear moduli, $w = G^{(1)}/G^{(2)}$. In the "spring bonding" model, the bonding property is solely determined by the stiffness of "shear spring" k . In the case that a single finite segment of the fiber undergoes uniform phase transformation, the phase transformation property is characterized by the phase transformation geometry parameter α . In this section, we discuss the relations of maximum shear stress with these parameters according to the numerical calculation for the case that a single finite segment of the fiber undergoes uniform phase transformation. The shear stress reaches its maximum at the intersection of fiber-matrix interface and phase boundary, i.e., $\bar{\sigma}_{rz}^{max} = |\bar{\sigma}_{rz}^{(n)}(1, 1)|$. Do not loss our purpose, some parameters in the plots are in the logarithmic scale. We will observe first the relations of the maximum shear stress on single parameter w , \bar{k} , or α . And then, we will consider the dependence of the maximum shear stress on two of the parameters to further study the correlation of those parameters.

Figure 5.9 shows the variation of the maximum shear stress $\bar{\sigma}_{rz}^{max}$ with the ratio of shear moduli $w = G^{(1)}/G^{(2)}$ for fixed $E^{(1)}$, $\alpha = 10$, and $\bar{k} = 10^{-5}$. It shows that the maximum shear stress decreases as w increases. Thus, for fixed matrix, the softer the fiber, the smaller the maximum shear stress. When $w = 1$, i.e., $E^{(1)} = E^{(2)}$, the maximum shear stress is not zero.

Figure 5.10 shows the variation of the maximum shear stress $\bar{\sigma}_{rz}^{max}$ with stiffness of "shear spring" \bar{k} for fixed the ratio of shear moduli $w = 10^{-2}$ and $\alpha = 10$. It shows that the maximum shear stress increases as \bar{k} increases. Thus, for fixed matrix and fiber, the softer the stiffness of the bonding spring, the smaller the maximum shear

stress.

Figure 5.11 shows the variation of the maximum shear stress $\bar{\sigma}_{rz}^{max}$ with the aspect ratio α for fixed $\bar{k} = 10^{-5}$ and $w = 10^{-2}$. It shows that the maximum shear stress increases as α increases. It also shows that the increase of the maximum shear stress is much quicker when α is small than when it large. It predicts that the system prefers a configuration with very small aspect ratio α as the fiber undergoing phase transformation to avoid shear stress concentration.

The dependance of maximum shear stress $\bar{\sigma}_{rz}^{max}$ on parameters w and \bar{k} for fixed $E^{(1)}$ and $\alpha = 10$ is shown in Figure 5.12. It seems to suggest that the maximum shear stress $\bar{\sigma}_{rz}^{max}$ is likely related to the difference between \bar{k} and w . Figure 5.13 plots the variation of maximum shear stress $\bar{\sigma}_{rz}^{max}$ with the ratio (\bar{k}/w) for fixed $E^{(1)}$ and $\alpha = 10$. It shows that the maximum shear stress decreases as the ratio (\bar{k}/w) decreases. The change of the maximum shear stress with the change of the ratio (\bar{k}/w) on is significant when \bar{k} smaller than w , while the change is very small when \bar{k} smaller than w .

Figure 5.14 and 5.15 show the relations of maximum shear stress $\bar{\sigma}_{rz}^{max}$ with parameters α and w for fixed $E^{(1)}$ and $\bar{k} = 10^{-5}$ and with α and \bar{k} for fixed $w = 10^{-2}$, respectively. The parallel lines with the α -axis in these figures indicate less correlation between α and w and between α and \bar{k} .

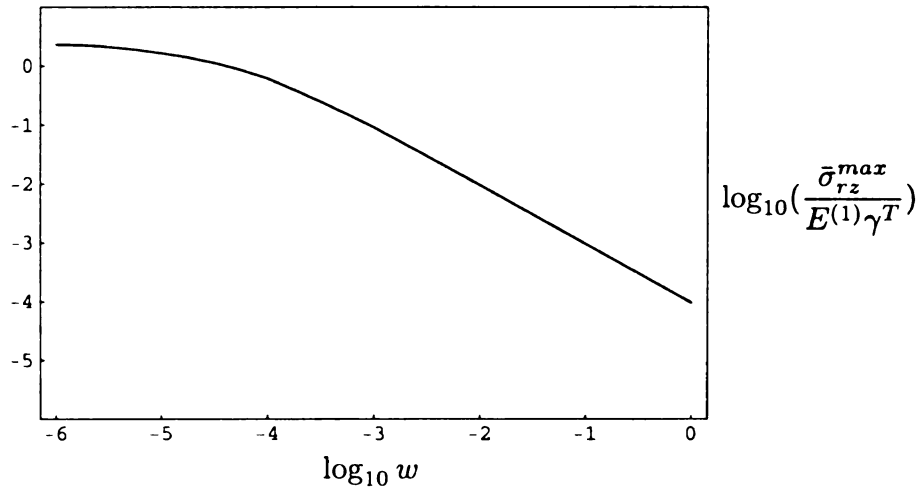


Figure 5.9. The variation of maximum shear stress $\bar{\sigma}_{rz}^{max}$ with the ratio of shear moduli $w = G^{(1)}/G^{(2)}$ for $\alpha = 10$ and $\bar{k} = 10^{-5}$.

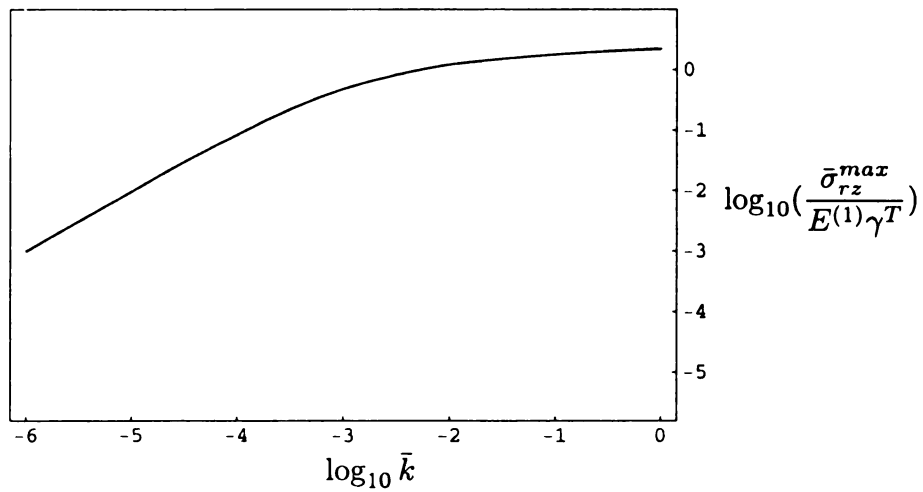


Figure 5.10. The variation of maximum shear stress $\bar{\sigma}_{rz}^{max}$ with \bar{k} for fixed $\alpha = 10$, and $w = 10^{-2}$.

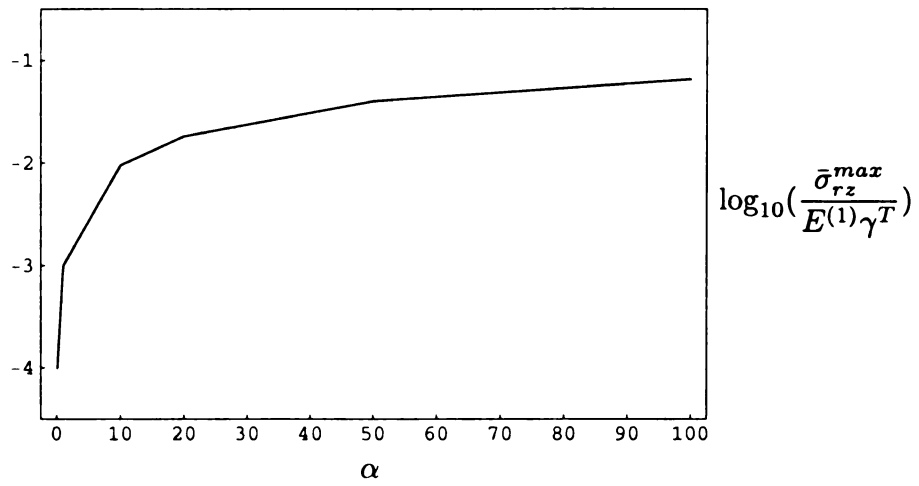


Figure 5.11. The variation of maximum shear stress $\bar{\sigma}_{rz}^{max}$ with parameters α for fixed $w = 10^{-2}$ and $\bar{k} = 10^{-5}$.

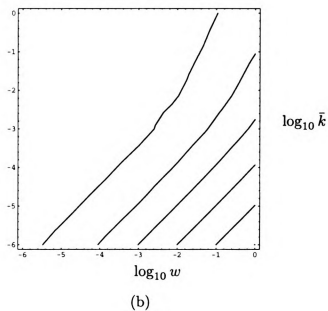
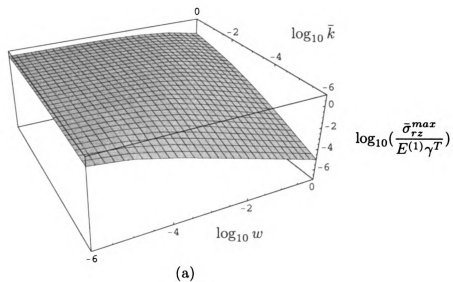
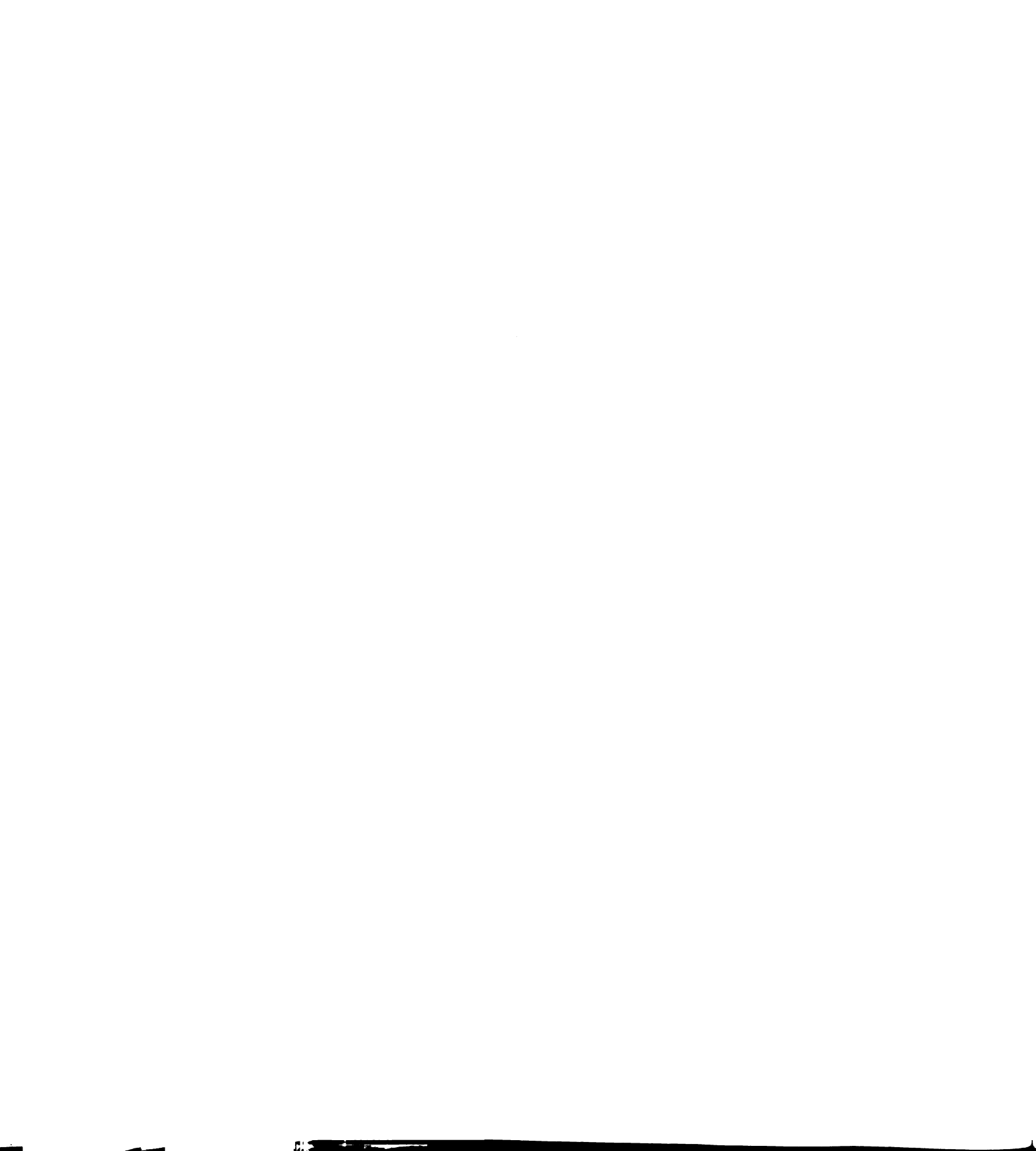


Figure 5.12. The maximum shear stress $\bar{\sigma}_{rz}^{max}$ as a function of parameters w and \bar{k} for fixed $\alpha = 10$. (a) The 3D plot, (b) the contour plot.



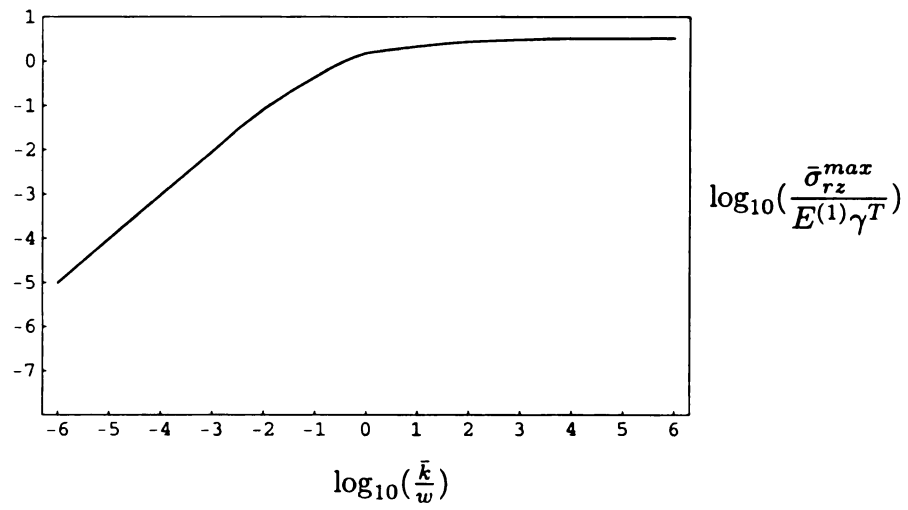


Figure 5.13. The variation of maximum shear stress $\bar{\sigma}_{rz}^{max}$ with the ratio (\bar{k}/w) for $\alpha = 10$.

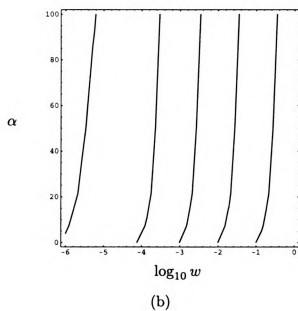
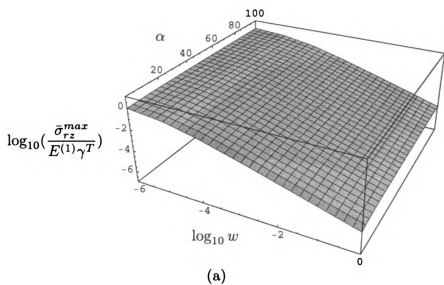
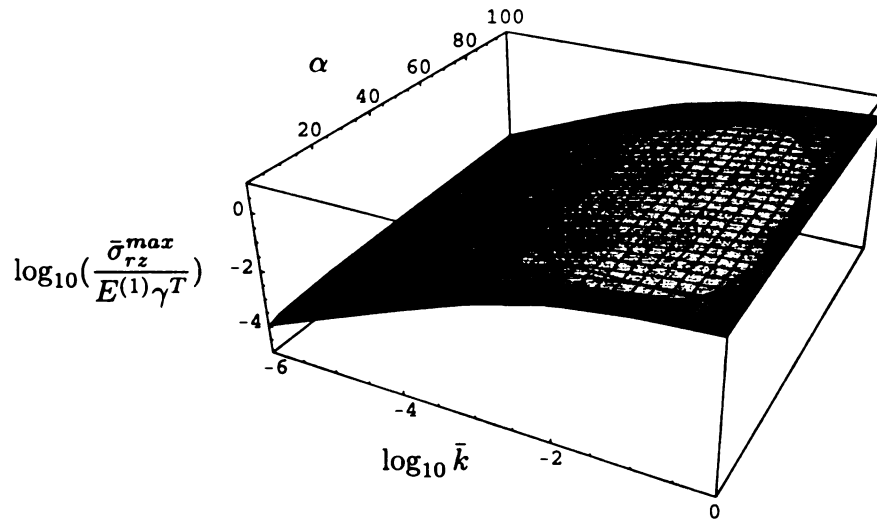
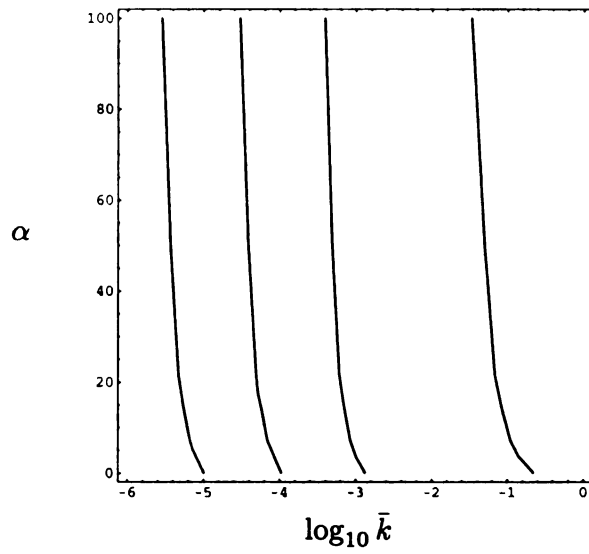


Figure 5.14. The maximum shear stress $\bar{\sigma}_{rz}^{max}$ as a function of parameters w and α for fixed $\bar{k} = 10^{-5}$. (a) The 3D plot, (b) the contour plot.



(a)



(b)

Figure 5.15. The maximum shear stress $\bar{\sigma}_{rz}^{max}$ as a function of parameters \bar{k} and α for fixed $w = 10^{-2}$. (a) The 3D plot, (b) the contour plot.

5.9 Remarks

The mechanical behavior of SMA fiber reinforced composite associate with phase transformation depends not only on the mechanical properties of the matrix and the fiber, including phase transformation, but also on the interaction between the fiber and matrix. In theoretical analysis, the interaction is modeled as certain bonding conditions. In the perfect bonding models as studied in chapter 3 and chapter 4, the displacement is assumed to be continuous across the fiber-matrix interface. However, the perfect bonding condition leads to singularities in stresses at the intersection of the fiber-matrix interface and the phase boundary of the fiber. To further study more general interaction between fiber and matrix, a “spring bonding” model is developed in this chapter. In this model, the radial displacement is still assumed continuous across the fiber-matrix interface while the axial displacement is allowed for discontinuous across the fiber-matrix interface. Such an axial displacement jump results in a shear stress with magnitude proportional to the magnitude of the jump. The elastostatic problem is still axisymmetric. The exact solutions for stresses, strains, and displacements are obtained for both general phase transformation and only one single finite segment of the fiber undergoing phase transformation. By using asymptotic analysis, moreover, it is approved that all the stresses are finite and continuous in both fiber and matrix. As $w \rightarrow 0$, the results to the rigid fiber with spring bonding model are obtained. As $k \rightarrow \infty$, the results reduce to those for the perfect bonding (elastic fiber) model.

Because the existence of phase boundary in the fiber, the shear stress concentrates at the intersection of the fiber-matrix interface and the phase boundary in the fiber. The magnitude of shear stress concentration depends on the material properties, bonding property, and phase transformation property. Based on numerical calculation of the results to the model, the influence of the ratio of shear moduli w , the stiffness of “shear spring” k , and aspect ratio α on the maximum shear stress

is discussed. The softer fiber, matrix, and bonding condition will reduce the shear stress concentration. The shear stress concentration increases as aspect ratio α increases. On influencing the shear stress concentration, there is a close correlation between parameters w and k , but α is less correlated with w and k .

CHAPTER 6. CONCLUSIONS AND FUTURE WORK

We have investigated the elastic deformations of SMA fibers reinforced composite associated with phase transformations in parts of the SMA fibers. To focus our attention on the interaction between the SMA fibers and the matrix, especially near the intersection of fiber-matrix interface and phase boundaries in the fiber, we have studied a simple model involving a single infinite fiber embedded in an infinite elastic matrix. Assume the sharp phase boundaries in the fiber are perpendicular to the axial direction of the fiber. The elastostatic problem is axisymmetrical, in which a solid cylinder (fiber) and a hollow cylinder (matrix) are bonded together.

A systematical method for studying this axisymmetrical elastostatic problem is developed. First, by introducing the Love's stress function, the elastostatic problem is reduced to a boundary value problem of PDE with only one unknown function. Next, by applying (generalized) Fourier transform, the problem is further reduced to an ODE. Then, the general solution to the Love's stress function in the Fourier transformed space can be obtained in terms of the modified Bessel functions of the first and the second kinds. Thus, the general solutions to stresses, strains, and displacements of the problem can also be expressed in terms of those modified Bessel functions. Finally, the exact solutions are found by applying corresponding bonding conditions. In the Fourier transformed space, those bonding or boundary conditions are linear algebraic equations with respect to unknown functions. This method may also be used to solve other axisymmetrical elastic problems.

Generally, the deformations of SMA fibers reinforced composite associated with phase transformations depend on the property of phase transformation in the SMA fiber, the material properties of the SMA fibers and the matrix, and the bonding conditions between the SMA fibers and the matrix. In this dissertation, we have studied the "perfect bonding rigid fiber" model, the "perfect bonding elastic

fiber” model, and the “spring bonding (elastic fiber)” model in details. The “spring bonding rigid fiber” model is dealt with as a special case of the “spring bonding (elastic fiber)” model. For each of those models, we have considered both cases of phase transformation pattern: general phase transformation and single finite segment phase transformation, with the emphasis on the latter.

In the study on the “perfect bonding rigid fiber” model, the influence of matrix on fiber is ignored. The phase transformation in the fiber is considered as constraint free. Under perfect bonding conditions, the constraint free phase transformation in the fiber directly gives rise to the boundary conditions for determining the deformation of the matrix. The exact solutions to the distributions of stress, strain, and displacement are obtained. For the case that a single finite segment of the fiber undergoes phase transformation, the normalized forms of the exact solution are presented. The numerical evaluation is performed. It is shown that across the phase boundary, the normal stresses have finite jumps whereas the shear stress approaches infinity. Further, by using asymptotic expansion technique, the singularities of the stresses are isolated. The jumps of the normal stresses and the intensity of singularity for the shear stress are determined by the material properties of matrix ($E^{(1)}, \nu^{(1)}$) and transformation strain γ^T , and are independent of the aspect ratio α . The singularity in shear stress indicates a severe stress concentration near the phase boundary. The solution provides a good approximation to the case that the fiber is much stronger than the matrix.

In more general cases, the matrix exerts a significant influence on deformations of the fiber, even constrains the phase transformation in the fiber. To take this effect into account, we have studied the “perfect bonding elastic fiber” model, in which the deformation of the fiber is also considered. The elastostatic problem maintains axisymmetrical with two separate cylindrical regions, which are connected by perfect bonding conditions. The exact solutions to stresses, strains, and displacements

in both the fiber and the matrix are obtained. The results for the case that only one single finite segment of the fiber undergoing phase transformation are presented in normalized variables. Particularly, when the fiber and the matrix have the same material properties, one obtains the solution for the problem that a cylindrical inclusion undergoes phase transformation. By asymptotic analysis, the solutions can be approximated by integrating to a sufficiently large value instead of to infinity. It is shown that inside the matrix and the fiber all stress components are continuous. However, on the fiber-matrix interface, all stress components have singularities across the phase boundary. The singularities of stresses are isolated. The numerical evaluation are also performed. All the results in the “perfect bonding elastic fiber” model are similar to the “perfect bonding rigid fiber” model. As w approaches ∞ , i.e., the fiber is very strong compared with matrix, the results reduce to those of “perfect bonding rigid fiber” model. As for the influence of the matrix on the deformation and the phase transformation in the fiber, it is shown that the constraint on the fiber increases with the increase of either w or α . The stiffer matrix exerts greater constraint on the phase transformation in the fiber. On the other hand, in the setting of composite, the phase transformation in the fiber may prefer a configuration with multi-piece small transformed segments to keep small α instead of a large transformed segment to avoid greater constraint from the matrix.

The studies on “perfect bonding rigid fiber” and “perfect bonding elastic fiber” models indicate that, under the assumption of perfect bonding conditions between the fiber and the matrix, the shear stress is singular at the intersection between the fiber-matrix interface and the phase boundary in the fiber. To further study more general interaction between fiber and matrix, a “spring bonding” model is developed. In this model, the radial displacement is still assumed continuous across the fiber-matrix interface while the axial displacement is allowed for discontinuity across the fiber-matrix interface. Such an axial displacement jump results in a shear stress

with magnitude proportional to the magnitude of the jump. The elastostatic problem is still axisymmetric. The exact solutions to stresses, strains, and displacements are obtained for both phase transformation patterns: general phase transformation and single finite segment phase transformation. By using asymptotic expansion, moreover, it is proved that all the stresses have no singularity in both fiber and matrix. As $w \rightarrow 0$, the results for the rigid fiber with spring bonding model are obtained. As $k \rightarrow \infty$, the results reduce to those for the perfect bonding (elastic fiber) model.

Even though there exists no stress singularity in the “spring bonding” model, the shear stress still concentrates at the intersection of the fiber-matrix interface and the phase boundary in the fiber. The magnitude of shear stress concentration depends on the properties of materials, bonding, and phase transformation. Based on numerical calculation of the results, the influence of the ratio of shear moduli w , the stiffness of “shear spring” k , and aspect ratio α on the maximum shear stress is discussed. The softer fiber, matrix, and bonding condition will reduce the shear stress concentration. The shear stress concentration increases as aspect ratio α increases. On influencing the shear stress concentration, there is a close correlation between parameters w and k , but α is less correlated with w and k . It is shown that the shear stress concentration is related to ratio $(\frac{k}{w})$ and α instead of to k , w , and α .

Through the studies on the “perfect bonding” model and the “spring bonding” model, we could also conclude that the stress singularities in a SMA fiber reinforced composite are the combined effect of phase boundary and perfect bonding interaction between fiber and matrix. The material properties of the fiber and the matrix as well as the transformation strain affect the intensity of stress singularities.

The following are some suggested directions for further studies.

Since the phase transformation in the SMA fiber is generally a large deforma-

tion, the induced elastic deformations in both the matrix and the fiber should also be large. Further studies on the nonlinear deformations of the composite associated with phase transformation in the SMA fiber are suggested. The studies could begin with development of the governing equations for general axisymmetric nonlinear deformations. Then, attention could be focused on certain specific hyperelastic material for some specific bonding condition to solve the problem.

In all the models studied in this dissertation, we assume there are sharp phase boundaries, so the strains in the SMA fiber suffer finite jumps across the phase boundaries. In terms of continuity of strain in the fiber, these are “discontinuous strain” models. On the other hand, it could be assumed that there exists an intermediate region in the fiber between each completely transformed and untransformed region. In this special region, there is a mixture of two phases. Assume that the volume fraction of the transformed phase changes continuously over this region. By taking the average of each cross section of the fiber, it is then modeled that the strain in the fiber changes continuously from transformed region to untransformed one. It could be called as “continuous strain” model. The method adopted in this dissertation could also be used to investigate the mechanical behavior of the material for this model.

In order to investigate local behavior, especially near the sharp phase boundary in SMA fiber during phase transformation, we have considered the dilute case involving a single SMA fiber embedded in an infinite elastic matrix. Further, we could study the non-dilute SMA fibers reinforced composites. To take the interaction between SMA fibers into account, we could model the composite as three concentric cylinders: a single infinite fiber is embedded in cylindrical elastic matrix, which is surrounded by infinite composite. A portion of the fiber is allowed to undergo phase transformation along the axial direction. A sharp phase boundary could be explicitly considered to study local behavior near the intersection between

the fiber-matrix interface and the phase boundary in the fiber. Assume the matrix is linearly elastic and isotropic. The infinite composite cylinder is assumed to be homogeneous, linear elastic, and transversely isotropic. The effective mechanical properties of the infinite composite cylinder could be analyzed using self-consistent method. The matrix and the infinite composite cylinder could be assumed perfectly bonded, while different bonding conditions between the fiber and the matrix could be investigated. By assuming both the fiber and the matrix undergoing general axisymmetrical deformations and the infinite composite cylinder doing axisymmetrical plane strain deformation, the problem could be modeled as a boundary value problem. The exact solutions to the problem could be then derived. According to the solutions, numerical calculations could be performed to illustrate the results. The asymptotic analysis will be carried out to further investigate stress concentration or possible singularities near the phase boundary of the SMA fiber. The comparisons could be made with the previous one single fiber model to study the interaction between SMA fibers.

REFERENCES

Abeyaratne R and Knowles JK (1988), On the dissipative response due to discontinuous strains in bars of unstable elastic material, *International Journal of Solids and Structures*, 24:10,1021–1044.

Abeyaratne R and Knowles JK (1993), A continuum model of a thermoelastic solid capable of undergoing phase transitions, *Journal of the Mechanics and Physics of Solids*, 41:3, 541–571.

Achenbach M and Müller I (1985), Simulation of material behaviour of alloys with shape memory, *Archives of Mechanics*, 37:6, 573–585.

Bekker A and Brinson LC (1997), Temperature-induced phase transformation in a shape memory alloy: Phase diagram based kinetics approach, *Journal of the Mechanics and Physics of Solids*, 45:6, 949–988.

Bekker A and Brinson LC (1998), Phase diagram based description of the hysteresis behavior of shape memory alloys, *Acta Materialia*, 46:10, 3649–3665.

Bekker A, Brinson LC, and Issen K (1998), Localized and diffuse thermoinduced phase transformation in 1-D shape memory alloys, *Journal of Intelligent Material Systems and Structures*, 9:5, 355–365.

Bell WW (1968), *Special Functions for Scientists and Engineers*, D. Van Nostrand Company Ltd, London.

Berman JB and White SR (1996), Theoretical modelling of residual and transformational stresses in SMA composites, *Smart Materials and Structures*, 5:6, 731–743.

Berveiller M, Patoor E, and Buisson M (1991), Thermomechanical Constitutive-Equations For Shape Memory Alloys, *Journal de Physique IV*, 1:C4, 387–396.

Birman V (1997) Review of mechanics of shape memory alloy structures, *Applied Mechanics Reviews*, 50:11, 629–645.

Birman V and Hopkins DA(1996) Micromechanics of composites with shape memory alloy fibers in uniform thermal fields, *AIAA Journal*, 34:9, 1905–1912.

Boyd JG and Lagoudas DC (1994), Thermomechanical response of shape memory composites *Journal of Intelligent Material Systems and Structures*, 5, 333–346.

Bracewell RN (1978), *The Fourier transform and its applications*, McGraw-Hill Book Company, Inc., New York, NY.

Brinson LC (1993), One dimensional constitutive behavior of shape memory alloys: thermomechanical derivation with non-constant material functions, *Journal of Intelligent Material Systems and Structures*, 4:2, 229–242.

Brinson LC, Bekker A, and Hwang S (1996), Deformation of shape memory alloys due to thermo-induced transformation, *Journal of Intelligent Material Systems and Structures*, 7:1, 97–107.

Brinson LC and Huang MS (1996), Simplifications and comparisons of shape memory alloy constitutive models, *Journal of Intelligent Material Systems and Structures*, 7:1, 108–114.

Buisson M, Patoor E, and Berveiller M (1991), Interfacial Motion In Shape Memory Alloys *Journal de Physique IV*, 1:C4, 463–466.

Courant R and Hilbert D (1989) *Methods of Mathematical Physics, Volume I*, John Wiley & Sons, Inc., New York.

Crawley EF (1994) Intelligent structures for aerospace: a technology overview and assessment, *AIAA Journal*, 32:8, 1689–1699.

Ericksen JL (1975), Equilibrium of bars, *Journal of Elasticity*, 5:3–4, 191–201,

Eshelby JD (1957), The determination of the elastic field of an ellipsoidal inclusion, and related problems, *Proceedings of the Royal Society, Series A Mathematical and Physical Sciences*, 241, 376–396.

Eshelby JD (1959), The elastic field outside an ellipsoidal inclusion, *Proceedings of the Royal Society, Series A Mathematical and Physical Sciences*, 252, 561–569.

Falk F (1980), Model free energy, mechanics, and thermodynamics of shape memory alloys, *Acta Metallurgica*, 28, 1773–1780.

Falk F (1983), One-dimensional model of shape memory alloys, *Archives of Mechanics*, 35:1, 63–84.

Fosdick RL and James RD (1981), The elastica and the problem of the pure bending for a non-convex stored energy function, *Journal of Elasticity*, 11, 165–186.

Griffel DH (1981), *Applied Functional Analysis*, Ellis Horwood Ltd., Chichester, England.

Hill R (1965), A self-consistent mechanics of composite materials, *Journal of the Mechanics and Physics of Solids*, 13, 213–222.

Hodgson DE, Wu MH, and Biermann RJ (1990), Shape memory alloys, *Metals Handbook*, tenth edition, Vol 2, ASM International, 897–902

Huang MS, Gao XJ, Brinson LC (2000), A multivariant micromechanical model for SMAs Part 2. Polycrystal model, *International Journal of Plasticity*, 16:10–11, 1371–1390.

Huang M and Brinson LC (1998), Multivariant model for single crystal shape memory alloy behavior, *Journal of the Mechanics and Physics of Solids*, 46:8, 1379–1409.

Gao XJ, Huang MS, and Brinson LC (2000), A multivariant micromechanical model for SMAs Part 1. Crystallographic issues for single crystal model, *International Journal of Plasticity*, 16:10–11, 1345–1369.

Ivshin Y and Pence TJ (1994), A constitutive model for hysteretic phase-transition behavior, *International Journal of Engineering Science*, 32:4, 681–704.

Ivshin Y and Pence TJ (1994), A thermomechanical model for a one variant shape-memory material, *Journal of Intelligent Material Systems and Structures*, 5:4, 455–473.

Lagoudas DC, Boyd JG, and Bo Z (1994), Micromechanics of active composites

with SMA fibers, *Journal of Engineering Materials and Technology ASME*, 116:3, 337–347.

Lewis G (1990), *Selection of Engineering Materials*, Printice-Hall, Inc., Englewood Cliffs, NJ.

Liang C and Rogers CA (1990), One-dimensional thermomechanical constitutive relations for shape memory materials, *Journal of Intelligent Material Systems and Structures*, 1, 207–234.

Love AEH (1944), *A Treatise on the Mathematical Theory of Elasticity*, Dover Publications, Inc., New York, NY.

Muki R and Sternberg E (1969), On the diffusion of an axial load from an infinite cylindrical bar embedded in an elastic medium, *International Journal of Solids and Structures*, 5, 587–605.

Müller I (1979), A model for a body with shape-memory, *Archive for Rational Mechanics and Analysis*, 70, 61–77.

Mura T (1982), *Micromechanics of defects in solids*, Martinus Nijhoff Publishers, The Hague, The Netherlands.

Nozaki S and Takahashi K (1994), Research activities on intelligent materials in Japan, *Proceedings of the Second International Conference on Intelligent Materials*, Edited by Rogers CA and Wallace GG, Technomic Publishing Co., Inc., Lancaster, PA, 1230–1241.

Olver FWJ (1974), *Asymptotics and special functions*, Academic Press, Inc., San Diego, CA.

Patoor E, Barbe P, Eberhardt A, and Berveiller M (1991), Internal-Stress Effect In The Shape Memory Behavior *Journal de Physique IV*, 1:C4, 95–100.

Patoor E, Eberhardt A, and Berveiller M (1996), Micromechanical modelling of superelasticity in shape memory alloys, *Journal de Physique IV*, 6:C1, 277–292.

Pence TJ (1986), On the emergence and propagation of a phase-boundary in

an elastic bar with a suddenly applied end load, *Journal of Elasticity*, 16:1, 3–42.

Pence TJ (1991), On the encounter of an acoustic shear pulse with a phase-boundary in an elastic-material - reflection and transmission behavior, *Journal of Elasticity*, 25:1, 31–74.

Pence TJ (1991), On the encounter of an acoustic shear pulse with a phase-boundary in an elastic-material - energy and dissipation, *Journal of Elasticity*, 26:2, 95–146.

Perkins J (1986), Shape-memory-effect alloys: basic principles, *Encyclopedia of Materials Science and Engineering*, Vol. 6, Edited by Bever MB, Pergamon Press and The MIT Press, 4365–4368.

Rogers CA, Barker DK, and Jaeger CA (1989), Introduction to smart materials and structures, *Smart Materials, Structures, and Mathematical Issues*, Technomic Publishing Co., Inc., Lancaster, PA.

Rosakis P and Tsai H (1995), Dynamic twinning processes in crystals, *International Journal of Solids and Structures*, 32:17–18, 2711–2723.

Shaw JA and Kyriakides S (1995), Thermomechanical aspects of NiTi, *Journal of the Mechanics and Physics of Solids*, 43:8, 1243–1281.

Tanaka K (1986a), Analysis of superplastic deformation during isothermal martensitic transformation, *Res Mechanica*, 17:3, 241–252.

Tanaka K (1986b), A thermomechanical sketch of shape memory effect: one-dimensional tensile behavior, *Res Mechanica*, 18:3, 251–263.

Timoshenko S and Goodier JN (1951), *Theory of Elasticity*, McGraw-Hill Book Company, Inc., New York, NY.

Tsai H and Rosakis P (2001), Quasi-steady growth of twins under stress, *Journal of the Mechanics and Physics of Solids*, 49, 289–312.

Wayman CM and Duerig TW (1990), An introduction to martensite and shape memory, *Engineering Aspects of Shape Memory Alloys*, Edited by Duerig TW,

Melton KN, Stöckel D, and Wayman CW, Butterworth-Heinemann Ltd., London, 3–20.

Wei ZG, Sandström R, and Miyazaki S (1998a), Shape-memory materials and hybrid composites for smart systems - Part I Shape-memory materials, *Journal of Materials Science*, 33, 3749–3762.

Wei ZG, Sandström R, and Miyazaki S (1998b), Shape-memory materials and hybrid composites for smart systems - Part II Shape-memory hybrid composites, *Journal of Materials Science*, 33, 3763–3783.

Wu XC and Pence TJ (1998), Two variant modeling of shape memory materials: Unfolding a phase diagram triple point, *Journal of Intelligent Material Systems and Structures*, 9:5, 335–354.

Yamada Y, Taya M, and Watanabe R (1993), Strengthening of metal matrix composite by shape memory effect, *Materials transactions, JIM*, 34:3, 254–260.

Zayed AI (1996), *Handbook of function and generalized function transformations*, CRC press, Inc., Boca Raton, FL.

Zhang XD, Rogers CA, and Liang C (1992), Modelling of the two-way shape memory effect, *Philosophical Magazine A*, 65:5, 1199–1215.

Zhong Z, Sun QP, and Tong P (2000), On the elastic axisymmetric deformation of a rod containing a single cylindrical inclusion, *International Journal of Solids and Structures*, 37, 5943–5955.

MICHIGAN STATE LIBRARIES



3 1293 02314 5901